MECHANISMS OF EPIGENETICS AND GENETICS IN LEUKEMOGENESIS

EDITED BY: Yonghui Li, Fei Gao and Shujun Liu
PUBLISHED IN: Frontiers in Oncology

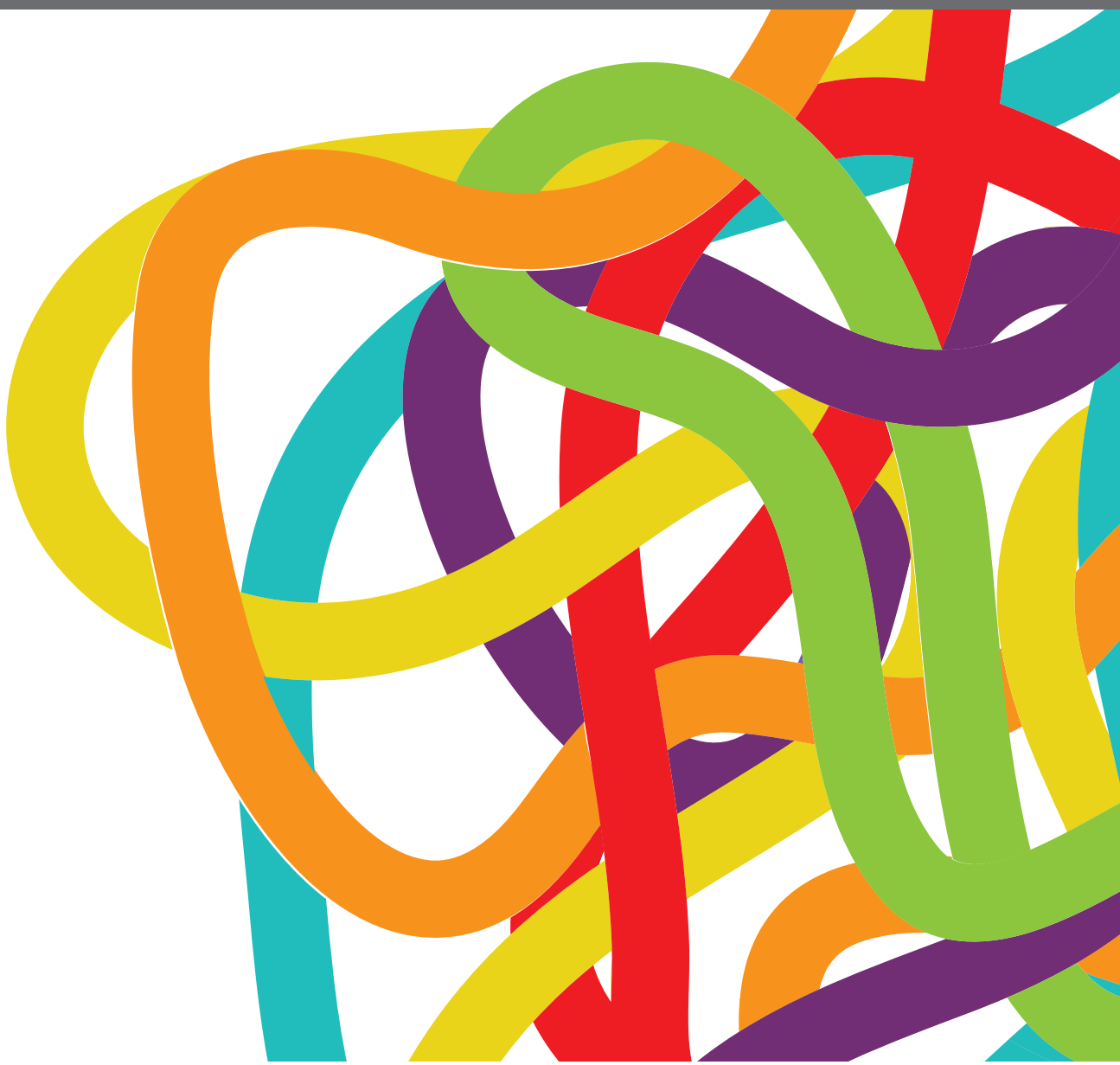

frontiers Research Topics

frontiers

ISSN 1664-8714
ISBN 978-2-88976-040-4
DOI 10.3389/978-2-88976-040-4

About Frontiers

Frontiers is more than just an open-access publisher of scholarly articles: it is a pioneering approach to the world of academia, radically improving the way scholarly research is managed. The grand vision of Frontiers is a world where all people have an equal opportunity to seek, share and generate knowledge. Frontiers provides immediate and permanent online open access to all its publications, but this alone is not enough to realize our grand goals.

Frontiers Journal Series

The Frontiers Journal Series is a multi-tier and interdisciplinary set of open-access, online journals, promising a paradigm shift from the current review, selection and dissemination processes in academic publishing. All Frontiers journals are driven by researchers for researchers; therefore, they constitute a service to the scholarly community. At the same time, the Frontiers Journal Series operates on a revolutionary invention, the tiered publishing system, initially addressing specific communities of scholars, and gradually climbing up to broader public understanding, thus serving the interests of the lay society, too.

Dedication to Quality

Each Frontiers article is a landmark of the highest quality, thanks to genuinely collaborative interactions between authors and review editors, who include some of the world's best academicians. Research must be certified by peers before entering a stream of knowledge that may eventually reach the public - and shape society; therefore, Frontiers only applies the most rigorous and unbiased reviews.
Frontiers revolutionizes research publishing by freely delivering the most outstanding research, evaluated with no bias from both the academic and social point of view. By applying the most advanced information technologies, Frontiers is catapulting scholarly publishing into a new generation.

What are Frontiers Research Topics?

Frontiers Research Topics are very popular trademarks of the Frontiers Journals Series: they are collections of at least ten articles, all centered on a particular subject. With their unique mix of varied contributions from Original Research to Review Articles, Frontiers Research Topics unify the most influential researchers, the latest key findings and historical advances in a hot research area! Find out more on how to host your own Frontiers Research Topic or contribute to one as an author by contacting the Frontiers Editorial Office: frontiersin.org/about/contact

MECHANISMS OF EPIGENETICS AND GENETICS IN LEUKEMOGENESIS

Topic Editors:
Yonghui Li, Shenzhen University General Hospital, China
Fei Gao, Beijing Genomics Institute (BGI), China
Shujun Liu, University of Minnesota Twin Cities, United States

Citation: Li, Y., Gao, F., Liu, S., eds. (2022). Mechanisms of Epigenetics and Genetics in Leukemogenesis. Lausanne: Frontiers Media SA. doi: 10.3389/978-2-88976-040-4

Table of Contents

frontiers | Frontiers in Oncology

EDITORIAL
published: 07 April 2022
doi: 10.3389/fonc.2022.896094

Editorial: Mechanisms of Epigenetics and Genetics in Leukemogenesis

Yonghui Li[1]*, *Fei Gao*[2] *and Shujun Liu*[3]

[1] Central Laboratory, Shenzhen Key Laboratory of Precision Medicine for Hematological Malignancies, Shenzhen University General Hospital, Shenzhen University Health Science Center, Shenzhen, China, [2] Shenzhen Branch, Guangdong Laboratory for Lingnan Modern Agriculture, Genome Analysis Laboratory of the Ministry of Agriculture, Agricultural Genomics Institute at Shenzhen, Chinese Academy of Agricultural Sciences, Shenzhen, China, [3] The Hormel Institute, University of Minnesota, Austin, MN, United States

Keywords: leukemia, epigenetics, genetics, immunotherapy, n^6-methyladenosine

Editorial on the Research Topic

Mechanisms of Epigenetics and Genetics in Leukemogenesis

According to the new cancer statistic report, the incidence and mortality of leukemia rank among the top ten of all cancers (1). Understanding the mechanism of leukemia is vitally important which might help us to identify novel markers and develop novel therapeutic strategies. With the development of science and technology, especially the sequencing technique, a number of studies have depicted the genetic and epigenetic landscape of leukemia (2–4). In the meanwhile, a large scale of databases containing different sequencing data of leukemia have been established and broadly open-accessed, for example, the TCGA database. It has been conclusively shown that genetic and epigenetic abnormalities contribute greatly to the generation, progression, and drug resistance of leukemia. However, the mechanism of leukemia is far from being fully elucidated. The articles in the Research Topic on *Mechanisms of Epigenetics and Genetics in Leukemogenesis* explored both genetic and epigenetic mechanisms in leukemia generation.

Genetic alterations to genes involved in hematopoiesis, tumor suppressor genes, and oncogenes can result in dramatic gene expression changes leading to leukemia. Zhang et al. showed that RUNX3 is highly expressed in acute myeloid leukemia (AML) cells. Further study revealed RUNX3 knockdown inhibits AML progression by altering the expression of genes involved in DNA damage and apoptosis. Su et al. reviewed CEBPA mutation in leukemia including current progress and future directions. Patients with different subtypes of CEBPA mutations showed different clinical features and different sensitivity to chemotherapy, which can be useful for optimizing the clinical management of AML patients with CEBPA mutations. Shi et al. showed that high CENPE expression is correlated with chemoresistance, while knockdown of CENPE expression *in vitro* suppresses the proliferation of myeloid leukemia cells and reverses the cytarabine (Ara-C) chemoresistance.

Since the beginning of the 21st century, epigenetics has entered a period of rapid development, especially in the field of biology and medicine. Examples of epigenetic modifications mainly include DNA methylation, histone modifications, chromatin remodeling, and non-coding RNAs. ASH1L is a histone methyltransferase that is essential in the generation and maintenance of MLL-AF9 leukemia. Aljazi et al. reported that ASH1L binds to the promoters and modifies the local histone H3K36me2 levels of MLL-AF9 target genes including *Hoxa9* and *Hoxa10*. SET8 regulates the

OPEN ACCESS

Edited and reviewed by:
Alessandro Isidori, AORMN Hospital, Italy

***Correspondence:**
Yonghui Li
yonghuililab@163.com

Specialty section:
This article was submitted to Hematologic Malignancies, a section of the journal Frontiers in Oncology

Received: *14 March 2022*
Accepted: *21 March 2022*
Published: *07 April 2022*

Citation:
Li Y, Gao F and Liu S (2022) Editorial: Mechanisms of Epigenetics and Genetics in Leukemogenesis. Front. Oncol. 12:896094. doi: 10.3389/fonc.2022.896094

histone H4 monomethylation at Lys 20 (H4K20me1), which is highly expressed in AML and associated with poor prognosis (Xu et al.). Targeting SET8 by LukS-PV induces apoptosis in leukemia. Besides methylation, histone acetylation plays a vital role in leukemogenesis. Zhang et al. made an elaborate review on the roles of histone deacetylases (HDAC) in AML with fusion proteins. lncRNA PPM1A-AS is highly expressed in T-cell acute lymphoblastic leukemia (T-ALL) and regulates genes in multiple signaling pathways. Li et al. confirmed that PPM1A-AS acts as an oncogene in T-ALL by promoting cell proliferation and inhibiting cell apoptosis. Another type of epigenetically regulated genes are those associated with immunity. According to the study from Xiao et al., Intercellular Adhesion Molecule-1 (ICAM-1), a crucial factor in tumor immunity, is epigenetically silenced by DNA methylation. The use of decitabine restores ICAM-1 expression and inhibits AML immune escape from NK cells. This study suggests that combining hypomethylating agent decitabine and NK cell infusion may be a potentially effective strategy in AML treatment.

Accumulated study of genetics and epigenetics in leukemogenesis facilitates the identification of possible novel biomarkers and the study of new targeted drugs, including the abovementioned CENPE (Shi et al.), ASH1L (Aljazi et al.), and SET8 (Xu et al.). In addition, HDAC inhibitors and hypomethylating agents (azacytidine, decitabine) have been widely used in clinical practice and the effect has been widely proved (5–7). In our Research Topic, Yin et al. reported a phase II clinical trial using a regimen combining chemotherapy, HDAC inhibitor, and hypomethylating agent in patients with relapsed/refractory AML. The completed remission (CR) rate is 42.9%, which suggests the double epigenetic priming regimen has good antileukemia activity. It indicates that a better understanding of the genetic and epigenetic mechanism of leukemogenesis has recently begun to increasingly influence the clinical decisions from diagnosis and risk stratification to individual therapeutic intervention.

In summary, the original articles, reviews, and clinical trials collected in this Research Topic represent an invaluable resource of insights on mechanisms of genetics and epigenetics in leukemogenesis. However, more studies, particularly on the interaction between genetics and epigenetics are needed to fully understand the mechanism of leukemogenesis, which will guide future clinical trials and lead to the development of new therapeutic strategies.

AUTHOR CONTRIBUTIONS

YL, FG, and SL are co-editors for this Research Topic. All authors contributed to the article and approved the submitted version.

FUNDING

YL was supported by National Natural Science Foundation of China (82070161, 81870134, and 81570137) and Beijing Natural Science Foundation (7202186).

ACKNOWLEDGMENTS

We are very grateful to all the authors who contributed to this Research Topic and for the interest shown by the scientific community.

REFERENCES

1. Siegel RL, Miller KD, Fuchs HE, Jemal A. Cancer Statistics, 2022. *CA Cancer J Clin* (2022) 72(1):7–33. doi: 10.3322/caac.21708
2. Shannon K, Armstrong SA. Genetics, Epigenetics, and Leukemia. *N Engl J Med* (2010) 363(25):2460–1. doi: 10.1056/NEJMe1012071
3. Fiñana C, Gómez-Molina N, Alonso-Moreno S, Belver L. Genomic and Epigenomic Landscape of Juvenile Myelomonocytic Leukemia. *Cancers (Basel)* (2022) 14(5):1335–54. doi: 10.3390/cancers14051335
4. Largeaud L, Bertoli S, Bérard E, Tavitian S, Picard M, Dufrechou S, et al. Genomic Landscape of Hyperleukocytic Acute Myeloid Leukemia. *Blood Cancer J* (2022) 12(1):4. doi: 10.1038/s41408-021-00601-5
5. Khateb A, Deshpande A, Feng Y, Finlay D, Lee JS, Lazar I, et al. The Ubiquitin Ligase RNF5 Determines Acute Myeloid Leukemia Growth and Susceptibility to Histone Deacetylase Inhibitors. *Nat Commun* (2021) 12(1):5397. doi: 10.1038/s41467-021-25664-7
6. Kennedy VE, Hui G, Azenkot T, Gaut D, Wieduwilt MJ, Oliai C, et al. Outcomes of Allogeneic Transplantation After Hypomethylating Agents With Venetoclax in Acute Myeloid Leukemia. *Am J Hematol* (2022). doi: 10.1002/ajh.26524
7. Wang H, Li Y, Lv N, Li Y, Wang L, Yu L. Predictors of Clinical Responses to Hypomethylating Agents in Acute Myeloid Leukemia or Myelodysplastic Syndromes. *Ann Hematol* (2018) 97(11):2025–38. doi: 10.1007/s00277-018-3464-9

Conflict of Interest: The authors declare that the research was conducted in the absence of any commercial or financial relationships that could be construed as a potential conflict of interest.

frontiers in Oncology

CASE REPORT
published: 26 August 2021
doi: 10.3389/fonc.2021.703612

Case Report: The Formation of a Truncated PAX5 Transcript in a Case of Ph-Positive Mixed Phenotype Acute Leukemia With dic(7;9)(p11-p13;p13)

Yan Yu[1,2,3†], Zhao Zeng[1,3†], Jundan Xie[1,2†], Qiongyu Lu[4†], Wenzhi Cai[1,2], Ruixi Zhang[1,2,3], Jinlan Pan[1,2], Yun Zhao[4], Aining Sun[1,2,3,5], Huiying Qiu[1,2] and Suning Chen[1,2,3*]*

[1] Jiangsu Institute of Hematology, National Clinical Research Center for Hematologic Diseases, The First Affiliated Hospital of Soochow University, Medical College of Soochow University, Suzhou, China, [2] Collaborative Innovation Center of Hematology, Soochow University, Suzhou, China, [3] Institute of Blood and Marrow Transplantation, Soochow University, Suzhou, China, [4] Cyrus Tang Hematology Center, Soochow University, Suzhou, China, [5] Key Laboratory of Thrombosis and Hemostasis of Ministry of Health, Suzhou, China

PAX5 plays a critical role in B-cell precursor development and is involved in various chromosomal translocations that involve the fusion of a portion of PAX5 to at least 49 different partners reported to date. Here, we identified a novel PAX5 fusion transcript in a Ph-positive mixed phenotype acute leukemia case with dic(7;9)(q13;q13), in which a translocation juxtaposes the 5' region of PAX5 and the ubiquitin-conjugating enzyme E2D4 (UBE2D4) to generate a PAX5-UBE2D4 fusion gene. To further explore the general characteristics and function of PAX5-UBE2D4, we cloned the full-length cDNA, which was amplified from the bone marrow of the patient. Interestingly, the fusion was located in the nucleus and negatively affected PAX5 transcription activity. Importantly, the fusion promoted tumor growth in nude mice and the proliferation of NIH3T3 cells *in vitro*. In conclusion, the fusion resulted in partial oncogenic activity, in contrast to the tumor suppressor activity of wild-type PAX5.

Keywords: Pax5, UBE2D4, MPAL, BCR/ABL, dic(7;9)

OPEN ACCESS

Edited by:
Yonghui Li,
Shenzhen University General Hospital, China

Reviewed by:
Rehan Khan,
Case Western Reserve University, United States
Yingchang Mi,
Chinese Academy of Medical Sciences and Peking Union Medical College, China
Xianping Shi,
Guangzhou Medical University, China

****Correspondence:***
Suning Chen
chensuning@suda.edu.cn
Huiying Qiu
qiuhuiying@suda.edu.cn

†These authors have contributed equally to this work

Specialty section:
This article was submitted to Hematologic Malignancies, a section of the journal Frontiers in Oncology

Received: *30 April 2021*
Accepted: *03 August 2021*
Published: *26 August 2021*

Citation:
Yu Y, Zeng Z, Xie J, Lu Q, Cai W, Zhang R, Pan J, Zhao Y, Sun A, Qiu H and Chen S (2021) Case Report: The Formation of a Truncated PAX5 Transcript in a Case of Ph-Positive Mixed Phenotype Acute Leukemia With dic(7;9)(p11-p13;p13). Front. Oncol. 11:703612. doi: 10.3389/fonc.2021.703612

INTRODUCTION

The transcription factor PAX5 plays a critical role in B-cell development and differentiation and has been considered to function as a tumor suppressor in B cell precursor acute lymphoblastic leukemia (BCP-ALL). PAX5 alterations, including deletions, mutations, and rearrangements, occur in approximately 30% of BCP-ALL cases. Chromosomal rearrangements account for 2–3% of cases (1–3). It has been well reported that a number of PAX5 rearrangements give rise to in-frame fusion transcripts that encode chimeric proteins that consistently retain the PAX5 DNA binding domain at the N terminus, but the C-terminal regions are derived from various partners, including transcription factors, kinases and structural proteins (4–8). To date, at least 58 fusions have been identified, and most of them have been found in association with BCP-ALL (9). Only a limited

number of the reported fusions were recurrent, such as PAX5-ETV6, PAX5-ELN, and PAX5-PML, while most have been found in single cases, such as PAX5/ASXL1 and PAX5/FOXP1 (9). In addition, half of the rearrangements have resulted in PAX5 fusions to genes in the opposite orientation, out-of-frame fusions or the expression of truncated isoforms (6). Here, we first identified a novel chromosomal dic(7;9) (p13;p13) translocation in a Ph-positive mixed phenotype acute leukemia (MPAL) patient, resulting in a PAX5 out-of-frame fusion with the ubiquitin-conjugating enzyme E2D4 (UBE2D4), which functions as a truncated PAX5. In addition, the fusion showed partial oncogenic activity, which was in contrast with the tumor suppressor ability of wild-type (WT) PAX5.

CASE DESCRIPTION

A 16-year-old boy was referred to our hospital in January 2010 with recurrent fever and weakness for one month. Physical examination indicated axillary lymphadenopathy and hepatosplenomegaly without anemic conjunctiva. The peripheral blood counts at diagnosis revealed multilineage cytopenia: hemoglobin 12 g/dL, white blood cells (WBCs) 12.87 x 109/L, and platelets 31 x 109/L. Bone marrow (BM) aspiration showed hypercellularity with 89.2% blasts and lymphatic changes. Flow cytometric analysis revealed that 23.4% of the BM blast cells were positive for HLA-DR, CD10, CD20, CD19, CD13, CD33, CD34, MPO and CD79a but negative for CD117, CD14, CD15, CD2, CD3, and CD7 (**Supplementary Figure 1**). Then, the patient was diagnosed with MPAL with co-expression of myeloid and B lymphoid lineage antigen according to the 2016 WHO classification. The karyotype of the bone marrow cells was 45, XY, dic(7;9)(p11-13;p13), t(9;22)(q34;q11) (8) /46, XY (9). The BCR/ABL (p190) fusion gene was detected by multiplex reverse transcription-polymerase chain reaction (RT-PCR), thereby confirming the diagnosis of Ph-positive mixed phenotype acute leukemia. The patient accepted tyrosine kinase inhibitor therapy and achieved remission, which was followed by 2 DVP chemotherapy sessions (with 70 mg daunorubicin, 4 mg vincristine and 20 mg dexamethasone). Unfortunately, the patient finally had a cytological relapse in the bone marrow and died 5 months after the initial diagnosis.

DISCUSSION AND CONCLUSION

Based on the karyotype of the patient, array comparative genomic hybridization (array-CGH) analysis was performed, and the results indicated that the breakpoints were located in the PAX5 and UBE2D4 genes and revealed the deletion of large parts of 9p and 7p (**Figure 1A**). When using the FISH (fluorescent *in situ* hybridization) probes RP11-652D9 and RP11-344B23 corresponding to the 5' and 3' sequences of the PAX5 gene, respectively, we observed a red signal and a yellow signal, which was consistent with the results of the array-CGH analysis (**Figure 1B** and **Supplementary Figure 2**). Then, RT-PCR amplification revealed the presence of PAX5-UBE2D4 fusion transcripts (**Supplementary Figure 3**). Sanger sequencing confirmed the out-of-frame fusion of PAX5 exon 7 (NM_016734) with UBE2D4 exon 2 (NM_015983.4), resulting in the analogous truncated PAX5 protein with the DNA binding (PBD) domain, OCT domain and homeodomain (HD) of PAX5 and an additional 19-amino acid tail, which does not correspond to any predicted functional domain (**Figure 1C**).

To investigate the function of the fusion, we amplified the full-length cDNA sequence of PAX5 and UBE2D4 that was retained in the fusion found in the patient, cloned it into a lentiviral vector (LV5, GenePharm Inc., Shanghai) and the pcDNA3.1 vector, and fused it with a 3×FLAG-tag. As **Figure 1D** shows, we observed nuclear localization of the fusion, which was expected since the fusion retained the nuclear localization signal of PAX5 (**Figure 1D** and **Supplementary Figure 4**). Furthermore, we co-transfected 293T cells with the CD19 promotor-LUC construct (PGL3), pcDNA-PAX5 and increasing amounts of the pcDNA-PAX5-UBE2D4 (PU) construct. The transcription of the luciferase reporter gene was significantly downregulated in the presence of the expression of PU alone compared with that observed in the presence of wt-PAX5 (**Figure 1E**). In addition, after concomitant transfection of wt-PAX5 and PU, PAX5-driven reporter gene transcription was downregulated (**Figure 1E**), indicating the dominant-negative activity of PU. To investigate the function of PU, HEL cells were transfected with PU (HEL-PU) and the vector (HEL-LV5). Then, the cells were subcutaneously injected into 6- to 8-week-old female nude mice (n=6-11). A total of 45.5% (5/11) of mice engrafted with HEL-PU cells developed tumors, which was obviously greater than the number of mice who developed tumors in the control (HEL-LV5, 33.3%, 2/6) group (**Figures 2A, B**). The mean volume of the tumors in the PU cohort was much larger than the control cohort (**Figure 2C**). In addition, the mean weight of the tumors in the HEL-PU group was the heaviest when compared with control group (**Figure 2D**). In contrast, the PU fusion showed at least partial oncogenic activity. Furthermore, NIH-3T3 cells expressing the PU fusion grew significantly faster than the control cells over 72 h and showed an increase in the number of colony forming units compared with the vector control-expressing cells (**Figures 2E, F**).

Dicentric (7;9)(p11-p13;p11-p13) is a very rare but recurrent abnormality in BCP-ALL patients as well as a limited number of cases involving PAX5 rearrangement. Indeed, we identified only 7 cases of dic(7;9) from among approximately thousands of cases with karyotypic data (**Supplementary Table 1**). Most cases with the translocation, dicentric abnormality or derivatives of chromosomes 7 and 9 involving PAX5 rearrangement mainly presented PAX5-LOC392027, PAX5-POM121, PAX5-ELN, and PAX5-AUTS2 (4, 8–14). Some aberrant PAX5 transcripts have also been reported, such as a case of MPAL that harbored der(9)t(7;9)(q11.2;p13) (10). To our knowledge, this is the first case of

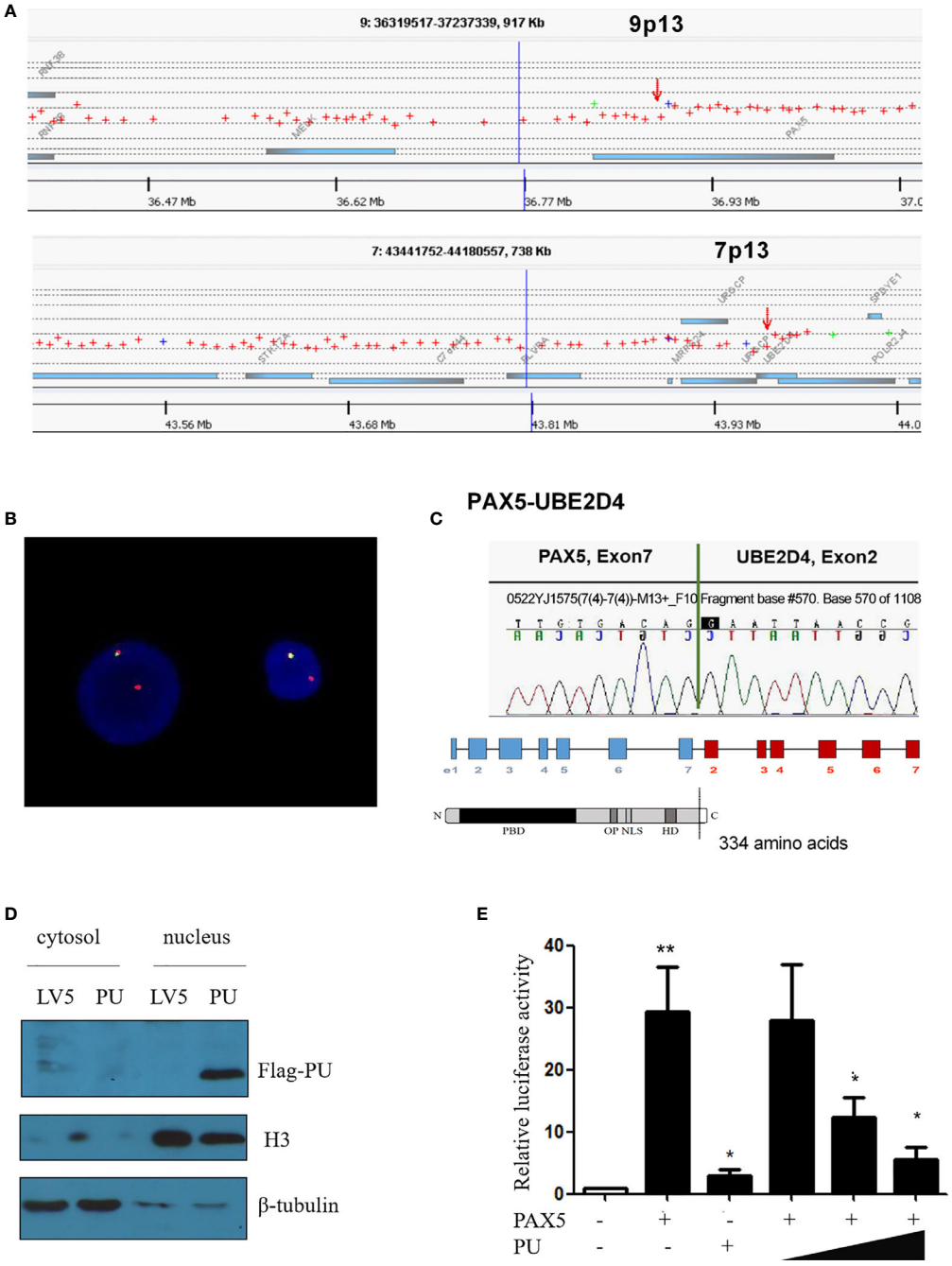

FIGURE 1 | **(A)** Array comparative genomic hybridization showing the breakpoints of 9p13/PAX5 and 7p13/UBE2D4. **(B)** FISH assay showing the splitting of the N terminus (green, RP11-344B23) and C-terminus (red, RP11-652D9) of WT PAX5. **(C)** Sanger sequencing confirmed that PAX5 exon 7 was fused out-of-frame with UBE2D4 exon 2, and the schematics show the domains of the PAX5-UBE2D4 (PU) fusion protein, including PBD (DNA-binding domain), OP (octapeptide motif), NLS (nuclear localization sequence) and HD (homeodomain), and an additional 19-amino acid tail encoded by the UBE2D4 gene. **(D)** Nuclear localization of the PU fusion protein as shown by a nucleus and cytosol separation assay. **(E)** The transcription activity of the PU fusion and its dominant negative effect on PAX5 transcription activity based on the CD19 promoter luciferase reporter assay. P values are from Fisher's exact test. *P ≤ 0.05, **P ≤ 0.01.

PAX5 rearrangement in a Ph-positive MAPL patient with dic (7;9). Previous studies showed that most malignant cells carrying PAX5 fusions displayed a simple karyotype (6). Coexistence of the t(9;22)(q34;q11) translocation, which resulted in the formation of the BCR-ABL1 p190 fusion in this study, might contribute to the cytogenetic complexity and suggest a poor prognosis. The partner genes involved in the PAX5 fusions were heterogeneous, but a partner involving a ubiquitin-related gene

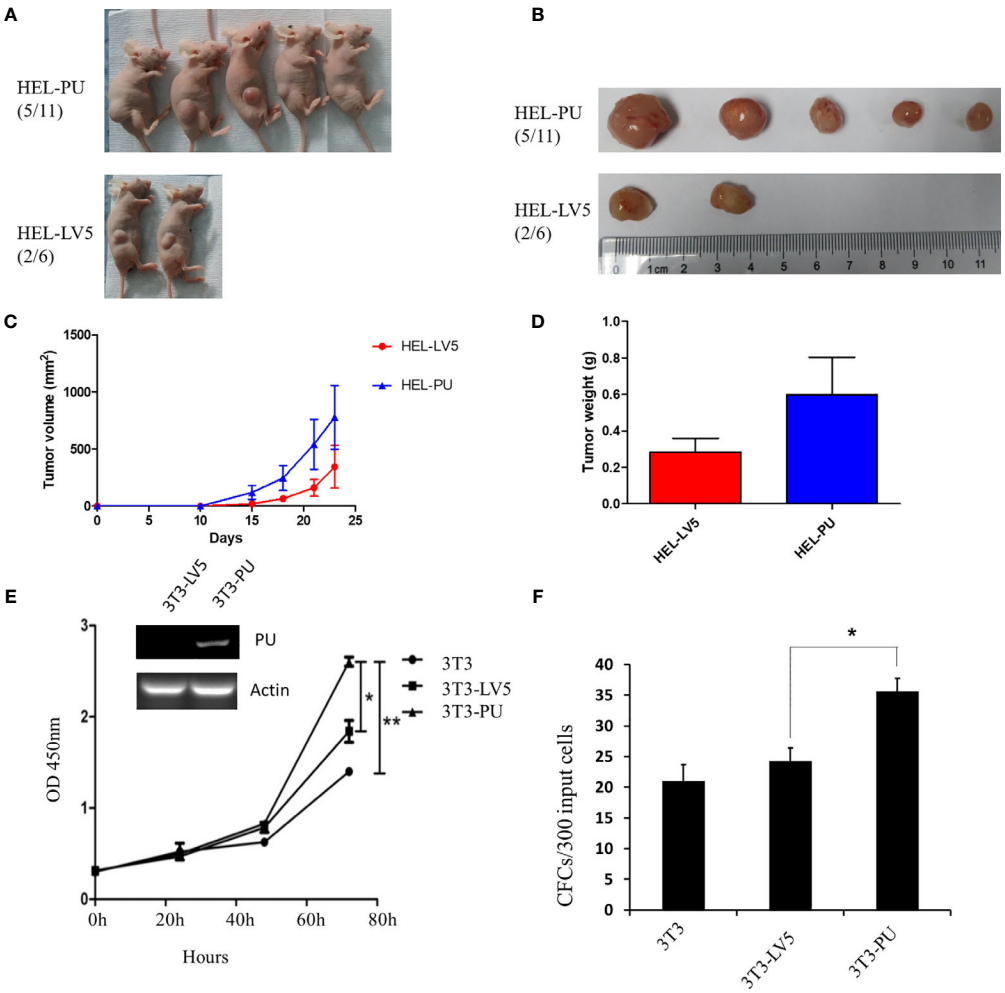

FIGURE 2 | The oncogenic activity of the PAX5-UBE2D4 (PU) fusion. **(A)** PAX5-UBE2D4 (PU) increases the number of tumors generated by subcutaneous injection of HEL cells into nude mice. **(B, C)** The sizes of the tumor masses and tumor weights **(D)** after injection of HEL cells expressing the indicated genes. **(E)** PU fusion promotes the proliferation and colony formation **(F)** of NIH-3T3 cells. P values are from Fisher's exact test. *P < 0.05, **P < 0.01.

was the first to be reported. Previous reports indicated that half of the PAX5 fusion genes gave rise to truncated PAX5 proteins, including those involving out-of-frame fusions (6). Consistently, the PAX5-UBE2D4 fusion showed the competitive inhibition of wt-PAX5 transactivating activity, similar to truncated PAX5. Furthermore, the PAX5-UBE2D4 fusion presented oncogenic activity in a nude mouse model. In contrast, WT PAX5 showed tumor suppressive ability both *in vivo* and *in vitro*.

PATIENT PERSPECTIVE

Since the diagnosis, the patient received and understood the cause of his illness, and the possible cause of premature death. Ultimately, he hoped to get the right treatment.

DATA AVAILABILITY STATEMENT

The original contributions presented in the study are included in the article/**Supplementary Material**. Further inquiries can be directed to the corresponding authors.

ETHICS STATEMENT

All procedures performed in studies involving human participants were in accordance with the ethical standards of the institutional and/or national research committee(s) and with the Helsinki Declaration (as revised in 2013). Written informed consent to participate in this study was provided by the participants' legal guardian/next of kin.

AUTHOR CONTRIBUTIONS

YY, ZZ, JX, and QL contributed equally to this study and performed most of the experiments. HQ and SC were the principal investigators. AS, WC, RZ, JP, and YZ analyzed and discussed the data. All authors contributed to the article and approved the submitted version.

FUNDING

This study was supported by grant from the National Key R&D Program of China (2019YFA0111000), the National Natural Science Foundation of China (81700140, 81873449, 81970142, 81900130, 81970136, 81970132), the Natural Science Foundation of the Jiangsu Higher Education Institution of China (18KJA320005, 18KJB320019), the Natural Science Foundation of Jiangsu Province (BK20190180), the priority academic program development of Jiangsu Higher Education Institution, the Innovation Capability Development Project of Jiangsu Province(BM2015004), the Translational Research Grant of NCRCH (2020WSB03, 2020WSB11, 2020WSB13) and the Open Project of Jiangsu Biobank of Clinical Resources (SBK202003001, SBK202003 003).

SUPPLEMENTARY MATERIAL

The Supplementary Material for this article can be found online at: https://www.frontiersin.org/articles/10.3389/fonc.2021.703612/full#supplementary-material

REFERENCES

1. Familiades J, Bousquet M, Lafage-Pochitaloff M, Béné MC, Beldjord K, De Vos J, et al. PAX5 Mutations Occur Frequently in Adult B-Cell Progenitor Acute Lymphoblastic Leukemia and PAX5 Haploinsufficiency Is Associated With BCR-ABL1 and TCF3-PBX1 Fusion Genes: A GRAALL Study. *Leukemia* (2009) 23:1989–98. doi: 10.1038/leu.2009.135
2. Mullighan CG, Goorha S, Radtke I, Miller CB, Coustan-Smith E, Dalton JD, et al. Genome-Wide Analysis of Genetic Alterations in Acute Lymphoblastic Leukaemia. *Nature* (2007) 446:758–64. doi: 10.1038/nature05690
3. Nebral K, Denk D, Attarbaschi A, König M, Mann G, Haas OA, et al. Incidence and Diversity of PAX5 Fusion Genes in Childhood Acute Lymphoblastic Leukemia. *Leukemia* (2009) 23:134–43. doi: 10.1038/leu.2008.306
4. Bousquet M, Broccardo C, Quelen C, Meggetto F, Kuhlein E, Delsol G, et al. A Novel PAX5-ELN Fusion Protein Identified in B-Cell Acute Lymphoblastic Leukemia Acts as a Dominant Negative on Wild-Type PAX5. *Blood* (2007) 109:3417–23. doi: 10.1182/blood-2006-05-025221
5. Cazzaniga G, Daniotti M, Tosi S, Giudici G, Aloisi A, Pogliani E, et al. The Paired Box Domain Gene PAX5 Is Fused to ETV6/TEL in an Acute Lymphoblastic Leukemia Case. *Cancer Res* (2001) 61:4666–70.
6. Coyaud E, Struski S, Prade N, Familiades J, Eichner R, Quelen C, et al. Wide Diversity of PAX5 Alterations in B-ALL: A Groupe Francophone De Cytogenetique Hematologique Study. *Blood* (2010) 115:3089–97. doi: 10.1182/blood-2009-07-234229
7. Nebral K, König M, Harder L, Siebert R, Haas OA, Strehl S. Identification of PML as Novel PAX5 Fusion Partner in Childhood Acute Lymphoblastic Leukaemia. *Br J Haematol* (2007) 139:269–74. doi: 10.1111/j.1365-2141.2007.06731.x
8. Denk D, Nebral K, Bradtke J, Pass G, Möricke A, Attarbaschi A, et al. PAX5-AUTS2: A Recurrent Fusion Gene in Childhood B-Cell Precursor Acute Lymphoblastic Leukemia. *Leukemia Res* (2012) 36:e178–81. doi: 10.1016/j.leukres.2012.04.015
9. *Atlas Genet Cytogenet Oncol Haematol* (2020). Available at: http://atlasgeneticsoncology.org//Anomalies/del9pALLID1064.html (Accessed August 15, 2020).
10. Amaki J, Matsushita H, Kitamura Y, Nagao R, Murayama H, Kojima M, et al. The Formation of an Aberrant PAX5 Transcript in a Patient With Mixed Phenotype Acute Leukemia Harboring der(9)t(7;9)(q11.2;p13). *Leukemia Res Rep* (2016) 5:14–7. doi: 10.1016/j.lrr.2016.04.001
11. Denk D, Bradtke J, König M, Strehl S. PAX5 Fusion Genes in (7;9)(q11.2;p13) Leukemia: A Case Report and Review of the Literature. *Mol Cytogenetics* (2014) 7:13. doi: 10.1186/1755-8166-7-13
12. Pan J, Xue Y, Wu Y, Wang Y, Shen J. Dicentric (7;9)(p11;p11) Is a Rare But Recurrent Abnormality in Acute Lymphoblastic Leukemia: A Study of 7 Cases. *Cancer Genet Cytogenet* (2006) 169:159–63. doi: 10.1016/j.cancergencyto.2006.03.016
13. Shetty D, Talker E, Chaubal K, Bhat V, Narula G. dic(7;9)(p11.1;p11.1) and del(7)(q36) as a Primary Abnormality in Childhood B-Cell Precursor ALL: A Case Report. *J Assoc Genet Technol* (2019) 45:121–3.
14. Gupta A, Reddy KG, Goyal M, Karwa P, Swarupa DG, Kasaragadda MR. dic (7;9) With Loss of Tp53 Gene in Acute Lymphoblastic Leukemia. *Indian J Pathol Microbiol* (2016) 59:571–3. doi: 10.4103/0377-4929.191790

Conflict of Interest: The authors declare that the research was conducted in the absence of any commercial or financial relationships that could be construed as a potential conflict of interest.

Publisher's Note: All claims expressed in this article are solely those of the authors and do not necessarily represent those of their affiliated organizations, or those of the publisher, the editors and the reviewers. Any product that may be evaluated in this article, or claim that may be made by its manufacturer, is not guaranteed or endorsed by the publisher.

frontiers in Oncology

REVIEW
published: 01 September 2021
doi: 10.3389/fonc.2021.741746

Roles of Histone Deacetylases in Acute Myeloid Leukemia With Fusion Proteins

Juan Zhang, Xuefeng Gao and Li Yu**

Department of Hematology and Oncology, International Cancer Center, Shenzhen Key Laboratory of Precision Medicine for Hematological Malignancies, Shenzhen University General Hospital, Shenzhen University Clinical Medical Academy, Shenzhen University Health Science Center, Shenzhen, China

Accurate orchestration of gene expression is critical for the process of normal hematopoiesis, and dysregulation is closely associated with leukemogenesis. Epigenetic aberration is one of the major causes contributing to acute myeloid leukemia (AML), where chromosomal rearrangements are frequently found. Increasing evidences have shown the pivotal roles of histone deacetylases (HDACs) in chromatin remodeling, which are involved in stemness maintenance, cell fate determination, proliferation and differentiation, *via* mastering the transcriptional switch of key genes. In abnormal, these functions can be bloomed to elicit carcinogenesis. Presently, HDAC family members are appealing targets for drug exploration, many of which have been deployed to the AML treatment. As the majority of AML events are associated with chromosomal translocation resulting in oncogenic fusion proteins, it is valuable to comprehensively understand the mutual interactions between HDACs and oncogenic proteins. Therefore, we reviewed the process of leukemogenesis and roles of HDAC members acting in this progress, providing an insight for the target anchoring, investigation of hyperacetylated-agents, and how the current knowledge could be applied in AML treatment.

Keywords: HDACs, AML, leukemogenesis, epigenetic modification, oncogenic fusion protein, chromosomal translocation

OPEN ACCESS

Edited by:
Shujun Liu,
University of Minnesota Twin Cities, United States

Reviewed by:
Yushi Yao,
Zhejiang University, China
Lin Fu,
The Second Affiliated Hospital of Guangzhou Medical University, China

****Correspondence:***
Li Yu
yuli@szu.edu.cn
Xuefeng Gao
xfgao@szu.edu.cn

Specialty section:
This article was submitted to Hematologic Malignancies, a section of the journal Frontiers in Oncology

Received: *15 July 2021*
Accepted: *11 August 2021*
Published: *01 September 2021*

Citation:
Zhang J, Gao X and Yu L (2021) Roles of Histone Deacetylases in Acute Myeloid Leukemia With Fusion Proteins. Front. Oncol. 11:741746. doi: 10.3389/fonc.2021.741746

INTRODUCTION

Acute myeloid leukemia (AML) is characterized by genetic mutations and epigenetic alterations, marked by uncontrollable proliferation, blocked differentiation, and anti-apoptosis (1–3). And the majority of AML events are correlative with abnormal chromosomal translocations, which generates the oncogenic fusion genes. Mounting studies have demonstrated the central roles of fusion genes in initiating the leukemogenesis (4–6). And the successful strategies are paralleled by the decrease or degradation of chimeric proteins (7, 8). Commonly, the fusion partner in chimeric protein acts as a transcriptional protein interacting with the recruited corepressor complexes, which alters the expression of target genes that maintain the homeostasis of myeloid development, conferring the foundation of leukemic transformation (9, 10). Thereby, master the potential elements interacting with the fusion proteins is the prerequisite for targeting such oncogenic chimera.

Epigenetic modification has been acknowledged to paly crucial roles in the oncogenic transforming including AML (11, 12). Generally, epigenetic modification is not dedicated to some specific genes but serving for a vital regulator of transcriptional factors, which hold the specific capacity of DNA binding, whereby determining the potential transcriptional outcome (13–15). Thereby, the function of epigenetic modification is closely related to the cell-specific situation where the transcription factors are involved.

Accumulating evidences have been presented that epigenetic aberration prominently contribute to the leukemogenesis (16–18). As one of the major epigenetic regulators, histone deacetylases (HDACs) are indispensable in gene transcription. Dysregulation of HDACs has long been recognized as a crucial driver to hematological malignancies from initiation to metastasis, because they determine the fate of tumor cells, directing the cell to proliferate, differentiate, or be quiescent (13, 19). Therefore, the orchestration of HDACs is closely related to the cell development of both normal cells and tumor cells.

As acetyl group removers, HDACs control the accessibility of chromatin for transcription factors through switching the acetylated status, which finely tunes the transcriptional level of transcription factors and epigenetic modifiers, involving in development, cellular homeostasis, and carcinogenesis (20–22). And deregulated HDACs are associated with cell differentiation arrest, cell cycle disruption, DNA damage, and cell death (13, 23). Targeting the dysfunctional deacetylation in AML provides a promising strategy benefit for tumor treatment (24, 25). And experimental and clinical functions of HDAC inhibitors have been described by a number of reports (26–31), but the detailed mechanism acted by HDACs has not been elaborated. Comprehensively harness the roles of HDAC family members acting in leukemogenesis will provide us more precise prevision against such malignancy.

AML is frequently associated with chromatin rearrangement, including translocation and inversion, which generate oncogenic fusion proteins, among of which four most common chimeric proteins should be paid more attention, including AML1-ETO, PML-RARα, CBFβ-MYH11, and MLL-MLLT3 (4, 6, 32–34). Here we attempt to summarize the mutual interactions between HDACs and oncogenic fusion proteins involved in AML, providing a reference for the precise application of HDAC inhibitors and novel drug exploration against AML.

ACUTE MYELOID LEUKEMOGENESIS AND CLASSIFICATION

Acute myeloid leukemogenesis is a complicated progress involved in genetic and epigenetic alterations, leading to uncontrolled proliferation, arrested differentiation, and myeloid dysfunction (1, 2). And the altered genes can be subdivided into five categories (**Figure 1**): Class I mutations, activators of

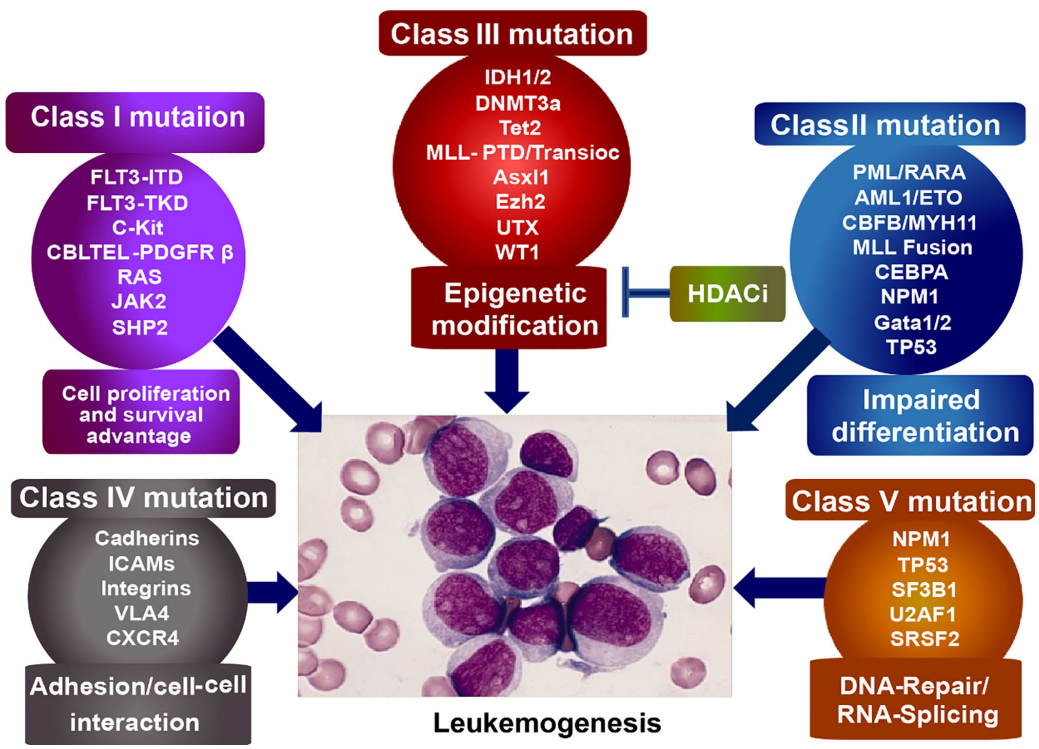

FIGURE 1 | Classification of mutagenic genes eliciting leukemogenesis. Class I mutation, provides tumor cells with survival/proliferation advantages; Class II mutation, disturbs the cell differentiation; Class III mutation, epigenetically dysregulates the tumor suppressor/activator; Class IV mutation, alters cell adhesion and cell-cell interaction, leading to the flexible motility and migration. Class V mutation, dysregulates DNA-repair and RNA-splicing.

tyrosine kinase, such as *c-Kit, Flt3*, and *BCR-ABL*, provide the hematopoietic progenitors with survival/proliferation advantage. Class II mutations, transcriptional factors such as *NPM1, CEBPA*, and *TP53* as well as oncogenic fusion genes (e. g. *AML1-ETO*, *PML-RARα*, and *CBFβ-MYH11*), arrest the differentiation of hematopoietic cells. Mutations emerging in either class I or class II do not result in leukemogenesis until the both happen to mutate. When differentiation of hematopoietic cells is hindered by Class II mutations, Class I mutations would autonomously proliferate, initiating the leukemogenesis. Class III mutations, epigenetic regulatory molecules (e. g. TET2, IDH1 and IDH2, DNMT3A, and HDACs), silence/activate the tumor suppressor genes/pro-tumor genes. And the class IV mutations involve genes that alter cell adhesion and cell-cell interaction, leading to the flexible motility and migration. Class V mutation includes genes dysregulating DNA-repair (e.g.TP53 and NPM1) and RNA-splicing (35–40). We focus on the epigenetic abnormalities of histone modification in the progression of leukemogenesis.

The subtypes of AML are majorly classified by two systems: French-American British (FAB) classification used earlier, and World Health Organization (WHO) classification, which has replaced the former (2). According to FAB classification (**Table 1**), AML can be grouped into eight subtypes from M0 to M7 based on the leukemic cell development and maturity. Among of them, M0 to M5 derived from the progenitors of white blood cells; M6 start with early forms of red blood cells; and M7 originates in the early forms of platelets (41–44).

According to WHO classification (45–50), AML is subdivided into 6 categories (**Table 2**): 1) AML with recurrent genetic abnormalities, involving in translocation, inversion, deletion, and mutation; 2) AML with myelodysplasia-related changes (MRC), a kind of multilineage dysplasia; 3) therapy-related myeloid neoplasms (t-MN), such as chemotherapy and radiation; 4) AML, not otherwise specified (NOS), including M0, 1, 2, 4, 5, 6, 7, acute basophilic leukemia, and acute panmyelosis with fibrosis; 5) myeloid sarcoma; 6) myeloid proliferations related to Down syndrome (DS). AML with recurrent genetic abnormalities

TABLE 1 | FAB subtype of AML.

FAB subtype	Stage of cell development	Percentage of adult AML patients	Prognostic stratification
0	AML with undifferentiated myeloblasts	5%	Worse
M1	AML with minimal maturation	15%	Average
M2	AML with maturation	25%	Better
M3	Acute promyelocytic leukemia (APL)	10%	Best
M4	Acute myelomonocytic leukemia	20%	Average
M4 eos	Acute myelomonocytic leukemia with eosinophilia	5%	Better
M5	Acute monocytic leukemia	10%	Average
M6	Acute erythroid leukemia	5%	Worse
M7	Acute megakaryoblastic leukemia	5%	Worse

TABLE 2 | WHO classification of AML.

WHO classification of Acute myeloid leukemia (AML)				
AML-associated oncofusion proteins				
Chromosomal translocation	**Oncofusion protein**	**Frequency of occurrence**	**Prognosis**	**FAB**
t (8,21)(q22;q22)	AML1-ETO	10-15%	Favorable	M2
t (15,17)(q22;q21)	PML-RARαβ	6-15%	Favorable	M3
inv (16)(p13q22)	CBFb-MYH11	3-10%	Favorable	M4
der(11q23)	MLL-fusions	5-8%	Variable	M4/M5
t (9,22)(q34;q11)	BCR-ABL1	1-2%	Adverse	M1/M2
t (6,9)(p22;q34)	DEK-NUP214	<1	Adverse	M2/M4
t (1,22)(p13;q13)	RBM15-MKL1	<1	Intermediate	M7
t (8,16)(p11;p13)	MYST3-CREBBP	<1	Adverse	M4/M5
t (7,11)(p15;p15)	NUP98 -HOXA9	<1	Intermediate	M2/M4
t (12,22)(p12;q11)	MN1-TEL	<1	Variable	M4/M7
inv (3)(q21;q26)	RPN1-EVI1	<1	Adverse	M1/M2/M4/M6/M7
t (16,21)(p11;q22)	FUS -ERG	<1	Adverse	M1/M2/M4/M5/M7

AML with mutations

NPM1; CEBPA (biallelic mutation); RUNX1; myelodysplasia-related changes; Therapy-related myeloid neoplasms

AML, not otherwise specified (NOS)

Undifferentiation; Minimal maturation; Maturation; Acute myelomonocytic leukemia; Acute monoblastic and monocytic leukemia; Pure erythroid leukemia; Acute megakaryoblastic leukemia; Acute basophilic leukemia; Acute panmyelosis with myelofibrosis; Myeloid sarcoma

Myeloid proliferations associated with Down syndrome
Transient abnormal myelopoiesis (TAM) associated with Down syndrome
Myeloid leukemia associated with Down syndrome

contains balanced translocation/inversion, and mutation. The balanced translocations include t (8,21) (q22;q22.1) (AML1-ETO); inv (16) (p13.1q22)(CBFβ-MYH11); t (9,11)(p21.3;q23.3) (PML-RARα); t (6,9) (p23;q34.1) (KMT2A-MLLT3); inv (3) (q21.3q26.2)(DEK-NUP214); t (1,22)(p13.3; q13.1) (Gata2, Mecom); Rbm15-MKL1, and Bcr-Abl1. Here we will discuss the four most common fusion proteins involved in AML, focusing on the roles of HDACs functioning in the fusion proteins.

HDACs CLASSIFICATION AND FUNCTIONS

Nucleosome, constituting the fundamental units of chromatin, is an octamer polymerized by four types of histones (H2A, H2B, H3, and H4), wrapped by 146 base-pair DNA. Each histone contains a structural domain and an unstructured tail of 25-40 amino acid residuals, which can be altered *via* post-translational modification, including acetylation, methylation, phosphorylation, and ubiquitination (51, 52). And the modification of histone residuals will determine the chromatin accessibility to transcription factors, keeping them activated or silent. Thereinto, the homeostasis of acetylation generally depends on the dynamic regulation of histone deacetylases (HDAC) and histone acetyltransferases (HAT) (53, 54).

HDAC and HAT play opposite roles in the epigenetic modification of chromatin, especially the histone proteins, where HATs allow the chromatin relaxed for gene transcription, and HDACs condense the chromatin making it inaccessible for transcriptional factors (**Figure 2**). HAT transfers the acetyl group from acetyl coenzyme A to lysine residual of histone N-terminal with positive charge, which binds to DNA strand with negative charge and prevents the chromatin from being condensed, thereby keeping the chromatin loosened available for the binding of transcription factors with DNA. Oppositely, HDACs favor to compact the chromatin, preventing the gene transcription. They remove the acetyl group from histone tail, and subsequently condense the chromatin, resulting in transcriptional inhibition (55–57). Therefore, the dysregulation is inevitable when the balance is disrupted between HDACs and HATs.

HDACs are universally spread in eukaryotes, which belong to a superfamily composed of 18 proteins with conserved deacetylase domain (21, 23). Based on the phylogenetic analysis, sequence homology to yeast protein, and domain organization, these proteins can be categorized into four

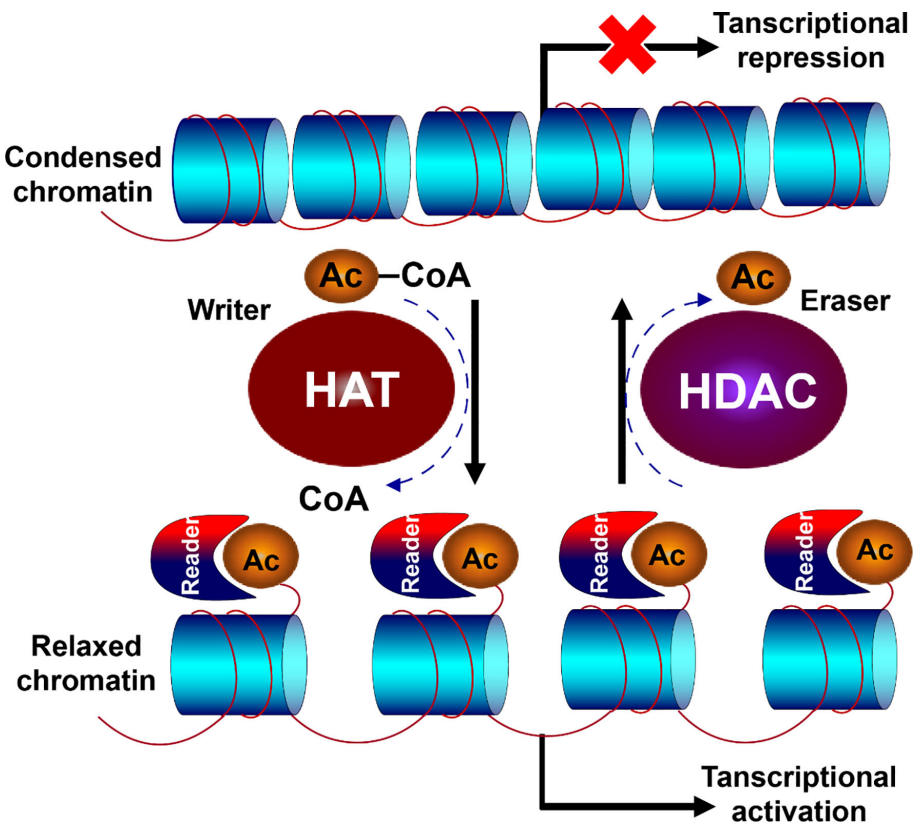

FIGURE 2 | Opposite function of HDACs and HATs. HDAC and HAT play opposite roles in the epigenetic modification of chromatin. HAT transfers the acetyl group from acetyl coenzyme A to lysine residual of histone N-terminal with positive charge, which binds to DNA strand with negative charge and prevents the chromatin from being condensed, allowing the chromatin relaxed for gene transcription. Oppositely, HDACs remove the acetyl group from histone tail, and subsequently condenses the chromatin, resulting in transcriptional inhibition.

families (class I, IIa, IIb, III and IV) (**Figure 3**). Three of them contain the Zn^{2+} dependent catalytic domain, which are referred to as classical HDACs, and class III members are NAD^{+}-dependent, called sirtuins, which possesses deacetylase activity but is unrelated to HDACs, and will not be involved here. Distinguished by structure, enzymatic function, and localization, they display similar and specific functions during the regulation of gene expression (13, 21, 58).

Class I HDAC family is consist of HDAC1, 2, 3, and 8, which are homologous to yeast protein reduced potassium dependency-3 (Rpd3) (21, 59). They are chiefly expressed in nuclear, consisted by classic deacetylase domain, nuclear localization signal, showing high enzymatic activity to their substrates. Approximately 400 amino acids consist of each member, the catalytic domain contains two histidine residues, two aspartic acid residues and one tyrosine residue with Zn^{2+}. And they generally function as gene transcriptional repressors. For instance, HDAC1 and HDAC2 bear closely identical structure and similar function, and usually work together in the repressive complexes, such as corepressor for element-1-silencing transcription factor (CoREST), nucleosome remodeling and deacetylase (NuRD), and transcription regulator family member switch-independent 3 (Sin3) complexes. HDAC3 generally emerges in another type of repressive complexes, such as N-CoR–SMRT complex. HDAC8 has been described to cooperate with SMAD3/4 complex, promoting the cell proliferation and migration (60–65).

According to the number of catalytic domains, Class II HDAC family can be subdivided into Class IIa (HDAC4, 5,7, 9) and Class IIb (HDAC6, 10), which can shuttle between nucleus and cytoplasm (66, 67). Class IIa HDAC members are grouped by a functionally important N-terminal domain, which mediates DNA-binding and nuclear-cytoplasmic shuttling. HDAC trafficking is regulated by nuclear export signal (NES) and binding sites for14-3-3 proteins. Upon 14-3-3 protein binding, cytoplasmatic retention or nuclear export of class IIa HDACs will be stimulated depending on the phosphorylation of 14-3-3 binding sites, which can be

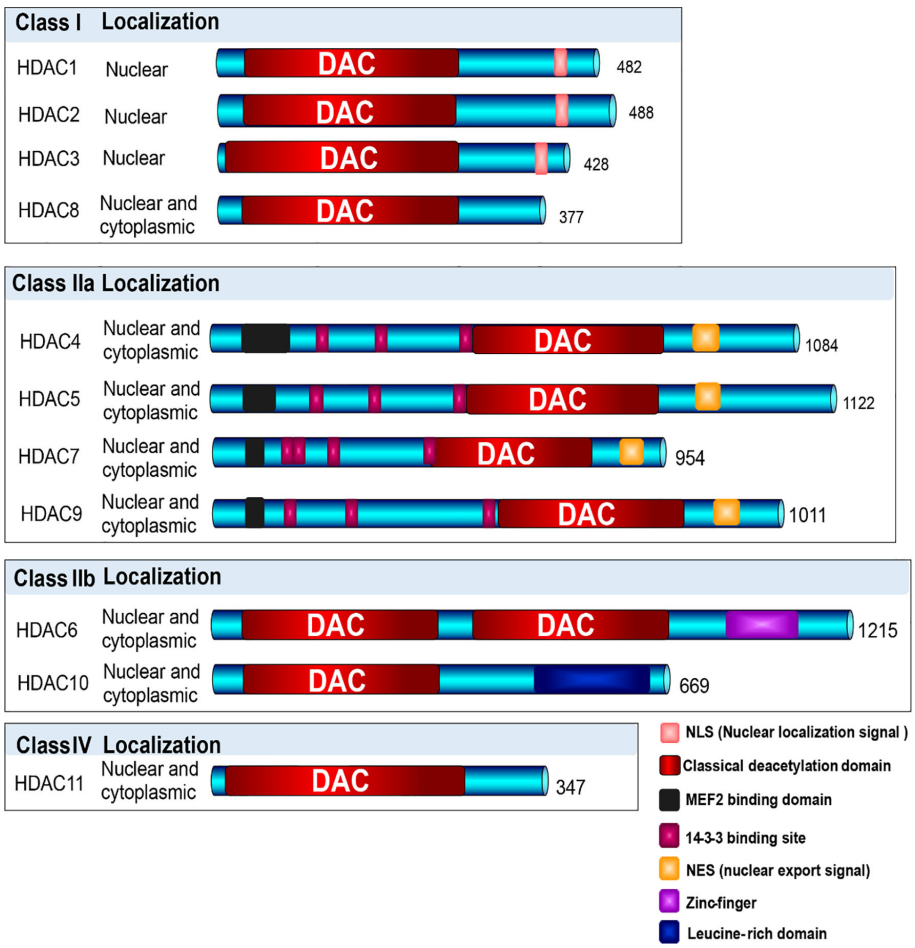

FIGURE 3 | Classification of HDACs. Based on the phylogenetic analysis, sequence homology to yeast protein, and domain organization, HDAC enzymes are categorized into four families (class I, IIa, IIb, III and IV). Three of them contain the Zn^{2+} dependent catalytic domain, which are referred to as classical HDACs, and class III members are NAD^{+}-dependent, which were not involved in this description. Class I HDACs contains HDAC1, 2, 3, and 8, which majorly localize in nuclear; Class II HDACs include Class IIa (HDAC4, 5, 7, 9) and Class IIb (HDAC6, 10), which shuttle between nuclear and cytoplasm; and Class IV contains only HDAC11, shuttling between nuclear and cytoplasm.

regulated by protein kinase-D, Ca^{2+}/calmodulin-dependent kinases (CaMKs), and checkpoint kinase-1 (CHK1). And subsequently the transcriptional repressors will be regulated *via* binding with myocyte enhancer factor 2 (MEF2) binding domain, conferring signal responsiveness to downstream genes. When bound with Class IIa HDACs, MEF2 makes them a transcriptional repressor, whereas bound with HATs p300, MEF2 then converted them into a transcriptional activator. And the deregulated balance of HDAC and HAT will subsequently lead to diseases (68–71). Class IIb HDACs are atypical ones. HDAC6 contains two deacetylase domains and a C-terminal zinc-finger, which functions as a major cytoplasmic deacetylase targeting alpha-tubulin and HSP90, regulating cell motility, adhesion, and chaperone function (72, 73). Besides, binding with ubiquitin *via* zinc finger domain HDAC6 can regulates the aggresome formation, autophagy, heat shock factor-1 (HSF-1), and function of platelet derived growth factor (PDGF) (74, 75). HDAC10 holds single deacetylation domain and a leucine-rich domain. It possesses properties of immunoregulator, against the tolerogenic molecule PD-L1, implying an epigenetic target for immunotherapy. Overexpression of HDAC10 has been demonstrated to accelerate the progress of carcinogenesis. Deletion of HDAC10 in antigen-presenting cells (APCs) can increase the expression of MHC class II molecules and repress the transcription of PD-L1, which is associated with enhancement of immune system (76–79).

HDAC11, as the sole member of Class IV HDAC family, structurally similar to class I and II, mainly distributes in nucleus and acts as a repressor of IL-10 (80). It can regulate the dynamic balance between immune activation and tolerance. Upregulation of HDAC11 has been shown in various cancer cells (81, 82).

Besides, an increasing number of non-histone proteins have been identified as substrates of HDACs, such as p53, Stat3, Hsp90, GATA1, Tubulin, and β-catenin, which display vital roles during the progress of carcinogenesis (83–85). *Via* deacetylation, HDAC1 can affect the stability of tumor suppressor gene p53, arresting the interaction with DNA, inverting the function of p53. HDAC1 can also directly lead to the deacetylation of GATA1, repressing the gene transcription. HDAC6 is associated with the modulation of Akt and Stat3 signaling *via* regulation of Hsp90 acetylation in multiple myeloma cells. Deletion of HDAC6 will result in reducing phosphorylation of Stat3, which results in related genes inactivation (22, 86, 87).

Taken together, HDACs participate in the regulation of key transcriptional factors involving in the gene transcription, cell apoptosis, cell cycles, and signal transduction, which depicts the pivotal roles of HDACs functioning in epigenetic modification and gene transcription. The histone modification determines the accessibility of chromatin, which will make genes activated or silent. Inevitably, dysregulated histone modification will lead to dysfunctional cell development, which is strongly associated with carcinogenesis. Disruption of specific HDACs usually associates with dysregulation of differentiation, proliferation, migration, chemotherapy resistance, and angiogenesis (**Figure 4**). Overexpression of HDAC usually emerges accompanying with leukemogenesis and the other tumor. They act to close the nucleosomes, inhibiting the expression of tumor suppressor genes. HDAC inhibitor, as an agonist of HDAC, can alter the abnormal hypoacetylation level of histone, and subsequently elicits cell differentiation and apoptosis, demonstrating the indispensable roles of HDACs in tumorigenesis (88–91). Harnessing the function of HDACs is the premise indicating to precisely target the master alterations.

HDACs IN LEUKEMOGENESIS

Although HDAC mutations in AML are relatively rare compared to solid tumors, HDAC proteins are abnormally recruited to oncogenic fusion proteins, such as AML1-ETO, CBFB-MYTH11, PML-RARα, and MLL-fusions, which function as vital roles in onsetting and promoting the progress of leukemogenesis (4, 13, 31). And HDAC inhibitors, as a series of compounds that neutralize the activities of HDACs, have long been utilized in treatment of AML for pre-clinical studies, which have some extend shown beneficial outcomes (26, 27, 30, 31). And the multiple functions of HDAC inhibitors have been discussed in numerous research articles and reviews (which will thereby not be included in this review). However, the mutual interaction between HDACs and AML has not been comprehensively described. And we choose the most frequent events of chromosomal translocation emerging in AML to elucidate the reciprocal functions of AML and HDACs.

HDACs IN AML WITH AML1-ETO

One of the well-studied AML subtypes is t (8, 21) AML, which occurs in approximately 10-15% of total AML cases, and 18-40% of M2 AML (92–95). The translocation is generated by the fusion of AML1 gene (Runx1) on 21q22.1 and ETO gene (Runx1T1) on 8q22, leading to the forming of AML1-ETO fusion protein (5, 34, 96). It can invert the original function of AML1, performing opposite function during the leukemogenesis. The fusion protein AML1-ETO provides the DNA-binding domain *via* the hematopoietic master regulator AML1 and transcriptional domain *via* ETO, targeting the AML1 target genes. It substitutes the original function of AML1 and disrupts cellular processes involved in the myeloid proliferation, differentiation, and genome stability (95, 97, 98).

To understand the mutual interactions between AML1-ETO and HDACs in detail, we firstly figure down the functions of AML1 and ETO in normal condition and AML1-ETO in tumorigenic environment. AML1 functions as a master organizer, which in charge of regulating the hematopoietic specific promoters and enhancers. It widely spreads in hematopoietic system, cooperating with multiple lineage-specific transcriptional regulators, such as the driving of endothelial hematopoietic transition (99, 100). AML1 gene on 21q22 is composed of nine exons, with three breakpoint cluster regions (BCR) in intron5. The structure of AML1 is composed of

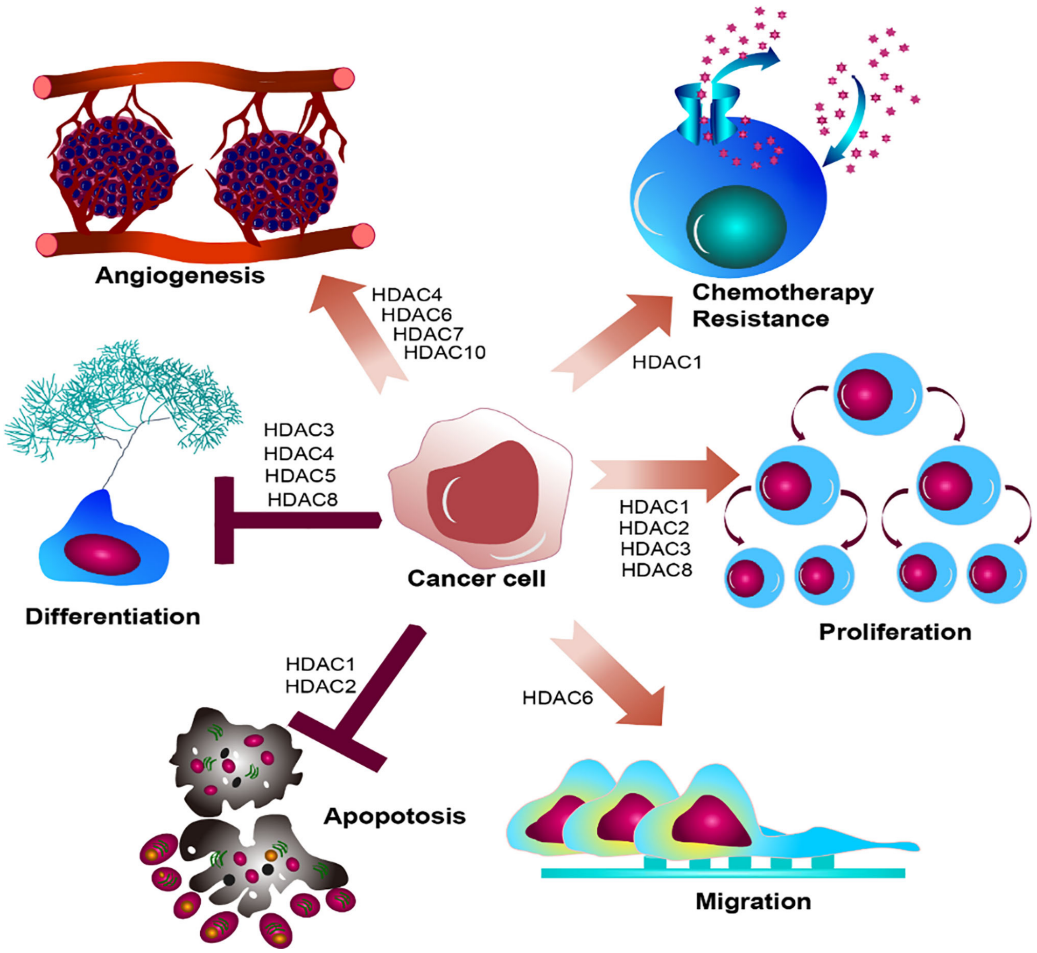

FIGURE 4 | Summary of HDACs functioning in cancer cell. HDAC family members determine biological effect of oncogenic hallmarks emerging in cancer cell, disrupting the regular cell development in cancer cell, leading to dysregulated differentiation, proliferation, migration, chemotherapy resistance, and angiogenesis.

conserved runt homology DNA binding domain (RHD), activation domain (AD), nuclear matrix-targeting signal (NMTS), proline-rich domain (PY), two inhibitory domains (ID), and an additional C-terminal motif with five amino acid (VWRPY), working as a recognition and recruitment signal for Groucho/TLE family. Besides, it contains two promoters: distal promoter P1 and proximal promoter P2. Both promoters include the AML1-binding sties, which can be regulated by itself and other AML1 transcriptional factors. RHD is in charge of recognizing and binding to DNA sequences, and localizing the AML1 transcriptional factors in nucleus. It also contributes to the binding of core biding factor β (CBFβ), which does not interact with DNA, but increases the α subunit affinity to DNA binding and stabilizes the complex (**Figure 5A**) (101–103).

AML1 functioning as an activator or repressor is determined by its interaction with corresponding transcriptional factors and co-factors, rather than itself features (95, 104, 105). It has been shown to interact with various chromatin modifiers and remodelers (**Figure 5B**). For instance, its activation can be stimulated by binding with lysine acetyl transferase MOZ (MYST3), and the same to transcriptional co-activators P300 and CBP. They function as integrators, which bind with AML1 and other transcriptional activators driving the hematopoietic promoters (106). ALY expressed in nucleus can bind to the activation domain of AML1, forming multimers and bridging the interaction of AML1 and other transcription factors. c-Yes tyrosine kinase associated protein (YAP) binds to PPPY motif in the AML1 C-terminal activation domain, enhancing the activity of AML1 (105, 107, 108).

Furthermore, AML1 may function as a repressor of HDAC complex (15). Researches have demonstrated that it can inhibit the transcription of p21 *via* binding the promoter of p21 with AML1 VWRPY Groucho/TLE interaction domain. Through binding with co-repressors such as Sin3A and Groucho/TLE, it recruits HDACs to repress the transcription (15). And the HDAC inhibitor Trichostatin A can impair such suppression, demonstrating that HDACs contribute to AML1-mediated inhibition. It is also associated with HDAC1, 2, 3 and histone H3 lysine 9 methyltransferase SUV39H1 (KMT1A), leading to transcriptional suppression. In myeloid cells, AML1 binding

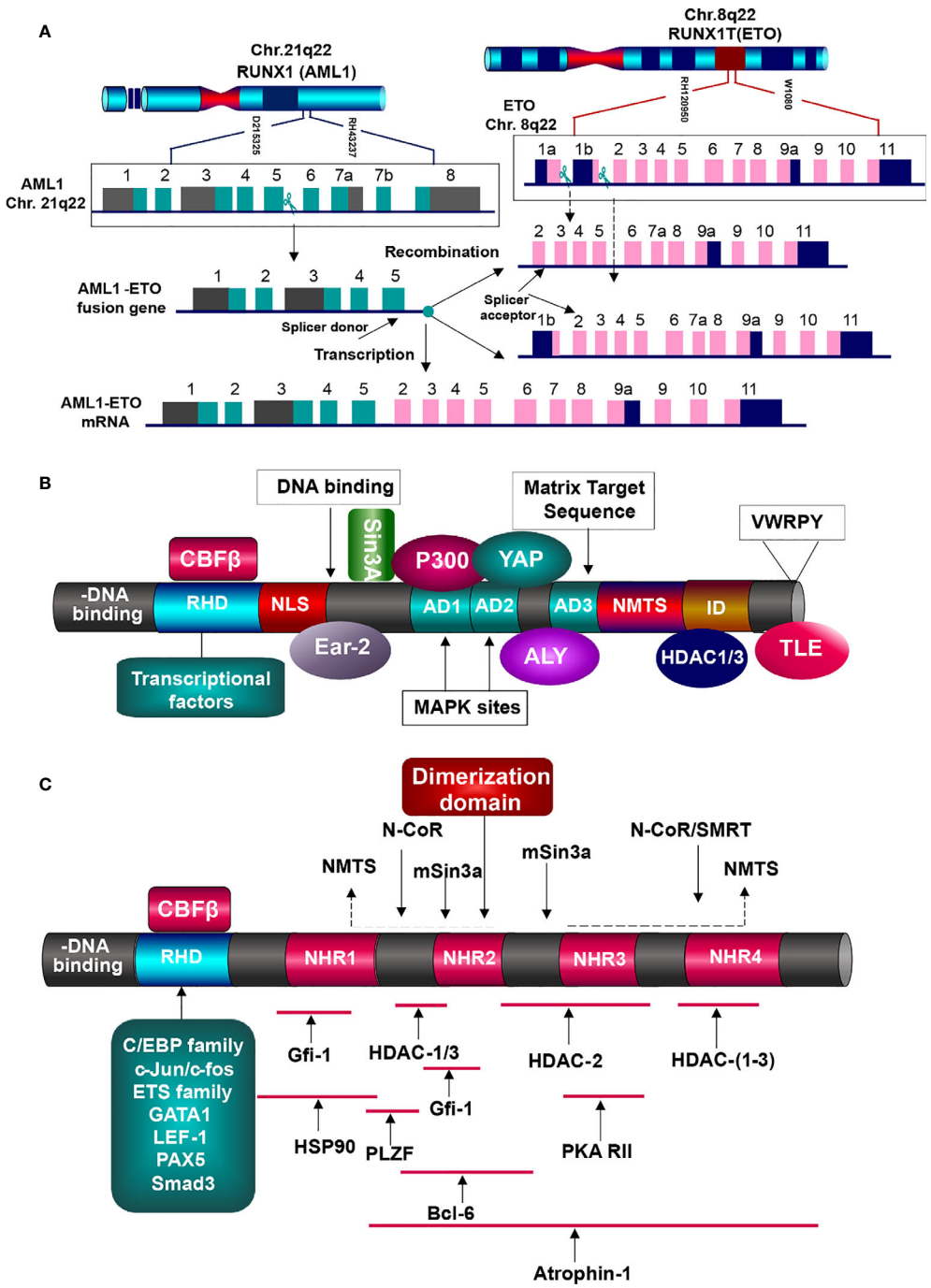

FIGURE 5 | Generation and function of AML1-ETO fusion protein. **(A)** Generation of AML1-ETO. ETO gene on Chr.8q22 is consist of 13 exons, containing two breakpoints, but one splicer acceptor in exon2. AML1 gene is made up of nine exons with one breakpoint and one splicer donor. Absence of splicer acceptor in exon1b, the two genes generate the only fusion mRNA. **(B)** AML1 protein structures and partner proteins. AML1 is composed of DNA-binding domain (RHD) and other domains related to signal transduction, transcriptional factors binding, epigenetic modifiers interaction, and TLE co-repression, which can interact with HATs (MOZ, CBP, and p300) and HDACs (HDAC1, 2, and 3), resulting in gene activation or inhibition. HATs, histone acetyltransferases; HDACs, histone deaccetylases; RHD, runt homology domain; NLS, nuclear localization signal; AD, activation domain; NMTS, nuclear matrix targeting signal; ID, inhibitory signal; VWRPY sequence. **(C)** AML1-ETO fusion protein and the interacting partners. AML1 contributes the DNA-binding domain RHD, which binds with various transcription factors, but lacks of domains to elicit regular functions. And nearly whole of ETO structure is involved in the fusion, including the four NHRs. They interat with corepressive complexes, HDACs, and other molecules, initiating the oncogenesis.

with CCAAT/enhancer binding protein alpha (C/EBPα) and PU.1 can activated the macrophage colony-stimulating factor receptor (M-CSFR) expression (104, 109).

Meanwhile, AML1 can also been inhibited by corresponding transcription factors. For instance, bound with forkhead box P3 (FOXP3), it can suppress the expression of interleukin2 (IL2) and interferon gamma (IFN-γ) in T regulatory cells. It is multifunctional in the regulation of hematopoiesis, including cell differentiation, proliferation, and apoptosis. And the aberration of AML1 will speculatively deregulate the normal cellular development, which is involved in carcinogenesis (15, 109).

Eight-twenty-one (ETO) gene on 8q22 is consist of 13 exons, with one BCR in intron1a and three BCRs in intron1b, which generate different variants but create the same fusion gene AML1-ETO, because it supplies only one splice acceptor in exon2, as the exon1b lacks of splice acceptor (104, 110). ETO protein possesses three proline-serine-threonine (PST)-rich regions and four conserved nervy homology regions (NHR), involved in neuronal development of Drosophila embryos. The PST-rich domains contain multiple potential kinase phosphorylation sites (SP and TP). NHR1 is homologous to the Drosophila TATA-box-associated factors, including TAF110. NHR2 domain, containing a hydrophobic amino-acid (a.a.) heptad repeat, plays crucial role in the oligomerization between ETO family members, forming homo-/hetero-dimerization. NHR3 is with predicted coiled-coil structure. NHR4 is homologous to myeloid-Nervy-DEAF1 (MYND) homology domain, with two predicted zinc-finger motifs, which is required for the protein-protein interaction. For instance, ETO is associated to the co-repressors mSin3 and nuclear receptor corepressor (N-CoR), thyroid hormone receptor (SMRT), as wells as HDAC1, 2, 3. Via binding with NHR4 DNA binding domain, it can interact with the co-repressors N-Cor, SMRT, and mSin3A, which will then tether the DNA-binding proteins to HDACs, resulting in repressive transcription (105, 111). Researches have shown that ETO and AML1-ETO can pull-down by HDAC activity *via* Co-IP, bearing out the repressive role of AML1-ETO through the recruitment of HDACs to AML1 target genes (112). Such function may instead of AML1 complex which originally worked as an activator involving in the histone acetyl transferases p300/CBP. It is similar to the leukemogenic mechanism of APL. Fusion proteins PML/PLZF-RARα increase the affinity of RARα to co-repressors and RARα target genes (113). It also interacts with Atrophin-1, chaperon heat-shock protein (HSP90), PLZF, Gfi-1, and Bcl-6, functioning as a corepressor of transcriptional factors. Via NHR1 and NHR2, ETO can binds to Gfi-1 and Gfi-1b, contributing to the recruitment of HDACs, which subsequently repress the activity of Gfi-1/Gfi-1b proteins (111, 112, 114). Depending on the DNA binding site provided by RHD of AML1, AML1-ETO may perform as a repressor or activator of the AML1 target genes (115).

In AML1-ETO fusion protein, the important features of AML1 are lost: 1) the c-terminal activation domain interacting with co-activators; 2) domains in charge of binding with co-repressors such as Sin3 and TLE; NLS domain functioning as nuclear matrix-targeting signal. And such lost will subsequently result in the dysregulation of hematopoiesis. The AML1-ETO fusion protein can affect the expression of both AML1 target genes and other related genes. As a part of AML1-ETO, AML1 recruits HDACs to the promoter, which suppress the expression of relative target genes. In normal, these target genes are required for regulating cell growth and preventing hemopoietic cells from transformation. And abnormally, the target genes are suppressed and lose their control, leading to cell overgrowth (107).

In t (8,21) AML, a number of genes critical to normal hematopoiesis are up-regulated by AML1, while AML1-ETO disrupts such trans-activation. AML1–ETO fusion protein recruits various transcriptional factors, epigenetic modifiers such as HDACs, PRMT1, and p300, forming the first aberration vital for the t (8,21) AML onset (13). And then it can collaborate with the secondary mutations including c-Kit, FLT3, and RAS. Via recruiting the HDAC1, 2, 3, AML1-ETO can silence the target genes and block the cell differentiation and transformation (95, 116). AML1 contributes the DNA binding domain RHD to a number of transcriptional factors (such as Ets-1, LEF-1, C/EBPα, PU.1, MEF, Pax5, and GATA1) and epigenetic modifiers, but defaults the subsequential elements for activation, which are replaced by nearly entire ETO. The well-known binding protein of AML1 is CBFβ, which efficiently binds to RHD of AML1 and is required for the its full transcriptional activation (**Figure 5B**) (117, 118).

HDAC1 is a binding partner of AML1 that takes part in the forming of corepressor complex with nuclear receptor corepressor (N-CoR) and mammalian Sin3 (mSin3A and B) (119, 120). And ETO can bind to the central domain of N-CoR, generating the AML1-ETO/N-CoR/mSin3/HDAC1 complex, remodeling of chromatin structure and transcriptional suppression, dysregulating the normal hematopoiesis (26, 121). Additionally, the substrates of HDACs are not only histone but also non-histone proteins, such as oncogenes, tumor-suppressor genes, and chaperones. One of the presentative tumor suppressors is TP53. Specifically interacting with TP53, HDAC1 combined with the corepressor complex can mediated its deacetylation, and subsequent degradation. As a classical tumor suppressor, TP53 is crucial to the process of hematopoiesis. The alteration of TP53 is associated with the AML progress and therapy responsiveness, and generally predicts poor prognosis (9). Although its mutation frequency is relatively low in AML (less than 10% of *de novo* AML cases) compared to solid tumors (more than50% of cases), the function of TP53 in AML could not be ignored, as dysfunctional wild-type (WT) TP53 appears in various AML entities, implying a more attention to be paid (122).

HDAC2 are nearly identical to HDAC1, and usually work together in repressive complexes, such as nucleosome remodeling and deacetylase (NuRD), switch independent 3 (Sin3), and corepressor of RE1 silencing transcription factor (CoREST) complexes. Inhibition of HDAC1 and HDAC2 leads to down-regulation of RAD51, BRCA1, and CHK1, which are crucial for the DNA damage response (DDR) and subsequent DNA double-strand break and apoptosis in AML cell lines. And AML-1-ETO can bind with HDAC1, 2, and 3 to repress the

AML1 target genes in t (8,21) AML (123). And HDAC6 deacetylates the chaperone Hsp90, eliciting the interaction with AML1-ETO protein, which can be dissociated by HDAC inhibitors that mediates the degradation of AML1-ETO protein.

HDAC11 may display a role in the immune system by regulating the immune cells. Antigen-presenting cells (APCs) plays critical role in T cell activation and tolerance, which is associated with HDAC11 (80). Up-regulation of HDAC11 can repress the expression of IL-10, and subsequently induce the APCs inflammation, which will prime naïve T cells and reactivate the response of tolerant $CD4^+$ T cells. Meanwhile, down-regulation of HDAC11 in APCs promotes the expression of IL-10 and impairs the T cell response. Therefore, HDAC11 may act as a decider in the immune activation and tolerance, implying the substantial role of HDAC11 in the immunotherapy, involving in AML (80).

HDACs IN AML WITH CBFβ-MYH11

The inv (16) translocation emerges in 8-10% of AML patients, which is associated with M4Eo AML. It is produced by the chromosomal breakpoints within core binding factor beta (CBFB) gene on 16q22 and smooth muscle myosin heavy chain gene (MYH11) gene on 16p13, encoding corresponding proteins: CBFβ and smooth muscle myosin heavy chain (SMMHC). And the oncogenic gene CBFB-MYH11 and fusion protein CBFβ-SMMHC will subsequently generated and arrest the differentiation of hematopoietic cells. Similar to AML with AML1-ETO, the original disorder of AML with CBFB-MYH11 derives from the disruption of hematopoietic function performed by the core binding factor (CBF).

CBF, as a heterodimer, is composed of CBFα (DNA-binding subunit) and CBFβ (partner of CBFα) (124). CBFα subunit is encoded by CBFA2 that is known as RUXN1 or AML1 gene. CBFβ does not directly bind with DNA, but enhances the affinity of CBFα to DNA, stabilizing the CBFα-DNA complex. CBFβ-SMMHC fusion protein displays a higher affinity to AML1 binding than wild type CBFβ. Additionally, it contains an additional AML1-binding domain in SMMHC portion. Therefore, AML1 is preferential to bind with CBFβ-SMMHC, which competes the RUNX1-binding site with CBFβ, resulting in the blocks of AML1 function and enhancement of the SMMHC activity. The dysregulation of CBFβ acts an indirect factor disrupting the function of AML1, whose pivotal functions in hematopoiesis has been described in t (8,21) AML. Both CBFA2 and CBFB genes are indispensable for the development of normal hematopoiesis, deletion of either gene will disrupt the definitive hematopoietic stem cells. CBFβ-SMMHC protein interacts with the pivotal transcription factor AML1, sequestering the normal essential hematopoietic function of AML1. It acts as a transcriptional repressor, interacting with transcriptional inhibitors and HDACs, repressing the transcription of corresponding genes.

HDAC1 is a binding partner of AML1. And further research showed that HDAC1 can bind to CBFβ-SMMHC complex, which colocalizes with the promoters of AML1 and CBFβ-SMMHC. As a key cofactor, HDAC1 participates in the forming of AML1: CBFβ-SMMHC complex, which is essential for the transcriptional activity of related genes, involving in leukemic cell differentiation block and pro-proliferation (125). Additionally, pharmacologic inhibition of HDAC1 contributes to the suppression of leukemogenesis with CBFβ-SMMHC (126, 127). And *in vivo*, it can decrease the mouse leukemic burden, showing an effective role of HDAC1 targeting the CBFβ-SMMHC protein (30).

HDAC8, as another member of class I HDAC, has been demonstrated to interact with CBFβ-SMMHC protein. Besides, it can also reduce the acetylation of P53, which is bound to CBFβ-SMMHC protein, and subsequently promote the transformation of CBFβ-SMMHC-related leukemic stem cells. And inhibition of HDAC8 will induce the apoptosis in inv (16) AML (128, 129).

HDACs IN ACUTE PROMYELOCYTIC LEUKEMIA WITH PML-RARA

The t (15,17) (q24;q21) translocation accounts for 10%-15% of acute promyelocytic leukemia (APL) issues. It is derived from the fusion of promyelocytic leukemia (PML) gene on 15q24 and retinoic acid receptor alpha (RARA) gene on 17q21, which is critical for the cellular transformation (130, 131).

PML gene is composed of nine exons that produces some alternative spliced transcripts variants, which share the N-terminal region, containing the RING-B-Box-Coiled-coil/tripartite motif (RBCC/TRIM) domain (132). Due to the alternative splicing, the isoforms of PML are different in central or C-terminal regions and the longest one is PML1, which harbors a nuclear export signal (NES) domain. In normal, PML mainly functions as a tumor suppressor. It can interact with over 170 proteins, most of which are mediated by the RBCC/TRIM domain leading to PML multimerization and organization or by other isoform-specific domains of PML. Conferred by these different binding interactions, PML is involved in proliferation and self-renewal of hematopoietic stem cells, epigenetic regulation in hematopoiesis, and p53-dependent/independent apoptosis and senescence (122). In addition, it is necessary for the formation of nuclear body (NB), which is associated with the protein release and sequestration, posttranscriptional modification, and promotion of nuclear issues (133).

RARA gene is consist of 10 exons producing two isoforms (RARA1 and RARA2) that are belonged to nuclear hormone receptor superfamily, acting as a nuclear transcriptional factor when retinoids are present, which is essential for the promyelocyte differentiation (130, 134). The RARA protein can interact with retinoid X receptor protein (RXRA), generating a heterodimer that acts as a transcription activator to bind with retinoic acid response elements (RARE). In the presence of ligand (all-trans retinoic acid (ATRA) or 9-cis retinoic acid), RARA binds to RXRA forming a heterodimer, which can interact with retinoic acid responsive elements (RARE). In the absence of ligand, RAR-RXR heterodimer recruits the transcriptional

corepressors, such as HDACs, Sin3, SMRT, and N-CoR, keeping transcriptional repression, which can be dissociated when ligand emerges (135). In normal, RARA is ligand-dependent determining the transcriptional switch, which is critical for the differentiation of normal myeloid hematopoietic cells (134). In APL, the fusion protein PML-RARA alters the function of PML and RARA, disrupting the nuclear structure and blocking the cell differentiation. Additionally, PML-RARA provide leukemic cells with a survival and proliferative advantage, leading to the superiority accumulation of tumor cells in APL (130). Besides, through inducing the deacetylation of p53, PML-RARA fusion protein can directly suppress the activity of p53, conferring leukemic blasts to escape from p53-dependent cancer surveillance. And such phenomenon is realized by the recruitment of HDACs to PML-RARA complex, which can result in the deacetylation of p53 (136, 137).

PML–RARA recruits HDACs leading to RARs suppress the transcription of RA target genes, which displays a central role in the oncogenic transformation of APL (132). The aberrant recruitment of HDACs induced by PML–RARA contributes to the differentiation blocks and accumulation of APL blasts, because it inappropriately represses the RAR target genes. RA functioning as a therapeutic agent is based on the mechanism that RA can lead to the dissociation of PML–RAR/HDAC complex and degradation of such fusion protein (138, 139). Furthermore, ATRA resistance can be neutralized by HDAC inhibitors (140), which should have been paid more attention. Deregulated HDAC3 acts as a crucial role in the progress of acute promyelocytic leukemia (APL) with PML-RARα fusion protein. HDAC4 can interact with the PLZF-RARα fusion protein, mediating the differentiation arrest (141, 142).

HDACs IN AML WITH MLL-MLLT3

The t (9,11) AML presents in 3-5% of AML events, generated by the fusion of mixed lineage leukemia (MLL) gene on 11q23 and mixed lineage leukemia translocated to chromosome 3 (MLLT3) gene on 9p22, producing the fusion protein MLL-MLLT3 (143, 144).

MLL gene is made up of 14 exons, encoding the histone lysine methyltransferase whereby it is also called KMT2A, which harbors powerful transforming potential associated with neoplastic diseases assisted by specific partners, such as AF9 (MLLT3), AF4, and ENL (MLLT1) (145). It orchestrates various facets of cell development, including cell fate determine, stem cell maintenance, and embryogenesis. MLL protein contains multiple conserved domains with specific functions: 1) three AT hooks domains in the N-terminal of MLL mediating itself to bind with minor groove of DNA with AT-rich; 2) a transcriptional repressive domain that is composed of cysteine-rich CXXC DNMT (DNA methyltransferase1) homology region, which can bind to unmethylated CpG islands; 3) four plant homeodomain (PHD) fingers that mediate the protein-protein interactions; 4) a transactivation domain that is employed to interact with CBP/p300 complex; 5) SET [Su(var)3–9, enhancer of zeste, and trithorax] domain in C-terminal, serving as a histone H3 methyltransferase. Carrying along with such multiple domains, MLL can generate complexes with various partners, such as tumor suppressor Menin (multiple endocrine neoplasia), cell cycle regulator E2Fs, and HDACs (146, 147).

Overexpression of HDAC1, 2, and 3 is frequently found in leukemia (13). They can interact with MLL fusion protein leading to dysregulated chromatin remodeling, which could be neutralized by chidamide (148). Targeting MLL dysfunction by HDAC inhibitors such as vorinostat and panobinostat may counteract the aggressive resistance in MLL-fusion leukemia (149). And mocetinostat, a class I HDAC inhibitor, can inhibit the HOXA9 expression in AML with MLL-AF9 (147). Researchers have purified the stable MLL complex, where HDAC1 and HDAC2 were found. Additionally, they have also demonstrated that the repressive domain of MLL can specifically bind with HDAC1 and HDAC2, which can be partially released by HDAC inhibitor TSA but not RD1domain, which implies that additional cofactors are involved in the complex to fully perform the repressive function. And through binding to PHD fingers, Cyp33 can increase the affinity of MLL to HDAC1. Hypoacetylated histone in chromatin is frequently involved in transcriptionally repressive status (148, 150, 151).

CONCLUDING REMARKS

HDACs serving as the pivotal epigenetic modifier of chromatin determine the chromatin accessibility to transcriptional factors, which is essential for specific gene transcription and oncogenic transformation. And the same to hematopoiesis, function of HDACs is indispensable, which determines the fate of hematopoietic cells, going through self-renewal, proliferation, differentiation, or apoptosis, terminating in various cell lineages (13, 14, 20). Thereby, dysregulation of HDACs inevitably leads to disruption of hematopoiesis (25, 91). It is necessary to concentrate on the investigation of HDACs functions.

The vital function of HDACs has long been acknowledged in the process of normal hematopoietic cell development and leukemogenesis, and numerous HDAC inhibitors have been applied in the treatment of various tumors but the mechanism of HDAC inhibitors serving in AML is elusive (20, 21). As the studies of HDACs function in AML increasing, we summarized the predominant importance in AML.

AML, with disrupted hematopoietic system, is usually hallmarked by oncogenic fusion proteins, majorly centralizing on AML1-ETO, CBFB-MYH11, PML-RARA, and MLL-AF9 (32, 33). HDAC inhibitors, the hyperacetylated agents, theoretically gear toward the alteration of the aberrant hypoacetylated status, providing a reasonable strategy against AML. They own the theoretical feasibility but practical hinderance, which provoked us to explore the precise function of HDAC, contributing to the utilization of HDAC inhibitors (152, 153). And mounting researches and reviews have demonstrated the roles of HDAC inhibitors in the treatment of AML. However, the function of HDACs in oncogenic molecules is rarely described (15, 26).

Although the relative material is of shortage, it is meaningful to elucidate the potential function of HDACs in AML, focusing on the oncogenic fusion proteins that provides a directing target against specific types of AML.

Besides, HDACs display immunoregulatory properties in integral level, which overall regulates the progress of leukemogenesis through modulating the master elements of immune system such as PD-L1, CTLA-4, Treg, and cytotoxic T lymphocyte (CTL), and antigen-presenting cell (APC) (154–156). For instance, expression of HDAC10 is associated with the presentation of MHC class II molecules in antigen presentation cells (157, 158). Members of HDACs participate in the different stages of T cell development, including $CD4^+$ T cell-mediated immunity (154, 159). That is to say, HDACs not only function with specific fusion proteins but also do regulate the entirety level of immune system which is involved in tumor microenvironment.

Attentions paid on HDACs usually focus on the HDAC inhibitors in the process of carcinogenesis, whereas the roles of HDACs have not got enough attention. It is necessary to harness the interaction between HDACs and leukemogenesis, which would precisely direct the investigation of novel HDAC inhibitors. Here, we summarized the current knowledge of HDACs functioning in leukemogenesis with oncogenic fusion proteins. They are closely associated with the suppression of oncogenic fusion genes, and can be blocked by HDAC inhibitors. However, pan-inhibitors presented various side effects and it can be improved by the specific HDAC inhibitors. And the searching of special targets is based on harnessing the traits of each HDAC member functioning in the epigenetic modification. The review summarized the functional properties of HDAC members, which may be useful for the exploration of specific HDAC inhibitors. Furthermore, HDACs is involved in the regulation of immune system, which may benefit to the investigation of novel agents or combinational drugs.

AUTHOR CONTRIBUTIONS

JZ drafted the manuscript. XG modified the manuscript. LY provided valuable advices, supervised, and approved the manuscript. All authors contributed to the article and approved the submitted version.

FUNDING

This work was supported by grants National Natural Science Foundation of China (82030076, 82000161, 82070161, 81970151, 81670162, and 81870134), China Postdoctoral Science Foundation (2018M640824), Chinese National Major Project for New Drug Innovation (2019ZX09201002003), Shenzhen Science and Technology Foundation (JCYJ20190808163601776, JCYJ20200109113810154). Shenzhen Key Laboratory Foundation (ZDSYS20200811143757022). Sanming Project of Shenzhen (SZSM202111004).

REFERENCES

1. Kantarjian H, Kadia T, DiNardo C, Daver N, Borthakur G, Jabbou E, et al. Acute Myeloid Leukemia: Current Progress and Future Directions. *Blood Cancer J* (2021) 11(2):41. doi: 10.1038/s41408-021-00425-3
2. Estey EH. Acute Myeloid Leukemia: 2021 Update On Risk-Stratification and Management. *Am J Hematol* (2020) 95(11):1368–98. doi: 10.1002/ajh.25975
3. De Kouchkovsky I, Abdul-Hay M. Acute Myeloid Leukemia: A Comprehensive Review and 2016 update'. *Blood Cancer J* (2016) 6(7): e441. doi: 10.1038/bcj.2016.50
4. Martens JH, Stunnenberg HG. The Molecular Signature of Oncofusion Proteins In Acute Myeloid Leukemia. *FEBS Lett* (2010) 584(12):2662–9. doi: 10.1016/j.febslet.2010.04.002
5. Tijchon E, Yi G, Mandoli A, Smits JGA, Ferrari F, Heuts BMH, et al. The Acute Myeloid Leukemia Associated AML1-ETO Fusion Protein Alters The Transcriptome and Cellular Progression In A Single-Oncogene Expressing *In Vitro* Induced Pluripotent Stem Cell Based Granulocyte Differentiation Model. *PLoS One* (2019) 14(12):e0226435. doi: 10.1371/journal.pone.0226435
6. Matsukawa T, Aplan PD. Clinical and Molecular Consequences of Fusion Genes in Myeloid Malignancies. *Stem Cells* (2020) 38(11):1366–74. doi: 10.1002/stem.3263
7. Pikman Y, Stegmaier K. Targeted Therapy for Fusion-Driven High-Risk Acute Leukemia. *Blood* (2018) 132(12):1241–7. doi: 10.1182/blood-2018-04-784157
8. Brien GL, Stegmaier K, Armstrong SA. Targeting Chromatin Complexes in Fusion Protein-Driven Malignancies. *Nat Rev Cancer* (2019) 19(5):255–69. doi: 10.1038/s41568-019-0132-x
9. Al-Harbi S, Aljurf M, Mohty M, Almohareb F, Ahmed SOA. An Update on the Molecular Pathogenesis and Potential Therapeutic Targeting of AML with t ((q22;q22.1);RUNX1-RUNX1T1. *Blood Adv* (2020) 4(1):229–38. doi: 10.1182/bloodadvances.2019000168
10. van Dijk AD, de Bont E, Kornblau SM. Targeted Therapy in Acute Myeloid Leukemia: Current Status and New Insights From a Proteomic Perspective. *Expert Rev Proteomics* (2020) 17(1):1–10. doi: 10.1080/14789450.2020.1717951
11. Goldman SL, Hassan C, Khunte M, Soldatenko A, Jong Y, Afshinnekoo K, et al. Epigenetic Modifications in Acute Myeloid Leukemia: Prognosis, Treatment, and Heterogeneity. *Front Genet* (2019) 10:133. doi: 10.3389/fgene.2019.00133
12. Dhall A, Zee BM, Yan F, Blanco MA. Intersection of Epigenetic and Metabolic Regulation of Histone Modifications in Acute Myeloid Leukemia. *Front Oncol* (2019) 9:432. doi: 10.3389/fonc.2019.00432
13. Wang P, Wang Z, Liu J. Role of HDACs in Normal and Malignant Hematopoiesis. *Mol Cancer* (2020) 19(1):5. doi: 10.1186/s12943-020-01182-w
14. Ropero S, Esteller M. The Role of Histone Deacetylases (HDACs) in Human Cancer. *Mol Oncol* (2007) 1(1):19–25. doi: 10.1016/j.molonc.2007.01.001
15. Li Y, Seto E. HDACs and HDAC Inhibitors in Cancer Development and Therapy. *Cold Spring Harb Perspect Med* (2016) 6(10):1–34. doi: 10.1101/cshperspect.a026831
16. Hiller JK, Schmoor C, Gaidzik VI, Schmidt-Salzmann C, Yalcin A, Abdelkarim M, et al. Evaluating the Impact of Genetic and Epigenetic Aberrations on Survival and Response in Acute Myeloid Leukemia Patients Receiving Epigenetic Therapy. *Ann Hematol* (2017) 96(4):559–65. doi: 10.1007/s00277-016-2912-7
17. Eriksson A, Lennartsson A, Lehmann S. Epigenetic Aberrations in Acute Myeloid Leukemia: Early Key Events During Leukemogenesis. *Exp Hematol* (2015) 43(8):609–24. doi: 10.1016/j.exphem.2015.05.009
18. Nebbioso A, Tambaro FP, Dell'Aversana C, Altucci L. Cancer epigenetics: Moving forward. *PLoS Genet* (2018) 14(6):e1007362. doi: 10.1371/journal.pgen.1007362

19. Hu D, Shilatifard A. Epigenetics of Hematopoiesis and Hematological Malignancies. *Genes Dev* (2016) 30(18):2021–41. doi: 10.1101/gad.284109.116
20. Gallinari P, Di Marco S, Jones P, Pallaoro M, Steinkuhler C. HDACs, Histone Deacetylation and Gene Transcription: From Molecular Biology to Cancer Therapeutics. *Cell Res* (2007) 17(3):195–211. doi: 10.1038/sj.cr.7310149
21. Milazzo G, Mercatelli D, Di Muzio G, Triboli L, De Rosa P, Perini G, et al. Histone Deacetylases (HDACs): Evolution, Specificity, Role in Transcriptional Complexes, and Pharmacological Actionability. *Genes (Basel)* (2020) 11(5):1–49. doi: 10.3390/genes11050556
22. Xia C, Tao Y, Li M, Che T, Qu J. Protein Acetylation and Deacetylation: An Important Regulatory Modification in Gene Transcription (Review). *Exp Ther Med* (2020) 20(4):2923–40. doi: 10.3892/etm.2020.9073
23. Lawlor L, Yang XB. Harnessing the HDAC-Histone Deacetylase Enzymes, Inhibitors and How These Can be Utilised In Tissue Engineering. *Int J Oral Sci* (2019) 11(2):20. doi: 10.1038/s41368-019-0053-2
24. Mithraprabhu S, Kalff A, Chow A, Khong T, Spencer A. Dysregulated Class I Histone Deacetylases Are Indicators of Poor Prognosis In Multiple Myeloma. *Epigenetics* (2014) 9(11):1511–20. doi: 10.4161/15592294.2014.983367
25. Patra S, Panigrahi DP, Praharaj PP, Bhol CS, Mahapatra KK, Mishra SR, et al. Dysregulation of Histone Deacetylases in Carcinogenesis and Tumor Progression: A Possible Link to Apoptosis And Autophagy. *Cell Mol Life Sci* (2019) 76(17):3263–82. doi: 10.1007/s00018-019-03098-1
26. Xu QY, Yu L. Epigenetic Therapies in Acute Myeloid Leukemia: The Role of Hypomethylating Agents, Histone Deacetylase Inhibitors and the Combination of Hypomethylating Agents With Histone Deacetylase Inhibitors. *Chin Med J (Engl)* (2020) 6):699–715. doi: 10.1097/CM9.0000000000000685
27. Blagitko-Dorfs N, Schlosser P, Greve G, Pfeifer D, Meier R, Baude A, et al. Combination Treatment of Acute Myeloid Leukemia Cells With DNMT and HDAC Inhibitors: Predominant Synergistic Gene Downregulation Associated With Gene Body Demethylation. *Leukemia* (2019) 33(4):945–56. doi: 10.1038/s41375-018-0293-8
28. Li X, Su Y, Madlambayan G, Edwards H, Polin L, Kushner J, et al. Antileukemic Activity and Mechanism of Action of the Novel PI3K and Histone Deacetylase Dual Inhibitor CUDC-907 in Acute Myeloid Leukemia. *Haematologica* (2019) 104(11):2225–40. doi: 10.3324/haematol.2018.201343
29. He Y, Xu L, Feng J, Wu K, Zhao Y, Huang H, et al. HDAC Inhibitor LBH589 Suppresses the Proliferation but Enhances the Antileukemic Effect of Human gammadeltaT Cells. *Mol Ther Oncolytics* (2020) 18:623–30. doi: 10.1016/j.omto.2020.08.003
30. Yu X, Li H, Hu P, Qing Y, Wang X, Zhu M, et al. Natural HDAC-1/8 Inhibitor Baicalein Exerts Therapeutic Effect in CBF-AML. *Clin Transl Med* (2020) 10(4):e154. doi: 10.1002/ctm2.154
31. San Jose-Eneriz E, Gimenez-Camino N, Agirre X, Prosper F. HDAC Inhibitors in Acute Myeloid Leukemia. *Cancers (Basel)* (2019) 11(11):1–24. doi: 10.3390/cancers11111794
32. Rapin N, Porse BT. Oncogenic Fusion Proteins Expressed in Immature Hematopoietic Cells Fail to Recapitulate the Transcriptional Changes Observed in Human AML. *Oncogenesis* (2014) 3:e106. doi: 10.1038/oncsis.2014.22
33. Lu C. Decoding the Function of an Oncogenic Transcription Factor: Finding the First Responders. *Mol Cell* (2021) 81(3):418–20. doi: 10.1016/j.molcel.2021.01.008
34. Singh AA, Mandoli A, Prange KH, Laakso M, Martens JH. AML Associated Oncofusion Proteins PML-RARA, AML1-ETO and CBFB-MYH11 Target RUNX/ETS-Factor Binding Sites to Modulate H3ac Levels and Drive Leukemogenesis. *Oncotarget* (2017) 8(8):12855–65. doi: 10.18632/oncotarget.14150
35. Panuzzo C, Signorino E, Calabrese C, Ali MS, Petiti J, Bracco E, et al. Landscape of Tumor Suppressor Mutations in Acute Myeloid Leukemia. *J Clin Med* (2020) 9(3):1–25. doi: 10.3390/jcm9030802
36. DiNardo CD, Cortes JE. Mutations in AML: Prognostic and Therapeutic Implications. *Hematol Am Soc Hematol Educ Program* (2016) 2016(1):348–55. doi: 10.1182/asheducation-2016.1.348
37. Wang RQ, Chen CJ, Jing Y, Qin JY, Li Y, Chen GF, et al. Characteristics and Prognostic Significance of Genetic Mutations in Acute Myeloid Leukemia Based on a Targeted Next-Generation Sequencing Technique. *Cancer Med* (2020) 9(22):8457–67. doi: 10.1002/cam4.3467
38. Dombret H. Gene Mutation and AML Pathogenesis. *Blood* (2011) 118 (20):5366–7. doi: 10.1182/blood-2011-09-379081
39. Lauber C, Correia N, Trumpp A, Rieger MA, Dolnik A, Bullinger L, et al. Survival Differences and Associated Molecular Signatures of DNMT3A-Mutant Acute Myeloid Leukemia Patients. *Sci Rep* (2020) 10(1):12761. doi: 10.1038/s41598-020-69691-8
40. Li Y, Lv X, Ge X, Yuan D, Ding M, Zhen C, et al. Mutational Spectrum and Associations With Clinical Features in Patients With Acute Myeloid Leukaemia Based on Nextgeneration Sequencing. *Mol Med Rep* (2019) 19 (5):4147–58. doi: 10.3892/mmr.2019.10081
41. Walter RB, Othus M, Burnett AK, Lowenberg B, Kantarjian HM, Ossenkoppele GJ, et al. Significance of FAB subclassification of "Acute Myeloid Leukemia, NOS" in the 2008 WHO Classification: Analysis of 5848 Newly Diagnosed Patients. *Blood* (2013) 121(13):2424–31. doi: 10.1182/blood-2012-10-462440
42. Schoch C, Schnittger S, Kern W, Dugas M, Hiddemann W, Haferlach T. Acute Myeloid Leukemia With Recurring Chromosome Abnormalities as Defined by the WHO-Classification: Incidence of Subgroups, Additional Genetic Abnormalities, FAB Subtypes and Age Distribution in an Unselected Series of 1,897 Patients With Acute Myeloid Leukemia. *Haematologica* (2003) 88(3):351–2.
43. Mrozek K, Eisfeld AK, Kohlschmidt J, Carroll AJ, Walker CJ, Nicolet D, et al. Complex Karyotype in De Novo Acute Myeloid Leukemia: Typical and Atypical Subtypes Differ Molecularly and Clinically. *Leukemia* (2019) 33 (7):1620–34. doi: 10.1038/s41375-019-0390-3
44. Hassan K, Qureshi M, Shafi S, Ikram N, Akhtar MJ. Acute Myeloid Leukemia-FAB Classification and Its Correlation With Clinico-Haematological Features. *J Pak Med Assoc* (1993) 43(10):200–3.
45. Arber DA, Orazi A, Hasserjian R, Thiele J, Borowitz MJ, Le Beau MM, et al. The 2016 Revision to the World Health Organization Classification of Myeloid Neoplasms and Acute Leukemia. *Blood* (2016) 127(20):2391–405. doi: 10.1182/blood-2016-03-643544
46. Zhang RD, Wang LY, Zheng HY. [Interpretation of the 2016 Revision to the World Health Organization Classification of Acute Leukemia]. *Zhonghua Er Ke Za Zhi* (2017) 55(1):15–8. doi: 10.3760/cma.j.issn.0578-1310.2017.01.003
47. Arber DA. The 2016 WHO Classification of Acute Myeloid Leukemia: What the Practicing Clinician Needs to Know. *Semin Hematol* (2019) 56(2):90–5. doi: 10.1053/j.seminhematol.2018.08.002
48. Hong M, He G. 2016 Revision to the WHO Classification of Acute Myeloid Leukemia. *J Transl Int Med* (2017) 5(2):69–71. doi: 10.1515/jtim-2016-0041
49. Jung J, Cho BS, Kim HJ, Han E, Jang W, Han K, et al. Reclassification of Acute Myeloid Leukemia According to the 2016 WHO Classification. *Ann Lab Med* (2019) 39(3):311–6. doi: 10.3343/alm.2019.39.3.311
50. Pourrajab F, Zare-Khormizi MR, Hashemi AS, Hekmatimoghaddam S. Genetic Characterization and Risk Stratification of Acute Myeloid Leukemia. *Cancer Manag Res* (2020) 12:2231–53. doi: 10.2147/CMAR.S242479
51. Marino-Ramirez L, Kann MG, Shoemaker BA, Landsman D. Histone Structure and Nucleosome Stability. *Expert Rev Proteomics* (2005) 2 (5):719–29. doi: 10.1586/14789450.2.5.719
52. Vaughan RM, Kupai A, Rothbart SB. Chromatin Regulation Through Ubiquitin and Ubiquitin-like Histone Modifications. *Trends Biochem Sci* (2021) 46(4):258–69. doi: 10.1016/j.tibs.2020.11.005
53. Morgan MAJ, Shilatifard A. Reevaluating the Roles of Histone-Modifying Enzymes and Their Associated Chromatin Modifications in Transcriptional Regulation. *Nat Genet* (2020) 52(12):1271–81. doi: 10.1038/s41588-020-00736-4
54. Binder H, Steiner L, Przybilla J, Rohlf T, Prohaska S, Galle J. Transcriptional Regulation by Histone Modifications: Towards a Theory of Chromatin Re-Organization During Stem Cell Differentiation. *Phys Biol* (2013) 10 (2):026006. doi: 10.1088/1478-3975/10/2/026006
55. Tessarz P, Kouzarides T. Histone core modifications regulating nucleosome structure and dynamics. *Nat Rev Mol Cell Biol* (2014) 15(11):703–8. doi: 10.1038/nrm3890
56. Kurumizaka H, Kujirai T, Takizawa Y. Contributions of Histone Variants in Nucleosome Structure and Function. *J Mol Biol* (2021) 433(6):166678. doi: 10.1016/j.jmb.2020.10.012
57. Zhao Z, Shilatifard A. Epigenetic Modifications of Histones in Cancer. *Genome Biol* (2019) 20(1):245. doi: 10.1186/s13059-019-1870-5

58. Seto E, Yoshida M. Erasers of Histone Acetylation: The Histone Deacetylase Enzymes. *Cold Spring Harb Perspect Biol* (2014) 6(4):a018713. doi: 10.1101/cshperspect.a018713
59. Kee HJ, Kook H. Roles and Targets of Class I and IIa Histone Deacetylases in Cardiac Hypertrophy. *J BioMed Biotechnol* (2011) 2011:928326. doi: 10.1155/2011/928326
60. Tang X, Li G, Su F, Cai Y, Shi L, Meng Y, et al. HDAC8 Cooperates With SMAD3/4 Complex to Suppress SIRT7 and Promote Cell Survival and Migration. *Nucleic Acids Res* (2020) 48(6):2912–23. doi: 10.1093/nar/gkaa039
61. Delcuve GP, Khan DH, Davie JR. Roles of Histone Deacetylases in Epigenetic Regulation: Emerging Paradigms From Studies With Inhibitors. *Clin Epigenet* (2012) 4(1):5. doi: 10.1186/1868-7083-4-5
62. Rajan A, Shi H, Xue B. Class I and II Histone Deacetylase Inhibitors Differentially Regulate Thermogenic Gene Expression in Brown Adipocytes. *Sci Rep* (2018) 8(1):13072. doi: 10.1038/s41598-018-31560-w
63. Chakrabarti A, Oehme I, Witt O, Oliveira G, Sippl W, Romier C, et al. HDAC8: A Multifaceted Target For Therapeutic Interventions. *Trends Pharmacol Sci* (2015) 36(7):481–92. doi: 10.1016/j.tips.2015.04.013
64. Millard CJ, Watson PJ, Fairall L, Schwabe JWR. Targeting Class I Histone Deacetylases in a "Complex" Environment. *Trends Pharmacol Sci* (2017) 38(4):363–77. doi: 10.1016/j.tips.2016.12.006
65. Millard CJ, Watson PJ, Celardo I, Gordiyenko Y, Cowley SM, Robinson CV, et al. Class I HDACs Share a Common Mechanism of Regulation by Inositol Phosphates. *Mol Cell* (2013) 51(1):57–67. doi: 10.1016/j.molcel.2013.05.020
66. Park SY, Kim JS. A Short Guide to Histone Deacetylases Including Recent Progress on Class II Enzymes. *Exp Mol Med* (2020) 52(2):204–12. doi: 10.1038/s12276-020-0382-4
67. Clocchiatti A, Florean C, Brancolini C. Class IIa HDACs: From Important Roles in Differentiation to Possible Implications in Tumourigenesis. *J Cell Mol Med* (2011) 15(9):1833–46. doi: 10.1111/j.1582-4934.2011.01321.x
68. Haberland M, Montgomery RL, Olson EN. The Many Roles of Histone Deacetylases in Development and Physiology: Implications For Disease and Therapy. *Nat Rev Genet* (2009) 10(1):32–42. doi: 10.1038/nrg2485
69. Di Giorgio E, Dalla E, Franforte E, Paluvai H, Minisini M, Trevisanut M, et al. Different Class IIa HDACs Repressive Complexes Regulate Specific Epigenetic Responses Related to Cell Survival in Leiomyosarcoma Cells. *Nucleic Acids Res* (2020) 48(2):646–64.
70. Bertos NR, Wang AH, Yang XJ. Class II Histone Deacetylases: Structure, Function, and Regulation. *Biochem Cell Biol* (2001) 79(3):243–52. doi: 10.1139/o01-032
71. Cante-Barrett K, Pieters R, Meijerink JP. Myocyte Enhancer Factor 2C in Hematopoiesis and Leukemia. *Oncogene* (2014) 33(4):403–10. doi: 10.1038/onc.2013.56
72. Kovacs JJ, Murphy PJ, Gaillard S, Zhao X, Wu JT, Nicchitta CV, et al. HDAC6 Regulates Hsp90 Acetylation and Chaperone-Dependent Activation of Glucocorticoid Receptor. *Mol Cell* (2005) 18(5):601–7. doi: 10.1016/j.molcel.2005.04.021
73. Pinzi L, Benedetti R, Altucci L, Rastelli G. Design of Dual Inhibitors of Histone Deacetylase 6 and Heat Shock Protein 90. *ACS Omega* (2020) 5(20):11473–80. doi: 10.1021/acsomega.0c00559
74. Kuta R, Larochelle N, Fernandez M, Pal A, Minotti S, Tibshirani M, et al. Depending on the Stress, Histone Deacetylase Inhibitors Act as Heat Shock Protein Co-Inducers in Motor Neurons and Potentiate Arimoclomol, Exerting Neuroprotection Through Multiple Mechanisms in ALS Models. *Cell Stress Chaperones* (2020) 25(1):173–91. doi: 10.1007/s12192-019-01064-1
75. Pernet L, Faure V, Gilquin B, Dufour-Guerin S, Khochbin S, Vourc'h C. HDAC6-Ubiquitin Interaction Controls the Duration of HSF1 Activation After Heat Shock. *Mol Biol Cell* (2014) 25(25):4187–94. doi: 10.1091/mbc.e14-06-1032
76. Liu X, Wang Y, Zhang R, Jin T, Qu L, Jin Q, et al. HDAC10 Is Positively Associated With PD-L1 Expression and Poor Prognosis in Patients With NSCLC. *Front Oncol* (2020) 10:485. doi: 10.3389/fonc.2020.00485
77. Wang L, Zheng S, Zhang L, Xiao H, Gan H, Chen H, et al. Histone Deacetylation 10 Alleviates Inflammation After Intracerebral Hemorrhage via the PTPN22/NLRP3 Pathway in Rats. *Neuroscience* (2020) 432:247–59. doi: 10.1016/j.neuroscience.2020.02.027
78. Powers J, Lienlaf M, Perez-Villarroel P, Deng S, Knox T, Villagra A, et al. Expression and Function of Histone Deacetylase 10 (HDAC10) in B Cell Malignancies. *Methods Mol Biol* (2016) 1436:129–45. doi: 10.1007/978-1-4939-3667-0_10
79. Boltz TA, Khuri S, Wuchty S. Promoter Conservation in HDACs Points to Functional Implications. *BMC Genomics* (2019) 20(1):613. doi: 10.1186/s12864-019-5973-x
80. Villagra A, Cheng F, Wang H, Suarez I, Glozak M, Maurin M, et al. The Histone Deacetylase HDAC11 Regulates The Expression of Interleukin 10 and Immune Tolerance. *Nat Immunol* (2009) 10(1):92–100. doi: 10.1038/ni.1673
81. Liu SS, Wu F, Jin YM, Chang WQ, Xu TM. HDAC11: A Rising Star in Epigenetics. *BioMed Pharmacother* (2020) 131:110607. doi: 10.1016/j.biopha.2020.110607
82. Yue L, Sharma V, Horvat NP, Akuffo AA, Beatty MS, Murdun C, et al. HDAC11 Deficiency Disrupts Oncogene-Induced Hematopoiesis in Myeloproliferative Neoplasms. *Blood* (2020) 135(3):191–207. doi: 10.1182/blood.2019895326
83. Kim E, Bisson WH, Lohr CV, Williams DE, Ho E, Dashwood RH, et al. Histone and Non-Histone Targets of Dietary Deacetylase Inhibitors. *Curr Top Med Chem* (2016) 16(7):714–31. doi: 10.2174/1568026615666150825125857
84. Peng L, Seto E. Deacetylation of Nonhistone Proteins by HDACs and the Implications in Cancer. *Handb Exp Pharmacol* (2011) 206:39–56. doi: 10.1007/978-3-642-21631-2_3
85. Toro TB, Watt TJ. Critical Review of Non-Histone Human Substrates of Metal-Dependent Lysine Deacetylases. *FASEB J* (2020) 34(10):13140–55. doi: 10.1096/fj.202001301RR
86. Keremu A, Aimaiti A, Liang Z, Zou X. Role of the HDAC6/STAT3 Pathway in Regulating PD-L1 Expression in Osteosarcoma Cell Lines. *Cancer Chemother Pharmacol* (2019) 83(2):255–64. doi: 10.1007/s00280-018-3721-6
87. Kumar S, Attrish D, Srivastava A, Banerjee J, Tripathi M, Chandra PS, et al. Non-Histone Substrates of Histone Deacetylases as Potential Therapeutic Targets in Epilepsy. *Expert Opin Ther Targets* (2021) 25(1):75–85. doi: 10.1080/14728222.2021.1860016
88. Feng Y, Endo M, Sugiyama H. Nucleosomes and Epigenetics from a Chemical Perspective. *Chembiochem* (2021) 22(4):595–612. doi: 10.1002/cbic.202000332
89. Wang ZA, Millard CJ, Lin CL, Gurnett JE, Wu M, Lee K, et al. Diverse Nucleosome Site-Selectivity Among Histone Deacetylase Complexes. *Elife* (2020) 9:1–19. doi: 10.7554/eLife.57663
90. Suraweera A, O'Byrne KJ, Richard DJ. Combination Therapy With Histone Deacetylase Inhibitors (HDACi) for the Treatment of Cancer: Achieving the Full Therapeutic Potential of HDACi. *Front Oncol* (2018) 8:92. doi: 10.3389/fonc.2018.00092
91. Sanaei M, Kavoosi F. Histone Deacetylases and Histone Deacetylase Inhibitors: Molecular Mechanisms of Action in Various Cancers. *Adv BioMed Res* (2019) 8:63. doi: 10.4103/abr.abr_142_19
92. Klaus M, Haferlach T, Schnittger S, Kern W, Hiddemann W, Schoch C. Cytogenetic Profile in De Novo Acute Myeloid Leukemia With FAB Subtypes M0, M1, and M2: A Study Based on 652 Cases Analyzed With Morphology, Cytogenetics, and Fluorescence In Situ Hybridization. *Cancer Genet Cytogenet* (2004) 155(1):47–56. doi: 10.1016/j.cancergencyto.2004.03.008
93. Reikvam H, Hatfield KJ, Kittang AO, Hovland R, Bruserud O. Acute Myeloid Leukemia With the t (8,21) Translocation: Clinical Consequences and Biological Implications. *J BioMed Biotechnol* (2011) 2011:104631. doi: 10.1155/2011/104631
94. Nishii K, Usui E, Katayama N, Lorenzo FT, Nakase K, Kobayashi T, et al. Characteristics of t (8,21) Acute Myeloid Leukemia (AML) with Additional Chromosomal Abnormality: Concomitant Trisomy 4 May Constitute a Distinctive Subtype of t (8,21) AML. *Leukemia* (2003) 17(4):731–7. doi: 10.1038/sj.leu.2402871
95. Kellaway S, Chin PS, Barneh F, Bonifer C, Heidenreich O. t(8,21) Acute Myeloid Leukemia as a Paradigm for the Understanding of Leukemogenesis at the Level of Gene Regulation and Chromatin Programming. *Cells* (2020) 9(12):1–13. doi: 10.3390/cells9122681
96. Licht JD. AML1 and the AML1-ETO Fusion Protein in the Pathogenesis of t (8,21) AML. *Oncogene* (2001) 20(40):5660–79. doi: 10.1038/sj.onc.1204593
97. Li X, Xu YB, Wang Q, Lu Y, Zheng YC, Wang YC, et al. Leukemogenic AML1-ETO Fusion Protein Upregulates Expression of Connexin 43: The

Role in AML 1-ETO-Induced Growth Arrest in Leukemic Cells. *J Cell Physiol* (2006) 208(3):594–601. doi: 10.1002/jcp.20695
98. DeKelver RC, Yan M, Ahn EY, Shia WJ, Speck NA, Zhang DE, et al. Attenuation of AML1-ETO Cellular Dysregulation Correlates With Increased Leukemogenic Potential. *Blood* (2013) 121(18):3714–7. doi: 10.1182/blood-2012-11-465641
99. Ichikawa M, Goyama S, Asai T, Kawazu M, Nakagawa M, Takeshita M, et al. AML1/Runx1 Negatively Regulates Quiescent Hematopoietic Stem Cells in Adult Hematopoiesis. *J Immunol* (2008) 180(7):4402–8. doi: 10.4049/jimmunol.180.7.4402
100. Okuda T, Nishimura M, Nakao M, Fujita Y. RUNX1/AML1: A Central Player in Hematopoiesis. *Int J Hematol* (2001) 74(3):252–7. doi: 10.1007/BF02982057
101. Tahirov TH, Inoue-Bungo T, Morii H, Fujikawa A, Sasaki M, Kimura K, et al. Structural Analyses of DNA Recognition by the AML1/Runx-1 Runt Domain and Its Allosteric Control by CBFbeta. *Cell* (2001) 104(5):755–67. doi: 10.1016/S0092-8674(01)00271-9
102. Yan M, Ahn EY, Hiebert SW, Zhang DE. RUNX1/AML1 DNA-Binding Domain and ETO/MTG8 NHR2-Dimerization Domain Are Critical to AML1-ETO9a Leukemogenesis. *Blood* (2009) 113(4):883–6. doi: 10.1182/blood-2008-04-153742
103. Elagib KE, Goldfarb AN. Oncogenic Pathways of AML1-ETO in Acute Myeloid Leukemia: Multifaceted Manipulation of Marrow Maturation. *Cancer Lett* (2007) 251(2):179–86. doi: 10.1016/j.canlet.2006.10.010
104. Ito Y, Bae SC, Chuang LS. The RUNX Family: Developmental Regulators in Cancer. *Nat Rev Cancer* (2015) 15(2):81–95. doi: 10.1038/nrc3877
105. Otalora-Otalora BA, Henriquez B, Lopez-Kleine L, Rojas A. RUNX Family: Oncogenes or Tumor Suppressors (Review). *Oncol Rep* (2019) 42(1):3–19. doi: 10.3892/or.2019.7149
106. Samarakkody AS, Shin NY, Cantor AB. Role of RUNX Family Transcription Factors in DNA Damage Response. *Mol Cells* (2020) 43(2):99–106. doi: 10.14348/molcells.2019.0304
107. Bonifer C, Levantini E, Kouskoff V, Lacaud G. Runx1 Structure and Function in Blood Cell Development. *Adv Exp Med Biol* (2017) 962:65–81. doi: 10.1007/978-981-10-3233-2_5
108. Mottis A, Mouchiroud L, Auwerx J. Emerging Roles of the Corepressors NCoR1 and SMRT in Homeostasis. *Genes Dev* (2013) 27(8):819–35. doi: 10.1101/gad.214023.113
109. Guenther MG, Barak O, Lazar MA. The SMRT and N-CoR Corepressors Are Activating Cofactors For Histone Deacetylase 3. *Mol Cell Biol* (2001) 21(18):6091–101. doi: 10.1128/MCB.21.18.6091-6101.2001
110. Chen-Wichmann L, Shvartsman M, Preiss C, Hockings C, Windisch R, Redondo Monte E, et al. Compatibility of RUNX1/ETO Fusion Protein Modules Driving CD34+ Human Progenitor Cell Expansion. *Oncogene* (2019) 38(2):261–72. doi: 10.1038/s41388-018-0441-7
111. van der Kouwe E, Staber PB. RUNX1-ETO: Attacking the Epigenome for Genomic Instable Leukemia. *Int J Mol Sci* (2019) 20(2):1–17. doi: 10.3390/ijms20020350
112. Hug BA, Lazar MA. ETO Interacting Proteins. *Oncogene* (2004) 23(24):4270–4. doi: 10.1038/sj.onc.1207674
113. Okumura AJ, Peterson LF, Okumura F, Boyapati A, Zhang DE. t (8,21)(q22; q22) Fusion Proteins Preferentially Bind to Duplicated AML1/RUNX1 DNA-Binding Sequences to Differentially Regulate Gene Expression. *Blood* (2008) 112(4):1392–401. doi: 10.1182/blood-2007-11-124735
114. Xiao Y, Liu Y. Recent Advances in the Discovery of Novel HSP90 Inhibitors: An Update From 2014. *Curr Drug Targets* (2020) 21(3):302–17. doi: 10.2174/1389450120666190829162544
115. Peterson LF, Zhang DE. The 8;21 Translocation in Leukemogenesis. *Oncogene* (2004) 23(24):4255–62. doi: 10.1038/sj.onc.1207727
116. Rulina AV, Spirin PV, Prassolov VS. Activated Leukemic Oncogenes AML1-ETO and c-kit: Role in Development of Acute Myeloid Leukemia and Current Approaches for Their Inhibition. *Biochem (Mosc)* (2010) 75(13):1650–66. doi: 10.1134/S0006297910130092
117. Roudaia L, Cheney MD, Manuylova E, Chen W, Morrow M, Park S, et al. CBFbeta is Critical for AML1-ETO and TEL-AML1 Activity. *Blood* (2009) 113(13):3070–9. doi: 10.1182/blood-2008-03-147207
118. Thiel VN, Giaimo BD, Schwarz P, Soller K, Vas V, Bartkuhn M, et al. Heterodimerization of AML1/ETO With CBFbeta is Required for Leukemogenesis But Not for Myeloproliferation. *Leukemia* (2017) 31(11):2491–502. doi: 10.1038/leu.2017.105
119. Liu S, Klisovic RB, Vukosavljevic T, Yu J, Paschka P, Huynh L, et al. Targeting AML1/ETO-Histone Deacetylase Repressor Complex: A Novel Mechanism For Valproic Acid-Mediated Gene Expression and Cellular Differentiation in AML1/ETO-Positive Acute Myeloid Leukemia Cells. *J Pharmacol Exp Ther* (2007) 321(3):953–60. doi: 10.1124/jpet.106.118406
120. Huang Y, Chen J, Lu C, Han J, Wang G, Song C, et al. HDAC1 and Klf4 Interplay Critically Regulates Human Myeloid Leukemia Cell Proliferation. *Cell Death Dis* (2014) 5:e1491. doi: 10.1038/cddis.2014.433
121. Wingelhofer B, Somervaille TCP. Emerging Epigenetic Therapeutic Targets in Acute Myeloid Leukemia. *Front Oncol* (2019) 9:850. doi: 10.3389/fonc.2019.00850
122. Prokocimer M, Molchadsky A, Rotter V. Dysfunctional Diversity of p53 Proteins in Adult Acute Myeloid Leukemia: Projections on Diagnostic Workup and Therapy. *Blood* (2017) 130(6):699–712. doi: 10.1182/blood-2017-02-763086
123. Guo C, Li J, Steinauer N, Wong M, Wu B, Dickson A, et al. Histone Deacetylase 3 Preferentially Binds and Collaborates With the Transcription Factor RUNX1 to Repress AML1-ETO-Dependent Transcription in t (8,21) AML. *J Biol Chem* (2020) 295(13):4212–23. doi: 10.1074/jbc.RA119.010707
124. Beghini A. Core Binding Factor Leukemia: Chromatin Remodeling Moves Towards Oncogenic Transcription. *Cancers (Basel)* (2019) 11(12):1–21. doi: 10.3390/cancers11121973
125. Richter LE, Wang Y, Becker ME, Coburn RA, Williams JT, Amador C, et al. HDAC1 Is a Required Cofactor of CBFbeta-SMMHC and a Potential Therapeutic Target in Inversion 16 Acute Myeloid Leukemia. *Mol Cancer Res* (2019) 17(6):1241–52. doi: 10.1158/1541-7786.MCR-18-0922
126. Biernacki MA, Foster KA, Woodward KB, Coon ME, Cummings C, Cunningham TM, et al. CBFB-MYH11 Fusion Neoantigen Enables T Cell Recognition and Killing of Acute Myeloid Leukemia. *J Clin Invest* (2020) 130(10):5127–41. doi: 10.1172/JCI137723
127. Cordonnier G, Mandoli A, Cagnard N, Hypolite G, Lhermitte L, Verhoeyen E, et al. CBFbeta-SMMHC Affects Genome-wide Polycomb Repressive Complex 1 Activity in Acute Myeloid Leukemia. *Cell Rep* (2020) 30(2):299–307.e293. doi: 10.1016/j.celrep.2019.12.026
128. Qi J, Singh S, Hua WK, Cai Q, Chao SW, Li L, et al. HDAC8 Inhibition Specifically Targets Inv(16) Acute Myeloid Leukemic Stem Cells by Restoring p53 Acetylation. *Cell Stem Cell* (2015) 17(5):597–610. doi: 10.1016/j.stem.2015.08.004
129. Spreafico M, et al. HDAC8: A Promising Therapeutic Target for Acute Myeloid Leukemia. *Front Cell Dev Biol* (2020) 8:844. doi: 10.3389/fcell.2020.00844
130. Liquori A, Ibanez M, Sargas C, Sanz MA, Barragan E, Cervera J. Acute Promyelocytic Leukemia: A Constellation of Molecular Events around a Single PML-RARA Fusion Gene. *Cancers (Basel)* (2020) 12(3). doi: 10.3390/cancers12030624
131. Geoffroy MC, de The H. Classic and Variants APLs, as Viewed from a Therapy Response. *Cancers (Basel)* (2020) 12(4):1–22. doi: 10.3390/cancers12040967
132. Martens JH, Brinkman AB, Simmer F, Francoijs KJ, Nebbioso A, Ferrara F, et al. PML-RARalpha/RXR Alters the Epigenetic Landscape in Acute Promyelocytic Leukemia. *Cancer Cell* (2010) 17(2):173–85. doi: 10.1016/j.ccr.2009.12.042
133. Guan D, Kao HY. The function, regulation and therapeutic implications of the tumor suppressor protein, PML. *Cell Biosci* (2015) 5:60. doi: 10.1186/s13578-015-0051-9
134. Saeed S, Logie C, Stunnenberg HG, Martens JH. Genome-Wide Functions of PML-RARalpha in Acute Promyelocytic Leukaemia. *Br J Cancer* (2011) 104(4):554–8. doi: 10.1038/sj.bjc.6606095
135. Liu XL, Liu HQ, Li J, Mao CY, He JT, Zhao X. Role of Epigenetic in Leukemia: From Mechanism to Therapy. *Chem Biol Interact* (2020) 317:108963. doi: 10.1016/j.cbi.2020.108963
136. Insinga A, Monestiroli S, Ronzoni S, Carbone R, Pearson M, Pruneri G, et al. Impairment of p53 Acetylation, Stability and Function By an Oncogenic Transcription Factor. *EMBO J* (2004) 23(5):1144–54. doi: 10.1038/sj.emboj.7600109
137. Molica M, Mazzone C, Niscola P, de Fabritiis P. TP53 Mutations in Acute Myeloid Leukemia: Still a Daunting Challenge? *Front Oncol* (2020) 10:610820. doi: 10.3389/fonc.2020.610820

138. Arteaga MF, Mikesch JH, Fung TK, So CW. Epigenetics in Acute Promyelocytic Leukaemia Pathogenesis and Treatment Response: A TRAnsition to Targeted Therapies. *Br J Cancer* (2015) 112(3):413–8. doi: 10.1038/bjc.2014.374
139. Singh AA, Petraglia F, Nebbioso A, Yi G, Conte M, Valente S, et al. Multi-Omics Profiling Reveals a Distinctive Epigenome Signature For High-Risk Acute Promyelocytic Leukemia. *Oncotarget* (2018) 9(39):25647–60. doi: 10.18632/oncotarget.25429
140. Leiva M, Moretti S, Soilihi H, Pallavicini I, Peres L, Mercurio C, et al. Valproic Acid Induces Differentiation and Transient Tumor Regression, But Spares Leukemia-Initiating Activity in Mouse Models of APL. *Leukemia* (2012) 26(7):1630–7. doi: 10.1038/leu.2012.39
141. Mehdipour P, Santoro F, Botrugno OA, Romanenghi M, Pagliuca C, Matthews GM, et al. HDAC3 Activity is Required for Initiation of Leukemogenesis in Acute Promyelocytic Leukemia. *Leukemia* (2017) 31 (4):995–7. doi: 10.1038/leu.2017.3
142. Chauchereau A, Mathieu M, de Saintignon J, Ferreira R, Pritchard LL, Mishal Z, et al. HDAC4 Mediates Transcriptional Repression by the Acute Promyelocytic Leukaemia-Associated Protein PLZF. *Oncogene* (2004) 23 (54):8777–84. doi: 10.1038/sj.onc.1208128
143. Biswas D, Milne TA, Basrur V, Kim J, Elenitoba-Johnson KS, Allis CD, et al. Function of Leukemogenic Mixed Lineage Leukemia 1 (MLL) Fusion Proteins Through Distinct Partner Protein Complexes. *Proc Natl Acad Sci U S A* (2011) 108(38):15751–6. doi: 10.1073/pnas.1111498108
144. Slany RK. MLL Fusion Proteins and Transcriptional Control. *Biochim Biophys Acta Gene Regul Mech* (2020) 1863(3):194503. doi: 10.1016/j.bbagrm.2020.194503
145. Marschalek R. Systematic Classification of Mixed-Lineage Leukemia Fusion Partners Predicts Additional Cancer Pathways. *Ann Lab Med* (2016) 36 (2):85–100. doi: 10.3343/alm.2016.36.2.85
146. Ney Garcia DR, Liehr T, Emerenciano M, Meyer C, Marschalek R, Pombode-Oliveira Mdo S, et al. Molecular Studies Reveal a MLL-MLLT3 Gene Fusion Displaced in a Case of Childhood Acute Lymphoblastic Leukemia With Complex Karyotype. *Cancer Genet* (2015) 208(4):143–7. doi: 10.1016/j.cancergen.2015.02.002
147. Lillico R, Lawrence CK, Lakowski TM. Selective DOT1L, LSD1, and HDAC Class I Inhibitors Reduce HOXA9 Expression in MLL-AF9 Rearranged Leukemia Cells, But Dysregulate the Expression of Many Histone-Modifying Enzymes. *J Proteome Res* (2018) 17(8):2657–67. doi: 10.1021/acs.jproteome.8b00118
148. Ye J, Zha J, Shi Y, Li Y, Yuan D, Chen Q, et al. Co-inhibition of HDAC and MLL-Menin Interaction Targets MLL-Rearranged Acute Myeloid Leukemia Cells via Disruption of DNA Damage Checkpoint and DNA Repair. *Clin Epigenet* (2019) 11(1):137. doi: 10.1186/s13148-019-0723-0
149. Ahmad K, Katryniok C, Scholz B, Merkens J, Loscher D, Marschalek R, et al. Inhibition of Class I HDACs Abrogates the Dominant Effect of MLL-AF4 by Activation Of Wild-Type MLL. *Oncogenesis* (2014) 3:e127. doi: 10.1038/oncsis.2014.39
150. Xia ZB, Anderson M, Diaz MO, Zeleznik-Le NJ. MLL Repression Domain Interacts With Histone Deacetylases, the Polycomb Group Proteins HPC2 and BMI-1, and the Corepressor C-Terminal-Binding Protein. *Proc Natl Acad Sci U S A* (2003) 100(14):8342–7. doi: 10.1073/pnas.1436338100
151. Lenard A, Xie HM, Pastuer T, Shank T, Libbrecht C, Kingsley M, et al. Epigenetic Regulation of Protein Translation in KMT2A-Rearranged AML. *Exp Hematol* (2020) 85:57–69. doi: 10.1016/j.exphem.2020.04.007
152. Li S, Mason CE, Melnick A. Genetic and Epigenetic Heterogeneity in Acute Myeloid Leukemia. *Curr Opin Genet Dev* (2016) 36:100–6. doi: 10.1016/j.gde.2016.03.011
153. Wouters BJ, Delwel R. Epigenetics and Approaches to Targeted Epigenetic Therapy in Acute Myeloid Leukemia. *Blood* (2016) 127(1):42–52. doi: 10.1182/blood-2015-07-604512
154. Ellmeier W, Seiser C. Histone Deacetylase Function in CD4(+) T Cells. *Nat Rev Immunol* (2018) 18(10):617–34. doi: 10.1038/s41577-018-0037-z
155. Yang Y, Wang Y. Role of Epigenetic Regulation in Plasticity of Tumor Immune Microenvironment. *Front Immunol* (2021) 12:640369. doi: 10.3389/fimmu.2021.640369
156. Boila LD, Sengupta A. Evolving Insights on Histone Methylome Regulation in Human Acute Myeloid Leukemia Pathogenesis and Targeted Therapy. *Exp Hematol* (2020) 92:19–31. doi: 10.1016/j.exphem.2020.09.189
157. Dahiya S, Beier UH, Wang L, Han R, Jiao J, Akimova T, et al. HDAC10 Deletion Promotes Foxp3(+) T-Regulatory Cell Function. *Sci Rep* (2020) 10 (1):424. doi: 10.1038/s41598-019-57294-x
158. Banik D, Moufarrij S, Villagra A. Immunoepigenetics Combination Therapies: An Overview of the Role of HDACs in Cancer Immunotherapy. *Int J Mol Sci* (2019) 20(9):1–29. doi: 10.3390/ijms20092241
159. Clara JA, Monge C, Yang Y, Takebe N. Targeting Signalling Pathways and the Immune Microenvironment of Cancer Stem Cells - A Clinical Update. *Nat Rev Clin Oncol* (2020) 17(4):204–32. doi: 10.1038/s41571-019-0293-2

Conflict of Interest: The authors declare that the research was conducted in the absence of any commercial or financial relationships that could be construed as a potential conflict of interest.

frontiers in Oncology

CLINICAL TRIAL
published: 03 September 2021
doi: 10.3389/fonc.2021.726926

A Phase II Trial of the Double Epigenetic Priming Regimen Including Chidamide and Decitabine for Relapsed/Refractory Acute Myeloid Leukemia

Jia Yin[1,2†], Chao-Ling Wan[1,2†], Ling Zhang[1,2†], Hao Zhang[3†], Lian Bai[4], Hai-Xia Zhou[1,2], Ming-Zhu Xu[1,2], Li-Yun Chen[1,2], Chong-Sheng Qian[1,2], Hui-Ying Qiu[1,2], Su-Ning Chen[1,2], Xiao-Wen Tang[1,2], De-Pei Wu[1,2], Yan-Ming Zhang[5], Ai-Ning Sun[1,2*] and Sheng-Li Xue[1,2*]*

[1] National Clinical Research Center for Hematologic Diseases, Jiangsu Institute of Hematology, The First Affiliated Hospital of Soochow University, Suzhou, China, [2] Institute of Blood and Marrow Transplantation, Collaborative Innovation Center of Hematology, Soochow University, Suzhou, China, [3] Department of Hematology, The Affiliated Hospital of Jining Medical College, Jining, China, [4] Department of Hematology, Canglang Hospital of Suzhou, Suzhou, China, [5] Department of Hematology, The Affiliated Huai'an Hospital of Xuzhou Medical University and The Second People's Hospital of Huai'an, Huai'an, China

Objective: To explore the role of chidamide, decitabine plus priming regimen in the salvage treatment of relapsed/refractory acute myeloid leukemia.

Methods: A clinical trial was conducted in relapsed/refractory acute myeloid leukemia patients using chidamide, decitabine, cytarabine, idarubicin, and granulocyte-colony stimulating factor, termed CDIAG, a double epigenetic priming regimen.

Results: Thirty-five patients were recruited. Three patients received 2 treatment cycles. In 32 evaluable patients and 35 treatment courses, the completed remission rate (CRR) was 42.9%. The median OS time was 11.7 months. The median OS times of responders were 18.4 months, while those of nonresponders were 7.4 months (P = 0.015). The presence of RUNX1 mutations was associated with a high CRR but a short 2-year OS (P = 0.023) and PFS (P = 0.018) due to relapse after treatment. The presence of IDH mutations had no effect on the remission rate (80.0% *vs*. 73.3%), but showed a better OS (2-year OS rate: 100.0% *vs*. 28.9%). Grade 3/4 nonhematological adverse events included pneumonia, hematosepsis, febrile neutropenia, skin and soft tissue infection and others.

Conclusion: The double epigenetic priming regimen (CDIAG regimen) showed considerably good antileukemia activity in these patients. Adverse events were acceptable according to previous experience. The study was registered as a clinical trial.

Clinical Trial Registration: https://clinicaltrials.gov/, identifier:NCT03985007

Keywords: epigenomics, histone deacetylase inhibitor (HDACi), CDIAG regimen, relapsed/refractory acute myeloid leukemia, salvage therapy

OPEN ACCESS

Edited by:
Fei GAO,
Beijing Genomics Institute (BGI), China

Reviewed by:
Sergiu Pasca,
Iuliu Haţieganu University of Medicine and Pharmacy, Romania
Garima Pandey,
Moffitt Cancer Center, United States

***Correspondence:**
Sheng-Li Xue
slxue@suda.edu.cn
Ai-Ning Sun
sunaining@suda.edu.cn
Yan-Ming Zhang
zhangyanming2005@126.com

†These authors have contributed equally to this work and share first authorship

Specialty section:
This article was submitted to Hematologic Malignancies, a section of the journal Frontiers in Oncology

Received: *17 June 2021*
Accepted: *20 August 2021*
Published: *03 September 2021*

Citation:
Yin J, Wan C-L, Zhang L, Zhang H, Bai L, Zhou H-X, Xu M-Z, Chen L-Y, Qian C-S, Qiu H-Y, Chen S-N, Tang X-W, Wu D-P, Zhang Y-M, Sun A-N and Xue S-L (2021) A Phase II Trial of the Double Epigenetic Priming Regimen Including Chidamide and Decitabine for Relapsed/Refractory Acute Myeloid Leukemia. Front. Oncol. 11:726926. doi: 10.3389/fonc.2021.726926

INTRODUCTION

Although treatment of Acute myeloid leukemia (AML) is rapidly progressing, approximately 10% to 40% of newly diagnosed AML patients cannot achieve complete remission (CR) through induction chemotherapy, and more than 50% of AML patients will ultimately relapse (1). For patients with relapsed/refractory (R/R) AML, the goal of chemotherapy varies from achieving long-term remission to providing a "bridge" to stem cell transplantation (SCT). Most conventional chemotherapeutic drugs have a low reinduction remission rate of nearly 1/3, poor tolerability and a prolonged bone marrow (BM) suppression stage, often leading to serious infection, high mortality, and a short survival (2). Therefore, it is crucial to explore and formulate reasonable and effective combined therapeutic strategies to undergo curative treatment with allogeneic stem cell transplantation (allo-SCT) in CR status (3).

Although several new small-molecule inhibitors have been developed (e.g., ABT-199, midostaurin, and *IDH1/2* inhibitor) and have shown promising results in R/R AML treatment, they are not currently commercially available in mainland China. In recent decades, epigenetic treatment for hypermethylation or histone deacetylation has been a major breakthrough in AML treatment (4). The application of DNA demethylation drugs involved in epigenetic regulation to elderly (age ≥ 60 years) AML and R/R AML patients was the IA category recommendation for first-line induction therapy in the NCCN guidelines (5). Chidamide is the first subtype-selective oral histone deacetylation inhibitor (HDACi) commercially available in mainland China and has been certified internationally by the FDA because it is effective in treating R/R peripheral T-cell lymphoma (PTCL) (6). Chidamide possesses potent HDAC inhibitory properties by terminating the deacetylation of histones H3 and H4 *via* inhibiting HDAC types 1, 2, 3, and 10. Selective targeting of individual HDACs causes differentiation, apoptosis, cell cycle inhibition, migration inhibition, susceptibility to chemotherapy and anti-angiogenesis (7, 8).

In the treatment of R/R AML with low-dose cytarabine and anthracycline combined with granulocyte-colony stimulating factor (G-CSF) (priming regimen) (9), the sensitizing effect of hematopoietic growth factors on leukemic cells enhances the cytotoxicity of chemotherapy in AML. Previous studies have suggested that the combination of decitabine with G-CSF, low-dose cytarabine and aclarubicin (DCAG) improved the CR rate and was well-tolerated in newly diagnosed elderly AML patients (10). Moreover, patients with R/R or high-risk AML were treated with the DCAG regimen, which was proven to overcome drug resistance and improve therapeutic efficacy (11). HDACis in monotherapy are modestly active in high-risk myelodysplastic syndrome (MDS) and AML, and *in vitro* evidence supports the synergy between hypomethylating agents (HMAs) and HDACis (12). Decitabine used concurrently or sequentially with vorinostat (an HDACi) was safe and well tolerated in patients with R/R AML (n=29), with responses observed in 15% of patients (13). Several of the above rationales led us to design a regimen that included chidamide, decitabine, idarubicin, cytarabine, and G-CSF (the CDIAG double epigenetic priming regimen) to treat patients with R/R AML.

MATERIALS AND METHODS

Patients

The trial was conducted at four medical centers (the First Affiliated Hospitals of Soochow University, Affiliated Hospital of Jining Medical University, Second People's Hospital of Huai'an, and Canglang Hospital of Suzhou), and the investigational agent chidamide was provided by Shenzhen Chipscreen Biosciences Ltd. (Shenzhen, China) under an agreement. All study subjects provided their voluntary, written informed consent. The current study was conducted in accordance with the Declaration of Helsinki. The protocol and all its amendments were approved by the Ethics Committee of the First Affiliated Hospital of Soochow University (ClinicalTrials.gov identifier NCT03985007).

Eligible patients met the R/R AML [non-acute promyelocytic leukemia (non-APL)] criteria (**Figure 1** and **Supplemental Table 1**). At enrollment, the patients were required to be 18 to 70 years of age and have an Eastern Cooperative Oncology Group (ECOG) performance status score less than 3, adequate organic function, and no severe complications, such as active infections and bleeding. Women of childbearing potential were required to practice adequate birth control while participating in the protocol. The exclusion criteria were as follows: unable to tolerate induction chemotherapy and a life expectancy of less than 1 month. The principal investigators performed BM morphology, immunophenotyping, cytogenetics, and molecular genetic analyses by reviewing central laboratory reports.

Study Design and Objectives

The therapeutic regimen comprised chidamide (30 mg orally twice every week for 2 weeks on days 1, 4, 8, and 11), decitabine [20 mg/m^2 intravenously daily for 5 days (d1-d5)], and the IAG regimen [cytarabine (10 mg/m^2 subcutaneously every 12 hrs. on days 4-17), idarubicin (5 mg intravenously every other day on days 4, 6, 8, 10, 12, and 14), and concurrent G-CSF (200 μg/m^2/day subcutaneously daily on days 3-17)] (**Supplemental Table 2**). The patients were removed from the study therapy for disease progression, symptomatic deterioration, or per patient request. Subsequent therapy after CDIAG for patients who did not receive SCT is described in detail in **Supplemental Table 3**. Supportive treatments, including G-CSF, the transfusion of RBCs or PLTs, and antibiotics, could be routinely administered during CDIAG treatment.

The primary objective of this phase II trial was to evaluate the ORR (confirmed CR, CRi, MLFS and PR) and CR (confirmed CR and CRi) rate by a BM examination based on central site review (**Supplemental Table 4**). The secondary objectives were to estimate the OS, PFS, and RFS and to assess toxicity. The OS duration was measured from the onset of CDIAG treatment until death due to any cause or censored for patients who remained alive at the time of assessment. PFS was defined as the time from

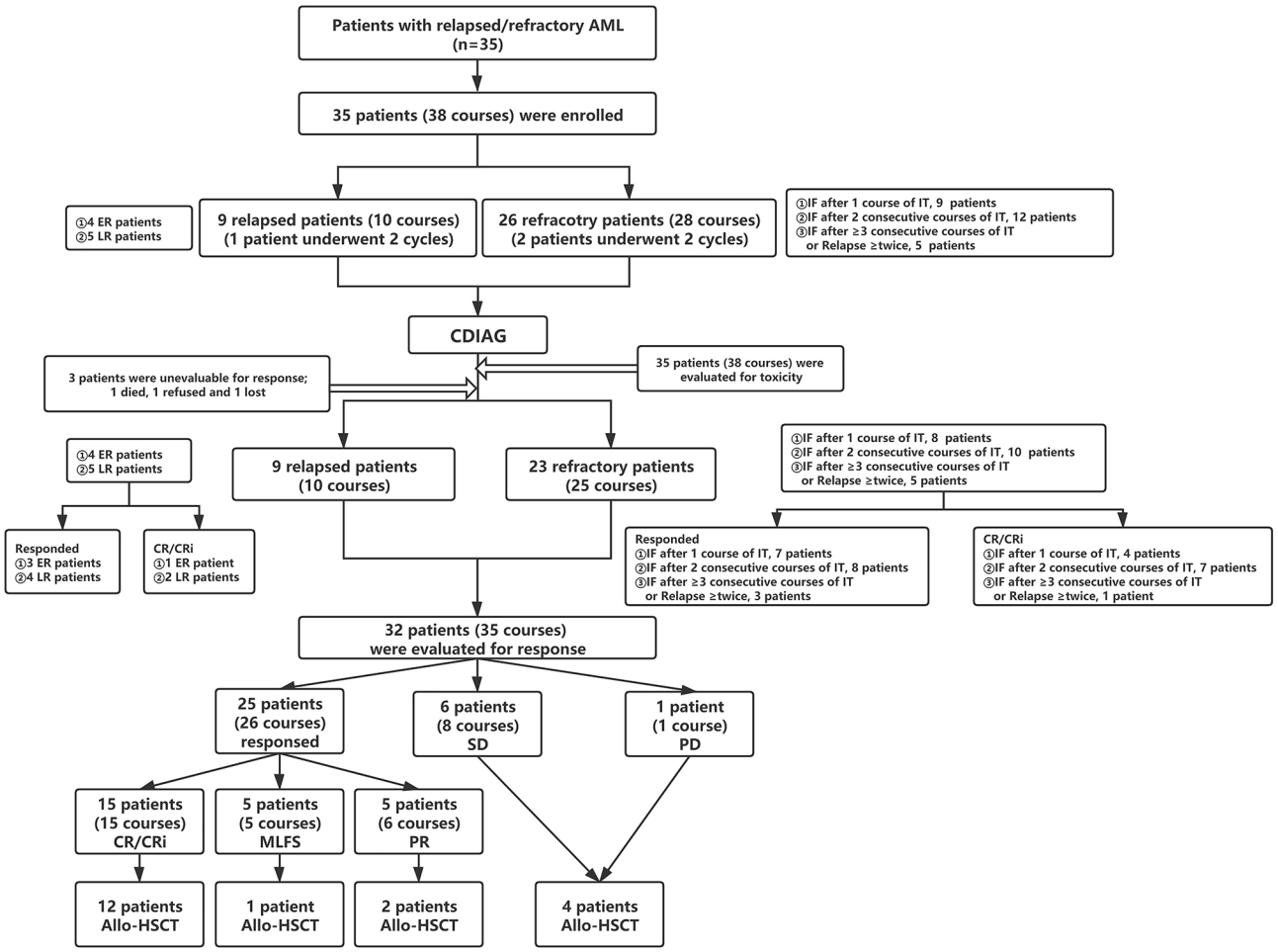

FIGURE 1 | Flow diagram for patient categorization and treatment. AML, acute myeloid leukemia; ER, early relapse; LR, late relapse; IT, induction therapy; IF, induction failure; CR, complete remission; Cri, CR with incomplete hematologic recovery; MLFS, morphologic leukemia-free state; PR, partial response; SD, stable disease, PD, progressive disease; Allo-HSCT, allogeneic hematopoietic stem cell transplantation.

the date of entry into the trial until the date of disease progression at any site, including distant metastasis or second primary tumors, or death. RFS was defined only for patients who achieved CR or CRi and was measured from the date of achieving remission until the date of relapse or death from any cause. Patients not known to have relapsed or died at the last follow-up were censored on the date they were last examined.

Assessments

Clinical data, biologic data (BM smears and MRD with 10-color MFC afforded $1{:}10^{-4}$ to $1{:}10^{-5}$ level sensitivity]), and response assessment were centrally reviewed. Twenty-four days after the start of treatment (7 days after the end of therapy), the efficacy was evaluated in the BM. Patients who did not achieve CR/CRi received a BM examination again 31 days after the commencement of treatment (14 days after the end of therapy), and the best BM response was documented. Patients who did not achieve CR/CRi after both assessments using our salvage chemotherapy regimen were allowed to receive a second course, but the evaluation was conducted for each course. Routine blood counts were monitored every day, and electrolyte levels, liver function, and creatinine levels were monitored twice weekly following CDIAG chemotherapy.

The response conditions were defined according to the 2017 ELN recommendations (3). Investigator-assessed AEs were graded according to the National Cancer Institute's Common Terminology Criteria for Adverse Events (NCI CTCAE version 5.0). Treatment-related mortality (TRM), adverse reactions in hematology (agranulocytosis days, PLT/RBC transfusion units) and nonhematological adverse reactions (**Supplemental Table 5**) (infection and organ injury) were recorded to evaluate toxicities. TRM was defined as death within 28 days after the initiation of IT.

Statistical Analysis

Thirty-five eligible patients were enrolled in this study. Standard statistical methods were used for all analyses in the trial: T-test for means between two groups, single-factor and multi-level

variance analyses for multiple groups, Fisher's exact test for categorical endpoints, Kaplan-Meier curves and the log-rank test for the time-to-event endpoints. Descriptive statistics (counts and percentages for categorical variables; mean and standard deviation, and medians and range for continuous variables) were used throughout the study. *P* values of 0.05 were considered significant for analysis. All statistical analyses were performed with Graphpad Prism (version 8.0.2). Patient age, sex, WHO classification, WBC count, BM blasts, SCT, previous HMA exposure (before CDIAG regimen), prognosis risk, response and R/R status, as well as treatments before CDIAG, were examined to assess their impact on the survival and remission rates. The follow-up cutoff date was defined as the end of June 2020.

RESULTS

Patient Characteristics

Thirty-five patients from four institutions who met the eligibility criteria were registered between 12/15/2016 and 03/29/2020 (**Table 1**). There were 19 male and 16 female patients, with a median age of 39.5 years (range, 18 to 68 years). The 35 patients included 28 (28/35, 80.0%) patients with AML, not otherwise specified (AML, NOS), 5 (5/35, 14.3%) patients with AML with myelodysplasia-related changes (AML-MRC), 1 (1/35, 2.9%) patient with AML with t(8;21)(q22;q22.1)/*RUNX1-RUNX1T1* and 1 (1/35, 2.9%) patient with AML with inv (16)(p13.1q22)/*CBFβ-MYH11*(concurrent with a *KIT* mutation). The most frequently mutated genes were *FLT3*-ITD (25.7%), *DNMT3A* (25.7%), *NPM1* (20.0%), *CEBPα* (20.0%), *WT1* (20.0%), *TET2* (17.1%), *IDH1/2* (14.3%), *NRAS* (11.4%) and *RUNX1* (11.4%).

Among the 35 patients, three were not evaluable for response and were refractory. Three of the remaining 32 eligible patients had completed 2 cycles; therefore, 32 patients and 35 courses were examined to assess efficacy (**Supplemental Table 6**). Regarding the disease status before CDIAG, 23 patients (25 courses) were refractory, and 9 patients (10 courses) relapsed. Four patients relapsed within 6 months (early relapse), 5 relapsed beyond 6 months (late relapse), 8 experienced induction failure (IF) after 1 course of IT (induction therapy), 10 had IF after 2 consecutive courses of IT, 3 had IF after ≥ 3 consecutive courses of IT, and 2 relapsed more than twice. On registering for this study, 2 patients were categorized as favorable risk, 4 as intermediate risk, and 26 as adverse risk with a poor prognosis according to the prognostic scoring system of R/R AML (**Supplemental Table 7**) (14). Nineteen of 32 (59.4%) eligible patients received allo-SCT after undergoing the prior CDIAG regimen (3 sibling donor type, 1 unrelated donor type, and 15 haploidentical donor type). Seven of 32 (21.9%) evaluable patients had received more than one cycle of HMA therapy before CDIAG.

TABLE 1 | Characteristics of the 35 enrolled patients.

Characteristic	Value
Relapsed/refractory	9/26
Male/female, No.	19/16
Age, median (range), y	39.5 (18-68)
WBC count, median (range), ×10exp9/L	26.0 (1.0-299.0)
Hemoglobin level, median (range), g/L	76 (48-127)
Platelet count, median (range), ×10exp9/L	54 (10-376)
BM blasts, median (range), %	63.0 (10-97.5)
WHO classification, No. (%)	
AML, NOS	28 (80.0)
AML with MRC	5 (14.3)
AML with t(8; 21)	1 (2.9)
AML with inv(16)	1 (2.9)
Prognosis risk for R/R AML, No. (%)	
Favorable	2 (5.7)
Intermediate	4 (11.4)
Poor	29 (82.9)
Prior HMA exposure (before the CDIAG regimen), No. (%)	
0	27 (77.1)
≥ 1	8 (22.9)
Subgroup classification of R/R AML, No. (%)	
Early relapse	4 (11.4)
Late relapse	5 (14.3)
IF after 1 course of IT	9 (25.7)
IF after 2 consecutive courses of IT	12 (34.3)
IF after ≥ 3 consecutive courses of IT	3 (8.6)
Relapse ≥ twice	2 (5.7)
Therapy after regimen, No. (%)	
SCT	19 (54.3)
Others	16 (45.7)
Genes Mutated, No. (%)	
FLT3-ITD mutated	9 (25.7)
DNMT3A mutated	9 (25.7)
NPM1 type A mutated	7 (20.0)
CEBPα biallelic mutated	7 (20.0)
WT1 mutated	7 (20.0)
TET2 mutated	6 (17.1)
IDH1/IDH2 mutated	5 (14.3)
RUNX1 mutated	4 (11.4)
NRAS mutated	4 (11.4)
FLT3-TKD mutated	3 (8.6)
U2AF1 mutated	2 (5.7)
TP53 mutated	2 (5.7)

R/R AML, relapsed/refractory AML; AML, NOS, AML, not otherwise specified; AML with MRC, AML with myelodysplasia-related changes; HMA, hypomethylating agent; SCT, stem cell transplantation; WBC, white blood cell; FLT3, FMS-like tyrosine kinase 3, FLT3-ITD, FLT3-internal tandem duplication; DNMT3A, DNA-methyltransferase 3A; NPM1, nucleophosmin 1; CEBPα, CCAAT/enhancer binding protein alpha; WT1, Wilms' tumor 1; IDH1, isocitrate dehydrogenase 1; IDH2, isocitrate dehydrogenase 2; TET2, Tet methylcytosine dioxygenase 2; RUNX1, runt-related transcription factor 1; NRAS, neuroblastoma RAS viral oncogene homolog; TP53, tumor protein 53; FLT3-TKD, FLT3-tyrosine kinase domain; U2AF1, U2 small nuclear RNA auxiliary factor 1.

Outcomes

Among the 35 patients, three withdrew before the evaluation. The overall response rate (ORR) for 35 assessable courses in 32 patients was 74.3% (95% confidence interval (CI): 59%-86%), the CR/CR with incomplete hematologic recovery (CRi) rate was 42.9% (95% CI: 25.6%-60.1%), the morphologic leukemia-free state (MLFS) rate was 14.3% (n=5), and the partial remission (PR) rate was 17.1% (n= 6). The stable disease (SD) rate was 22.9% (n= 8), and the progressive disease (PD) rate was 2.9% (n= 1). The median follow-up time was 22.1 months (range, 8.2-48.6 months) for this patient cohort. The median overall survival (OS) time was 11.7 months, and the median progression-free survival (PFS) time was 11.7 months. The survival outcomes of the entire cohort of 32 patients are shown in **Figure 2**. The 2-year

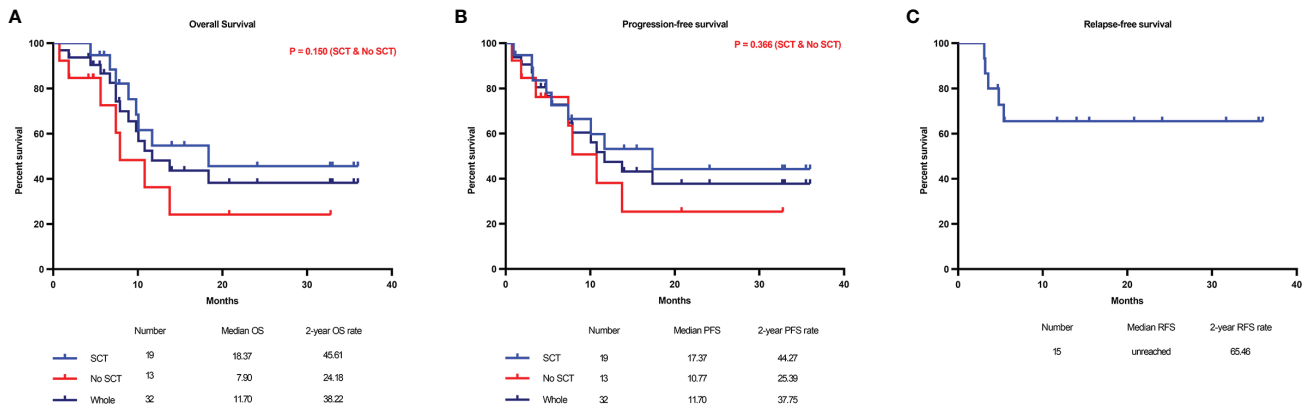

FIGURE 2 | Main study results. Kaplan–Meier graphs illustrating the overall survival **(A)** and progression-free survival **(B)** of all 32 refractory/relapsed (R/R) acute myeloid leukemia (AML) patients after the CDIAG regimen and the distinction of overall survival between patients with or without transplantation. The 2-year relapse-free survival (RFS) rate was 40.7% in 15 patients who achieved CR/CRi **(C)**.

OS, PFS and relapse-free survival (RFS) rates were 38.2% (**Figure 2A**), 37.8% (**Figure 2B**), and 65.5% (**Figure 2C**), respectively (RFS was evaluated in 15 patients who achieved CR/CRi). The primary and secondary endpoints are summarized in **Table 2**.

The ORR for the 10 CDIAG induction courses in 9 relapsed patients was 70.0% (7/10) (3 of 4 courses in 4 patients who had an early relapse and 4 of 6 courses in 5 patients who had a late relapse before CDIAG). The CR/CRi rate for the 10 courses in 9 relapsed patients was 30.0% (3/10) (only 1 of 4 courses in 4 patients who had an early relapse and 2 of 6 courses in 5 patients who had a late relapse). No difference was found in the ORR/CRR or survival rates between patients who had early and late relapses (**Table 3**).

The ORR for the 25 CDIAG induction courses in 23 refractory patients was 76.0% (19/25) (7 of 8 courses in 8 patients who had IF after 1 course of IT, 9 of 12 courses in 10 patients who had IF after 2 consecutive courses of IT, and only 3 of 5 courses in 5 patients who had IF after ≥ 3 consecutive courses of IT or relapsed ≥ twice). The CR/CRi rate for the 25 courses in 23 refractory patients was 48.0% (12/25) (4 of 8 courses in 8 patients who had IF after 1 course of IT, 7 of 12 courses in 10 patients who had IF after 2 consecutive courses of IT, and only 1 of 5 patients who had IF after ≥ 3 consecutive courses of IT or relapsed ≥ twice achieved CR/CRi by CDIAG reinduction). Among all the refractory subgroups, the best CRR of 58.3% was achieved in 12 courses of 10 patients who had IF after 2 consecutive courses of IT (**Table 3**). The 2-year OS and PFS rates for the three refractory groups were 28.6%, 60.0%, 0% and 28.6%, 54.0%, 0.0%, respectively (**Table 4**).

Five subgroups among the entire cohort of R/R AML patients had different OS and PFS rates (P = 0.011 and 0.044, respectively), in which patients who had IF after ≥ 3 consecutive courses of IT or relapsed ≥ twice had the worst survival rate, and patients who had late relapse achieved the best survival rate (**Table 4**, **Figure 3A**, and **Supplemental Figure 1A**). The 2-year OS and PFS rates of relapsed and refractory patients were 51.4% vs. 32.7% and 51.4% vs. 31.5% (P = 0.422 and 0.250), respectively.

The median OS and PFS times for patients who achieved a response were 18.4 and 17.4 months, respectively, while those for nonresponders were 7.4 and 7.4 months, respectively. Additionally, OS and PFS were significantly longer in responders than in nonresponders (P = 0.015 and 0.041, respectively) (**Table 4**, **Figure 3B**, and **Supplemental Figure 1B**). The 2-year OS and PFS rates for the 25 patients who achieved a response were 46.8% and 46.0%, respectively, while those for nonresponders (7 patients without a response after CDIAG) were 0.0% and 0.0%, respectively. The median OS and PFS rates for 15 patients who achieved CR were not available, while those for patients who did not were 10.1 and 10.1 months, respectively. The 2-year OS and PFS rates for patients who achieved CR were 58.7% and 57.3%, respectively, while those for 17 patients who could not achieve CR after CDIAG were 18.6%

TABLE 2 | Primary and secondary patient endpoints.

Endpoint (evaluable patients=32, courses= 35)	Value
Overall response, No. (%)	26 (74.3%)
Complete remission, No. (%)	15 (42.9%)
CR, No. (%)	9 (25.7%)
CRi, No. (%)	6 (17.1%)
Morphologic leukemia-free state, No. (%)	5 (14.3%)
Partial remission, No. (%)	6 (17.1%)
Stable disease, No. (%)	8 (22.9%)
Progressive disease, No. (%)	1 (2.9%)
Median OS time	11.7 months
Median PFS time	11.7 months
2-year OS rate	38.2%
2-year PFS rate	37.8%
2-year RFS rate	65.5%

OS, overall survival; PFS, progression-free survival; RFS, relapse-free survival. The ORR and CRR were evaluated for 35 courses in 32 patients. OS and PFS were evaluated in 32 patients. RFS was evaluated in 15 patients who achieved CR.

TABLE 3 | Clinical responses of R/R AML patients with subgroup univariate analysis.

Variable	Response	P-Value	OR* (95% CI)	CR/CRi	P-Value	OR* (95% CI)
Overall	26/35 (74.3%)			15/35 (42.9%)		
Age						
<51 years	22/28 (75.6%)	0.340	0.364 (0.063-2.089)	13/28 (46.4%)	0.669	0.462 (0.076-2.793)
≥51 years	4/7 (57.1%)			2/7 (28.6%)		
Sex						
Male	16/21 (76.2%)	1.000	1.280 (0.276-5.934)	11/21 (52.4%)	0.163	2.750 (0.651-11.624)
Female	10/14 (71.4%)			4/14 (28.6%)		
Blast						
<0.3	3/8 (37.5%)	**0.015**	9.583 (1.613-56.952)	2/8 (25.0%)	**0.450**	2.786 (0.475-16.345)
≥0.3	23/27 (85.2%)			13/27 (48.1%)		
WBC						
<14 × 10E9/L	7/12 (58.3%)	0.220	3.393 (0.703-16.385)	3/12 (25.0%)	0.123	3.273 (0.700-15.291)
≥14 × 10E9/L	19/23 (82.6%)			12/23 (52.2%)		
HB						
<65 g/L	7/11 (63.6%)	0.416	2.171 (0.450-10.486)	2/11 (18.2%)	0.069	5.318 (0.943-29.993)
≥65 g/L	19/24 (79.2%)			13/24 (54.2%)		
PLT						
<40 × 10E9/L	12/14 (85.7%)	0.262	0.333 (0.058-1.919)	7/14 (50.0%)	0.486	0.615 (0.157-2.419)
≥40 × 10E9/L	14/21 (66.7%)			8/21 (38.1%)		
Previous HMA or not						
Yes	5/7 (71.4%)	0.632	0.625 (0.093-4.222)	3/7 (42.9%)	0.576	0.813 (0.150-0.404)
No	20/25 (80.0%)			12/25 (48.0%)		
Prognostic score of R/R AML*						
Favorable/intermediate risk	5/7 (71.4%)	1.000	1.200 (0.189-7.628)	2/7 (28.6%)	0.672	2.167 (0.358-13.110)
Adverse risk	21/28 (75.0%)			13/28 (46.4%)		
Relapsed/Refractory						
Relapsed	7/10 (70.0%)	0.694	1.357 (0.265-6.958)	3/10 (30.0%)	0.458	2.154 (0.451-10.287)
Refractory	19/25 (76.0%)			12/25 (48.0%)		
Relapsed/Refractory subgroup						
Early relapse	3/4 (75.0%)	0.765	0.909 (0.484-1.705)	1/4 (25.0%)	0.661	1.132 (0.651-1.969)
Late relapse	4/6 (66.7%)			2/6 (30.0%)		
IF after 1 course of IT	7/8 (87.5%)			4/8 (50.0%)		
IF after 2 consecutive courses of IT	9/12 (75.0%)			7/12 (58.3%)		
IF after ≥ 3 consecutive courses of IT or relapse ≥ twice	3/5 (60.0%)			1/5 (20.0%)		
Genes Mutated						
FLT3-ITD^{mut}	7/10 (70.0%)	0.694	0.737 (0.144-3.778)	3/10 (30.0%)	0.458	0.464 (0.097-2.217)
FLT3-ITD^{wt}	19/25 (76.0%)			12/25 (48.0%)		
DNMT3A^{mut}	6/9 (66.7%)	0.665	0.600 (0.114-3.153)	3/9 (33.3%)	0.700	0.583 (0.119-2.849)
DNMT3A^{wt}	20/26 (76.9%)			12/26 (46.2%)		
NPM1 type A^{mut}	3/7 (42.9%)	**0.055**	0.163 (0.027-0.969)	2/7 (28.6%)	**0.669**	0.462 (0.076-2.793)
NPM1 type A^{wt}	23/28 (82.1%)			13/28 (46.4%)		
CEBPα biallelic^{mut}	5/7 (71.4%)	1.000	0.833 (0.131-5.297)	4/7 (57.1%)	0.669	2.061 (0.385-11.035)
CEBPα biallelic^{wt}	21/28 (75.0%)			11/28 (39.3%)		
WT1^{mut}	6/7 (85.7%)	0.648	2.400 (0.248-23.236)	4/7 (57.1%)	0.669	2.061 (0.385-11.035)
WT1^{wt}	20/28 (71.4%)			11/28 (39.3%)		
TET2^{mut}	3/6 (50.0%)	0.156	0.261 (0.042-1.635)	3/6 (50.0%)	1.000	1.417 (0.243-8.256)
TET2^{wt}	23/29 (79.3%)			12/29 (41.4%)		
IDH1/IDH2^{mut}	4/5 (80.0%)	0.747	1.455 (0.141-15.039)	2/5 (40.0%)	1.000	0.872 (0.127-6.003)
IDH1/IDH2^{wt}	22/30 (73.3%)			13/30 (43.3%)		
RUNX1^{mut}	4/4 (100.0%)	**0.303**	Not reached	4/4 (100.0%)	**0.026**	Not reached
RUNX1^{wt}	21/31 (67.7%)			11/31 (35.9%)		
NRAS^{mut}	2/3 (66.7%)	0.758	0.667 (0.053-8.372)	2/3 (66.7%)	0.794	2.923 (0.239-35.681)
NRAS^{wt}	24/32 (75.0%)			13/32 (40.6%)		
FLT3-TKD^{mut}	2/3 (66.7%)	0.758	0.667 (0.053-8.372)	2/3 (66.7%)	0.794	2.923 (0.239-35.681)
FLT3-TKD^{wt}	24/32 (75.0%)			13/32 (40.6%)		

OR, odds ratio.

The bolded text means that there are significant differences between groups.

and 18.7%, respectively (P = 0.067 and 0.179, respectively) (**Table 4**, **Figure 3C**, and **Supplemental Figure 1C**).

The minimal residual disease (MRD) of flow cytometry (FCM) was analyzed in 29 patients and divided into the following three groups: 6 patients had MRD ≥ 10-1, 15 patients had MRD <10-1 and >10-3, 8 patients had MRD ≤10-3. The OS of the three groups were consistent with the clinical estimate. The lowest MRD group achieved the best survival (2-year OS rate: 75.0%), the MRD ≥ 10-1 group showed the worst OS and PFS (2-year OS rate: 0.0%), and the survival of the

TABLE 4 | Overall survival and progress-free survival univariate analysis.

Variable	Alive (%)	HR (95%CI)	Median OS (months)	2-year OS (%)	P-Value	HR (95%CI)	Median PFS (months)	2-year PFS (%)	P-Value
Overall	17/35(48.6)	-	11.7	38.2	-	-	11.7	37.8	-
Age									
< 51 years	13/25(52.0)	1.470(0.470-4.605)	10.1	32.1	0.545	1.586(0.525-4.796)	10.8	31.3	0.462
≥ 51 years	4/7(57.1)	0.680(0.217-2.130)	Not reached	53.6		0.630(0.209-1.906)	Not reached	53.3	
Sex									
Male	10/19(52.6)	0.642(0.213-1.98)	18.4	43.5	0.391	0.711(0.244-2.073)	11.7	41.5	0.501
Female	7/13(53.8)	1.558(0.516-4.701)	10.1	29.0		1.407(0.483-4.104)	10.8	31.1	
BM-Blast									
< 0.3	3/6(42.9)	1.550(0.359-6.698)	8.9	Not reached	0.487	1.458(0.350-6.070)	7.4	Not reached	0.549
≥ 0.3	14/26(53.8)	0.645(0.149-2.787)	13.8	39.5		0.686(0.165-2.857)	13.8	38.9	
WBC									
< 14 × 10E9/L	5/10(50.0)	1.151(0.383-3.464)	10.1	30.9	0.795	1.052(0.362-3.058)	10.8	30.9	0.925
≥ 14 × 10E9/L	12/22(54.5)	0.869(0.289-2.613)	13.8	40.5		0.951(0.327-2.765)	13.8	40.1	
HB									
< 65 g/L	3/9(33.3)	2.240(0.672-7.463)	7.9	15.2	0.112	2.067(0.639-6.684)	7.4	15.2	0.147
≥ 65 g/L	14/23(60.9)	0.447(0.134-1.488)	13.8	49.2		0.484(0.150-1.564)	13.8	47.7	
PLT									
< 40 × 10E9/L	7/13(53.8)	0.790(0.286-2.183)	18.4	34.0	0.652	0.966(0.360-2.587)	11.7	31.1	0.944
≥ 40 × 10E9/L	10/19(52.6)	1.265(0.458-3.494)	10.1	39.0		1.036(0.387-2.776)	10.1	40.9	
Previous HMA or not									
Yes	3/7(42.6)	1.885(0.477-7.449)	8.9	Not reached	0.267	1.830(0.471-7.110)	5.4	Not reached	0.285
No	14/25(51.9)	0.531(0.134-2.097)	13.8	38.9		0.546(0.141-2.123)	11.7	37.9	
Prognostic score of R/R AML[†]									
Favorable/intermediate risk	2/6(33.3)	1.750(0.458-6.687)	8.9	20.0	0.324	1.485(0.419-5.271)	7.9	20.0	0.484
Adverse risk	15/26(57.7)	0.572(0.150-2.185)	18.4	43.4		0.673(0.190-2.390)	13.8	42.4	
Relapsed/Refractory									
Relapsed	6/9(66.7)	0.601(0.198-1.825)	Not reached	51.4	0.422	0.489(0.171-1.397)	Not reached	51.4	0.250
Refractory	12/23(52.2)	1.664(0.548-5.055)	11.7	32.7		2.045(0.716-5.844)	11.7	31.5	
Relapsed/Refractory subgroup									
Early relapse	2/4(50.0)	-	10.1	33.3	**0.011**	-	10.1	33.3	**0.044**
Late relapse	4/5(80.0)		Not reached	66.7			Not reached	66.7	
IF after 1 course of IT	3/8(37.5)		13.8	28.6			13.8	28.6	
IF after 2 consecutive courses of IT	7/10(70.0)		Not reached	60.0			Not reached	54.0	
IF after ≥ 3 consecutive courses of IT or relapse ≥ twice	1/5(20.0)		7.4	0.0			5.4	0.0	
Genes Mutated									
FLT3-ITD^{mut}	5/9(55.6)	1.014(0.322-3.195)	13.8	45.7	0.981	0.936(0.307-2.850)	13.8	48.6	0.908
FLT3-ITD^{wt}	12/23(52.2)	0.987(0.313-3.110)	10.8	35.6		1.068(0.351-3.253)	10.8	34.4	
DNMT3A^{mut}	6/9(66.7)	0.516(0.175-1.519)	Not reached	62.2	0.292	0.701(0.246-1.999)	Not reached	53.3	0.531
DNMT3A^{wt}	11/23(47.8)	1.937(0.658-5.701)	10.1	28.7		1.427(0.500-4.071)	10.1	29.8	
NPM1 type A^{mut}	3/7(42.9)	1.765(0.460-6.773)	13.8	26.8	0.320	1.407(0.405-4.886)	13.8	26.8	0.549
NPM1 type A^{wt}	14/25(56.0)	0.567(0.148-2.174)	11.7	41.4		0.711(0.205-2.469)	11.7	40.0	
CEBPα biallelic^{mut}	4/7(57.1)	1.081(0.296-3.948)	8.9	42.9	0.904	1.430(0.409-4.999)	7.4	35.7	0.531
CEBPα biallelic^{wt}	13/25(52.0)	0.925(0.253-3.380)	11.7	36.5		0.699(0.200-2.444)	13.8	37.4	
WT1^{mut}	4/7(57.1)	1.160(0.308-4.365)	10.8	25.0	0.816	1.015(0.288-3.585)	11.7	26.7	0.981
WT1^{wt}	13/25(52.0)	0.862(0.229-3.243)	13.8	40.6		0.985(0.279-3.477)	13.8	39.1	
TET2^{mut}	3/6(50.0)	1.866(0.389-8.947)	7.4	27.8	0.319	1.989(0.492-8.045)	7.4	22.2	0.218

(Continued)

TABLE 4 | Continued

Variable	Alive (%)	HR (95%CI)	Median OS (months)	2-year OS (%)	P-Value	HR (95%CI)	Median PFS (months)	2-year PFS (%)	P-Value
TET2^{wt}	14/26(53.8)	0.536(0.112-2.571)	13.77	39.8		0.503(0.124-2.034)	13.8	40.7	
IDH1/IDH2^{mut}	5/5(100.00)	0.280(0.079-0.997)	Not reached	100.0	**0.050**	0.278(0.082-0.939)	Not reached	100.0	**0.039**
IDH1/IDH2^{wt}	12/27(44.4)	3.566(1.003-12.680)	10.1	28.8		3.595(1.065-12.140)	10.1	28.2	
RUNX1^{mut}	0/4(0.00)	0.294(0.053-1.630)	7.8	0.0	**0.023**	0.283(0.495-1.622)	4.5	0.0	**0.018**
RUNX1^{wt}	18/31(58.1)	3.405(0.613-18.900)	18.4	46.1		3.531(0.616-20.220)	17.4	44.6	
NRAS^{mut}	1/3(33.3)	1.413(0.258-7.736)	10.8	0.0	0.642	1.485(0.263-8.394)	11.7	0.0	0.593
NRAS^{wt}	16/29(55.2)	0.708(0.129-3.877)	13.8	41.4		0.673(0.119-3.805)	13.8	40.5	
FLT3-TKD^{mut}	1/3(33.3)	1.084(0.234-5.027)	13.8	33.3	0.915	1.022(0.230-4.555)	13.8	33.3	0.976
FLT3-TKD^{wt}	16/29(55.2)	0.922(0.199-4.277)	11.7	38.7		0.978(0.220-4.357)	11.7	38.1	
Response									
Yes	15/25(60.0)	0.296(0.066-1.341)	18.4	46.8	**0.015**	0.358(0.087-1.469)	17.4	46.0	**0.041**
No	2/7(28.6)	3.374(0.746-15.260)	7.4	0.0		2.797(0.681-11.490)	7.4	0.0	
CR/CRi									
Yes	10/15(66.7)	0.384(0.1384-1.067)	Not reached	58.7	**0.067**	0.511(0.191-1.365)	Not reached	57.3	**0.179**
No	7/17(41.2)	2.603(0.938-7.224)	10.1	18.6		1.959(0.733-5.236)	10.1	18.7	
MRD									
$\geq 10^{-1}$	2/6(33.3)	-	7.40	0.0	**<**	-	7.4	0.0	**0.005**
$<10^{-1}$ and $\geq 10^{-3}$	8/15(53.3)		18.4	43.1	**0.0001**		17.4	40.2	
$<10^{-3}$	7/8(87.5)		Not reached	75.0			Not reached	75.0	
SCT or not									
Yes	11/19(57.9)	0.485(0.160-1.467)	18.4	45.6	**0.150**	0.639(0.226-1.810)	17.4	44.3	**0.366**
No	6/13(46.2)	2.062(0.682-6.235)	7.9	24.2		1.564(0.553-4.427)	10.8	25.4	
SCT with a response or not									
Yes	9/15(60.0)	0.194(0.011-3.528)	Not reached	51.3	**0.017**	0.387(0.044-3.430)	17.4	48.9	**0.204**
No	2/4(50.0)	5.146(0.283-93.420)	7.4	0.0		2.584(0.292-22.910)	7.4	0.0	
SCT with CR/CRi or not									
Yes	8/12(66.7)	0.438(0.097-1.975)	Not reached	60.0	0.227	0.605(0.150-2.440)	Not reached	57.1	0.447
No	3/7(42.9)	2.282(0.506-10.290)	10.1	22.9		1.651(0.410-6.650)	10.1	22.9	
Responders underwent SCT or not									
Yes	9/15(60.0)	0.493(0.117-2.075)	Not reached	51.3	0.260	0.710(0.193-2.617)	17.4	48.9	0.579
No	6/10(60.0)	2.027(0.482-8.521)	10.8	36.0		1.408(0.382-5.186)	10.8	39.4	
CR/CRi underwent SCT or not									
Yes	8/12(66.7)	0.523(0.341-8.106)	Not reached	60.0	0.558	0.956(0.108-8.450)	Not reached	57.1	0.965
No	2/3(66.7)	1.902(0.123-29.320)	13.2	Not reached		1.049(0.118-9.294)	Not reached	66.7	

†Prognostic score was graded by the European Prognostic Index score in ELN. HR, hazards ratio.
The bolded text means that there are significant differences between groups.

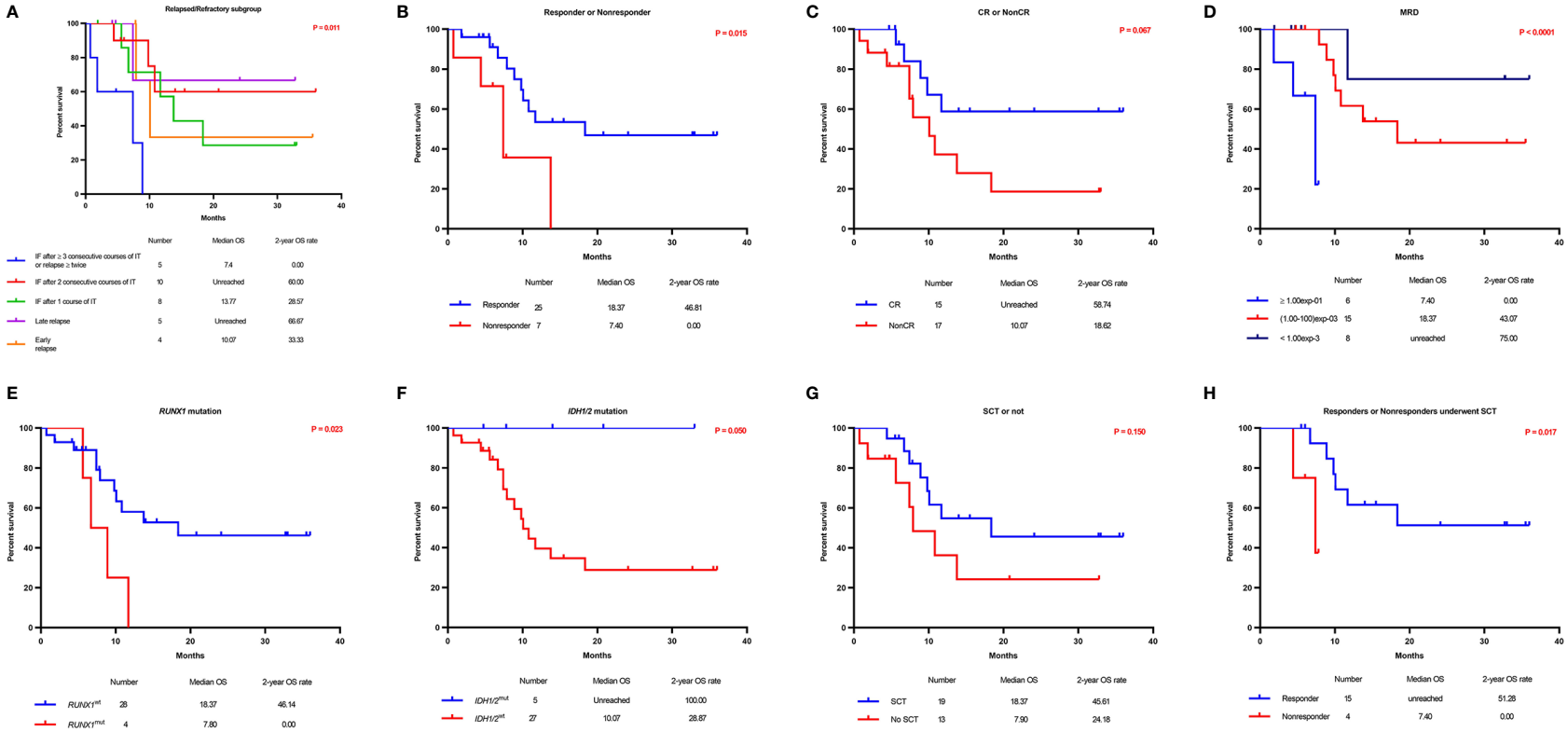

FIGURE 3 | Overall survival according to prognostic characteristics and treatment allocation. Kaplan–Meier graphs illustrating the overall survival of 32 R/R AML patients with 5 different subgroups **(A)**, responders *versus* nonresponders **(B)**, patients who achieved CR *versus* those who did not **(C)**, patients according to the MRD status **(D)**, patients with *RUNX1*^{mut} *versus RUNX1*^{wt} **(E)**, patients with *IDH*^{mut} *versus IDH*^{wt} **(F)**, patients who received SCT *versus* those who did not **(G)**, and responders who underwent SCT *versus* nonresponders who underwent SCT **(H)**.

MRD <10-1 and >10-3 group was intermediate (2-year OS rate, 43.1 months). The survival difference among the three groups was statistically significant (OS: P < 0.0001; PFS: P = 0.005) (**Table 4**, **Figure 3D**, and **Supplemental Figure 1D**).

Among the 32 evaluable patients, all 4 with a RUNX1 gene mutation achieved CR after one course of the CDIAG regimen. However, in 28 patients with wild-type RUNX1, the response rate for 31 CDIAG induction courses was 67.7% (21/31), and the CR rate was 35.9% (11/31). The CRR in the RUNX1mut group was significantly higher than that in the RUNX1wt group (P = 0.026) (**Table 3**). The presence of the RUNX1 mutations was associated with a short median OS (7.8 *vs*. 18.4 months; P = 0.023) and PFS (4.5 *vs*. 17.4 months; P = 0.018) times, with a 2-year OS rate of 0.0% *vs*. 46.1% and a 2-year PFS rate of 0.0% *vs*. 44.6% (**Table 4**, **Figure 3E**, and **Supplemental Figure 1E**).

No significant difference was found in the response rate between five IDHmut (including IDH1 and IDH2) patients and 22 IDHwt patients (80.0% *vs*. 73.3%; P = 0.747). All five IDHmut patients were still alive. The survivals of these two groups were obviously different (2-year OS rate: 100.0% *vs*. 28.9%, P = 0.050; 2-year PFS rate, 100.0% *vs*. 28.2%, P = 0.039) (**Table 4**, **Figure 3F**, and **Supplemental Figure 1F**).

The ORR for 10 courses in 9 FLT3-ITDmut patients after the CDIAG regimen reached 70.0% (7/10) and that for 25 courses in 23 FLT3-ITDwt patients reached 76.0% (19/25). The CRR for 10 courses in 9 FLT3-ITDmut patients reached 30.0% (3/10) and that for 25 courses in 23 FLT3-ITDwt patients reached 48.0% (12/25). No difference was found in the ORR or CRR between FLT3-ITDmut and FLT3-ITDwt patients (P = 0.694 and 0.458, respectively), but FLT3-ITDwt patients showed a shorter median OS time (10.8 *vs*. 13.8 months, P = 0.981) and PFS time (10.77 *vs*. 13.77 months, P = 0.908) (**Table 4**). Additionally, no significant correlation was found between mutations in other genes (CEBPα, DNMT3A, NPM1, TET2, WT1, NRAS, FLT3-TKD) and the remission or survival rate.

Among the entire cohort, nineteen of the 32 eligible patients (59.4%) successfully bridged to SCT after CDIAG treatment. The 2-year OS and PFS rates of the 19 patients who had undergone SCT were 45.6% and 44.3%, respectively, and the rates of the 13 patients who did not undergo SCT were 24.2% and 25.4%, respectively. No significant difference was found in the OS or PFS between these groups (P = 0.150 and 0.366, respectively) (**Table 4**, **Figure 3G**, and **Supplemental Figure 1G**).

Among the 19 patients who had undergone SCT, the 2-year OS rate of 15 responders was significantly higher than that of 4 nonresponders (51.3% *vs*. 0.0%; P = 0.017), but no difference was found in the 2-year PFS rate (48.9% *vs*. 0.0%; P = 0.204) (**Table 4**, **Figure 3H**, and **Supplemental Figure 1H**). For the 25 responders, the 2-year OS and PFS rates of the 15 responders who had undergone SCT were not significantly different from those of the 10 responders who had not undergo SCT (51.3% *vs*. 36.0%, P = 0.260; 48.9% *vs*. 39.4%, P = 0.579).

Of the 10 patients who achieved a response after CDIAG but did not receive SCT, four (including one who achieved CR) died from PD, two were lost to follow-up with a PD status, two (including one who achieved CR) were alive with a PD status, and only two (including one who achieved CR) were alive with a remission status under chemotherapy at the time of analysis.

At the time of analysis, five of 10 patients who received SCT from haploidentical donors survived and achieved CR; 1 died because of TRM, 3 died from relapse, and one was alive after relapse. One patient who received SCT from a sibling donor was lost to follow-up, and 1 patient who received a transplant from an unrelated donor remained alive and achieved CR. No early TRM (within 60 days of SCT) occurred in the 19 patients who had undergone SCT after the CDIAG regimen.

No difference was found in the ORR (71.4%, 5/7 *vs*. 80.0%, 20/25; P = 0.632), CRR (42.9%, 3/7 *vs*. 48.0%, 12/25; P = 0.576), median OS time (8.9 *vs*. 13.8 months, P = 0.267) or median PFS time (5.4 *vs*. 11.7 months, P = 0.285) between patients who had been treated with or without HMA (primary decitabine). Additionally, the 2-year OS and PFS rates were not significantly different between the groups (not reached *vs*. 38.9% and not reached *vs*. 37.9% (**Table 4**).

No significant difference was found in the ORR and CRR between groups with different prognosis risks: the ORR and CRR for 7 courses in 6 patients with a favorable or intermediate risk were 71.4% (5/7) and 28.6% (2/7), respectively, while those for 28 courses in 26 patients with an adverse risk were 75.0% (21/28) and 46.4% (13/28), respectively (P = 1.000 and 0.672, respectively); the 2-year OS rates were 20.0% *vs*. 43.4%, and the 2-year PFS rates were 20.0% *vs*. 42.4%, respectively, comparing the two groups (P = 0.324 and 0.484, respectively) (**Table 4** and **Supplemental Table 2**).

Age, sex, BM blasts, the white blood cell (WBC) count, the hemoglobin count and the platelet (PLT) count did not affect the response rates.

Safety

Thirty-five patients received 38 courses of IT. Thus, all the toxicological evaluations were performed during these 38 courses.

For hematological adverse events (AEs), the median time for neutropenia was 18.4 (0-77) days, and G-CSF injections were administered in 34 of 38 courses because the neutrophil count was less than 1.0×10exp9/L. All the patients received red blood cell (RBC) transfusions at an average of 6 Units (1200 mL) because the hemoglobin levels were below 60 g/L. Additionally, all the patients required platelet transfusions at an average of 7.3 units per course because the platelet counts were below 10×10exp9/L.

The nonhematological AEs are summarized in **Supplemental Table 3**. Two (5.3%) patients died of AEs that were deemed treatment-related (both because of severe deterioration of liver and kidney function after the infective shock). Overall, the treatment was well tolerated, although most side effects were grade 3. The reason for this high rate of grade 3 AEs was that, in most cases, inflammation required intravenous treatment and blood transfusion in the hypoimmune state.

DISCUSSION

The outcome of R/R AML remains poor, and treatment options are very limited. Exploring an effective and well-tolerated combination therapy is urgent. In the preclinical studies, chidamide and decitabine, two epigenetic modifiers, revealed a significant synergistic effect in both AML cell lines and primary R/R AML cells. In this phase II prospective multicenter trial, of the 32 evaluable patients treated with the CDIAG regimen, the ORR was 74.3% and CR/CRi rate was 42.9%, with a median OS of 11.7 months and a 2-year OS rate of 38.2%. Patients who achieved a response or MRD levels below 10^{-3} have a significantly better OS and PFS than those without. The clinical results were encouraging because many poor-risk individuals were enrolled and 81% of the patients had adverse cytogenetics.

SCT was plausibly the best salvage treatment option for R/R AML until the development of effective and available novel drugs (15). SCT for AML yields good results when administered to patients in a CR status (16). In a previously published prospective study, sixty-seven percent of remitters received allo-transplantation in CR2, providing a superior survival rate than no stem cell transplantation (5-year OS rate: 42% *vs*. 16%) (17). In our study, 19 patients bridged to SCT after the CDIAG regimen. Their 2-year overall survival rate was higher than that of the non-SCT group (45.6% *vs*. 24.2%; P=0.150). The results were consistent with our expectations, suggesting that the CDIAG protocol could reduce the leukemia burden before transplantation and provide a bridge for subsequent transplantation. Responders after CDIAG should receive transplantation as soon as possible.

Among our entire cohort of refractory and relapsed patients, those with PIF after ≥ 3 consecutive courses of IT or who relapsed ≥ twice had the worst OS and PFS. The 2-year survival rate of these patients was 0.0%. The patients with a late relapse had the best survival rate of 66.7%. Importantly, the survival rate of the refractory patients receiving one course of IT was worse than that of patients who received two consecutive courses of IT because of the high proportion (4/8) of *FLT3*-ITD mutations in the former group. Most studies thus far have suggested no difference in the response rate with or without previous HMA exposure (18). Although no significantly difference, patients who had received HMA therapy had a shorter OS time than those who had not. The median OS time was 8.90 months for previous HMA exposure vs. 13.8 months for no previous HMA exposure (P = 0.267). (**Table 4**). The possible mechanism underlying the shorter tendency in the survival times of such patients could be due to the drug resistance property after screening by HMA drugs.

Importantly, the response rate was improved in patients with *RUNX1* mutations (100%; 4 of 4 patients), but the increased sensitivity could not compensate for the poor prognosis associated with *RUNX1* mutation (19). The 2-year OS and PFS rates for 28 *RUNX1*^{wt} patients (courses=31) and 4 *RUNX1*^{mut} patients were 46.1% vs. 0% and 44.6% *vs*. 0.0%, respectively (P = 0.023 and 0.018, respectively). *RUNX1* is an important regulator of myeloid differentiation and effective hematopoiesis (20). HDAC1 and 3 bind to *RUNX1* and regulate the transcription activity of *RUNX1 (*21). Whether chidamide binds competitively to HDAC1 and 3 against *RUNX1* and plays a role in CDIAG IT deserves further exploration. Interestingly, even the presence of *IDH* mutation did not affect the CR rate but achieved better OS and PFS. Although several studies have investigated the incidence and prognosis of *IDH* mutations in patients with AML, the significance of *IDH* mutations on AML outcome has been unclear (22). Better survival might benefit from the impact of *IDH* on histone modifications and DNA methylation (23, 24). As mentioned above, no difference was found in the response or survival rate between *FLT3*-ITD^{mut} and *FLT3*-ITD^{wt} patients, but *FLT3*-ITD^{mut} patients had worse outcomes. Recently, Hu et al. revealed a novel resistance pathway involving *FLT3*-ITD^{mut}: in AML cells, *FLT3*-ITD^{mut} upregulates HDAC8, thereby promoting the persistence of *FLT3*-ITD^{mut} AML cells even in the presence of an *FLT3* inhibitor (25). This view confirms our findings. *FLT3*-ITD^{mut} patients achieved a poor response, and 4 of 7 responders with *FLT3*-ITD^{mut} ultimately achieved PD with poor outcomes, likely because of the ineffectiveness of chidamide for selectively inhibiting HDAC1, 2, 3 and 10 instead of HDAC8.

Despite the clinical activity of chidamide combination therapy in R/R AML patients, toxicity is still commonly observed in this cohort. The degree of cytopenia and resulting complications reported in our study are not higher than those reported in treatment-naïve patients or other R/R populations, although the rates and degrees of baseline cytopenia were higher (26). We found that infections of grade 3 or higher were observed in nearly half of the cohort (18 courses), and 2 of the 18 courses developed infectious shock. Three patients died within 4 weeks after treatment, 2 of the 3 patients developed severe infection and shock, and one patient persistently maintained no response and died after receiving chemotherapy. Even with these toxicities, in our study, the median OS and PFS times were 11.7 and 11.7 months, respectively, and the 2-year OS and PFS rates were 38.2% and 37.8%, respectively, which are equivalent or superior to those of conventional salvage therapy (27).

CONCLUSION

The CDIAG regimen was well tolerated and associated with a higher clinical response rate than expected in the context of salvage therapy for R/R AML. The regimen delays disease progression and reduces the leukemia burden before transplantation, providing eligible patients with the chance of proceeding to allo-SCT. Our results show that epigenetic agents combining cytotoxic agents may represent a promising direction for patients with R/R AML. Further evaluations in larger population are needed to seek biological indicators benefiting from this regimen.

DATA AVAILABILITY STATEMENT

The original contributions presented in the study are included in the article/**Supplementary Material**. Further inquiries can be directed to the corresponding authors.

ETHICS STATEMENT

The studies involving human participants were reviewed and approved by the Ethics Committee of the First Affiliated Hospital of Soochow University. The patients/participants provided their written informed consent to participate in this study.

AUTHOR CONTRIBUTIONS

JY contributed to data curation, formal analysis, visualization, and writing-original draft. C-LW contributed to writing-original draft and visualization. LZ contributed to data curation. HZ contributed to methodology and investigation. LB contributed to methodology and investigation. H-XZ contributed to investigation and resources. M-ZX contributed to investigation and resources. L-YC contributed to investigation and resources. C-SQ contributed to investigation and resources. H-YQ contributed to methodology and validation. S-NC contributed to methodology and validation. X-WT contributed to investigation and resources. D-PW contributed to conceptualization, supervision, and writing-review and editing. Z-YM contributed to methodology and investigation. A-NS contributed to conceptualization, funding acquisition, supervision, and writing-review. S-LX contributed to conceptualization, funding acquisition, supervision, resources, and writing-review. All authors contributed to the article and approved the submitted version.

FUNDING

This work was supported by grants from the National Natural Science Foundation of China (Grant No. 81970138), Translational Research Grant of NCRCH (Grant No. 2020ZKMB05), Jiangsu Province "333" project, Jiangsu Province Medical Youth Talent Program (Grant No. QNRC2016719), a C class sponsored project from Jiangsu Provincial Six Talent Peaks (Grant No. 2016-WSN-123) and Gusu Key Medical Talent Program (Grant No. GSWS2019007).

ACKNOWLEDGMENTS

The authors would like to thank the investigators and patients who participated in the CDIAG trial and Shenzhen Chipscreen Biosciences Ltd.(Shenzhen, China) for providing chidamide for this clinical trial.

SUPPLEMENTARY MATERIAL

The Supplementary Material for this article can be found online at: https://www.frontiersin.org/articles/10.3389/fonc.2021.726926/full#supplementary-material

REFERENCES

1. Cheson BD, Bennett JM, Kopecky KJ, Büchner T, Willman CL, Estey EH, et al. Revised Recommendations of the International Working Group for Diagnosis, Standardization of Response Criteria, Treatment Outcomes, and Reporting Standards for Therapeutic Trials in Acute Myeloid Leukemia. *J Clin Oncol* (2003) 21:4642–9. doi: 10.1200/jco.2003.04.036
2. Döhner H, Estey EH, Amadori S, Appelbaum FR, Büchner T, Burnett AK, et al. Diagnosis and Management of Acute Myeloid Leukemia in Adults: Recommendations From an International Expert Panel, on Behalf of the European LeukemiaNet. *Blood* (2010) 115:453–74. doi: 10.1182/blood-2009-07-235358
3. Döhner H, Estey E, Grimwade D, Amadori S, Appelbaum FR, Büchner T, et al. Diagnosis and Management of AML in Adults: 2017 ELN Recommendations From an International Expert Panel. *Blood* (2017) 129:424–47. doi: 10.1182/blood-2016-08-733196
4. Cashen AF, Schiller GJ, O'Donnell MR, DiPersio JF. Multicenter, Phase II Study of Decitabine for the First-Line Treatment of Older Patients With Acute Myeloid Leukemia. *J Clin Oncol* (2010) 28:556–61. doi: 10.1200/jco.2009.23.9178
5. Al-Ali HK, Jaekel N, Junghanss C, Maschmeyer G, Krahl R, Cross M, et al. Azacitidine in Patients With Acute Myeloid Leukemia Medically Unfit for or Resistant to Chemotherapy: A Multicenter Phase I/II Study. *Leuk Lymphoma* (2012) 53:110–7. doi: 10.3109/10428194.2011.606382
6. Pan DS, Yang Q-J, Fu X, Shan S, Zhu JZ, Zhang K, et al. Discovery of an Orally Active Subtype-Selective HDAC Inhibitor, Chidamide, as an Epigenetic Modulator for Cancer Treatment. *Med Chem Commun* (2014) 5:1789–96. doi: 10.1039/C4MD00350K
7. Witt O, Deubzer HE, Milde T, Oehme I. HDAC Family: What are the Cancer Relevant Targets? *Cancer Lett* (2009) 277:8–21. doi: 10.1016/j.canlet.2008.08.016
8. Khan AN, Tomasi TB. Histone Deacetylase Regulation of Immune Gene Expression in Tumor Cells. *Immunol Res* (2008) 40:164–78. doi: 10.1007/s12026-007-0085-0
9. Yamada K, Furusawa S, Saito K, Waga K, Koike T, Arimura H, et al. Concurrent Use of Granulocyte Colony-Stimulating Factor With Low-Dose Cytosine Arabinoside and Aclarubicin for Previously Treated Acute Myelogenous Leukemia: A Pilot Study. *Leukemia* (1995) 9:10–4.
10. Li J, Chen Y, Zhu Y, Zhou J, Xu Y, Li Y, et al. Efficacy and Safety of Decitabine in Combination With G-CSF, Low-Dose Cytarabine and Aclarubicin in Newly Diagnosed Elderly Patients With Acute Myeloid Leukemia. *Oncotarget* (2015) 6:6448–58. doi: 10.18632/oncotarget.3361
11. Jiang X, Wang Z, Ding B, Yin C, Zhong Q, Carter BZ, et al. The Hypomethylating Agent Decitabine Prior to Chemotherapy Improves the Therapy Efficacy in Refractory/Relapsed Acute Myeloid Leukemia Patients. *Oncotarget* (2015) 6:33612–22. doi: 10.18632/oncotarget.5600
12. Cameron EE, Bachman KE, Myöhänen S, Herman JG, Baylin SB. Synergy of Demethylation and Histone Deacetylase Inhibition in the Re-Expression of Genes Silenced in Cancer. *Nat Genet* (1999) 21:103–7. doi: 10.1038/5047
13. Kirschbaum M, Gojo I, Goldberg SL, Bredeson C, Kujawski LA, Yang A, et al. A Phase 1 Clinical Trial of Vorinostat in Combination With Decitabine in Patients With Acute Myeloid Leukaemia or Myelodysplastic Syndrome. *Br J Haematol* (2014) 167:185–93. doi: 10.1111/bjh.13016
14. Kurosawa S, Yamaguchi T, Miyawaki S, Uchida N, Sakura T, Kanamori H, et al. Prognostic Factors and Outcomes of Adult Patients With Acute Myeloid

Leukemia After First Relapse. *Haematologica* (2010) 95:1857–64. doi: 10.3324/haematol.2010.027516
15. Middeke JM, Herbst R, Parmentier S, Bug G, Hänel M, Stuhler G, et al. Long-Term Follow-Up and Impact of Comorbidity Before Allogeneic Hematopoietic Stem Cell Transplantation in Patients With Relapsed or Refractory Acute Myeloid Leukemia-Lessons Learned From the Prospective BRIDGE Trial. *Biol Blood Marrow Transpl* (2017) 23:1491–7. doi: 10.1016/j.bbmt.2017.05.014
16. Freeman SD, Hills RK, Virgo P, Khan N, Couzens S, Dillon R, et al. Measurable Residual Disease at Induction Redefines Partial Response in Acute Myeloid Leukemia and Stratifies Outcomes in Patients at Standard Risk Without NPM1 Mutations. *J Clin Oncol* (2018) 36:1486–97. doi: 10.1200/jco.2017.76.3425
17. Burnett AK, Goldstone A, Hills RK, Milligan D, Prentice A, Yin J, et al. Curability of Patients With Acute Myeloid Leukemia Who did Not Undergo Transplantation in First Remission. *J Clin Oncol* (2013) 31:1293–301. doi: 10.1200/jco.2011.40.5977
18. Aldoss I, Yang D, Aribi A, Ali H, Sandhu K, Al Malki MM, et al. Efficacy of the Combination of Venetoclax and Hypomethylating Agents in Relapsed/Refractory Acute Myeloid Leukemia. *Haematologica* (2018) 103:e404–7. doi: 10.3324/haematol.2018.188094
19. Della Porta MG, Gallì A, Bacigalupo A, Zibellini S, Bernardi M, Rizzo E, et al. Clinical Effects of Driver Somatic Mutations on the Outcomes of Patients With Myelodysplastic Syndromes Treated With Allogeneic Hematopoietic Stem-Cell Transplantation. *J Clin Oncol* (2016) 34:3627–37. doi: 10.1200/jco.2016.67.3616
20. Grimwade D, Ivey A, Huntly BJ. Molecular Landscape of Acute Myeloid Leukemia in Younger Adults and Its Clinical Relevance. *Blood* (2016) 127:29–41. doi: 10.1182/blood-2015-07-604496
21. Giannini G, Cabri W, Fattorusso C, Rodriquez M. Histone Deacetylase Inhibitors in the Treatment of Cancer: Overview and Perspectives. *Future Med Chem* (2012) 4:1439–60. doi: 10.4155/fmc.12.80
22. DiNardo CD, Propert KJ, Loren AW, Paietta E, Sun Z, Levine RL, et al. Serum 2-Hydroxyglutarate Levels Predict Isocitrate Dehydrogenase Mutations and Clinical Outcome in Acute Myeloid Leukemia. *Blood* (2013) 121:4917–24. doi: 10.1182/blood-2013-03-493197
23. Lev Maor G, Yearim A, Ast G. The Alternative Role of DNA Methylation in Splicing Regulation. *Trends Genet* (2015) 31:274–80. doi: 10.1016/j.tig.2015.03.002
24. Garrett-Bakelman FE, Melnick AM. Mutant IDH: A Targetable Driver of Leukemic Phenotypes Linking Metabolism, Epigenetics and Transcriptional Regulation. *Epigenomics* (2016) 8:945–57. doi: 10.2217/epi-2016-0008
25. Long J, Jia MY, Fang WY, Chen XJ, Mu LL, Wang ZY, et al. FLT3 Inhibition Upregulates HDAC8 via FOXO to Inactivate P53 and Promote Maintenance of FLT3-ITD+ Acute Myeloid Leukemia. *Blood* (2020) 135:1472–83. doi: 10.1182/blood.2019003538
26. Hatsumi N, Miyawaki S, Yamauchi T, Takeshita A, Komatsu N, Usui N, et al. Phase II Study of FLAGM (Fludarabine + High-Dose Cytarabine + Granulocyte Colony-Stimulating Factor + Mitoxantrone) for Relapsed or Refractory Acute Myeloid Leukemia. *Int J Hematol* (2019) 109:418–25. doi: 10.1007/s12185-019-02606-0
27. Giles F, O'Brien S, Cortes J, Verstovsek S, Bueso-Ramos C, Shan J, et al. Outcome of Patients With Acute Myelogenous Leukemia After Second Salvage Therapy. *Cancer* (2005) 104:547–54. doi: 10.1002/cncr.21187

Conflict of Interest: The authors declare that the research was conducted in the absence of any commercial or financial relationships that could be construed as a potential conflict of interest.

frontiers in Oncology

ORIGINAL RESEARCH
published: 08 October 2021
doi: 10.3389/fonc.2021.754093

Histone H3K36me2-Specific Methyltransferase ASH1L Promotes MLL-AF9-Induced Leukemogenesis

Mohammad B. Aljazi[1], *Yuen Gao*[1], *Yan Wu*[1], *George I. Mias*[1,2] *and Jin He*[1]*

[1] Department of Biochemistry and Molecular Biology, College of Nature Sciences, Michigan State University, East Lansing, MI, United States, [2] Institute for Quantitative Health Science and Engineering, Michigan State University, East Lansing, MI, United States

ASH1L and MLL1 are two histone methyltransferases that facilitate transcriptional activation during normal development. However, the roles of ASH1L and its enzymatic activity in the development of MLL-rearranged leukemias are not fully elucidated in *Ash1L* gene knockout animal models. In this study, we used an *Ash1L* conditional knockout mouse model to show that loss of ASH1L in hematopoietic progenitor cells impaired the initiation of MLL-AF9-induced leukemic transformation *in vitro*. Furthermore, genetic deletion of ASH1L in the MLL-AF9-transformed cells impaired the maintenance of leukemic cells *in vitro* and largely blocked the leukemia progression *in vivo*. Importantly, the loss of ASH1L function in the *Ash1L*-deleted cells could be rescued by wild-type but not the catalytic-dead mutant ASH1L, suggesting the enzymatic activity of ASH1L was required for its function in promoting MLL-AF9-induced leukemic transformation. At the molecular level, ASH1L enhanced the MLL-AF9 target gene expression by directly binding to the gene promoters and modifying the local histone H3K36me2 levels. Thus, our study revealed the critical functions of ASH1L in promoting the MLL-AF9-induced leukemogenesis, which provides a molecular basis for targeting ASH1L and its enzymatic activity to treat MLL-AF9-induced leukemias.

Keywords: MLL1, ASH1L, histone modification, H3K36me2, leukemogenesis, MLL-AF9 fusion

OPEN ACCESS

Edited by:
Fei Gao,
Beijing Genomics Institute (BGI), China

Reviewed by:
Palash C. Maity,
Universität Ulm, Germany
Gerardo Ferrer,
Josep Carreras Leukaemia Research Institute (IJC), Spain

***Correspondence:**
Jin He
hejin1@msu.edu

Specialty section:
This article was submitted to Hematologic Malignancies, a section of the journal Frontiers in Oncology

Received: *05 August 2021*
Accepted: *17 September 2021*
Published: *08 October 2021*

Citation:
Aljazi MB, Gao Y, Wu Y, Mias GI and He J (2021) Histone H3K36me2-Specific Methyltransferase ASH1L Promotes MLL-AF9-Induced Leukemogenesis. Front. Oncol. 11:754093. doi: 10.3389/fonc.2021.754093

INTRODUCTION

The MLL rearrangement (MLLr) caused by 11q23 chromosomal translocations creates a variety MLL fusion proteins that drive the acute lymphoblastic and myeloid leukemia development, which accounts for approximate 5-10% acute leukemias in human patients (1–5). Despite recent progression in the development of chemotherapies against leukemias, the overall prognosis for the MLLr leukemias remains poor (6, 7).

MLL1 protein is a histone lysine methyltransferase (KMTase) that contains a SET (Su(var)3-9, Enhancer-of-zeste and Trithorax) domain to catalyze trimethylation of histone H3 lysine 4 (H3K4me3) (8). Functionally, MLL1 belongs to the Trithorax-group (TrxG) proteins that antagonize the Polycomb-group (PcG)-mediated gene silencing and facilitate transcriptional activation (9). In 11q23 chromosomal translocations, the *N*-terminal portion of MLL1 is fused

with a variety of fusion partners to generate different oncogenic MLL fusion proteins that function as disease drivers leading to leukemia development (10–12). Previous studies have revealed that the *N*-terminal portion of MLL fusion proteins interacts with MENIN and LEDGF (Lens Epithelium-Derived Growth Factor), which is critical for the recruitment of MLL fusion proteins to chromatin, whereas the *C*-terminal fusion partners interact with various trans-activators to induce transcriptional activation (13–17). However, since the MLL fusion proteins lack the intrinsic histone H3K4 methyltransferase activity due to loss of the SET domain located in the *C*-terminal portion of MLL1 (10), it is unclear whether other histone modifications are required for the MLL fusion proteins-induced gene expression and leukemogenesis.

Recently, another member of TrxG proteins, ASH1L (Absent, Small, or Homeotic-Like 1), was found to play important roles in normal hematopoiesis and leukemogenesis (8, 18, 19). Biochemically, ASH1L is a histone KMTase that mediates dimethylation of histone H3 lysine 36 (H3K36me2) (20). Similar to MLL1, ASH1L facilitates gene expression through antagonizing PcG-mediated gene silencing (8). Previous studies have shown that ASH1L and MLL1 co-occupies the same transcriptional regulatory regions, and loss of either ASH1L or MLL1 reduces the expression of common genes (21–23), suggesting ASH1L and MLL1 function synergistically to activate gene expression during normal development. However, the significance of ASH1L and its-mediated histone H3K36me2 in the MLLr-associated leukemogenesis has not been addressed in the *Ash1L* gene knockout animal models.

In this study, we used an *Ash1L* conditional knockout mouse model to show that loss of ASH1L in hematopoietic progenitor cells (HPCs) impaired the initiation of MLL-AF9-induced leukemic transformation *in vitro*. Furthermore, genetic deletion of ASH1L in the MLL-AF9-transformed cells impaired the maintenance of leukemic cells *in vitro* and largely blocked the leukemia progression *in vivo*. Importantly, the loss of ASH1L function in the *Ash1L*-deleted cells could be rescued by ectopic expression of wild-type but not the catalytic-dead mutant ASH1L, suggesting the enzymatic activity of ASH1L was required for its function in promoting MLL-AF9-induced leukemic transformation. At the molecular level, ASH1L activated the MLL-AF9 target gene expression by directly binding to the gene promoters and modifying the local histone H3K36me2 levels. Thus, our study revealed the critical functions of ASH1L in MLL-AF9-induced leukemogenesis and raised the possibility that ASH1L might serve as a potential therapeutic target for the treatment of MLL-AF9-induced leukemias.

MATERIALS AND METHODS

Mice

The *Ash1L* conditional knockout mice were generated as previously reported (24). To generate inducible *Ash1L* deletion, mice were crossed with Rosa26-CreER^{T2} mice that were obtained from The Jackson Laboratory. All mice for this study were backcrossed to C57BL/6 mice for at least five generations to reach pure genetic background prior to conducting experiments. All mouse experiments were performed with the approval of the Michigan State University Institutional Animal Care & Use Committee.

Hematopoietic Progenitor Isolation and Culture

Hematopoietic progenitor cells were isolated from femurs of 4- to 6-week C57BL/6 mice. The red blood cells in the bone marrows were lysed by ammonium chloride solution (Stem Cell Technologies 07800) and filtered with a 70-μm nylon filter. The c-KIT$^+$ HPCs were isolated using c-KIT antibody-conjugated IMag (BD Biosciences) beads. HPCs cells were maintained in RMPI1640 medium supplemented with 10% FBS, 1% MEM non-essential amino acids, 1% Glutamax, 10 ng/mL, 2-mercaptoethanol, and 50 ng/mL mSCF (PeproTech), 10 ng/mL mIL-6 (PeproTech), and 10 ng/mL mIL-3 (PeproTech). To induce CRE-mediated recombination *in vitro*, 4-hydroxy-tamoxifen (Sigma-Aldrich) was resuspended in DMSO and supplemented into the culture medium with concentration of 250 nM.

Retroviral and Lentiviral Vector Production and Transduction

The pMIG-FLAG-MLL-AF9 retroviral vectors as obtained from Addgene (Plasmid #71443). Retroviral vectors were generated by co-transfection of retroviral vectors with pGag-pol, pVSVG 293T cells using CalPhos mammalian transfection kit (TaKaRa). After 48hrs post transfection, viral supernatant was harvested, filtered through a 0.45 μm membrane, and concentrated by ultracentrifugation. The lentiviral system was obtained from the National Institutes of Health AIDS Research and Reference Reagent Program. To generate GFP expression vectors, the GFP cDNA was PCR amplified, fused with P2A and puromycin resistant cassette and cloned into the SpeI/EcoRI sites under the EF1α promoter. To generate lentiviral viruses, the transducing vectors pTY, pHP and pHEF1α–VSVG were co-transfected into HEK293T cells. The supernatant was collected at 24, 36 and 48 hours after transfection, filtered through a 0.45 μm membrane and concentrated by ultracentrifugation. Retroviral and lentiviral transduction of HPCs was performed by spin inoculation for 1 hour at 800g, in RMPI1640 medium supplemented with 10% FBS, 1x MEM non-essential amino acids (Life Technologies), 1x Glutamax (Life Technologies), 1x sodium pyruvate (Life Technologies), and 10 ng/mL mIL-3 (PeproTech).

Serial Methylcellulose Replating Assay and Leukemia Transplantation

The colony formation assays were conducted by plating 500 cells into methylcellulose media consisting of Iscove MDM (Life Technologies) supplemented with FBS, BSA, insulin-transferrin (Life Technologies), 2-mercaptoethanol, 50 ng/mL mSCF (PeproTech), 10 ng/mL mIL-6 (PeproTech), 10 ng/mL mIL-3 (PeproTech), and 10 ng/mL GM-CSF (PeproTech). After 7-10

days, the colony numbers were counted under a microscope. The colonies were picked up, and cells were pooled and replated onto secondary methylcellulose plates. Three rounds of replating were performed for each experiment. For leukemia transplantation, recipient C57BL/6 mice were subjected to total body irradiation at a dose of 11 Gy with the use of a X-RAD 320 biological irradiator. Donor cells (5×10^5) and radiation protector cells (5×10^5) isolated from BM were mixed in 1× PBS and transplanted into the recipient mice through retro-orbital injection. The mice were fed with water supplemented with trimethoprim/sulfamethoxazole for 4 weeks after transplantation.

FACS Analysis

For FACS analysis, cells were stained with antibodies in staining buffer (1× PBS, 2% FBS) and incubated at 4°C for 30 minutes. The samples were washed once with staining buffer before subjected to FACS analysis with the use of a BD LSRII. The antibodies used in this study include anti–Mac-1(eBioscience), anti–Gr-1(eBioscience), anti–c-KIT (eBioscience).

Western Blot Analysis

Total proteins were extracted by RIPA buffer and separated by electrophoresis by 8-10% PAGE gel. The protein was transferred to the nitrocellulose membrane and blotted with primary antibodies. The antibodies used for Western Blot and IP-Western Blot analyses included: rabbit anti-ASH1L (1:1000, in house) (24) and IRDye 680 donkey anti-rabbit second antibody (1: 10000, Li-Cor). The images were developed by Odyssey Li-Cor Imager (Li-Cor).

Quantitative RT-PCR and ChIP-qPCR Assays

RNA was extracted and purified from cells with the use of Qiashredder (QIAGEN) and RNeasy (QIAGEN) spin columns. Total RNA (1 μg) was subjected to reverse transcription using Iscript reverse transcription supermix (Bio-Rad). cDNA levels were assayed by real-time PCR using iTaq universal SYBR green supermix (Bio-Rad) and detected by CFX386 Touch Real-Time PCR detection system (Bio-Rad). Primer sequences for qPCR are listed in **Supplementary Table 3**. The expression of individual genes is normalized to expression level of *Gapdh*. ChIP assays that used rabbit anti-ASH1L antibody (in house), rabbit anti-H3K36me2 antibody (Abcam), rabbit anti-Flag antibody (Cell Signaling) were carried out according to the previously reported protocol with the following modifications (25): ~2 ug antibodies were used in the immunoprecipitation, and chromatin-bound beads were washed 3 times each with TSEI, TSEII, and TESIII followed by 2 washes in 10mM Tris, pH 7.5, 1mM EDTA. Histone modification ChIPs were carried out as previously reported (26). DNA that underwent ChIP was analyzed by quantitative PCR (qPCR), and data are presented as the percentage of input as determined with CFX manager 3.1 software. The amplicons were designed to locate at 1.0-kb upstream of transcriptional starting sites (TSS) and transcription ending sties (TES) of *Hoxa9/Hoxa10* genes. The mouse intracisternal A-particle LTR repeat elements were included as a negative control for the ASH1L binding. The ChIP primers for the mouse IAP LTR were purchased from Cell Signaling (85916, Cell Signaling). Other qPCR and ChIP primers are listed in **Supplementary Table 3**, respectively.

RNA-Seq Sample Preparation for HiSeq4000 Sequencing

RNA was extracted and purified from cells using QI shredder (Qiagen) and RNeasy (Qiagen) spin columns. Total RNA (1 μg) was used to generate RNA-seq library using NEBNext Ultra Directional RNA library Prep Kit for Illumina (New England BioLabs, Inc) according to the manufacturer's instructions. Adapter-ligated cDNA was amplified by PCR and followed by size selection using agarose gel electrophoresis. The DNA was purified using Qiaquick gel extraction kit (Qiagen) and quantified both with an Agilent Bioanalyzer and Invitrogen Qubit. The libraries were diluted to a working concentration of 10nM prior to sequencing. Sequencing on an Illumina HiSeq4000 instrument was carried out by the Genomics Core Facility at Michigan State University.

RNA-Seq Data Analysis

RNA-Seq data analysis was performed essentially as described previously. All sequencing reads were mapped mm9 of the mouse genome using Tophat2 (27). The mapped reads were normalized to reads as Reads Per Kilobase of transcript per Million mapped reads (RPKM). The differential gene expression was calculated by Cuffdiff program and the statistic cutoff for identification of differential gene expression is $p < 0.01$ and 1.5-fold RPKM change between samples (28). The heatmap and plot of gene expression were generated using plotHeatmap and plotProfile in the deepTools program (29). The differential expressed gene lists were input into the David Functional Annotation Bioinformatics Microarray Analysis for the GO enrichment analyses (https://david.ncifcrf.gov/).

Statistical Analysis

All statistical analyses were performed using GraphPad Prism 9 (GraphPad Software). Parametric data were analyzed by a two-tailed *t* test or two-way ANOVA test for comparisons of multiple samples. The post-transplantation survivals were analyzed by the Gehan-Breslow-Wilcoxon test. *P* values < 0.05 were considered statistically significant. Data are presented as mean ± SEM.

RESULTS

ASH1L Promotes the Initiation of MLL-AF9-Induced Leukemic Transformation *In Vitro*

To examine the function of ASH1L in MLL-AF9-induced leukemogenesis, we generated an *Ash1L* conditional knockout (*Ash1L*-cKO) mouse line in which two *LoxP* elements inserted into the exon 4 flanking regions (24). A CRE recombinase-mediated deletion of exon 4 resulted in altered splicing of mRNA that created a premature stop codon before the sequences encoding the first functional AWS (associated with SET)

domain (**Figures 1A, B**). The *Ash1L*-cKO mice were further crossed with the Rosa26-CreER^{T2} mice to generate a tamoxifen-inducible *Ash1L* knockout line (*Ash1L*$^{2f/2f}$;Rosa26-CreER^{T2}), which allowed us to study the function of ASH1L in leukemogenesis *in vitro* and *in vivo*.

Using this *Ash1L*-cKO mouse model, we investigate the role of ASH1L in the initiation of MLL-AF9-induced leukemic transformation. To this end, we isolated the bone marrow cells from wild-type (*Ash1L*$^{+/+}$;*Cre-ER*^{T2}) and *Ash1L*-cKO (*Ash1L*$^{2f/2f}$; *Cre-ER*^{T2}) mice, respectively. The c-KIT^{+} HPCs were further

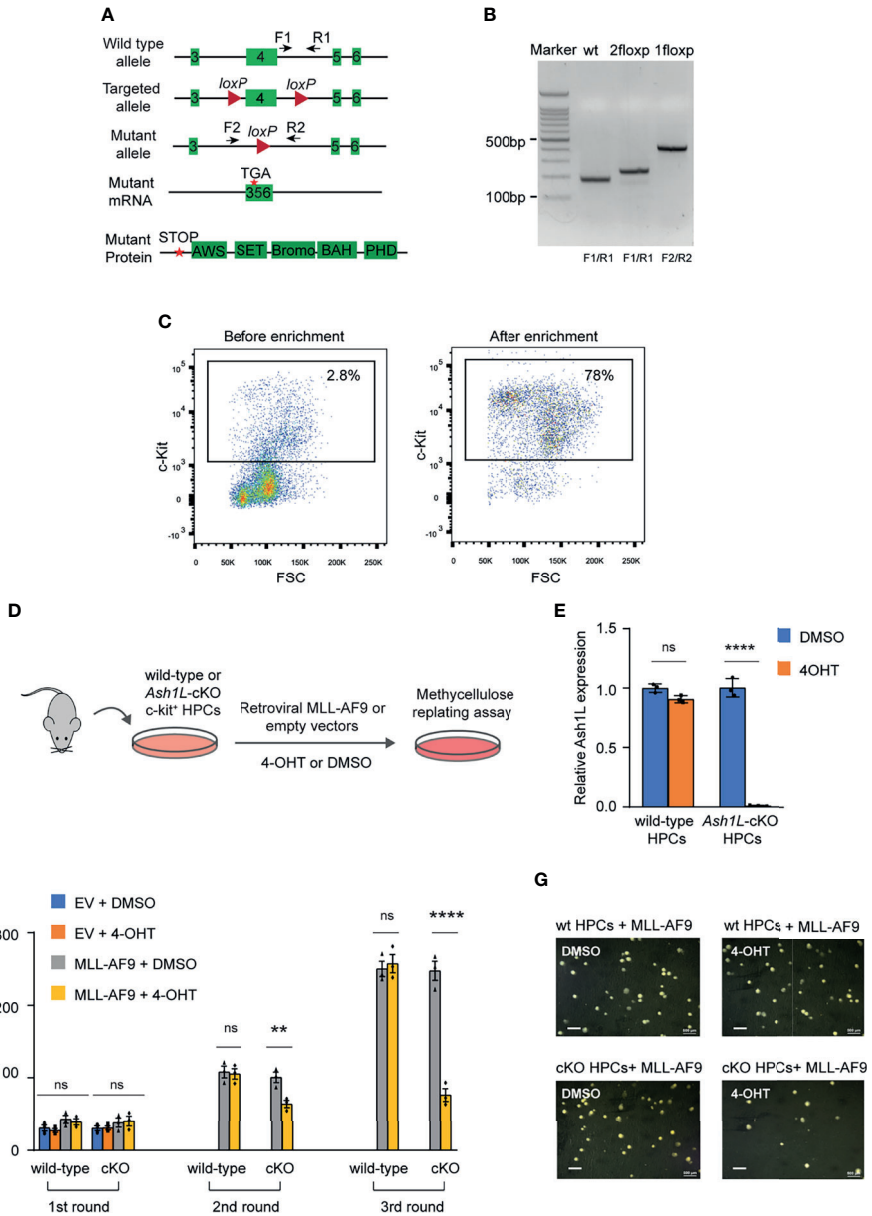

FIGURE 1 | ASH1L is required for the initiation of MLL-AF9-induced leukemic transformation. **(A)** Diagram showing the strategy for the generation of *Ash1L* conditional knockout mice. CRE-mediated deletion of exon 4 results in an altered spliced mRNA with a premature stop codon, which generates a truncated protein without all functional AWS, SET, Bromo, BAH and PHD domains. The arrows labeled as F and R represent the genotyping primers. **(B)** Genotyping results showing the PCR results of wild-type, 2 floxP, and 1 floxP alleles. **(C)** FACS analysis showing the c-KIT+ HPC populations before and after enrichment with c-KIT antibody-conjugated beads. **(D)** Schematic experimental procedure. **(E)** qRT-PCR analysis showing the *Ash1L* expression levels in wild-type and *Ash1L*-cKO cells after treated with 4-OHT or DMSO. The results were normalized against levels of *Gapdh* and the expression level in DMSO-treated cells was arbitrarily set to 1. The error bars represent mean ± SEM, n = 3 per group. ****$P < 0.0001$, ns, not significant. **(F)** Methylcellulose replating assays showing the colony numbers for each round of plating. The error bars represent mean ± SEM, n = 3 per group. **$P < 0.01$; ****$P < 0.0001$, ns, not significant. **(G)** Photos showing the representative colony formation on methylcellulose plates for each group. Bar = 0.5 mm.

enriched by the c-KIT antibody-conjugated magnetic beads (**Figure 1C**). The HPCs were cultured in the HPC medium supplemented with murine IL-3, IL-6, and SCF for three days, and followed by transduction of retroviral vectors expressing a *MLL1-AF9* fusion gene or control empty viruses (EV). After transduction, the cells were cultured in the suspension medium with 4-hydroxytamoxifen (4-OHT) for five days to induce *Ash1L* gene deletion in the *Ash1L*-cKO HPCs (**Figure 1D**). The quantitative RT-PCR (qRT-PCR) analysis showed that the *Ash1L* expression reduced to less than 5% at the mRNA level in the *Ash1L*-deleted cells (**Figure 1E**). To investigate the effect of *Ash1L* loss on the initiation of MLL-AF9-induced leukemic transformation *in vitro*, we performed serial colony replating assays by plating the cells on the semi-solid methylcellulose medium to examine the leukemic transformation. The results showed that although the cells transduced with *MLL-AF9* or empty vectors had comparable colony numbers in the first round of plating, the cells transduced with control empty vectors did not form colonies in the following rounds of replating. In contrast, both wild-type and *Ash1L*-cKO HPCs transduced with *MLL-AF9* retroviruses formed colonies in all three rounds of plating, indicating successful leukemic transformation by the *MLL-AF9* transgene *in vitro*. Notably, compared to the MLL-AF9-transduced wild-type cells, the *Ash1L*-deleted cells had reduced colony numbers in the second and third rounds of plating, suggesting that loss of *Ash1L* in HPCs compromised the MLL-AF9-induced leukemic transformation (**Figures 1F, G**), suggesting ASH1L promotes the MLL-AF9-induced leukemic transformation *in vitro*.

ASH1L Facilitates the Maintenance of MLL-AF9-Induced Leukemic Cells *In Vitro*

Next, we examined the functional role of *Ash1L* in maintaining the MLL-AF9-transformed cells. To this end, we transduced both wild-type and *Ash1L*-cKO HPCs with *MLL-AF9* retroviruses and plated the transduced cells onto the methylcellulose medium. After three rounds of replating, the transformed colonies were manually picked and cultured in the suspension medium supplemented with 4-OHT for 5 days to induce deletion of *Ash1L* in the *Ash1L*-cKO cells. The cells were further maintained in suspension culture without 4-OHT for 5 days before plated onto the methylcellulose to examine the colony formation (**Figure 2A**). The results showed that compared to the wild-type MLL-AF9-transformed cells, the *Ash1L*-deleted cells had marked reduced colony formation (**Figures 2B, C**), suggesting that ASH1L facilitated the maintenance of MLL-AF9 transformed cells *in vitro*.

To examine cellular responses to the *Ash1L* depletion, we performed the FACS analysis to examine cell death in response

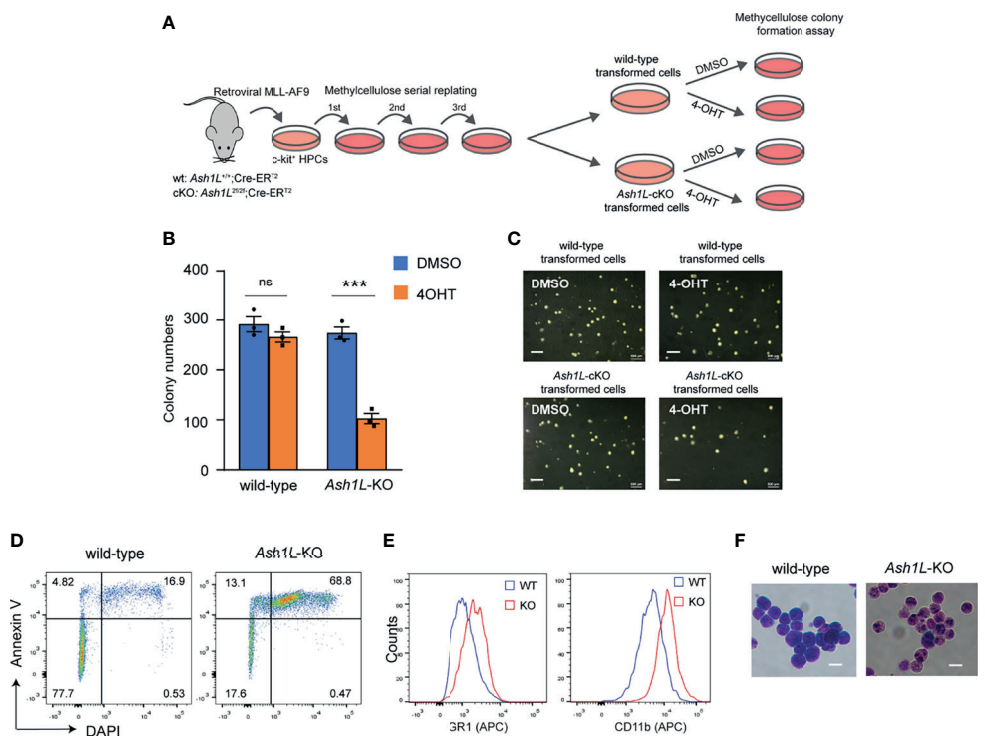

FIGURE 2 | ASH1L is required for the maintenance of MLL-AF9-induced leukemic cells *in vitro*. **(A)** Schematic experimental procedure. **(B)** Methylcellulose colony formation assays showing the colony numbers. The error bars represent mean ± SEM, n = 3 per group. ***$P < 0.001$; ns, not significant. **(C)** Photos showing the representative colony formation on methylcellulose plates for each group. Bar = 0.5 mm. **(D)** Representative FACS results showing the Annexin V+ and DAPI+ populations of wild-type and *Ash1L*-KO MLL-AF9-transformed cells. **(E)** Representative FACS results showing the GR-1 and CD11b expression of wild-type and *Ash1L*-KO MLL-AF9-transformed cells. **(F)** Photos showing the Wright-Giemsa staining of wild-type and *Ash1L*-KO MLL-AF9-transformed cells. Bar = 10 μm.

to the loss of *Ash1L* in the MLL-AF9-transformed cells. The results showed that compared to the wild-type cells, the *Ash1L*-deleted cells had increased populations of both early apoptotic cells (Annexin V+/DAPI-) and late dead cells (Annexin V+/DAPI+) (**Figure 2D**), suggesting that the loss of *Ash1L* induced cell death of MLL-AF9-transformed cells. Moreover, FACS analyses showed that compared to the wild-type transformed cells, the *Ash1L*-deleted cells had increased expression of myeloid differentiation surface markers CD11b and GR-1 (**Figure 2E**). Morphologically, the wild-type transformed cells displayed leukoblast-like morphology with enlarged dark stained nuclei, while the *Ash1L*-deleted cells had light-stained and segmented nuclei, a feature indicating the differentiation towards matured myeloid cells (**Figure 2F**). Taken together, these results suggested that ASH1L facilitated the maintenance of MLL-AF9-transformed cells through suppressing cell death and differentiation.

ASH1L Promotes the MLL-AF9-Induced Leukemia Development *In Vivo*

To determine the role of ASH1L in the MLL-AF9-induced leukemogenesis *in vivo*, we performed leukemia transplantation assays and monitor the leukemia development in recipient mice. To this end, the wild-type and *Ash1L*-deleted MLL-AF9-transformed cells were labeled with GFP by transduction with lentiviral-GFP vectors, mixed with normal protective bone marrow cells, and transplanted into the total-body-irradiated (TBI) syngeneic recipient mice (**Figure 3A**). Four weeks after transplantation, FACS analysis showed that the mice transplanted with wild-type leukemic cells had higher GFP+ leukemic cell populations in the peripheral blood compared to the mice received with *Ash1L*-KO leukemic cells (**Figure 3B**), which was consistent with the higher leukemic cell numbers in the peripheral blood smears and splenomegaly found in the mice transplanted with wild-type leukemic cells (**Figures 3C, D**). All mice transplanted with wild-type leukemic cells died within 3 months after transplantation, and the median survival time was around 8.5 weeks. In contrast, the mice transplanted with *Ash1L*-deleted cells had significant longer survival time (Chi square = 10.73, df = 1, p = 0.0011) compared to the mice transplanted with wild-type leukemic cells (**Figure 3E**). These results suggested that ASH1L in the MLL-AF9-transformed leukemic cells promoted the development and progression of leukemia *in vivo*.

The Enzymatic Activity of ASH1L Is Required for Its Function in Promoting MLL-AF9-Induced Leukemic Transformation

Next, we set out to determine whether the histone methyltransferase activity of ASH1L was required for its function in promoting MLL-AF9-induced leukemic transformation. To this end, the *Ash1L*-cKO HPCs were infected with retroviruses expressing *MLL-AF9* transgene, followed by transduced with lentiviral vectors expressing either wild-type ASH1L or catalytic-dead mutant ASH1L(H2214A) (21). The transformed cells were treated with 4-OHT to induce deletion of endogenous *Ash1L* gene (**Figure 4A**). Western blot analysis showed that both wild-type and mutant exogenous ASH1L had a similar expression level (**Figure 4B**). The cells were further plated onto the methylcellulose medium to examine the colony formation (**Figure 4A**). The results showed that compared to the wild-type ASH1L-expressed cells, the cells with

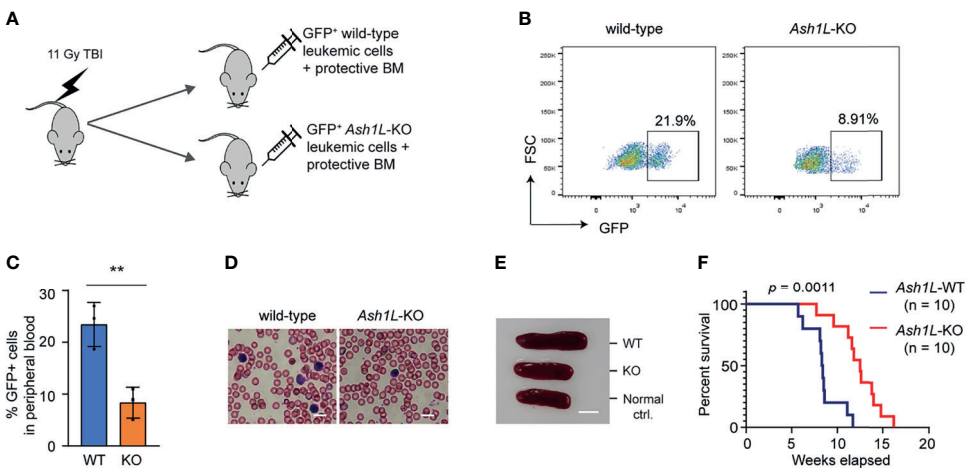

FIGURE 3 | ASH1L promotes the MLL-AF9-induced leukemia development *in vivo*. **(A)** Schematic experimental procedure. **(B)** Representative FACS analysis showing the GFP+ leukemic cell populations in the peripheral blood of mice transplanted with wild-type or *Ash1L*-KO MLL-AF9-transformed cells. **(C)** Quantitative results showing the percentage of GFP+ leukemic cell populations in the peripheral blood of mice transplanted with wild-type or *Ash1L*-KO MLL-AF9-transformed cells. The error bars represent mean ± SEM, n = 3 per group. $^{**}P < 0.01$. **(D)** Photos showing the leukemic cells in the peripheral blood smear of mice transplanted with wild-type or *Ash1L*-KO MLL-AF9-transformed cells. Bar = 10 μm. **(E)** Photos showing the representative spleen size from the normal control mice (Normal ctrl.), mice transplanted with wild-type (WT) or *Ash1L*-KO (KO) MLL-AF9-transformed cells. The samples were collected at post-transplantation 4 weeks. Bar = 5 mm. **(F)** Kaplan-Meier survival curve of mice transplanted with wild-type or *Ash1L*-KO MLL-AF9-transformed cells. *P* value calculated using a Gehan-Breslow-Wilcoxon test. n = 10 mice per group.

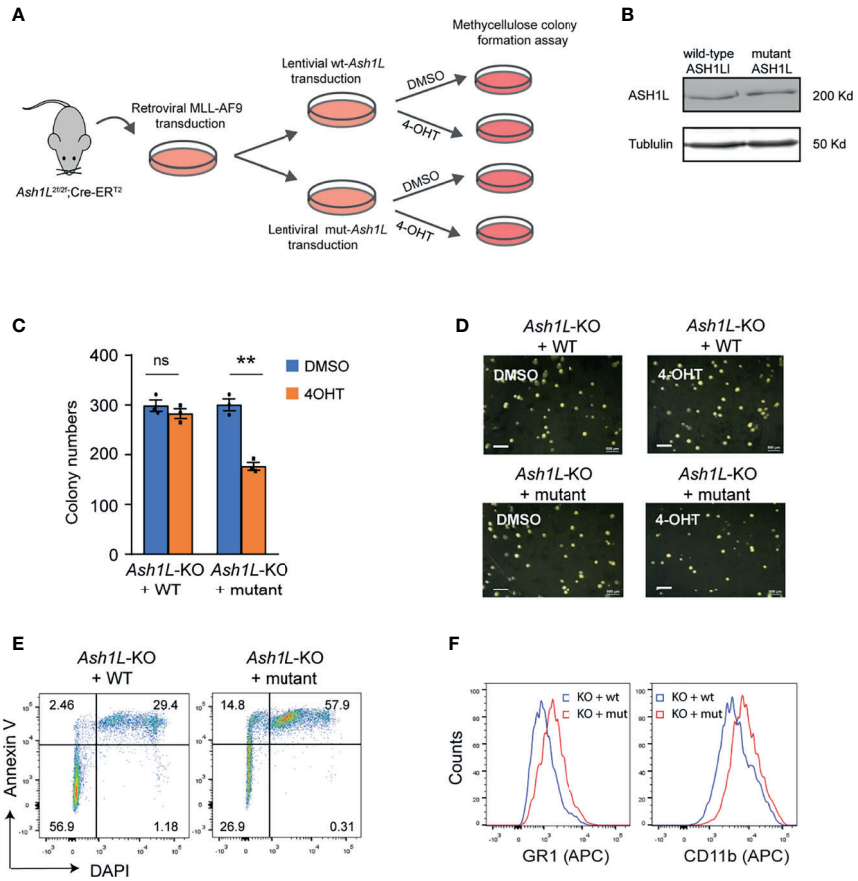

FIGURE 4 | The enzymatic activity of ASH1L is required for its function in promoting MLL-AF9-induced leukemic transformation. **(A)** Schematic experimental procedure. **(B)** WB analysis showing the ectopic expression of wild-type and mutant ASH1L. **(C)** Methylcellulose colony formation assays showing the colony numbers. The error bars represent mean ± SEM, n = 3 per group. $^{**}P < 0.01$; ns, not significant. **(D)** Photos showing the representative colony formation on methylcellulose plates for each group. Bar = 0.5 mm. **(E)** Representative FACS results showing the Annexin V+ and DAPI+ populations of *Ash1L*-KO cells rescued with wild-type and mutant ASH1L. **(F)** Representative FACS results showing the GR1 and CD11b expression of *Ash1L*-KO cells rescued with wild-type and mutant ASH1L.

ectopic expression of catalytic-dead mutant ASH1L had reduced colony formation (**Figures 4C, D**). Similar to the *Ash1L*-deleted cells, the *Ash1L*-deleted cells rescued with mutant ASH1L had increased cell death and upregulated expression of myeloid differentiation markers of CD11b and GR-1 (**Figures 4E, F**). These results suggested that ASH1L histone methyltransferase activity was required for its function in promoting MLL-AF9-induced leukemogenesis by inhibiting cell death and blocking myeloid differentiation.

ASH1L Facilitates the MLL-AF9-Induced Leukemogenic Gene Expression

To examine the molecular mechanisms underlying the function of ASH1L in promoting MLL-AF9-induced leukemogenesis, we performed RNA-seq analyses to examine the transcriptome changes in normal HPCs, wild-type and *Ash1L*-deleted MLL-AF9-tranformed cells. The results showed that compared to normal HPCs, the MLL-AF9-transformed cells had 1,021 upregulated and 1,228 downregulated genes (cutoff: fold changes > 1.5, FDR < 0.05), respectively (**Figure 5A**). The gene ontology (GO) enrichment analysis showed that both upregulated and downregulated genes were involved in immune processes and inflammatory responses (cutoff: FDR < 0.05) (**Supplementary Tables 1** and **2**), suggesting that MLL-AF9 fusion proteins disrupted the normal differentiation and mis-regulated the normal function of myeloid cells. Notably, multiple genes, such as *Hoxa5*, *Hoxa7*, *Hoxa9*, *Hoxa10* and *MeisI* that were known to mediate the MLL-AF9-induced leukemogenesis, were highly expressed in the MLL-AF9-transformed cells (**Figure 5B**). Further RNA-seq analysis showed that compared to MLL-AF9-transformed wild-type cells, the *Ash1L*-deleted cells had 372 upregulated gene and 472 downregulated genes (cutoff: fold changes > 1.5, FDR < 0.05), respectively (**Figure 5C**). Cross-examining these two data sets revealed that 105 genes, including *Hoxa5*, *Hoxa7*, *Hoxa9*, *Hoxa10*, and *MeisI* that were highly expressed in the wild-type MLL-AF9-transformed cells, were downregulated in the *Ash1L*-deleted cells (**Figures 5D, E**). Altogether, these results suggested

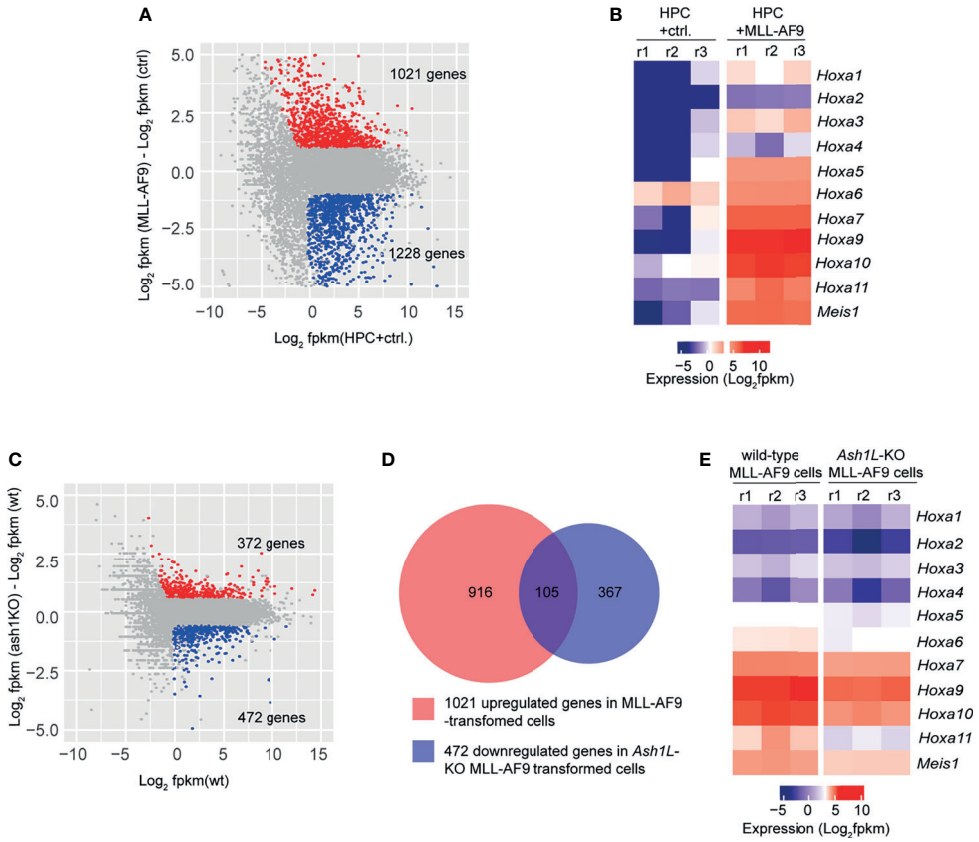

FIGURE 5 | ASH1L facilitates the MLL-AF9-induced leukemogenic gene expression. **(A)** Plot showing 1021 up- and 1228 down-regulated genes in the MLL-AF9-transformed cells compared to the normal HPCs. **(B)** Heatmap showing the upregulation of *Hoxa* gene cluster and *Meisl* in the MLL-AF9-transformed cells compared to normal HPCs. **(C)** Plot showing 372 up- and 472 down-regulated genes in the *Ash1L*-KO MLL-AF9-transformed cells compared to the wild-type MLL-AF9-transformed cells. **(D)** Venn diagram showing the 105 genes upregulated in the MLL-AF9-transformed cells and downregulated in the *Ash1L*-KO cells. **(E)** Heatmap showing the *Hoxa* gene cluster and *Meisl* downregulated in the *Ash1L*-KO cells compared to the wild-type MLL-AF9-transformed cells.

that ASH1L promoted the MLL-AF9-induced leukemogenesis by facilitating the MLL-AF9-induced leukemic gene expression.

ASH1L Binds and Mediates the Histone H3K36me2 Modification at *Hoxa9* and *Hoxa10* Gene Promoters

To determine whether ASH1L directly regulated the expression of MLL-AF9 target genes, we performed chromatin immunoprecipitation (ChIP) coupled with quantitative PCR (ChIP-qPCR) assays to examine the ASH1L occupancy, MLL-AF9 occupancy, and histone H3K36me2 modification at the gene promoters, transcriptional starting sites (TSS), transcriptional ending sites (TES) of *Hoxa9* and *Hoxa10*, two MLL-AF9 target genes that were shown to be activated in the wild-type transformed cells and have reduced expression in the *Ash1L*-deleted cells (**Figures 5B, E**). The results showed that both ASH1L occupancy and histone H3K36me2 were enriched at the *Hoxa9* and *Hoxa10* promoters compared to that on the TES and the long terminal repeat (LTR) of intracisternal A-particle (IAP) (**Figures 6A–E**). Furthermore, compared to wild-type MLL-AF9-transformed cells, both ASH1L occupancy and histone H3K36me2 modification were reduced at the gene promoters in the *Ash1L*-deleted cells (**Figures 6A–E**), suggesting that ASH1L bound to the *Hoxa9* and *Hoxa10* gene promoters directly and mediated local histone H3K36me2 modification. However, the MLL-AF9 occupancy at both gene promoters did not show significant difference between wild-type and *Ash1L*-deleted MLL-AF9-transformed cells (**Figures 6F, G**), suggesting the ASH1L-mediated histone H3K36me2 did not affect the binding of MLL-AF9 fusion protein to the gene promoters.

DISCUSSION

Chromosomal 11q23 translocations generate various MLL fusion proteins that contain the *N*-terminal portion of MLL1 and different fusion partners including AF9 (30, 31). Previous studies have demonstrated that the *N*-terminal MLL1 is critical for the recruitment of MLL fusion proteins to chromatin through its CxxC-zinc finger (CxxC-zf) domain and its interacting proteins MENIN and LEDGF, while the *C*-terminal fusion partners interact with multiple trans-activators to induce

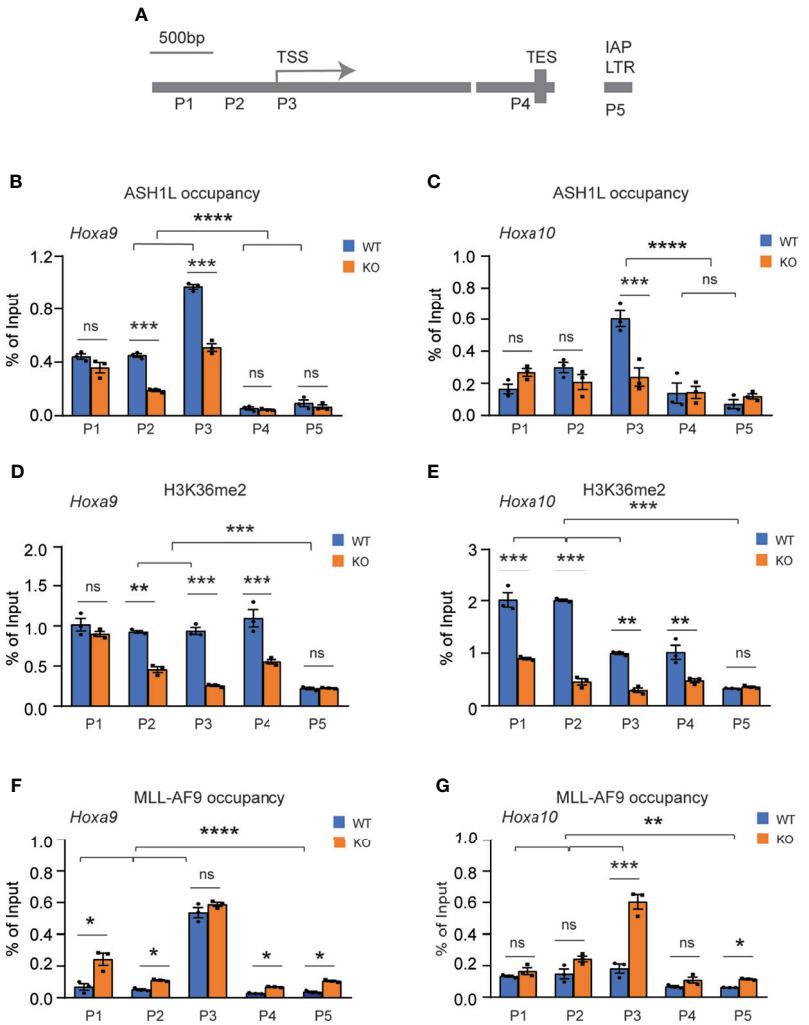

FIGURE 6 | ASH1L binds and mediates histone H3K36me2 modification at *Hoxa9* and *Hoxa10* gene promoters. **(A)** Plot showing the locations of ChIP-qPCR amplicons at the *Hoxa9* and *Hoxa10* gene loci and LTR of intracisternal A-particle (IAP). **(B, C)** ChIP-qPCR analysis showing the ASH1L occupancy at *Hoxa9* and *Hoxa10* gene loci in the wild-type and *Ash1L*-KO MLL-AF9-transformed cells. **(D, E)** ChIP-qPCR analysis showing the histone H3K36me2 at *Hoxa9* and *Hoxa10* gene loci in the wild-type and *Ash1L*-KO MLL-AF9-transformed cells. **(F, G)** ChIP-qPCR analysis showing the MLL-AF9 occupancy at *Hoxa9* and *Hoxa10* gene loci in the wild-type and *Ash1L*-KO MLL-AF9-transformed cells. Note: for panels **(B–E)**, the error bars represent mean ± SEM, n = 3 biological replicates. $^{*}P < 0.05$, $^{**}P < 0.01$, $^{***}P < 0.001$; $^{****}P < 0.0001$; ns, not significant.

transcriptional activation (16). Since the MLL fusion proteins lose the MLL1 C-terminal SET domain and its-associated histone H3K4 methyltransferase activity, it is unclear whether other histone KMTase-mediated histone modifications are required for the MLL fusion proteins to activate leukemogenic gene expression and induce leukemia development.

ASH1L is another member of TrxG proteins that facilitate transcriptional activation (8). Biochemically, ASH1L is a histone KMTase mediating histone H3K36me2 modification (20). Recent studies reported that ASH1L and MLL1 co-occupied the same gene promoters to activate gene expression, suggesting ASH1L and MLL function synergistically in activating gene expression in normal development and leukemogenesis (19, 21–23). However, the functional roles of ASH1L and its-mediated histone H3K36me2 in the MLLr-associated leukemogenesis have not been addressed using *Ash1L* gene knockout animal models.

In this study, we used an *Ash1L* conditional knockout mouse model to show that ASH1L and its histone methyltransferase activity are required for promoting the MLL-AF9-induced leukemogenesis. First, genetic deletion of ASH1L in normal HPCs largely impairs the MLL-AF9-induced colony formation in serial methylcellulose replating assays (**Figure 1**), suggesting ASH1L promotes the initiation of MLL-AF9-induced leukemic transformation. Second, loss of ASH1L in the MLL-AF9-transformed cells largely impaired the colony formation *in vitro* and delayed the leukemia development in the recipient mice transplanted with leukemic cells (**Figures 2** and **3**), suggesting ASH1L facilitates the maintenance of MLL-AF9-transformed cells

in vitro and leukemia progression *in vivo*. Importantly, the impaired ASH1L's function in the *Ash1L*-KO cells could be rescued by the wild-type but not the catalytic-dead mutant ASH1L (**Figure 4**), suggesting that the histone methyltransferase activity is required for its function in promoting MLL-AF9-induced leukemogenic transformation, which is consistent with a recent study showing that the SET domain is required for the MLL-AF9-induced leukemic transformation (32).

At the cellular level, we observed that the loss of ASH1L in MLL-AF9-transformed cells induced cell death and myeloid differentiation, which could be rescued by the wild-type but not the catalytic-dead mutant ASH1L (**Figures 2**, **4**), suggesting that ASH1L promotes MLL-AF9-induced leukemic transformation though inhibiting cell apoptosis and blocking cell differentiation. The results are consistent with the molecular findings that ASH1L is required for the full activation of MLL-AF9 target genes including *Hoxa* gene cluster and *MeisI* (**Figure 5**), which are known to play important roles in leukemogenesis through inhibiting cell death and blocking normal cell differentiation (33–35). Finally, the ChIP assays showed that both ASH1L occupancy and histone H3K36me2 modification were enriched at the promoters of MLL-AF9 target genes *Hoxa9* and *Hoxa10* in the wild-type transformed cells (**Figure 6**), indicating the ASH1L regulates the MLL-AF9 target genes through directly chromatin binding and its-mediated histone H3K36me2 modification.

Previous studies have shown that the PWWP domain of LEDGF is required for the recruitment of MLL fusion proteins through its binding to histone H3K36me2 (13, 15, 16). However, our ChIP analysis did not reveal reduction of MLL-AF9 occupancy at the *Hoxa9* and *Hoxa10* promoters in the *Ash1L*-KO cells (**Figures 6F, G**), suggesting the MLL-AF9 fusion protein could bind to its target regions though other recruiting mechanisms, such as the CxxC-zf domain-mediated binding to unmethylated CpG-rich promoters (36), and the reduced H3K36me2 at gene promoters in the *Ash1L*-KO cells impaired the *Hoxa* gene expression through mechanisms other than the recruitment of MLL-AF9 fusion protein.

Our current study has some limitations: (i) since this study includes a single type of MLLr, MLL-AF9 fusion protein, to induce leukemia development in mice, it is unclear whether ASH1L has the similar function in promoting other MLLr-induced leukemogenesis; (ii) although *Ash1L* deletion induces cell death, some MLL-AF9-transformed cells survive *in vitro* and *in vivo*, suggesting the MLL-AF9-transformed cells have heterogenous responses to the *Ash1L* depletion. However, the underlying mechanisms are not addressed by our current study. These fundamental questions merit further investigation for a better understating of the function of ASH1L in broad MLLr-associated leukemogenesis.

In summary, our study reveals that the histone H3K36me2-specific methyltransferase ASH1L and its enzymatic activity play an important role in promoting the MLL-AF9-induced leukemogenesis, which provides an important molecular basis for targeting ASH1L and its enzymatic activity to treat MLL-AF9-induced leukemias.

DATA AVAILABILITY STATEMENT

The datasets presented in this study can be found in online repositories. The names of the repository/repositories and accession number(s) can be found below: NCBI GEO; GSE183413.

ETHICS STATEMENT

The animal study was reviewed and approved by Michigan State University Institutional Animal Care & Use Committee.

AUTHOR CONTRIBUTIONS

JH conceived the project. MA, YG, YW, and JH performed the experiments. JH and GM performed the sequencing data analysis. MA and JH interpreted the data and wrote the manuscript. All authors contributed to the article and approved the submitted version.

FUNDING

This work was supported by the National Institute Health NIH grant R01GM127431.

ACKNOWLEDGMENTS

MSU genomics core facility processed the next-generation sequencing.

SUPPLEMENTARY MATERIAL

The Supplementary Material for this article can be found online at: https://www.frontiersin.org/articles/10.3389/fonc.2021.754093/full#supplementary-material

REFERENCES

1. Berger R, Bernheim A, Sigaux F, Daniel MT, Valensi F, Flandrin G. Acute Monocytic Leukemia Chromosome Studies. *Leuk Res* (1982) 6(1):17–26. doi: 10.1016/0145-2126(82)90039-X
2. Nakamura T, Alder H, Gu Y, Prasad R, Canaani O, Kamada N, et al. Genes on Chromosomes 4, 9, and 19 Involved in 11q23 Abnormalities in Acute Leukemia Share Sequence Homology and/or Common Motifs. *Proc Natl Acad Sci U S A* (1993) 90(10):4631–5. doi: 10.1073/pnas.90.10.4631
3. De Braekeleer M, Morel F, Le Bris MJ, Herry A, Douet-Guilbert N. The MLL Gene and Translocations Involving Chromosomal Band 11q23 in Acute Leukemia. *Anticancer Res* (2005) 25(3B):1931–44.
4. Vermaelen K, Barbieri D, Michaux JL, Tricot G, Casteels-Van Daele M, Noens L, et al. Anomalies of the Long Arm of Chromosome 11 in Human

Myelo- and Lymphoproliferative Disorders. I. Acute Nonlymphocytic Leukemia. *Cancer Genet Cytogenet* (1983) 10(1):105–16. doi: 10.1016/0165-4608(83)90111-5
5. Ayton PM, Cleary ML. Molecular Mechanisms of Leukemogenesis Mediated by MLL Fusion Proteins. *Oncogene* (2001) 20(40):5695–707. doi: 10.1038/sj.onc.1204639
6. Chessells JM, Harrison CJ, Kempski H, Webb DK, Wheatley K, Hann IM, et al. Clinical Features, Cytogenetics and Outcome in Acute Lymphoblastic and Myeloid Leukaemia of Infancy: Report From the MRC Childhood Leukaemia Working Party. *Leukemia* (2002) 16(5):776–84. doi: 10.1038/sj.leu.2402468
7. Hilden JM, Dinndorf PA, Meerbaum SO, Sather H, Villaluna D, Heerema NA, et al. Analysis of Prognostic Factors of Acute Lymphoblastic Leukemia in Infants: Report on CCG 1953 From the Children's Oncology Group. *Blood* (2006) 108(2):441–51. doi: 10.1182/blood-2005-07-3011
8. Kingston RE, Tamkun JW. Transcriptional Regulation by Trithorax-Group Proteins. *Cold Spring Harb Perspect Biol* (2014) 6(10):a019349. doi: 10.1101/cshperspect.a019349
9. Schuettengruber B, Chourrout D, Vervoort M, Leblanc B, Cavalli G. Genome Regulation by Polycomb and Trithorax Proteins. *Cell* (2007) 128(4):735–45. doi: 10.1016/j.cell.2007.02.009
10. Slany RK. The Molecular Biology of Mixed Lineage Leukemia. *Haematologica* (2009) 94(7):984–93. doi: 10.3324/haematol.2008.002436
11. Winters AC, Bernt KM. MLL-Rearranged Leukemias-An Update on Science and Clinical Approaches. *Front Pediatr* (2017) 5:4. doi: 10.3389/fped.2017.00004
12. Chan AKN, Chen CW. Rewiring the Epigenetic Networks in MLL-Rearranged Leukemias: Epigenetic Dysregulation and Pharmacological Interventions. *Front Cell Dev Biol* (2019) 7:81. doi: 10.3389/fcell.2019.00081
13. Yokoyama A, Somervaille TC, Smith KS, Rozenblatt-Rosen O, Meyerson M, Cleary ML. The Menin Tumor Suppressor Protein is an Essential Oncogenic Cofactor for MLL-Associated Leukemogenesis. *Cell* (2005) 123(2):207–18. doi: 10.1016/j.cell.2005.09.025
14. Shun MC, Botbol Y, Li X, Di Nunzio F, Daigle JE, Yan N, et al. Identification and Characterization of PWWP Domain Residues Critical for LEDGF/p75 Chromatin Binding and Human Immunodeficiency Virus Type 1 Infectivity. *J Virol* (2008) 82(23):11555–67. doi: 10.1128/JVI.01561-08
15. Yokoyama A, Cleary ML. Menin Critically Links MLL Proteins With LEDGF on Cancer-Associated Target Genes. *Cancer Cell* (2008) 14(1):36–46. doi: 10.1016/j.ccr.2008.05.003
16. Yokoyama A. Transcriptional Activation by MLL Fusion Proteins in Leukemogenesis. *Exp Hematol* (2017) 46:21–30. doi: 10.1016/j.exphem.2016.10.014
17. Okuda H, Kawaguchi M, Kanai A, Matsui H, Kawamura T, Inaba T, et al. MLL Fusion Proteins Link Transcriptional Coactivators to Previously Active CpG-Rich Promoters. *Nucleic Acids Res* (2014) 42(7):4241–56. doi: 10.1093/nar/gkt1394
18. Jones M, Chase J, Brinkmeier M, Xu J, Weinberg DN, Schira J, et al. Ash1l Controls Quiescence and Self-Renewal Potential in Hematopoietic Stem Cells. *J Clin Invest* (2015) 125(5):2007–20. doi: 10.1172/JCI78124
19. Zhu L, Li Q, Wong SH, Huang M, Klein BJ, Shen J, et al. ASH1L Links Histone H3 Lysine 36 Dimethylation to MLL Leukemia. *Cancer Discov* (2016) 6(7):770–83. doi: 10.1158/2159-8290.CD-16-0058
20. Yuan W, Xu M, Huang C, Liu N, Chen S, Zhu B. H3K36 Methylation Antagonizes PRC2-Mediated H3K27 Methylation. *J Biol Chem* (2011) 286(10):7983–9. doi: 10.1074/jbc.M110.194027
21. Miyazaki H, Higashimoto K, Yada Y, Endo TA, Sharif J, Komori T, et al. Ash1l Methylates Lys36 of Histone H3 Independently of Transcriptional Elongation to Counteract Polycomb Silencing. *PLoS Genet* (2013) 9(11):e1003897. doi: 10.1371/journal.pgen.1003897
22. Gregory GD, Vakoc CR, Rozovskaia T, Zheng X, Patel S, Nakamura T, et al. Mammalian ASH1L Is a Histone Methyltransferase That Occupies the Transcribed Region of Active Genes. *Mol Cell Biol* (2007) 27(24):8466–79. doi: 10.1128/MCB.00993-07
23. Tanaka Y, Kawahashi K, Katagiri Z, Nakayama Y, Mahajan M, Kioussis D. Dual Function of Histone H3 Lysine 36 Methyltransferase ASH1 in Regulation of Hox Gene Expression. *PLoS One* (2011) 6(11):e28171. doi: 10.1371/journal.pone.0028171
24. Gao Y, Duque-Wilckens N, Aljazi MB, Wu Y, Moeser AJ, Mias GI, et al. Loss of Histone Methyltransferase ASH1L in the Developing Mouse Brain Causes Autistic-Like Behaviors. *Commun Biol* (2021) 4(1):756. doi: 10.1038/s42003-021-02282-z
25. Aljazi MB, Gao Y, Wu Y, Mias GI, He J. Cell Signaling Coordinates Global PRC2 Recruitment and Developmental Gene Expression in Murine Embryonic Stem Cells. *iScience* (2020) 23(11):101646. doi: 10.1016/j.isci.2020.101646
26. He J, Shen L, Wan M, Taranova O, Wu H, Zhang Y. Kdm2b Maintains Murine Embryonic Stem Cell Status by Recruiting PRC1 Complex to CpG Islands of Developmental Genes. *Nat Cell Biol* (2013) 15(4):373–84. doi: 10.1038/ncb2702
27. Kim D, Pertea G, Trapnell C, Pimentel H, Kelley R, Salzberg SL. TopHat2: Accurate Alignment of Transcriptomes in the Presence of Insertions, Deletions and Gene Fusions. *Genome Biol* (2013) 14(4):R36. doi: 10.1186/gb-2013-14-4-r36
28. Trapnell C, Hendrickson DG, Sauvageau M, Goff L, Rinn JL, Pachter L. Differential Analysis of Gene Regulation at Transcript Resolution With RNA-Seq. *Nat Biotechnol* (2013) 31(1):46–53. doi: 10.1038/nbt.2450
29. Ramirez F, Dündar F, Diehl S, Grüning BA, Manke T. deepTools: A Flexible Platform for Exploring Deep-Sequencing Data. *Nucleic Acids Res* (2014) 42 (Web Server issue):W187–91. doi: 10.1093/nar/gku365
30. Krivtsov AV, Armstrong SA. MLL Translocations, Histone Modifications and Leukaemia Stem-Cell Development. *Nat Rev Cancer* (2007) 7(11):823–33. doi: 10.1038/nrc2253
31. Dobson CL, Warren AJ, Pannell R, Forster A, Lavenir I, Corral J. The mll-AF9 Gene Fusion in Mice Controls Myeloproliferation and Specifies Acute Myeloid Leukaemogenesis. *EMBO J* (1999) 18(13):3564–74. doi: 10.1093/emboj/18.13.3564
32. Rogawski DS, Deng J, Li H, Miao H, Borkin D, Purohit T, et al. Discovery of First-in-Class Inhibitors of ASH1L Histone Methyltransferase With Anti-Leukemic Activity. *Nat Commun* (2021) 12(1):2792. doi: 10.1038/s41467-021-23152-6
33. Sitwala KV, Dandekar MN, Hess JL. HOX Proteins and Leukemia. *Int J Clin Exp Pathol* (2008) 1(6):461–74.
34. Domsch K, Papagiannouli F, Lohmann I. The HOX-Apoptosis Regulatory Interplay in Development and Disease. *Curr Top Dev Biol* (2015) 114:121–58. doi: 10.1016/bs.ctdb.2015.07.014
35. Magli MC, Largman C, Lawrence HJ. Effects of HOX Homeobox Genes in Blood Cell Differentiation. *J Cell Physiol* (1997) 173(2):168–77. doi: 10.1002/(SICI)1097-4652(199711)173:2<168::AID-JCP16>3.0.CO;2-C
36. Ayton PM, Chen EH, Cleary ML. Binding to Nonmethylated CpG DNA is Essential for Target Recognition, Transactivation, and Myeloid Transformation by an MLL Oncoprotein. *Mol Cell Biol* (2004) 24(23):10470–8. doi: 10.1128/MCB.24.23.10470-10478.2004

Conflict of Interest: GM has consulted for Colgate-Palmolive North America.

The remaining authors declare that the research was conducted in the absence of any commercial or financial relationships that could be construed as a potential conflict of interest.

Publisher's Note: All claims expressed in this article are solely those of the authors and do not necessarily represent those of their affiliated organizations, or those of the publisher, the editors and the reviewers. Any product that may be evaluated in this article, or claim that may be made by its manufacturer, is not guaranteed or endorsed by the publisher.

frontiers in Oncology

ORIGINAL RESEARCH
published: 12 October 2021
doi: 10.3389/fonc.2021.725336

Runt-Related Transcription Factor 3 Promotes Acute Myeloid Leukemia Progression

Wenwen Zhang[1,2†], *Qian Ma*[1,2,3†], *Bing Long*[4†], *Zhangyi Sun*[1,2], *Lingling Liu*[4*], *Dongjun Lin*[1*] *and Minyi Zhao*[1*]

[1] Department of Hematology, The Seventh Affiliated Hospital, Sun Yat-sen University, ShenZhen, China, [2] Key Laboratory of Stem Cells and Tissue Engineering, Zhongshan School of Medicine, Sun Yat-sen University, Ministry of Education, Guangzhou, China, [3] Department of Clinical Laboratory, Peking University First Hospital, Beijing, China, [4] Department of Hematology, The Third Affiliated Hospital, Sun Yat-sen University, Guangzhou, China

OPEN ACCESS

Edited by:
Fei Gao,
Beijing Genomics Institute (BGI), China

Reviewed by:
Hao Wang,
Northwestern University, United States
Guangjin Pan,
Guangzhou Institutes of Biomedicine and Health (CAS), China

***Correspondence:**
Minyi Zhao
zhaomy26@mail.sysu.edu.cn
Dongjun Lin
lindj@mail.sysu.edu.cn
Lingling Liu
liull35@mail.sysu.edu.cn

[†]*These authors have contributed equally to this work*

Specialty section:
This article was submitted to Hematologic Malignancies, a section of the journal Frontiers in Oncology

Received: *15 June 2021*
Accepted: *17 September 2021*
Published: *12 October 2021*

Citation:
Zhang W, Ma Q, Long B, Sun Z, Liu L, Lin D and Zhao M (2021) Runt-Related Transcription Factor 3 Promotes Acute Myeloid Leukemia Progression. Front. Oncol. 11:725336. doi: 10.3389/fonc.2021.725336

Acute myeloid leukemia (AML) is an aggressive hematological malignancy with high relapse/refractory rate. Genetic and epigenetic abnormalities are driving factors for leukemogenesis. RUNX1 and RUNX2 from the Runt-related transcription factor (RUNX) family played important roles in AML pathogenesis. However, the relationship between RUNX3 and AML remains unclear. Here, we found that *RUNX3* was a super-enhancer-associated gene and highly expressed in AML cells. The Cancer Genome Atlas (TCGA) database showed high expression of *RUNX3* correlated with poor prognosis of AML patients. We observed that *Runx3* knockdown significantly inhibited leukemia progression by inducing DNA damage to enhance apoptosis in murine AML cells. By chromatin immunoprecipitation sequencing (ChIP-seq) analysis, we discovered that RUNX3 in AML cells mainly bound more genes involved in DNA-damage repair and antiapoptosis pathways compared to that in normal bone marrow cells. *Runx3* knockdown obviously inhibited the expression of these genes in AML cells. Overall, we identified *RUNX3* as an oncogene overexpressed in AML cells, and *Runx3* knockdown suppressed AML progression by inducing DNA damage and apoptosis.

Keywords: RUNX3, super-enhancer, acute myeloid leukemia, cell cycle, apoptosis, DNA repair

INTRODUCTION

Acute myeloid leukemia (AML) is one of the most common hematologic malignancies that is characterized by clonal expansion of abnormally differentiated myeloid blasts (1, 2). High treatment failure rate of AML that is caused by frequent relapses and limited treatments challenges the clinical management of AML (3). Genetic and epigenetic abnormalities, such as NPM1 mutation, DNMT3a mutation, and MLL rearrangement, are determinants of AML pathogenesis and always relate to AML prognosis (4). Consequently, it is imperative to further decipher the genetic and epigenetic characteristics of AML to identify more new molecular targets for AML treatment improvement.

Super-enhancer is a special enhancer identified to enhance the transcription of key oncogenes in various cancer cells, such as prostate cancer cells, T cell acute lymphocytic leukemia cells, and multiple myeloma cells (5–7). In mouse AML cells, some genes critical in leukemogenesis, including

Myc, *Meis1*, and *Runx2*, are also super-enhancer-associated genes (8), which indicates that super-enhancers may dedicate to AML pathogenesis.

The Runt-related transcription factor (RUNX) family consists of three members, RUNX1, RUNX2, and RUNX3. The tumor-related functions of RUNX1 and RUNX2 were well studied. Especially, RUNX1 plays a critical role in AML pathogenesis (9). Meanwhile, RUNX3 was the least investigated (10). As a transcription factor, the heterodimer of RUNX3 and a beta subunit form a complex that binds to the core DNA sequence found in a number of enhancers and promoters and further activate or suppress transcription (11). RUNX3 was previously regarded as a tumor-suppressor gene for its inactivation promotes the progression of gastric cancer, lung cancer, colorectal cancer, and bladder cancer by upregulating oncogenes, such as *YBX1* and *GLI1*, or abrogating ARF–P53 pathway (12–16). Conversely, RUNX3 is overexpressed and exhibits oncogenic activities in ovarian cancers, basal cell carcinomas, and head and neck cancers (17–19). As well, RUNX3 overexpression drives the transformation of myelodysplastic syndrome, another myeloid malignancy, by repressing RUNX1 (20) and predicts poor prognosis in childhood AML (21). However, the relationship between RUNX3 and AML pathogenesis remains mysterious.

In this study, we discovered that RUNX3 is a super-enhancer-associated gene and highly expressed in AML cells. *Runx3* knockdown in murine AML cells efficiently impeded AML progress. Furthermore, we proved that RUNX3 bound and upregulated the expression of genes involved in DNA repair and antiapoptosis pathways to promote AML progression.

RESULTS

RUNX3 Is a Super-Enhancer-Associated Gene Only Highly Expressed in Acute Myeloid Leukemia Cells Instead of in Normal Blood Cells

To identify super-enhancer-associated genes that are unique in AML cells, we analyzed H3K27ac chromatin immunoprecipitation sequencing (ChIP-Seq) data of three types of normal blood cells, including neutrophils (NEs), monocytes (MOs), and hematopoietic stem cell progenitor cells (HSPCs), and AML cells (AML1#–3#). We found 3,436 super-enhancer-associated genes in normal blood cells. Meanwhile, 528 super-enhancer-associated genes were consistently identified in AML cells (**Figure 1A**). Furthermore, two independent RNA sequencing (RNA-seq) datasets (GSE128910 and GSE138702) were analyzed and revealed that 485 genes were identified as being differentially expressed (adjusted $p < 0.05$) with ≥1.5-fold differential expression between the groups were consistently overexpression. Accordingly, we found three abnormally highly expressed genes (*RUNX3*, *TMEM50B*, and *TGOLN2*) those were super-enhancer-associated genes only in AML cells (**Figure 1A** and **Supplementary Figure S1**). Furthermore, we analyzed The Cancer Genome Atlas (TCGA) database and found that only *RUNX3* expression was positively associated with poor prognosis in AML (*RUNX3*, p = 0.02; *TMEM50B*, p = 0.14; *TGOLN2*, p = 0.81; **Figure 1B**). Moreover, we observed that the expression level of *RUNX3* was remarkably higher in bone marrow cells from AML patients than that from healthy volunteers (15.39-fold increase; **Figure 1C** and **Table 1**). Consistently, both mRNA and protein levels of RUNX3 in MLL-AF9-induced murine AML cells were significantly elevated compared to those in normal murine bone marrow cells (7.72-fold increase of *Runx3* mRNA expression; **Figures 1D–F**).

Taken together, we demonstrate that *RUNX3* is a super-enhancer-associated gene only highly expressed in AML cells instead of in normal blood cells and probably exerts pro-tumor function on AML cells.

Runx3 Knockdown Inhibits Acute Myeloid Leukemia Progression *In Vivo*

To further explore the potential pro-tumor role of *Runx3* in AML, equal numbers of control (Vector) or *Runx3* knockdown (*Runx3* KD) murine AML cells were transplanted into syngeneic wild-type (WT) recipients (**Figure 2A**). To evaluate the effects of *Runx3* reduction, we first sorted green fluorescent protein $(GFP)^+$ leukemia cells from Vector and *Runx3* KD AML mice and confirmed that shRNA specific for *Runx3* led to decreased RUNX3 expression by qRT-PCR and Western blot analysis (80.3% reduction of *Runx3* mRNA expression; **Figures 2B, C** and **Supplementary Figure S2**). We found that *Runx3* KD significantly ablated AML cells in the peripheral blood (PB) [79.5% reduction on day 28 (d28), 46.9% reduction on d45; **Figures 2D, E**] and reduced disease burden in the bone marrow (37.4% reduction on leukemic cell frequency, 47.2% reduction on leukemic cell number; **Figure 2F**). Furthermore, the spleen and liver of AML mice were significantly enlarged, and *Runx3* knockdown significantly alleviated these symptoms (44.9% and 35.7% reduction of spleen weight and liver weight, respectively; **Figure 2G**). Consistently, histological analysis showed that AML mice in *Runx3* KD group had fewer leukemia cell infiltration in the peripheral blood, spleen, and liver (**Figure 2H**). Importantly, *Runx3* knockdown significantly prolonged the survival of AML mice [Median overall survival (MOS) 81 days in *Runx3* knockdown group compared to 56 days in vector control group; **Figure 2I**].

These results demonstrate that *Runx3* knockdown suppresses the progression of MLL-AF9-induced AML in mice, which supports our hypothesis that *Runx3* is oncogenic in AML.

Runx3 Knockdown Induces DNA Damage and Apoptosis in Acute Myeloid Leukemia Cells *In Vivo*

We next investigated how *Runx3* knockdown suppressed the development of AML. Through flow cytometric analysis of control (Vector) or *Runx3* KD AML cells, we found a slight increase in the percentage of G2/S/M-phase cells and G0-phase cells, accompanied by a minor decrease in the percentage of G1-phase cells after *Runx3* knockdown (1.14-fold and 1.34-fold

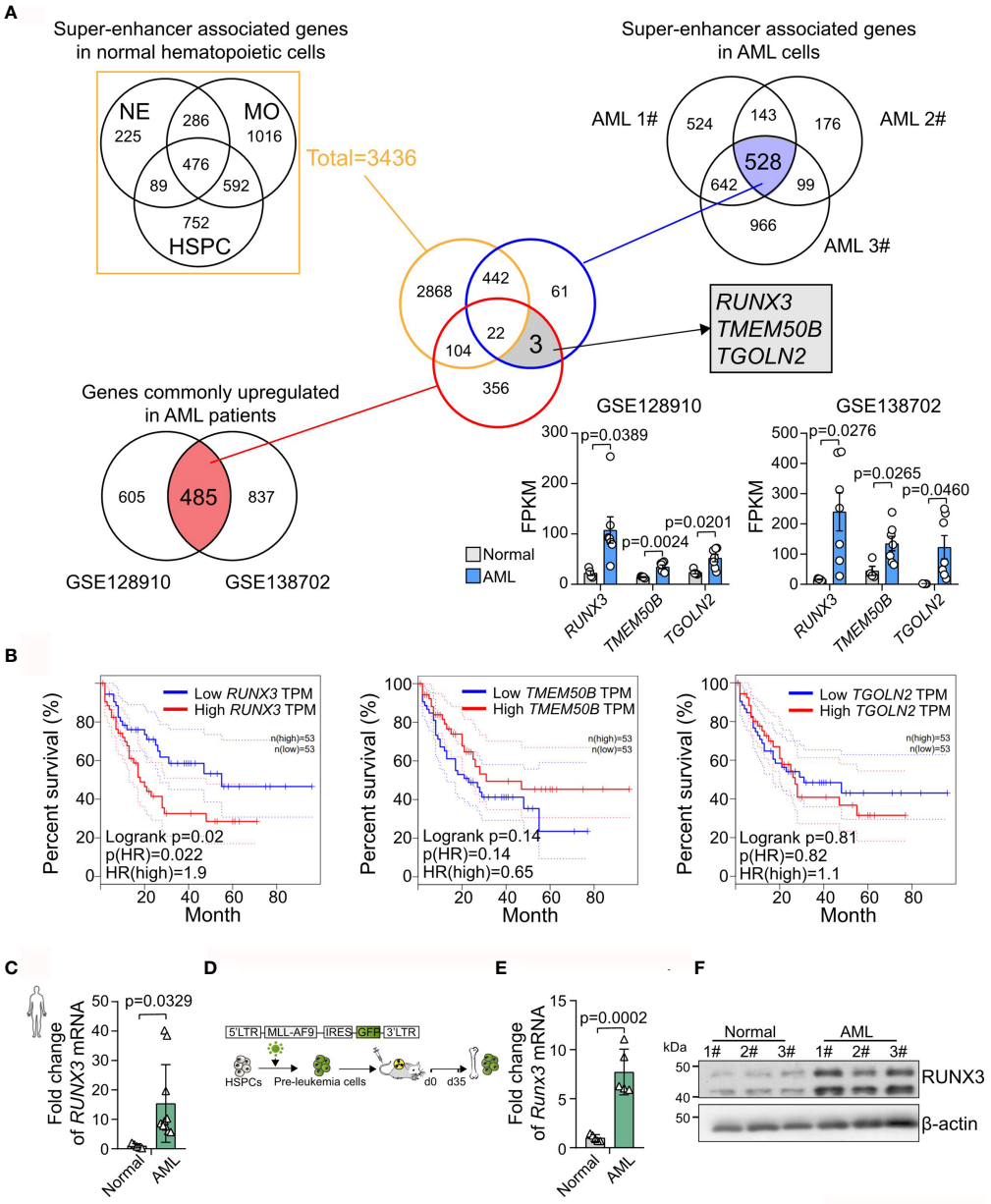

FIGURE 1 | *RUNX3* is a super-enhancer-associated gene only highly expressed in acute myeloid leukemia (AML) cells instead of in normal blood cells. **(A)** Experimental scheme to search for specific and highly expressed super-enhancer-associated genes in AML cells. **(B)** The Kaplan–Meier survival curves of *RUNX3*, *TMEM50B*, and *TGOLN2* in The Cancer Genome Atlas (TCGA)-LAML database. **(C)** The *RUNX3* mRNA expression of bone marrow cells from healthy volunteers (n = 5) or AML patients (n = 10). **(D)** Experimental scheme for panels **(E, F)**. **(E)** qRT-PCR and **(F)** Western blot showing that RUNX3 expression was increased in murine leukemic cells from primary transplant mice compared with normal mouse bone marrow cells. ACTIN was used to show equal loading. Symbols represent an individual mouse.

increase in G2/S/M-phase cells and G0-phase cells, 12.8% reduction in G1-phase cells, respectively; **Figure 3A** and **Supplementary Figure S3**). Reduction of *Runx3* in leukemic cells therefore appeared to induce G0/G1 arrest, which was consistent with a reduction of leukemia burden. Furthermore, *Runx3* knockdown obviously increased DNA damage in AML cells (1.81-fold increase in γ-H2AX$^+$ cells, 3.93-fold increase in γ-H2AX foci per cell; **Figures 3B, C**). Annexin V and 7-AAD double staining showed that upon *Runx3* knockdown, the percentage of total apoptotic cells in AML cells was remarkably increased to 13.4% compared with 8.6% in control group (1.56-fold increase) (**Figure 3D**).

Altogether, these results illustrate that *Runx3* knockdown induces DNA damage and apoptosis in leukemia cells *in vivo*.

TABLE 1 | Clinical sample information.

	Sample number	Patient's identification number	Age	Subtype	Tumor burden (%) in BM	Red blood cell (RBC,10^12/L)	White blood cell (WBC,10^9/L)	Platelet (10^9/L)
AML	1 #	695438	29	M5	29.8	66	25.9	55
Patients	2#	665972	19	M2	36.3	63	49.9	23
	3#	687524	34	M1	75.7	39	36.6	75
	4#	742586	49	M5	54.6	38	46.4	45
	5#	675823	58	M5	79.2	48	62.1	46
	6#	668545	44	M1	68.2	56	66.6	45
	7#	698657	35	M1	58.3	44	35.5	68
	8#	699982	61	M5	59.1	55	73.2	38
	9#	659325	52	M4	27.5	67	21.1	48
	10#	695837	61	M4	52.8	50	45.5	61
	Sample Number	**Gender**	**Age**					
Healthy	1#	Male	36					
Volunteers	2#	Female	42					
	3#	Female	21					
	4#	Male	28					
	5#	Male	31					

Clinical sample information of 10 acute myeloid leukemia (AML) patients and five healthy volunteers for ***Figure 1C****.*

RUNX3 Binds to Cell Cycle-Related Genes in Both Normal Bone Marrow Cells and Acute Myeloid Leukemia Cells but Specifically to DNA Repair and Antiapoptosis-Related Genes Only in Acute Myeloid Leukemia Cells

To determine the molecular mechanism of the oncogenic activity of RUNX3 in AML cells, we analyzed the genomic distribution of RUNX3 in bone marrow cells from normal mice and AML mice by RUNX3 chromatin immunoprecipitation followed by next-generation sequencing (ChIP-seq). The bone marrow cells from primary AML mice were collected 35 days after transplantation at which point the percentage of AML cells (GFP^+ cells) was 97.5% (**Figure 4A** and **Supplementary Figures S4A, B**). The number of RUNX3 peaks and corresponding genes in the leukemia group was significantly higher than those in the normal cells (**Figure 4B**). RUNX3 peaks were enriched at introns, promoters, intergenic sites, and exons of genes in normal cells and leukemia cells (**Figure 4C**). By analyzing RUNX3-bound genes in normal bone marrow cells and AML cells, we found that 4,667 genes were able to be bound by RUNX3 in both normal bone marrow cells and AML cells. There were 5,845 RUNX3-bound genes that could be found in AML cells but not in normal bone marrow cells (**Figure 4D**).

To further explore the difference between RUNX3-bound genes in normal bone marrow cells and AML cells, Gene Ontology (GO) enrichment analysis was performed. We found that most of the 4,667 RUNX3-bound genes in both types of cells were cell cycle-related genes, but the RUNX3 peak values were higher in AML cells (**Supplementary Figures S4C, D**). More importantly, most of the 5,845 genes specifically bound by RUNX3 in AML cells were related to DNA repair and the negative regulation of apoptosis, such as *Chek1*, *Ddb1*, *Rad51c*, *Rpa2*, *Bcl-2*, and *Mcl-1* (**Figures 4E, F**). Surprisingly, many classical AML-related oncogenes that have been reported were found to be bound by RUNX3 in AML cells, such as *Myc*, *Cd93* (22), *Kit*, *Ikzf2* (23), *Fto* (24), and *Sox4* (25) (**Supplementary Figure S4E**). Furthermore, we discovered that RUNX3 tended to bind with these classical genes related to DNA repair, antiapoptosis, and leukemogenesis around their promoter areas (**Figure 4F** and **Supplementary Figure S4E**). Interestingly, RUNX3 bound some classical DNA-repair genes at their enhancer areas, while it bound no antiapoptotic genes at their enhancer areas (**Supplementary Figure S4F**).

These results indicate that RUNX3 probably directly regulates genes related to cell cycle, DNA repair, and apoptosis in AML cells.

Runx3 Knockdown Inhibits the Expression Levels of Genes Involved in DNA Repair, Antiapoptosis, and Cell Cycle Pathways in Acute Myeloid Leukemia Cells

To prove the regulatory role of RUNX3 in the expression of DNA repair, antiapoptosis, and cell cycle-related genes that it binds to, we detected the expression of the above genes in murine AML cells under *Runx3* knockdown by qRT-PCR. Transcriptional analysis showed that *Runx3* knockdown decreased the expression level of cell cycle-related genes that RUNX3 binds to, such as *Cdk4*, *Ccnd1*, *Ccnd2*, *Cdk2*, *Ccna1*, and *Ccnb1* (36.4%, 21.1%, 52.3%, 52.0%, 29.9%, and 45.4% reduction, respectively) in murine AML cells (**Supplementary Figure S5**). More importantly, in murine AML cells, *Runx3* knockdown also significantly reduced the expression of DNA-repair (*Chek1*, *Ddb1*, *Rad51c*, *Rpa2*, *Rpa3*, *Xrcc1*, and *Xrcc4*) (36.4%, 48.7%, 46.4%, 56.8%, 62.1%, 56.3%, and 28.6% reduction, respectively)- and antiapoptosis (*Bcl2*, *Bcl2l10*, *Bcl2l12*, and *Mcl1*) (43.3%, 48.5%, 63.3%, and 43.4% reduction, respectively)-related genes that RUNX3 binds to only in AML cells (**Figures 5A, B**). Consistently, the expression of several genes associated with leukemogenesis that has been reported was obviously reduced after RUNX3 knockdown in murine AML cells (*Myc*, *Kit*, and *Ikzf2*) (63.8%, 62.6%, and 47.1% reduction, respectively) (**Figure 5C**).

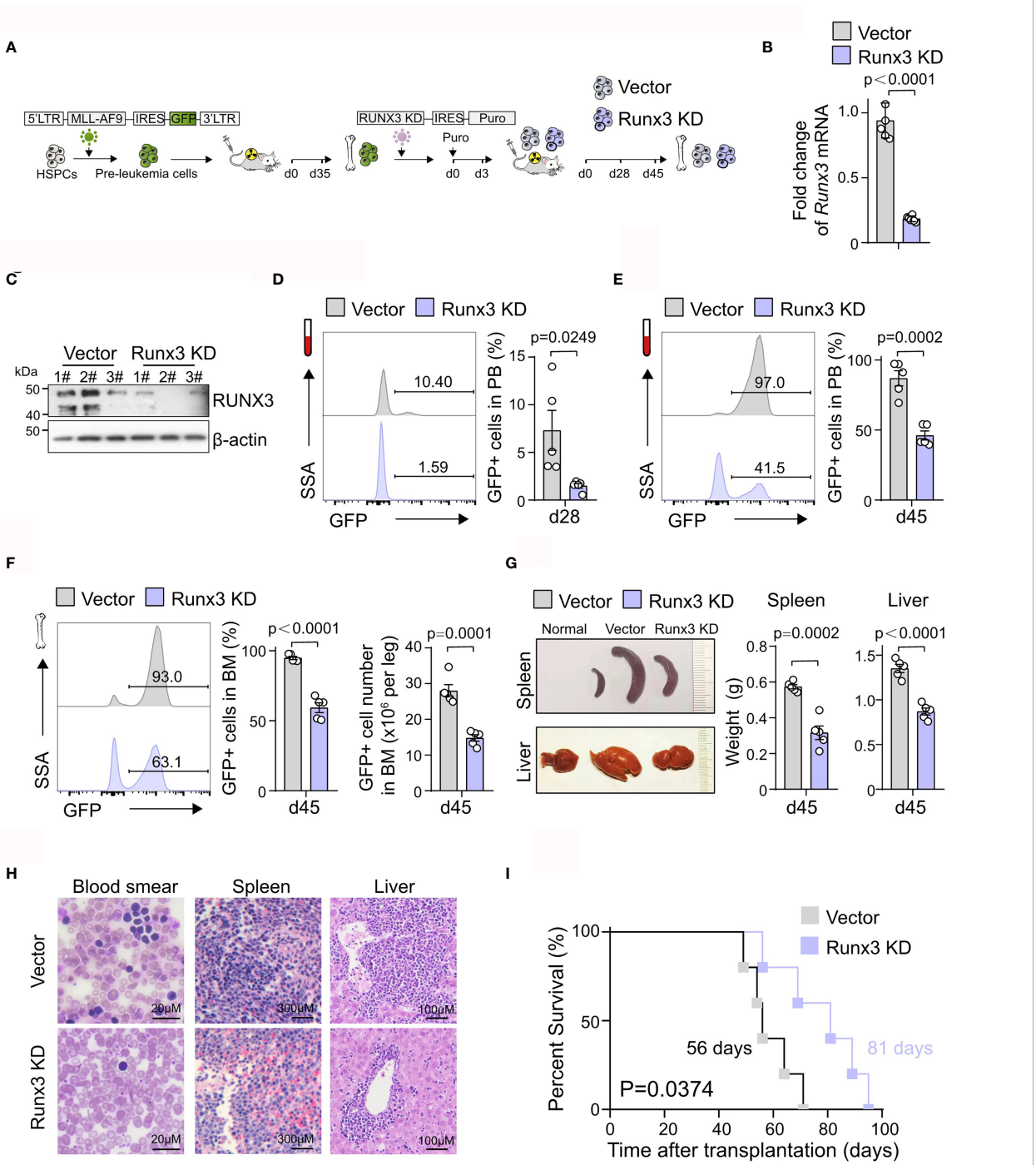

FIGURE 2 | *Runx3* knockdown inhibits acute myeloid leukemia (AML) progression *in vivo*. **(A)** Experimental scheme for investigating RUNX3 role in AML progression *in vivo*. **(B)** qRT-PCR analysis showing *Runx3* knockdown in sorted AML cells from bone marrow of scramble control (Vector) and *Runx3* knockdown (*Runx3* KD) AML mice at day 45 posttransplantation. Each dot represents a mouse. **(C)** Western blot analysis showing RUNX3 knockdown. **(D)** Representative cytometric flow plots (left) and statistic results (right) show that *Runx3* knockdown decreases leukemia burden in peripheral blood (PB) at day 28 posttransplantation (n = 5 mice). **(E)** The percentage of green fluorescent protein $(GFP)^+$ AML cells in the PB at day 45 posttransplantation (n = 5 mice). **(F)** Representative cytometric flow plots (left), the percentage of GFP^+ AML cells (middle), and the number of GFP^+ leukemic cells (right) in bone marrow (BM) at day 45 posttransplantation (n = 5 mice). **(G)** Representative image of spleen (upper left), liver (bottom left), and quantitative analysis of spleen weight (middle) and liver weight (right) from scramble control and *Runx3* knockdown AML mice (n = 5 mice). **(H)** Wright–Giemsa staining of blood smear and H&E staining of spleen and liver from scramble control and *Runx3* knockdown AML mice. Scale bar: blood smear 20 μm, spleen 300 μm, liver 100 μm. **(I)** Survival analysis of mice transplanted with scramble control or *Runx3* knockdown AML cells. Data shown are combined from two independent transplants. (n = 5 mice). p = 0.0374, log-rank test.

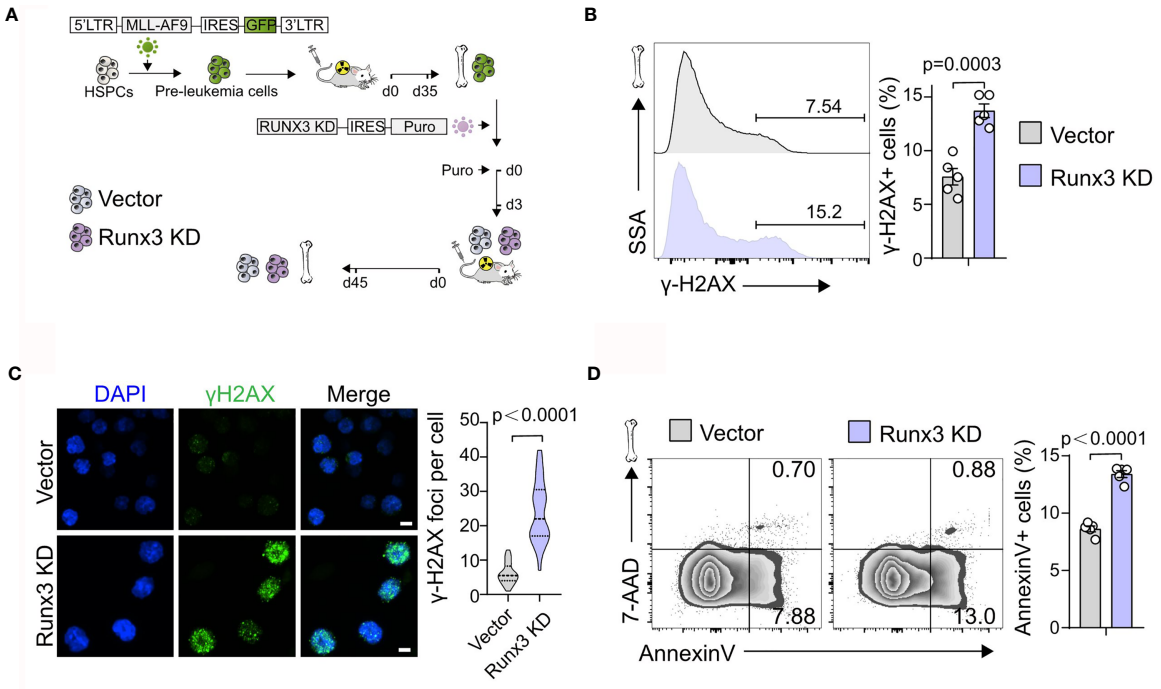

FIGURE 3 | *Runx3* knockdown induces DNA damage and apoptosis in AML cells *in vivo*. **(A)** Experimental scheme for getting *Runx3* knockdown AML cells induced by MLL-AF9. **(B)** Representative flow cytometry (FCM) plots and quantitative analysis show the percentage of γ-H2AX$^+$ cells in scramble control and *Runx3* knockdown AML cells (n = 5 mice). **(C)** CLSM images of γ-H2AX expression and quantification of γ-H2AX foci per cell (30 cells in each group) in scramble control and *Runx3* knockdown AML cells. Nuclear DNA was counterstained with DAPI. Scale bar = 50 μm. **(D)** *Runx3* knockdown increases apoptosis. Representative FCM plots (left) and statistical results (right) show the percentage of apoptotic cells in scramble control and *Runx3* knockdown AML cells. Bone marrow cells were stained for Annexin V and 7-AAD (n = 5 mice).

Taken together, these results illustrate that *Runx3* knockdown inhibits the expression levels of cell cycle-, DNA repair-, antiapoptosis-, and leukemogenesis-related genes in AML cells.

DISCUSSION

Genetic and epigenetic abnormalities drive leukemogenesis and determine the prognosis of AML (4). They are complex and dynamically evolving (26). There is still much work to do to uncover the full genetic and epigenetic landscape of AML. In our study, we found that RUNX3 was an obvious highly expressed gene in AML cells. According to TCGA-LAML database, the high expression of RUNX3 was positively related to poor prognosis of AML patients. These discoveries suggest a potential role of RUNX3 in AML progression.

As reported, diverse solid tumors, including gastric, colorectal, lung, and bladder cancers, exhibit low expression of RUNX3 (27). Low expression of RUNX3 is caused by gene deletion and epigenetic alteration. Epigenetic alteration is the most common one (28). The *RUNX3* gene is regulated by two promoters, P1 and P2. At the P2 promoter, there is a large CpG island that is often hypermethylated in tumor cells to silence RUNX3 (29). However, the P2 promoter in AML cells is unmethylated, and demethylating agents fail to increase RUNX3 expression level in AML cells (21). Moreover, we discovered that *RUNX3* in AML cells was regulated by a super-enhancer that had strengthened transcriptional regulating ability. These evidences explain why differs from that in other solid tumor cells, RUNX3 expression in AML cells is elevated.

The function of RUNX3 in cancers is controversial. Primarily, RUNX3 was reported as a tumor-suppressor gene in multiple cancers (12–14). Then, in ovarian cancers and head and neck cancers, RUNX3 showed oncogenic activity (17, 19). Consistent with the human information from TCGA database, our results showed that *Runx3* knockdown in MLL-AF9-induced AML cells retarded AML progression. This indicates that RUNX3 probably plays a pro-tumor role in AML. RUNX3 regulates transcription by binding enhancers and promoters (11). So, we performed ChIP-seq in both murine normal bone marrow cells and AML cells to investigate the mechanism of the oncogenic activity of RUNX3 in AML. We further discovered that compared to that in normal bone marrow cells, RUNX3 in AML cells tended to bind genes enriched in DNA repair (*Chek1*, *Ddb1*, *Rad51c*, and *Rpa2*), antiapoptosis (*Bcl2*, *Bcl2l10*, *Bcl2l12*, and *Mcl1*), and leukemogenesis (*Myc*, *Cd93*, *Kit*, *Ikzf2*, *Fto*, and *Sox4*) pathways. *Myc* is a classical oncogene in various cancers. The activation of *Myc* by RUNX3 had already been demonstrated to be the main cause of the oncogenic function of RUNX3 (30, 31). Also, *Ddb1*, *Chek1*, and *Rad51c* are essential genes involved in DNA-damage repair of AML cells (32, 33). *Bcl2* and *Mcl1* are critical antiapoptosis genes and successfully used as

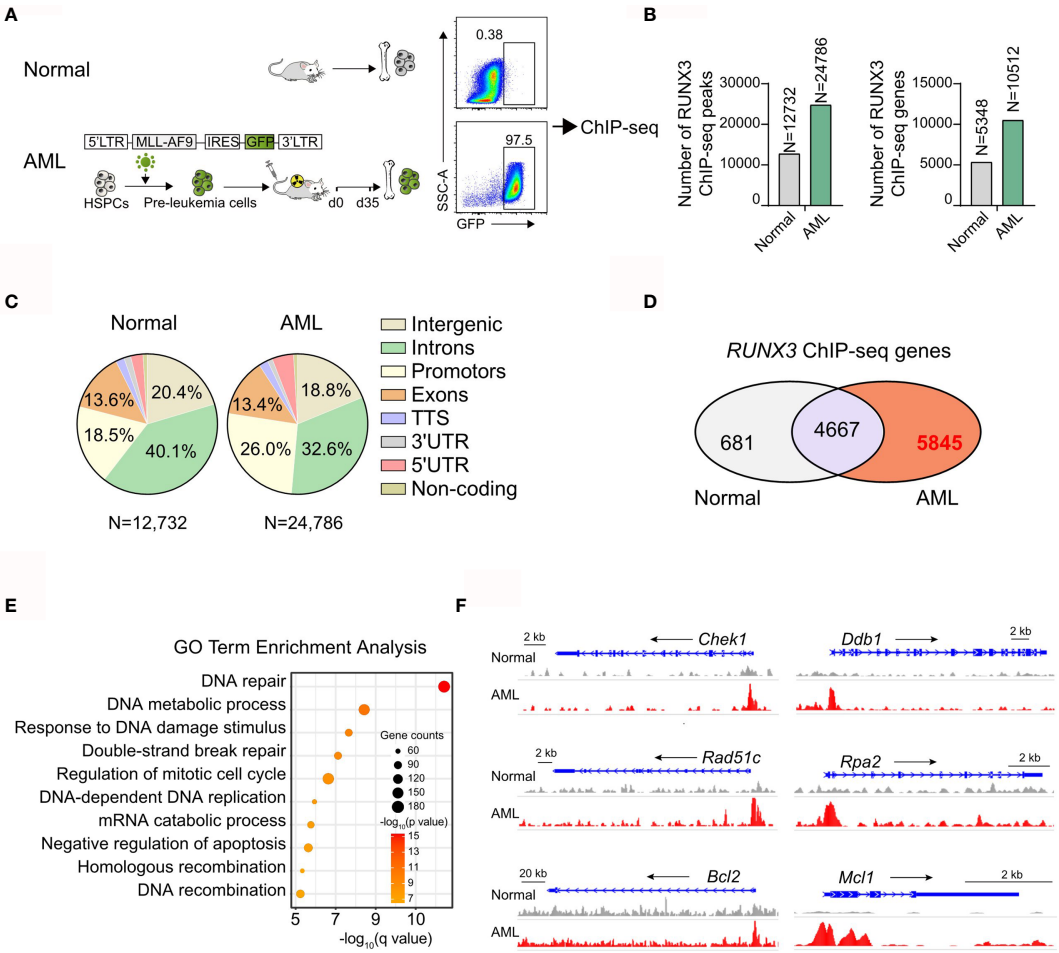

FIGURE 4 | RUNX3 specifically to DNA repair and anti-apoptosis related genes only in AML cells. Chromatin immunoprecipitation sequencing (ChIP-seq) results for RUNX3 in whole bone marrow cells from normal mice or MLL-AF9 AML mice. **(A)** Experimental scheme. **(B)** Number of RUNX3 ChIP-seq peaks and genes identified by HOMER. **(C)** Pie charts show the genomic distribution of ChIP-seq peaks for RUNX3 in whole bone marrow cells from normal mice (left) or MLL-AF9 AML mice (right). Representation of the annotated regions is shown for comparison. **(D)** Venn diagram of the RUNX3-bound 5,348 genes in normal bone marrow cells and the RUNX3-bound 10,512 genes in AML bone marrow cells. **(E)** Gene Ontology (GO) term enrichment analysis of 5,845 genes that can be bound by RUNX3 in leukemia cells but not be bound in normal bone marrow cells. **(F)** Genome browser views of the distribution of RUNX3 ChIP-seq peaks in DNA repair (*Chek1*, *Ddb1*, *Rad51c*, and *Rpa2*)- and antiapoptosis (*Bcl-2* and *Mcl-1*)-related gene loci.

treatment targets for AML (34). We demonstrated that in murine AML cells, RUNX3 mainly bound these classical genes at their promoter sites. With combined analysis of public datasets of H3K27ac ChIP-seq, we discovered that RUNX3 bound some key DNA-repair factors at their enhancer areas. However, we failed to find RUNX3 that bound any antiapoptotic factors at their enhancer areas. Our results further proved that *Runx3* knockdown significantly downregulated the expression of these DNA-repair and antiapoptotic genes in murine AML cells. This suggests that RUNX3 directly upregulates the expression of DNA-repair genes by controlling both their promoters and enhancers while upregulating the expression of antiapoptotic genes only by controlling their promoters. Decreased expression of DNA-repair genes resulted in increased DNA damage, which ultimately collaborated with the influence of reduced antiapoptotic factors to induce more apoptosis of AML cells *in vivo*. Also, our results showed that RUNX3 knockdown slightly disturbed the normal cell cycle of AML cells *in vivo*. Altogether, we elucidate that RUNX3 promotes AML progression not only by activating *Myc* transcription but also by directly regulating oncogene network covering DNA repair and apoptosis. Further studies are warranted to determine the detailed mechanism of how RUNX3 regulates the oncogene network.

Collectively, our study identified RUNX3 as an oncogene in AML, which conferred a new treatment target for AML therapy.

MATERIALS AND METHODS

Animals

The C57BL/6 mice and CD45.1 mice (6–8 weeks old, weighing 18–22 g) were all raised in the specific pathogen-free (SPF)-level animal breeding facility of the Experimental Animal Center of

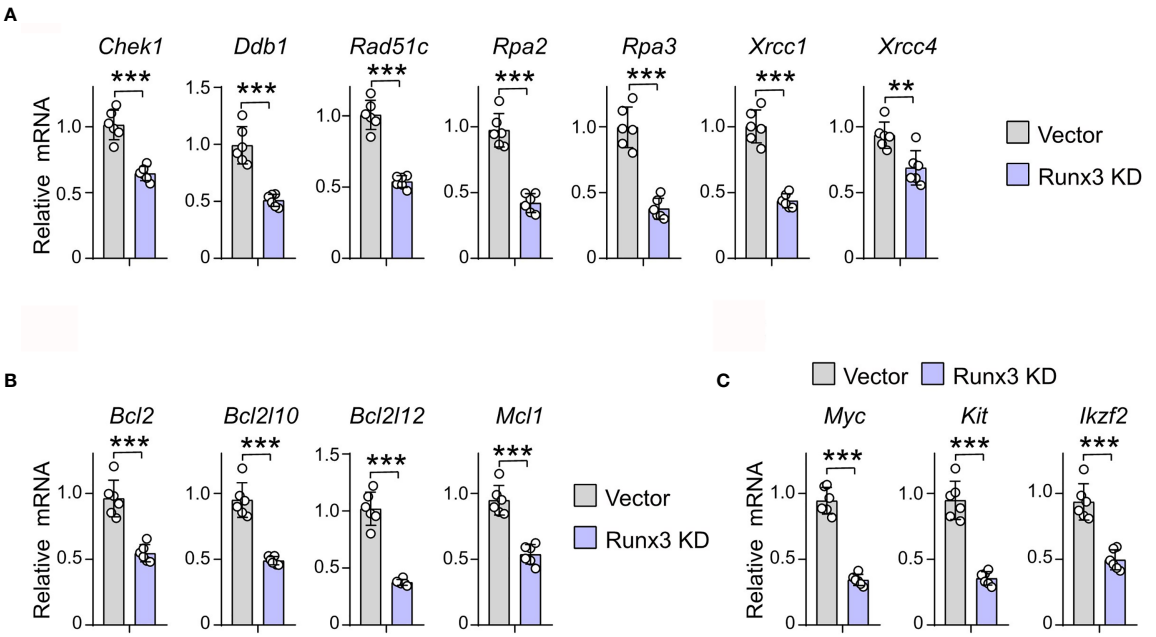

FIGURE 5 | *Runx3* knockdown inhibits the expression levels of genes involved in DNA repair and anti-apoptosis pathways in AML cells. **(A–C)** The relative mRNA expression level of DNA repair **(A)**, antiapoptosis **(B)**, and leukemogenesis **(C)** related genes that RUNX3 binds to only in AML cells. Data represent mean ± SEM of six mice. **p < 0.01, ***p < 0.001. ns, not significant.

Zhongshan Medical College, Sun Yat-sen University. All experimental procedures followed the experimental guidelines outlined in the Animal Care Principles and were approved by the Animal Care and Use Committee of Sun Yat-sen University.

Definition of Enhancers and Super-Enhancers

We downloaded H3K27ac ChIP-seq data from a public database (NE SRR1915572, MO SRR787551, HSPC SRR2094192, AML1# SRR3503794, AML2# SRR3503797, AML2# SRR3503801, mouse GSE117443). Enhancers were stitched, and super-enhancers were identified using ROSE (https://bitbucket.org/young_computation/rose). Briefly, constituent enhancers were stitched together if they are within a certain distance and ranked by their input-subtracted signal of H3K27ac. And then, we separated super-enhancers from typical enhancers by identifying an inflection point of H3K27ac signal; the slope here was 1. We run ROSE with a stitching distance of 12,500 bp and allowed enhancers within 12,500 bp to be stitched together. In addition, we used a transcription start site (TSS) exclusion zone of 5,000 bp. Finally, Rose GeneMapper tool was used to annotate the genes within the 50-kb range of the super-enhancers.

Survival Analysis of the Genes in The Cancer Genome Atlas Dataset

LAML data from TCGA were used to perform validation with the Gene Expression Profiling Interactive Analysis (GEPIA) database (http://gepia.cancer-pku.cn) (35). Furthermore, Kaplan–Meier curves were generated from the GEPIA database. The overall survival (OS) was estimated using the log-rank test, and p-value <0.05 was considered to denote statistically significant data.

Patient Specimens

The AML patients' specimens used in this study were derived from the routine clinical management in the Third Affiliated Hospital, Sun Yat-sen University. The procedure was approved by the ethics committee of the Third Affiliated Hospital, Sun Yat-sen University in accordance with the international guidelines and the ethical standards outlined in the Declaration of Helsinki. Mononuclear cells were isolated from the patient bone marrow with Ficoll-Hypaque and then processed to extract mRNA.

Quantitative RT-PCR

Total mRNA was extracted from sorted GFP^+ cells using MagZol™ Reagent (R4801-03, Magen) according to the manufacturer's instructions. mRNA purity and quantity were determined with NanoDrop (Thermo Scientific) before qPCR analysis. For qRT-PCR, equal amounts of mRNA samples were reverse transcribed into cDNA using the TransScript All-in-One First-Strand cDNA Synthesis SuperMix for qPCR (One-Step gDNA Removal) Kit (AT341, Transgen). Quantitative real-time PCR was performed on Bio-Rad CFX96 Touch™ Real-Time PCR Detection system using SYBR Green I Master Mix reagent (11203ES03, YEASEN).

Western Blotting

The same number of GFP^+ bone marrow cells from control or *Runx3* knockdown AML mice was sorted into phosphate buffered

saline (PBS) with 2% fetal bovine serum (FBS). The cells then were washed with PBS and lysed by radio immunoprecipitation assay (RIPA). Equal amounts of protein extracts were fractionated by 10% sodium dodecyl sulfate–polyacrylamide gel electrophoresis (SDS-PAGE) and transferred to a polyvinylidene fluoride (PVDF) membrane (IPVH00010, Merck Millipore). After being blocked with 5% non-fat milk in Tris-buffered saline with Tween-20 (TBST, pH 7.6) for 1 h at room temperature, the membranes were incubated with primary antibodies: anti-RUNX3/AML2 (D6E2) (mouse, 1:1,000, 9647, Cell Signaling Technology) and anti-β-actin (rabbit, 1:1,000, 4970, Cell Signaling Technology) overnight at 4°C and then incubated with secondary antibodies (rabbit, 1:10,000, W401B, Promega; mouse, 1:10,000, W402B, Promega) for 1 h at room temperature. The blots were detected by X-ray film or digital imaging system (Odyssey Fc).

Acute Myeloid Leukemia Mouse Model

The 293T cells were transfected with retroviral plasmids MSCV-MLL-AF9-IRES-GFP containing MLL-AF9 and GFP cDNA sequences. Bone marrow cells from C57 mice treated with 5-fluorouracil (5-FU) for 5 days were infected with retrovirus twice with 24-h interval. The 400K infected cells were mixed with 100K protective cells to intravenously inject into WT recipient mice irradiated with a 9-Gy lethal dose. The number of animals used per experiment is shown in the figure legends.

Constructs

Runx3 knockdown shRNA (GAAGAGTTTCACGCTCACAAT) was cloned into pLKO.1-puro (8453, Addgene). *Runx3* knockdown and control lentivirus were prepared by HEK293T transfected by pLKO.1-puro together with psPAX2, pMD2G packaging vectors. MLL-AF9-GFP$^+$ bone marrow cells were harvested from AML mice at 35 days after transplantation. These cells were infected with *Runx3* knockdown or control lentivirus and further selected by 1 μg ml^{-1} puromycin for 72 h. The 200K GFP$^+$ cells screened by puromycin were mixed with 100K protective cells to intravenously inject into CD45.2$^+$ recipient mice irradiated with a 4.5-Gy sublethal dose.

γ-H2AX Immunofluorescence Staining

The cells were transferred to a glass slide and allowed to stand for 1 h to make the cells adhere to the glass slide. After fixation with 4% paraformaldehyde (PFA) for 15 min, cells were permeabilized with 0.5% Triton X-100 at room temperature for 30 min, blocked with 10% goat serum solution at room temperature for 1 h, washed, and incubated with γ-H2AX primary antibody (Biolegend, Cat 613404) overnight. After that, the secondary antibody was added dropwise and incubated at room temperature for 1 h, and the high-speed confocal imaging system (Dragonfly CR-DFLY-202 2540) was used for imaging. The γ-H2AX foci in 30 cells were counted in each group.

Flow Cytometry

Take 20–30 μl of peripheral blood through the tail vein of the mouse and add to the anticoagulation tube. Take the bone marrow cells from the femur and tibia of the sacrificed mice. The red blood cells were lysed, and the bone marrow cells were filtered using a 100-μm cell strainer. Monoclonal antibodies to Mac-1 (M1/70, Biolegend), Gr-1 (RB6-8C5, Biolegend), c-Kit (2B8, Biolegend), Lin mix (Gr1, CD4, CD3, CD8a, Ter119, B220, IgM) (Biolegend), CD34 (MEC14.7, Biolegend), Sca1 (D7, Biolegend), FcγRII/III (93, Biolegend), IL-7Ra (A7R34, Biolegend) (all used as 50 ng per million cells) were used where indicated. After incubation with antibodies, the samples were analyzed using the Attune NxT flow cytometer (Thermo), and the results were analyzed using FlowJo software. Here, 7-aminoactinomycin D (7-AAD) (A1310, Life Technologies) was used to exclude dead cells.

Chromatin Immunoprecipitation

Bone marrow cells were harvested from MLL-AF9-induced AML mice 35 days after transplantation, and bone marrow cells from normal syngeneic mice with the same age served as controls, five mice for each group. Here, 1% formaldehyde in PBS was used to crosslink the cells for 10 min, followed by quenching with 125 mM glycine on ice. Cells were collected and flash frozen in liquid nitrogen, then stored at -80°C for use. Frozen crosslinked cells were thawed on ice and then resuspended in lysis buffer I (50 mM HEPES-KOH pH 7.5, 140 mM NaCl, 1 mM EDTA, 10% glycerol, 0.5% NP-40, 0.25% Triton X-100, protease inhibitors). After rotating for 10 min at 4°C, the cells were collected and resuspended in lysis buffer II (10 mM Tris-HCl pH 8.0, 200 mM NaCl, 1 mM EDTA, 0.5 mM EGTA, protease inhibitors). After rotating for 10 min at 4°C, the cells were collected and resuspended in sonication buffer (20 mM Tris-HCl pH 8.0, 150 mM NaCl, 2 mM EDTA pH 8.0, 0.1% SDS, 1% Triton X-100, protease inhibitors) for sonication. Sonicated lysates were cleared once by centrifugation at 16,000 g for 10 min at 4°C. Input material was reserved as control. The remainder was incubated with magnetic beads bound with anti-RUNX3/AML2 (D6E2) antibody (mouse, 1:1,000, 9647, Cell Signaling Technology) to enrich for DNA fragments overnight at 4°C. Beads were washed with wash buffer (50 mM HEPES-KOH pH 7.5, 500 mM LiCl, 1 mM EDTA pH 8.0, 0.7% Na-deoxycholate, 1% NP-40) and TE buffer (10 mM Tris-HCl pH 8.0, 1 mM EDTA, 50 mM NaCl) in order. Beads were removed by incubation at 65°C for 30 min in elution buffer (50 mM Tris-HCl pH 8.0, 10 mM EDTA, 1% SDS). Crosslinks were reversed overnight at 65°C. To purify eluted DNA, 200 ml TE was added, and then RNA was degraded by incubation in 8 μl 10 mg/ml RNase A at 37°C for 2 h. Protein was degraded by addition of 4 μl 20 mg/ml^{-1} proteinase K and incubation at 55°C for 2 h. Phenol:chloroform:isoamyl alcohol extraction was performed followed by an ethanol precipitation. The DNA was then resuspended in 5 0ml TE. Library preparation was performed with a DNA Library Prep Kit (Vazyme, #TD501); libraries were amplified for seven cycles and were size-selected with Beckman AMPure XP beads. Two biological replicates were performed for each group.

ChIP-Seq Data Analysis

We aligned the ChIP-Seq data to the mm9 reference genome by bowtie2 with default parameter, followed by removing the multiple aligned reads, PCR duplications with samtools. To

eliminate the impact of "Problematic genomic regions", we downloaded the ENCODE blacklist (Consortium, 2012) and discarded the reads aligning this region through bedtools. Finally, we used macs2 to calling peaks with control, setting a q value cutoff of 0.05.

Gene Ontology Analysis

To find the GO terms enriched in RUNX3-bound genes, The clusterProfiler (36) package in R was utilized for the identification and visualization of enriched pathways among differentially expressed genes identified as described above. The functions "enrichGO" were used to identify overrepresented pathways based on the GO databases. Significance in the enrichment analysis was based on p.adjust <0.05. For **Figures 4E, G**, we reported 10 significant GO Biological Process terms and their associated q values.

Statistics

Data are expressed as means ± SEM. For all experiments, except the determination of survival, data were analyzed by Student's *t*-tests, and differences were considered statistically significant if $p < 0.05$. The survival of the two groups was analyzed using a log-rank test, and differences were considered statistically significant if $p < 0.05$. * $p < 0.05$, ** $p < 0.01$, *** $p < 0.001$.

DATA AVAILABILITY STATEMENT

The datasets presented in this study can be found in online repositories. The names of the repository/repositories and accession number(s) can be found below: NCBI BioProject PRJNA741044.

ETHICS STATEMENT

The studies involving human participants were reviewed and approved by the ethics committee of the Third Affiliated Hospital, Sun Yat-sen University (SYSU). The patients/participants provided their written informed consent to participate in this study.

AUTHOR CONTRIBUTIONS

WZ, QM, BL and ZS designed and performed most of the experiments and analyzed the data. BL and LL contributed to animal experiments and patient sample assay.WZ and MZ wrote the paper. LL, DL, and MZ supervised the project. All authors contributed to the article and approved the submitted version.

FUNDING

We would like to thank the National Natural Science Foundation of China (NSFC 81870127), National Natural Science Foundation of China (NSFC 81700149), Sanming Project of Medicine in Shenzhen (SZSM201911004), and Research support foundation for post doctors in the seventh affiliated hospital, Sun Yat-sen University (ZSQYRSFPD0017) for generous support.

SUPPLEMENTARY MATERIAL

The Supplementary Material for this article can be found online at: https://www.frontiersin.org/articles/10.3389/fonc.2021.725336/full#supplementary-material

Supplementary Figure 1 | *RUNX3* is super-enhancer-associated gene in AML cells. Enhancers in three normal blood cells and three AML cells ranked based on H3K27ac signal intensity.

Supplementary Figure 2 | *Runx3* knock-down is on the target. The relative mRNA expression level of *Runx1* and *Runx2* in sorted scramble control (Vector) and *Runx3* knock-down (*Runx3* KD) AML cells. Data represent mean ± s.e.m of 6 mice. ns, not significant.

Supplementary Figure 3 | *Runx3* knock-down impedes cell cycle progression in AML cells. Representative FACS plots (left) and quantitative analysis (right) of cell cycle in scramble control (Vector) and Runx3 knock-down (Runx3 KD) AML cells at day 45 post-transplantation (n=5 mice).

Supplementary Figure 4 | RUNX3 binds to cell cycle related genes and AML-related oncogenes both in normal bone marrow cells and AML cells. **(A, B)** Cell surface marker analysis of primary AML cells for ChIP-seq. Flow analysis of the bone marrow cells from AML mice 35 days after primary transplantation. The most commonly markers were used, such as $GFP^+CD11b^+Gr\text{-}1^+$, $GFP^+c\text{-}Kit^+$, $Gr\text{-}1^-c\text{-}Kit^+$ **(A)**, and $GFP^+Lin^-Sca\text{-}1^-IL\text{-}7R^-c\text{-}Kit^+CD34^+Fc\gamma RII/III^{high}$ **(B)** leukemia stem cells. **(C)** GO term enrichment analysis of 4667 genes that can be bound by RUNX3 in both normal bone marrow cells and AML cells. **(D)** Genome browser views of cell cycle related genes (*Mki67, Cdkn1b, Cdk4, and Ccnd1*) loci showing the distribution of RUNX3 ChIP-seq peaks. **(E)** RUNX3 directly binds to AML-related oncogenes. Genome browser views of AML-related oncogenes (*Myc, Cd93, Kit, Ikzf2, Fto* and *Sox4*) loci showing the distribution of RUNX3 ChIP-seq peaks. **(F)** Genome browser views of the distribution of RUNX3 and H3K27ac ChIP-seq peaks in DNA repair (*Rad54b, Rad51c, Chek1* and *Ddb2*) and anti-apoptosis *(Bcl-2 and Mcl-1)* related gene loci.

Supplementary Figure 5 | *Runx3* knock-down inhibits the expression levels of cell cycle-related genes in AML cells. The relative mRNA expression level of cell cycle related genes which RUNX3 binds to in sorted scramble control (Vector) and *Runx3* knock-down (*Runx3* KD) AML cells. Data represent mean ± s.e.m of 6 mice. *$p < 0.05$, **$p < 0.01$, ***$p < 0.001$.

REFERENCES

1. Khwaja A, Bjorkholm M, Gale R, Levine R, Jordan C, Ehninger G, et al. Acute Myeloid Leukaemia. *Nat Rev Dis Primers* (2016) 2:16010. doi: 10.1038/nrdp.2016.10
2. Short N, Rytting M, Cortes J. Acute Myeloid Leukaemia. *Lancet (London England)* (2018) 392(10147):593–606. doi: 10.1016/S0140-6736(18)31041-9
3. DeWolf S, Tallman M. How I Treat Relapsed or Refractory AML. *Blood* (2020) 136(9):1023–32. doi: 10.1182/blood.2019001982
4. Cai S, Levine R. Genetic and Epigenetic Determinants of AML Pathogenesis. *Semin Hematol* (2019) 56(2):84–9. doi: 10.1053/j.seminhematol.2018.08.001
5. Chen X, Ma Q, Shang Z, Niu Y. Super-Enhancer in Prostate Cancer: Transcriptional Disorders and Therapeutic Targets. *NPJ Precis Oncol* (2020) 4(1):31. doi: 10.1038/s41698-020-00137-0

6. Hnisz D, Abraham B, Lee T, Lau A, Saint-André V, Sigova A, et al. Super-Enhancers in the Control of Cell Identity and Disease. *Cell* (2013) 155(4):934–47. doi: 10.1016/j.cell.2013.09.053
7. Jia Y, Chng W, Zhou J. Super-Enhancers: Critical Roles and Therapeutic Targets in Hematologic Malignancies. *J Hematol Oncol* (2019) 12(1):77. doi: 10.1186/s13045-019-0757-y
8. Minzel W, Venkatachalam A, Fink A, Hung E, Brachya G, Burstain I, et al. Small Molecules Co-Targeting Ckiα and the Transcriptional Kinases CDK7/9 Control AML in Preclinical Models. *Cell* (2018) 175(1):171–85.e25. doi: 10.1016/j.cell.2018.07.045
9. Bullinger L, Döhner K, Döhner H. Genomics of Acute Myeloid Leukemia Diagnosis and Pathways. *J Clin Oncol Off J Am Soc Clin Oncol* (2017) 35 (9):934–46. doi: 10.1200/JCO.2016.71.2208
10. Deltcheva E, Nimmo R. RUNX Transcription Factors at the Interface of Stem Cells and Cancer. *Biochem J* (2017) 474(11):1755–68. doi: 10.1042/BCJ20160632
11. Levanon D, Eisenstein M, Groner Y. Site-Directed Mutagenesis Supports a Three-Dimensional Model of the Runt Domain. *J Mol Biol* (1998) 277(3):509–12. doi: 10.1006/jmbi.1998.1633
12. Li Q, Ito K, Sakakura C, Fukamachi H, Inoue K, Chi X, et al. Causal Relationship Between the Loss of RUNX3 Expression and Gastric Cancer. *Cell* (2002) 109(1):113–24. doi: 10.1016/S0092-8674(02)00690-6
13. Su H, Fan G, Huang J, Qiu X. YBX1 Regulated by Runx3-miR-148a-3p Axis Facilitates non-Small-Cell Lung Cancer Progression. *Cell Signal* (2021) 85:110049. doi: 10.1016/j.cellsig.2021.110049
14. Kim B, Na Y, Kim J, Jeong Y, Park S, Jo M, et al. RUNX3 Suppresses Metastasis and Stemness by Inhibiting Hedgehog Signaling in Colorectal Cancer. *Cell Death differ* (2020) 27(2):676–94. doi: 10.1038/s41418-019-0379-5
15. Kim W, Kim E, Jeong P, Quan C, Kim J, Li Q, et al. RUNX3 Inactivation by Point Mutations and Aberrant DNA Methylation in Bladder Tumors. *Cancer Res* (2005) 65(20):9347–54. doi: 10.1158/0008-5472.CAN-05-1647
16. Lee Y, Lee J, Jang J, Chi X, Kim J, Li Y, et al. Runx3 Inactivation Is a Crucial Early Event in the Development of Lung Adenocarcinoma. *Cancer Cell* (2013) 24(5):603–16. doi: 10.1016/j.ccr.2013.10.003
17. Lee C, Chuang L, Kimura S, Lai S, Ong C, Yan B, et al. RUNX3 Functions as an Oncogene in Ovarian Cancer. *Gynecol Oncol* (2011) 122(2):410–7. doi: 10.1016/j.ygyno.2011.04.044
18. Salto-Tellez M, Peh B, Ito K, Tan S, Chong P, Han H, et al. RUNX3 Protein is Overexpressed in Human Basal Cell Carcinomas. *Oncogene* (2006) 25 (58):7646–9. doi: 10.1038/sj.onc.1209739
19. Kudo Y, Tsunematsu T, Takata T. Oncogenic Role of RUNX3 in Head and Neck Cancer. *J Cell Biochem* (2011) 112(2):387–93. doi: 10.1002/jcb.22967
20. Yokomizo-Nakano T, Kubota S, Bai J, Hamashima A, Morii M, Sun Y, et al. Overexpression of RUNX3 Represses RUNX1 to Drive Transformation of Myelodysplastic Syndrome. *Cancer Res* (2020) 80(12):2523–36. doi: 10.1158/0008-5472.CAN-19-3167
21. Cheng C, Li L, Cheng S, Lau K, Chan N, Wong R, et al. Transcriptional Repression of the RUNX3/AML2 Gene by the T (8,21) and Inv(16) Fusion Proteins in Acute Myeloid Leukemia. *Blood* (2008) 112(8):3391–402. doi: 10.1182/blood-2008-02-137083
22. Iwasaki M, Liedtke M, Gentles A, Cleary M. CD93 Marks a Non-Quiescent Human Leukemia Stem Cell Population and Is Required for Development of MLL-Rearranged Acute Myeloid Leukemia. *Cell Stem Cell* (2015) 17(4):412–21. doi: 10.1016/j.stem.2015.08.008
23. Park S, Cho H, Thornton A, Barlowe T, Chou T, Chhangawala S, et al. IKZF2 Drives Leukemia Stem Cell Self-Renewal and Inhibits Myeloid Differentiation. *Cell Stem Cell* (2019) 24(1):153–65.e7. doi: 10.1016/j.stem.2018.10.016
24. Li Z, Weng H, Su R, Weng X, Zuo Z, Li C, et al. FTO Plays an Oncogenic Role in Acute Myeloid Leukemia as a N-Methyladenosine RNA Demethylase. *Cancer Cell* (2017) 31(1):127–41. doi: 10.1016/j.ccell.2016.11.017
25. Zhang H, Alberich-Jorda M, Amabile G, Yang H, Staber P, Di Ruscio A, et al. Sox4 is a Key Oncogenic Target in C/Ebpα Mutant Acute Myeloid Leukemia. *Cancer Cell* (2013) 24(5):575–88. doi: 10.1016/j.ccr.2013.09.018
26. Papaemmanuil E, Gerstung M, Bullinger L, Gaidzik V, Paschka P, Roberts N, et al. Genomic Classification and Prognosis in Acute Myeloid Leukemia. *N Engl J Med* (2016) 374(23):2209–21. doi: 10.1056/NEJMoa1516192
27. Chen F, Liu X, Bai J, Pei D, Zheng J. The Emerging Role of RUNX3 in Cancer Metastasis (Review). *Oncol Rep* (2016) 35(3):1227–36. doi: 10.3892/or.2015.4515
28. Chuang L, Ito Y. RUNX3 is Multifunctional in Carcinogenesis of Multiple Solid Tumors. *Oncogene* (2010) 29(18):2605–15. doi: 10.1038/onc.2010.88
29. Bangsow C, Rubins N, Glusman G, Bernstein Y, Negreanu V, Goldenberg D, et al. The RUNX3 Gene–Sequence, Structure and Regulated Expression. *Gene* (2001) 279(2):221–32. doi: 10.1016/S0378-1119(01)00760-0
30. Date Y, Ito K. Oncogenic RUNX3: A Link Between P53 Deficiency and MYC Dysregulation. *Mol Cells* (2020) 43(2):176–81. doi: 10.14348/molcells.2019.0285
31. Selvarajan V, Osato M, Nah G, Yan J, Chung T, Voon D, et al. RUNX3 is Oncogenic in Natural Killer/T-Cell Lymphoma and is Transcriptionally Regulated by MYC. *Leukemia* (2017) 31(10):2219–27. doi: 10.1038/leu.2017.40
32. Boudny M, Trbusek M. ATR-CHK1 Pathway as a Therapeutic Target for Acute and Chronic Leukemias. *Cancer Treat Rev* (2020) 88:102026. doi: 10.1016/j.ctrv.2020.102026
33. Kotake Y, Zeng Y, Xiong Y. DDB1-CUL4 and MLL1 Mediate Oncogene-Induced P16ink4a Activation. *Cancer Res* (2009) 69(5):1809–14. doi: 10.1158/0008-5472.CAN-08-2739
34. Ramsey H, Fischer M, Lee T, Gorska A, Arrate M, Fuller L, et al. A Novel MCL1 Inhibitor Combined With Venetoclax Rescues Venetoclax-Resistant Acute Myelogenous Leukemia. *Cancer Discov* (2018) 8(12):1566–81. doi: 10.1158/2159-8290.CD-18-0140
35. Tang Z, Li C, Kang B, Gao G, Li C, Zhang Z. GEPIA: A Web Server for Cancer and Normal Gene Expression Profiling and Interactive Analyses. *Nucleic Acids Res* (2017) 45:W98–W102. doi: 10.1093/nar/gkx247
36. Yu G, Wang L, Han Y, He Q. Clusterprofiler: An R Package for Comparing Biological Themes Among Gene Clusters. *Omics J Integr Biol* (2012) 16 (5):284–7. doi: 10.1089/omi.2011.0118

Conflict of Interest: The authors declare that the research was conducted in the absence of any commercial or financial relationships that could be construed as a potential conflict of interest.

frontiers in Oncology

ORIGINAL RESEARCH
published: 13 October 2021
doi: 10.3389/fonc.2021.751834

Acute Myeloid Leukemia Epigenetic Immune Escape From Nature Killer Cells by ICAM-1

Yang Xiao[1†], Jinghong Chen[2†], Jia Wang[1†], Wei Guan[1], Mengzhen Wang[1], Linlin Zhang[1], Zhiding Wang[3], Lixin Wang[2*] and Li Yu[1,2*]*

[1] Department of Hematology and BMT Center, Chinese PLA General Hospital, Beijing, China, [2] Department of Hematology and Oncology, International Cancer Center, Shenzhen Key Laboratory, Shenzhen University General Hospital, Shenzhen University Health Science Center, Shenzhen University, Shenzhen, China, [3] Beijing Institute of Basic Medical Sciences, Beijing, China

OPEN ACCESS

Edited by:
Shujun Liu,
University of Minnesota Twin Cities, United States

Reviewed by:
Frederic Baron,
University of Liège, Belgium
Marianna Rossi,
Fondazione Ospedale San Matteo (IRCCS), Italy

***Correspondence:**
Li Yu
yuli@szu.edu.cn
Lixin Wang
wanglixin1991@sohu.com
Zhiding Wang
wzdfjfn@126.com

[†]These authors have contributed equally to this work

Specialty section:
This article was submitted to Hematologic Malignancies, a section of the journal Frontiers in Oncology

Received: *02 August 2021*
Accepted: *27 September 2021*
Published: *13 October 2021*

Citation:
Xiao Y, Chen J, Wang J, Guan W, Wang M, Zhang L, Wang Z, Wang L and Yu L (2021) Acute Myeloid Leukemia Epigenetic Immune Escape From Nature Killer Cells by ICAM-1. Front. Oncol. 11:751834. doi: 10.3389/fonc.2021.751834

Acute myeloid leukemia (AML), a malignant disorder of hemopoietic stem cells. AML can escape immunosurveillance of natural killer (NK) by gene mutation, fusions, and epigenetic modification, while the mechanism is not clearly understood. Here we show that the expression of Intercellular adhesion molecule-1 (ICAM-1, CD54) is silenced in AML cells. Decitabine could upregulate ICAM-1 expression, which contributes to the NK-AML cell conjugates and helps NK cells kill AML cells. We also show that ICAM-1 high expression can reverse the AML immune evasion and activate NK cells function *in vivo*. This study suggests that a combination of the hypomethylating agent and NK cell infusion could be a new strategy to cure AML.

Keywords: AML, ICAM-1, NK, methylation, immune escape

HIGHLIGHTS

- AML can escape immunosurveillance. The mechanism of AML immune evasion is not clearly understood.
- The expression of ICAM-1 is silenced, which could be reversed by decitabine. Thus, decitabine can help NK cells recognize and kill AML cells, which reverses AML immune evasion.
- This study suggests that the hypomethylating agent decitabine in combination with NK cell infusion may be a working strategy to cure AML.

BACKGROUND

AML is a heterogeneous disease from the biological and clinical standpoint with increasing incidence, high mortality, and a very poor prognosis (1, 2). Current therapies show also a high rate of relapse (3). AML has neoplastic changes and clonal proliferation due to gene mutation, fusions, and epigenetic modification, ultimately resulting in the inhibition of normal hematopoiesis and escape from immunosurveillance (4).

Immunotherapy based on mechanisms of immune surveillance has been recognized as a potential therapeutic strategy for numerous cancer elimination (5). Immunotherapy with strategies aimed at boosting the immune response has pushed NKs into the spotlight (2). Intercellular adhesion molecule-1 is a membrane glycoprotein of the Ig superfamily and plays an important role in inflammatory processes and immune responses (6). Studies showed that promoting the NK-AML cell conjugate formation by upregulating lymphocyte-function associated (LFA) antigen expression on NK cells and by inducing ICAM-1 expression on AML cells could increase their cytotoxic activities (7). Thus, restoring ICAM-1 expression in AML may combine the benefit of targeting AML cells and NK-mediated killing. However, limited studies are relating to how to increase the ICAM-1 expression on the surface of AML cells.

Decitabine is a valuable treatment option in AML patients (8). An important mechanism of tumor immune response evasion by cancer cells lies in their ability to display the loss of antigenicity, resulting in less potent for immune cells and substances in cancer elimination (5). A hypomethylating agent has favorable effects on anti-tumor immune response by reactivating the tumor suppressor genes (9). Hypomethylating agents such as decitabine have favorable effects on anti-tumor immune evasion response and limit the ability of cancer cells to alter the expression of tumor-associated antigens by regulating a range of immunomodulatory pathway-related genes (10).

In our previous studies, we found AML was epigenetic silenced (11–13) and could escape immunosurveillance by CD80 (14) and CD48 (15, 16). In this study, we found ICAM-I was also epigenetic silenced in AML and escaped the NK cell killing function. Decitabine is implicated in the regulation of ICAM-1 expression and reverses the AML-NK dysfunction.

MATERIALS AND METHODS

Mice

Male BALB/c mice (6- to 8-weeks-old) were obtained from SPF (Beijing) Biotechnology. All the mice were bred and maintained in the Laboratory Animal Center of Chinese PLA General Hospital, under specific pathogen-free conditions and were treated in strict compliance with the guidelines for the care and use of laboratory animals set out by the Laboratory Animal Center of Chinese PLA General Hospital, the protocol was approved by the Committee on the Ethics of Animal Experiments of Chinese PLA General Hospital (16). All the efforts were made to minimize suffering.

For the *in vivo* study, mice were separated into three groups (five each), and each mouse was injected intravenously (i.v.) with WEHI-3 (2.5×10^5) on Day 1. For decitabine treatment, each mouse was injected intraperitoneally (i.p.) 0.5 mg/kg/day from Day 1 to Day 3. For NK cell infusion, NK cells were separated from the spleen by the NK Cell Isolation Kit (Miltenyi), and each mouse was injected intravenously (i.v.) with 1×10^6 NK cells on Day 3. For the observation of the tumor burden in the mouse spleen and liver, the mice were sacrificed by CO_2 inhalation on Day 17 after WEHI-3 injection, when the mice of the control group started to paralyze and be dying. Isoflurane inhalation was used for any anaesthetization. Spleen and liver were stained with H&E for histological analysis.

Database Analysis

173 AML patients' and 70 healthy donors' samples were analyzed the ICAM-1 RNA sequencing expression data of The Cancer Genome Atlas (TCGA) database by GEPIA (17).

Cell Culture

Human cell lines NK92, HL60, and NB4 cells were maintained in RPMI 1640 medium and mouse cell line WEHI-3 cells were maintained in DMEM medium, supplemented with 50 μg/mL streptomycin, 50 IU penicillin, and 10% fetal bovine serum. All the cell lines are obtained from ATCC and culture at 37°C in 5% CO_2. For decitabine stimulation, the cell lines were cultured with decitabine for 72 h and decitabine was re-supplement every 24 h. Human cell lines (HL60 and NB4) were cultured with 1 μmol/mL decitabine. The mouse cell line WEHI-3 was cultured with 0.25 μmol/mL decitabine.

RNA Extraction and Analysis

Total RNA was extracted from cells using the TRIzol RNA Isolation Reagents (Thermo Fisher Scientific). RNA was reverse-transcribed in a 25 μL reaction volume using AMV Reverse Transcriptase (Promega), and then cDNA was amplified using KAPA SYBR FAST qPCR Kits (Kapa Biosystems). The relative expression of the gene of interest was determined using the 2–ΔΔCt method, with GAPDH as the internal control (18). The primers used were: Human ICAM-1: Forward: GGCATTGTTCTCTAATGTCTCCG, Reverse: GTCGAGCTTTGGGATGGTAG; Mouse ICAM-1: Forward: TTGGGCATAGAGACCCCGTT, Reverse: GCACATTGCT CAGTTCATACACC; 18S: Forward: TTGACGGAAGGGC ACCACCAG, Reverse: CATACCAGGAAATGAGCTTGA.

Cytometric Analysis

All the cell experiments were prepared on ice and cells were washed with FACS buffer. All the samples were incubated with 2.4G2 anti-Fc receptors (BD Pharmingen) before incubation with other antibodies. Fluorescence conjugated anti-mouse CD54 (Biolegend, YN1.7.4) and Pacific Blue anti-human ICAM-1 (Biolegend, HA58) antibodies were used. All the flow cytometry data were acquired with NAVIOS (BECKMAN) and analyzed by FlowJo software (Tree Star).

NK Cells Isolation

The NK Cell Isolation Kit (Miltenyi) was used for the untouched isolation mouse NK cells from spleen cells, which were activated by IL-2 and incubated in 5% CO_2 for 24 hours.

The Adhesion Between NK Cells and WEHI-3 Cells

NK cells were divided into PBS and Decitabine (DAC) groups. The WEHI-3 cells that were treated or untreated with decitabine

from Day 1 to Day 3 were collected on Day 4. The PBS and DAC groups of WEHI-3 were added into each well of NK cells. WEHI-3 untreated with decitabine and without NK cells was considered as a blank group for cytometric analysis.

NK Killing Assay

NK killing assay was described previously (16). In brief, the control cells were stained with CellTrace CFSE Cell Proliferation Kit (ThermoFisher Scientific), and the Decitabine treated cells were stained with CellTrace Far-red (ThermoFisher Scientific). Then the control cells and the Decitabine treated cells were plated on a 96-well plate. For ICAM-1 blocking, 20 mg/mL of anti-mouse ICAM-1 antibody (Biolegend, YN1/1.7.4) were added to each well. Then NK cells were added to each well and 20-24 h later the samples were analyzed by Flow Cytometer. Human cell lines (HL60 and NB4) were co-cultured with NK92 cells. The mouse cell line WEHI-3 was cultured with NK cells separated from mouse. The No NK group as control, the ratio of NK group was decitabine treated and untreated cell co-culture with NK cells. The CON and anti-ICAM-1 groups were percentages (1- normalized Treated/Untreated). The CON means the specific killing of decitabine treated and untreated cell co-culture with NK cells. The anti-ICAM-1 group means the specific killing of decitabine treated and untreated cell co-culture with NK cells and ICAM-1 antibody blocking.

Statistical Analysis

Data were expressed as the mean ± standard deviation. Differences between groups were analyzed using the t-test. The mouse model survival analysis was showed as Kaplan-Meier. A P-value less than 0.05 was considered to be significant. GraphPad Prism software (version 7.00) was used for All the statistical procedures. All the flow cytometry data were analyzed by FlowJo-V10 software.

RESULTS

ICAM-1 Silenced in AML Patients and Reversed by Hypomethylating

To determine the role of ICAM-1 in the AML patients, ICAM-1 mRNA expression was analyzed in the bone marrow or peripheral blood of 70 healthy controls and 173 AML patients from The Cancer Genome Atlas (TCGA) by GEPIA (16, 17). ICAM-1 mRNA expression was significantly lower in patients than in normal healthy individuals (**Figure 1A**). ICAM-1 expression on AML cells could increase NK cells cytotoxic activities. reversed the ICAM-1 expression could inhibit the AML immune escape. Q-PCR analysis showed that the hypomethylating agent decitabine can increase ICAM-1 mRNA expression on AML cell lines HL60 ($p < 0.0001$), NB4 ($p < 0.0001$), and WEHI-3 ($p = 0.0006$). The Q-PCR results (**Figures 1B**–**D**) showed that decitabine increased ICAM-1 mRNA expression, which was confirmed by FACS analysis for protein expression on the surface of HL60, NB4, and WEHI-3 cells (**Figures 1E**–**G**). These findings indicate that decitabine increases ICAM-1 expression and reveals a novel mechanism of a therapeutic hypomethylating agent for AML. By the Bisulfite Sequencing PCR analysis, WEHI-3 gene promoter methylation was decreased by decitabine treatment (**Figures 1H, I**). Thus, this hypomethylating agent could increase the ICAM-1 expression by decrease promoter methylation. Thus, decitabine may restore ICAM-1 expression and inhibit AML immune evasion from NK cells.

Decitabine Inhibits AML Immune Escape From NK Cells by ICAM-1

To determine if decitabine influence the NK cell to find AML, WEHI-3 cells were treated or untreated with decitabine and co-cultured with sorted NK cells (**Figure 2A**). FACS analysis showed that the adhesion ratio between NK cells and WEHI-3 treated with DAC was enhanced ($p = 0.0009$), with the PBS as the control group (**Figure 2B**). The cells that adhere to NK cells account for 9.29% among the WEHI-3 cells treated with DAC, while 1.26% among the WEHl-3 cells treated with PBS. And the data showed that the NK cell killing rate increased significantly. NK cells can kill more HL60 (**Figure 2C**), NB4 (**Figure 2D**) and WEHI-3 (**Figure 2E**) cells treated with decitabine than cells treated with PBS. To determine whether decitabine inhibits AML immune escape through ICAM-1 *in vitro*, WEHI-3 cells were treated with or without decitabine, then co-cultured with mouse NK cells with or without the ICAM-1 antibody to block ICAM-1. The NK cell killing function was inhibited by ICAM-1 antibody blockage (**Figure 2F**). Thus, decitabine could increase NK cell killing *via* ICAM-1 *in vitro*.

AML Immune Evasion Was Decreased by ICAM-1 *In Vivo*

To determine whether decitabine could inhibit AML immune escape *in vivo*, BALB/c mice were injected with WEHI-3 and mouse NK cells, and their survival and tumor burden was monitored. The mice were randomly divided into control, DAC, and DAC + ICAM-1 antibody groups ($n = 5$). Firstly, to assessing survival, the mice were bred until the first signs of paralysis determined the end of observation for each mouse. The survival of the DAC group was significantly longer compared to the control (**Figure 3A**, Kaplan-Meier, $p = 0.0019$). When injected with the ICAM-1 antibody, the survival time of the DAC + ICAM-1 antibody group decreased compared to the DAC group ($p = 0.0278$). These findings indicate that decitabine could increase mouse survival time *via* ICAM-1 *in vivo*. To assess tumor burden and invasion in the spleen, the mice were sacrificed on the 17th day after the WEHI-3 injection. After WEHI-3 inoculation, the AML cells invaded the spleen and liver, formed extramedullary masses. The number of tumor masses in the DAC group decreased compared to the control group ($p = 0.0003$) (**Figures 3B, C**). When injected with the ICAM-1 antibody, the number of tumor masses of the DAC group was less than the DAC + ICAM-1 antibody group ($p = 0.0023$) (**Figures 3B, C**). H&E staining of livers (**Figure 3D**) and spleens (**Figure 3E**) showed more tumor masses and invasion than the DAC group. Thus, decitabine could inhibit AML immune

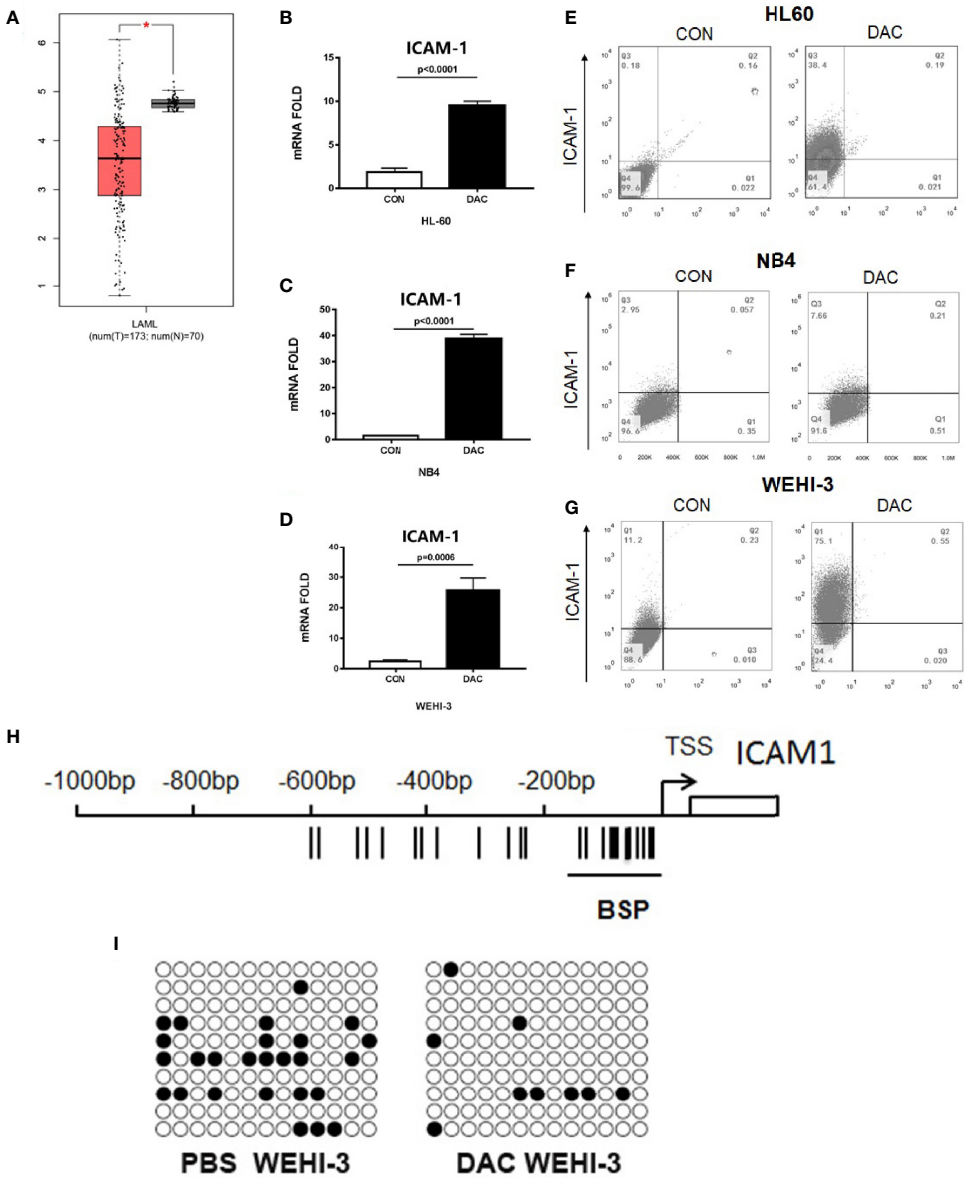

FIGURE 1 | ICAM-1 silenced in AML patients and reversed by hypomethylating. **(A)** The ICAM-1 mRNA Chip analysis of 70 healthy controls (N) and 173 AML patients (T) (TCGA). Q-PCR anlysis of ICAM-1 mRNA expression in **(B)** HL-6, **(C)** NB4, and **(D)** WEHI-3 cells treated with or without decitabine (mean ± SD, n=4). FACS analysis of ICAM-1 expression in **(E)** HL60, **(F)** NB4, and **(G)** WEHI-3 (n=3, typical data). **(H)** Bisulfite sequencing PCR of mouse ICAM-1 methylation sequencing fragment. **(I)** Methylation rate of WEHI-3 treated and untreated with DAC reached 20% [left] and 6.92% [right], respectively.

evasion in the spleen *in vivo* and improve mouse survival by increasing ICAM-1 expression on the AML cell surface and enhancing NK cell killing function.

DISCUSSION

This is the first study that implicates methylation in the regulation of AML ICAM-1 expression, and we show that the hypomethylating agent decitabine could increase ICAM-1 expression, which in turn reverses AML immune evasion from NK cells.

Epigenetic modification in cancers is critical for the immune cell interactions, which including DNA, histone, and chromatin structure modifications (19). Emerging evidence and our works (15, 16) show that tumors could use various epigenetic mechanisms to immune escape. Epigenetic targeting agents are becoming attractive immunomodulatory drugs and will have major impacts on immunotherapy. Tumor epigenetics down-

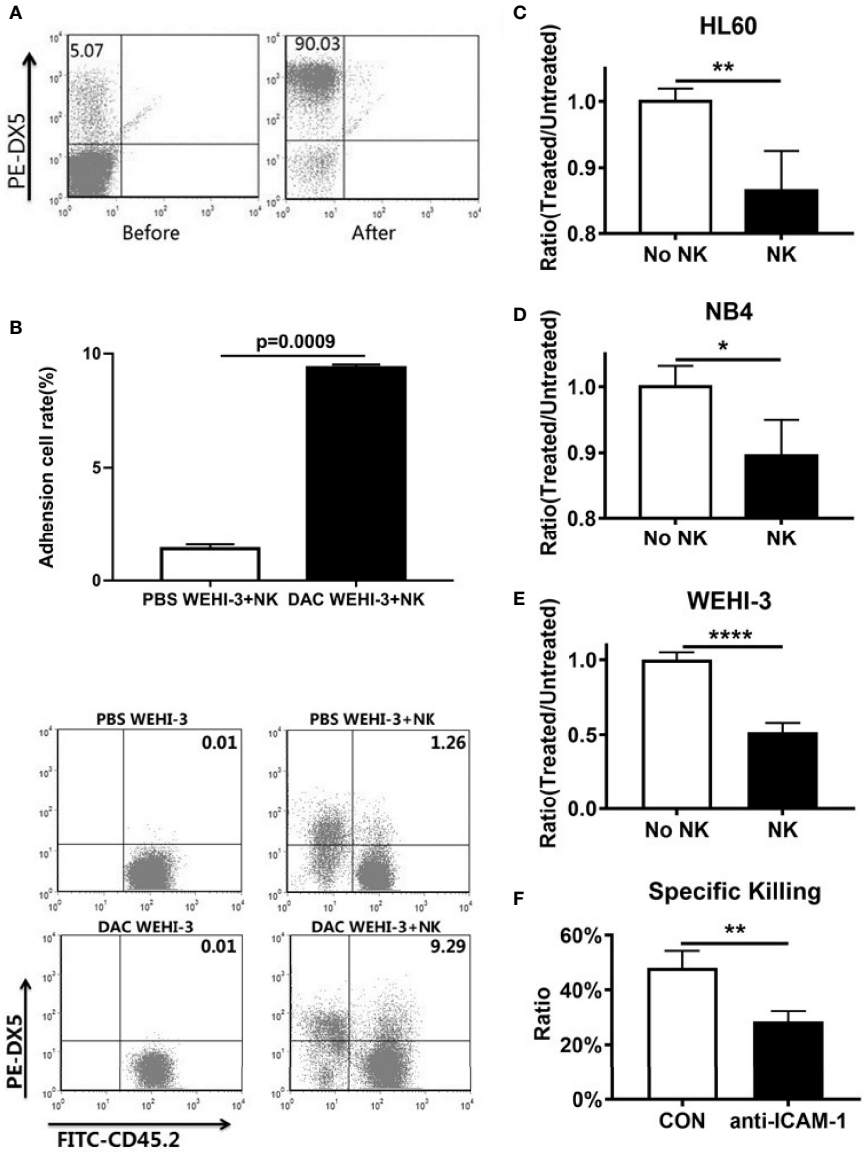

FIGURE 2 | ICAM-1 expression and NK killing rate increased by hypomethylating *in vitro*. **(A)** Purity of NK cells before and after magnetic bead sorting. **(B)** The adhesion between NK cells and DAC WEHI-3 cells was significantly enhanced (mean ± SD, n=3, repeat three times). DAC enhanced NK cells' sensitivity to **(C)** NB4, **(D)** HL60, and **(E)** WEHI-3, cells (mean ± SD, n=4). **(F)** The NK cell killing rate of decitabine treated or untreated with WEHI-3 cells, and then co-cultured with NK cells with or without the ICAM-1 antibody to block ICAM-1 for 24h (mean ± SD, n=4). *p < 0.05, **p < 0.01, ****p < 0.0001.

regulation antigen-presenting (20) and other immune molecular, which become invisible to T cell and other immune cells. Hypermethylation can reverse the MHC-I antigen presentation (21). In our previous studies, AML cells can escape immunosurveillance of NK cells by downregulating CD48 expression on AML cell surface (16). AML cells with downregulated CD48 through epigenetic modification increase DNA methylation and decrease histone acetylation (15).

NK cells play a vital role in AML eradication. Increased ICAM-1 expression contributes to the NK-AML cell conjugates and helps NK cells kill AML cells. Other mechanistic studies also reveal that the increased cytotoxic activity correlates with an increased conjugate formation by upregulating LFA expression on NK cells and by inducing ICAM-1 expression on AML cells (7).

The expression of ICAM-1 on AML cells is silenced, while our findings showed that decitabine could upregulate ICAM-1 expression on AML cells and inhibit AML immune evasion. The mechanism of hypomethylating agent decitabine on ICAM-1 expression is still unclear and required to be

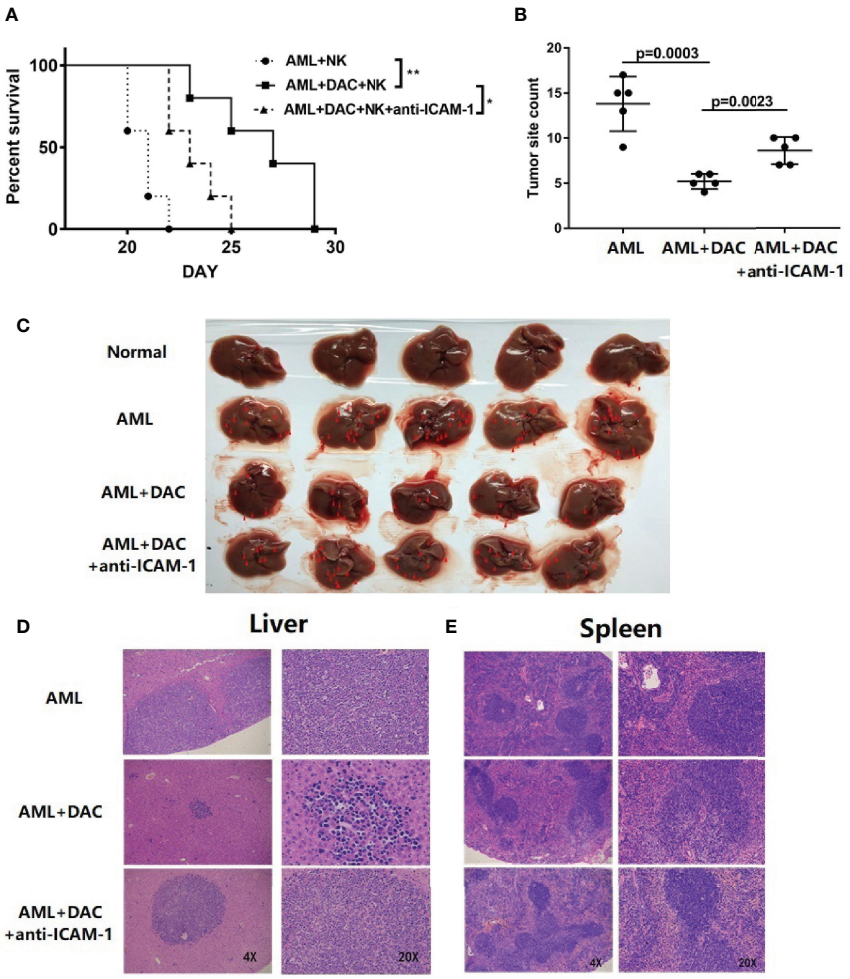

FIGURE 3 | ICAM-1 inhibits AML immune escape *in vivo*. **(A)** Survival of BALB/c mice injected with WEHI-3 cells supplemented or not supplemented with ICAM-1 antibody on Day 1, and then injected decitabine from Day 1 to Day 3, finally injected with NK cells on Day 3 (n=5). **(B, C)** The tumor site and count of mouse livers on 17 days after injection (mean ± SD, n=5). H&E staining of **(D)** livers and **(E)** spleen. *p < 0.05; **p < 0.01.

explored. Our findings indicated that decitabine may be potentially utilized to modulates the immune system and help to cure AML with other drugs.

DATA AVAILABILITY STATEMENT

The original contributions presented in the study are included in the article/supplementary material. Further inquiries can be directed to the corresponding authors.

ETHICS STATEMENT

The animal study was reviewed and approved by the Committee on the Ethics of Animal Experiments of Chinese PLA General Hospital.

AUTHOR CONTRIBUTIONS

Conception and design of the study: LY, LW, and ZW. Acquisition, analysis, and interpretation of data: YX, JC, and JW. Contribution of administrative, experimental, analytic, or material support: WG, MW, and LZ. Writing-Original Draft Preparation: YX and JC. Editing: ZW. All authors contributed to the article and approved the submitted version.

FUNDING

Chinese National Major Project for New Drug Innovation (2019ZX09201002003). National Natural Science Foundation of China (82030076, 2070161, 81970151, 81670162 and 81870134). Shenzhen Science and Technology Foundation (JCYJ20190808163601776, JCYJ20200109113810154). Shenzhen Key Laboratory Foundation (ZDSYS20200811143757022). Sanming Project of Shenzhen (SZSM202111004).

REFERENCES

1. Hansrivijit P, Gale RP, Barrett J, Ciurea SO. Cellular Therapy for Acute Myeloid Leukemia - Current Status and Future Prospects. *Blood Rev* (2019) 37:100578. doi: 10.1016/j.blre.2019.05.002
2. Baragano Raneros A, Lopez-Larrea C, Suarez-Alvarez B. Acute Myeloid Leukemia and NK Cells: Two Warriors Confront Each Other. *Oncoimmunology* (2019) 8(2):e1539617. doi: 10.1080/2162402X.2018.1539617
3. Coombs CC, Tallman MS, Levine RL. Molecular Therapy for Acute Myeloid Leukaemia. *Nat Rev Clin Oncol* (2016) 13(5):305–18. doi: 10.1038/nrclinonc.2015.210
4. Higginson IJ, Wilcock A, Johnson MJ, Bajwah S, Lovell N, Yi D, et al. Randomised, Double-Blind, Multicentre, Mixed-Methods, Dose-Escalation Feasibility Trial of Mirtazapine for Better Treatment of Severe Breathlessness in Advanced Lung Disease (BETTER-B Feasibility). *Thorax* (2020) 75(2):176–9. doi: 10.1136/thoraxjnl-2019-213879
5. Xu J, Niu T. Natural Killer Cell-Based Immunotherapy for Acute Myeloid Leukemia. *J Hematol Oncol* (2020) 13(1):167. doi: 10.1186/s13045-020-00996-x
6. Simmons D, Makgoba MW, Seed B. ICAM, an Adhesion Ligand of LFA-1, is Homologous to the Neural Cell Adhesion Molecule NCAM. *Nature* (1988) 331(6157):624–7. doi: 10.1038/331624a0
7. Parameswaran R, Ramakrishnan P, Moreton SA, Xia Z, Hou Y, Lee DA, et al. Repression of GSK3 Restores NK Cell Cytotoxicity in AML Patients. *Nat Commun* (2016) 7:11154. doi: 10.1038/ncomms11154
8. Santini V, Ossenkoppele GJ. Hypomethylating Agents in the Treatment of Acute Myeloid Leukemia: A Guide to Optimal Use. *Crit Rev Oncol Hematol* (2019) 140:1–7. doi: 10.1016/j.critrevonc.2019.05.013
9. Kantarjian H, Issa JP, Rosenfeld CS, Bennett JM, Albitar M, DiPersio J, et al. Decitabine Improves Patient Outcomes in Myelodysplastic Syndromes: Results of a Phase III Randomized Study. *Cancer* (2006) 106(8):1794–803. doi: 10.1002/cncr.21792
10. Daver N, Boddu P, Garcia-Manero G, Yadav SS, Sharma P, Allison J, et al. Hypomethylating Agents in Combination With Immune Checkpoint Inhibitors in Acute Myeloid Leukemia and Myelodysplastic Syndromes. *Leukemia* (2018) 32(5):1094–105. doi: 10.1038/s41375-018-0070-8
11. Li Y, Gao L, Luo X, Wang L, Gao X, Wang W, et al. Epigenetic Silencing of microRNA-193a Contributes to Leukemogenesis in T(8;21) Acute Myeloid Leukemia by Activating the PTEN/PI3K Signal Pathway. *Blood* (2013) 121 (3):499–509. doi: 10.1182/blood-2012-07-444729
12. Fu L, Huang W, Jing Y, Jiang M, Zhao Y, Shi J, et al. AML1-ETO Triggers Epigenetic Activation of Early Growth Response Gene L, Inducing Apoptosis in T(8;21) Acute Myeloid Leukemia. *FEBS J* (2014) 281(4):1123–31. doi: 10.1111/febs.12673
13. Yu L, Liu C, Vandeusen J, Becknell B, Dai Z, Wu YZ, et al. Global Assessment of Promoter Methylation in a Mouse Model of Cancer Identifies ID4 as a Putative Tumor-Suppressor Gene in Human Leukemia. *Nat Genet* (2005) 37 (3):265–74. doi: 10.1038/ng1521
14. Wang LX, Mei ZY, Zhou JH, Yao YS, Li YH, Xu YH, et al. Low Dose Decitabine Treatment Induces CD80 Expression in Cancer Cells and Stimulates Tumor Specific Cytotoxic T Lymphocyte Responses. *PloS One* (2013) 8(5):e62924. doi: 10.1371/journal.pone.0062924
15. Wang Z, Guan W, Wang M, Chen J, Zhang L, Xiao Y, et al. AML1-ETO Inhibits Acute Myeloid Leukemia Immune Escape by CD48. *Leuk Lymphoma* (2021) 62(4):937–43. doi: 10.1080/10428194.2020.1849680
16. Wang Z, Xiao Y, Guan W, Wang M, Chen J, Zhang L, et al. Acute Myeloid Leukemia Immune Escape by Epigenetic CD48 Silencing. *Clin Sci (Lond)* (2020) 134(2):261–71. doi: 10.1042/CS20191170
17. Tang Z, Li C, Kang B, Gao G, Li C, Zhang Z. GEPIA: A Web Server for Cancer and Normal Gene Expression Profiling and Interactive Analyses. *Nucleic Acids Res* (2017) 45(W1):W98–102. doi: 10.1093/nar/gkx247
18. Wang Z, Li G, Dou S, Zhang Y, Liu Y, Zhang J, et al. Tim-3 Promotes Listeria Monocytogenes Immune Evasion by Suppressing Major Histocompatibility Complex Class I. *J Infect Dis* (2020) 221(5):830–40. doi: 10.1093/infdis/jiz512
19. Cao J, Yan Q. Cancer Epigenetics, Tumor Immunity, and Immunotherapy. *Trends Cancer* (2020) 6(7):580–92. doi: 10.1016/j.trecan.2020.02.003
20. Leone P, Shin EC, Perosa F, Vacca A, Dammacco F, Racanelli V. MHC Class I Antigen Processing and Presenting Machinery: Organization, Function, and Defects in Tumor Cells. *J Natl Cancer Inst* (2013) 105(16):1172–87. doi: 10.1093/jnci/djt184
21. Luo N, Nixon MJ, Gonzalez-Ericsson PI, Sanchez V, Opalenik SR, Li H, et al. DNA Methyltransferase Inhibition Upregulates MHC-I to Potentiate Cytotoxic T Lymphocyte Responses in Breast Cancer. *Nat Commun* (2018) 9(1):248. doi: 10.1038/s41467-017-02630-w

Conflict of Interest: The authors declare that the research was conducted in the absence of any commercial or financial relationships that could be construed as a potential conflict of interest.

frontiers in Oncology

ORIGINAL RESEARCH
published: 20 October 2021
doi: 10.3389/fonc.2021.718791

LukS-PV Induces Apoptosis *via* the SET8-H4K20me1-PIK3CB Axis in Human Acute Myeloid Leukemia Cells

Liang Fei Xu[1†], Lan Shi[1†], Shan Shan Zhang[1], Peng Sheng Ding[1], Fan Ma[1], Kai Di Song[1], Ping Qiang[1], Wen Jiao Chang[1], Yuan Yuan Dai[1], Yi De Mei[2] and Xiao Ling Ma[1,2]*

[1] The First Affiliated Hospital of USTC, Division of Life Sciences and Medicine, University of Science and Technology of China, Hefei, China, [2] University of Science and Technology of China, School of Life Sciences and Medicine, USTC Life Sciences, Hefei, China

OPEN ACCESS

Edited by:
Yonghui Li,
Shenzhen University General Hospital, China

Reviewed by:
Michael Diamantidis,
University Hospital of Larissa, Greece
Hussein A. Abbas,
MD Anderson Cancer Center, United States

***Correspondence:**
Xiao Ling Ma
maxiaoling@ustc.edu.cn

[†]These authors have contributed equally to this work and share first authorship

Specialty section:
This article was submitted to Hematologic Malignancies, a section of the journal Frontiers in Oncology

Received: 23 July 2021
Accepted: 22 September 2021
Published: 20 October 2021

Citation:
Xu LF, Shi L, Zhang SS, Ding PS, Ma F, Song KD, Qiang P, Chang WJ, Dai YY, Mei YD and Ma XL (2021) LukS-PV Induces Apoptosis via the SET8-H4K20me1-PIK3CB Axis in Human Acute Myeloid Leukemia Cells. Front. Oncol. 11:718791. doi: 10.3389/fonc.2021.718791

Evidence suggests that histone modification disorders are involved in leukemia pathogenesis. We previously reported that LukS-PV, a component of Panton–Valentine leukocidin (PVL), has antileukemia activities that can induce differentiation, increase apoptosis, and inhibit proliferation of acute myeloid leukemia (AML) cells. Furthermore, LukS-PV inhibited hepatoma progression by regulating histone deacetylation, speculating that LukS-PV may exert antileukemia activity by targeting histone modification regulators. In this study, the results showed that LukS-PV induced apoptosis by downregulating the methyltransferase SET8 and its target histone H4 monomethylated at Lys 20 (H4K20me1). Furthermore, chromatin immunoprecipitation sequencing and polymerase chain reaction identified the kinase *PIK3CB* as a downstream target gene for apoptosis mediated by SET8/H4K20me1. Finally, our results indicated that LukS-PV induced apoptosis *via* the PIK3CB-AKT-FOXO1 signaling pathway by targeting SET8. This study indicates that SET8 downregulation is one of the mechanisms by which LukS-PV induces apoptosis in AML cells, suggesting that SET8 may be a potential therapeutic target for AML. Furthermore, LukS-PV may be a drug candidate for the treatment of AML that targets epigenetic modifications.

Keywords: epigenetics, AML, LukS-PV, apoptosis, SET8

INTRODUCTION

Acute myeloid leukemia (AML) is a heterogeneous clonal disorder of hematopoietic progenitor cells, which is characterized by immature myeloid cell proliferation and bone marrow failure with a short course (1). AML occurs predominantly in older adults who are more than 60 years of age (2). Although hematopoietic stem cell transplantation combined with chemotherapy has substantially

Abbreviations: AML, acute myeloid leukemia; FCM, flow cytometry; ChIP, chromatin immunoprecipitation; SET-NC, SET8 negative control; SET8-OE, SET8 overexpression; SET8-SiRNA, SET8 small interfering RNA.

improved therapy for young adults, approximately 80% of older adults still succumb to the disease or related therapeutic toxicity. Thus, it is important to identify more targeted therapies for AML.

In recent years, bacterial toxins have received increasing attention as potential anticancer drugs because of their specificity and cytotoxicity, and bacterial toxin-containing anticancer drugs have entered clinical trials (3, 4). Panton–Valentine leukocidin (PVL) is a two-component pore-forming cytosolic toxin secreted by *Staphylococcus aureus*. It was first discovered by Van de Velde and isolated from hemolysin by Panton and Valentine in 1932 (5, 6). PVL is composed of LukF-PV and LukS-PV protein subunits encoded by *lukF-PV* and *lukS-PV* genes, respectively (7). PVL belongs to the pore-forming toxin family and has been reported to induce lysis of human polymorphonuclear neutrophils (8, 9). LukS-PV first binds to a specific receptor on the membrane of neutrophils, and LukF-PV binds to LukS-PV to form a dimer. The LukS-PV–LukF-PV dimers combine to form a ring structure, which is inserted into the cellular membrane and forms a planar vertical transmembrane pore that induces necrosis and apoptosis (10, 11). Our previous study demonstrated that the LukS-PV subunit alone did not cause perforation cytotoxicity; however, this subunit displayed antileukemia activity *in vitro* and *in vivo* without noticeable side effects in mice (12). Sun et al. reported that LukS-PV regulated microRNA-125a-3p-induced THP-1 cell differentiation and apoptosis by downregulating NF1 and BCL2 (13). Zhang et al. found that LukS-PV induced AML apoptosis by targeting the C5a receptor (14). Additionally, LukS-PV induced differentiation by activating the ERK signaling pathway and c-JUN/c-FOS in AML cells (15). The above investigations indicate that LukS-PV exerts antileukemia activity through several mechanisms and targets, and whether it has other mechanisms of action deserves further study.

Comprehensive genomic profiling of AML has shown that dysregulation of histone modifications plays an essential role in leukemia pathogenesis, and emerging evidence suggests that histone modification is a major epigenetic determinant for gene expression and is frequently dysregulated in AML (16). Moreover, histone modifications are potentially reversible, which provides opportunities for targeted therapy for AML. DOT1L methyltransferase inhibitors have been used extensively to reduce the leukemia burden in a variety of AML models with mixed lineage leukemia rearrangements (17). Tranylcypromine, an LSD1 inhibitor, either alone or in combination with all-trans retinoic acid, disrupted the oncogenic program of mixed lineage leukemia and induced expression of myeloid differentiation genes in AML cells with rearrangements (18). These studies suggest that histone modifications are potentially promising targets for leukemia therapy. Furthermore, in another study, we demonstrated that LukS-PV inhibited the proliferation and induced apoptosis in hepatocellular carcinoma (HCC) cells by downregulating histone acetylation (19), suggesting that LukS-PV may regulate histone epigenetic modifiers. However, whether LukS-PV exerts antileukemia activity by targeting regulators of histone modification remains unclear. Therefore, in this study, we investigated the underlying molecular mechanisms by which LukS-PV exerts antileukemia activities to determine whether this protein regulated histone modifications in AML cells.

MATERIALS AND METHODS

Cell Culture and Reagents

Human acute leukemia cell lines HL-60 and NB4 were obtained from the Shanghai Institute for Biological Sciences (Shanghai, China). Cells were cultured in RPMI-1640 medium (Gibco, Grand Island, NY, USA) supplemented with 10% fetal bovine serum (HyClone, Logan, UT, USA) and 1% penicillin/streptomycin in an incubator at 37°C with 5% CO_2. The medium was changed every 2–3 days. The PIK3CB inhibitor GSK2636771 and SET8 inhibitor UNC0379 were purchased from MedChemExpress (Shanghai, China).

Total RNA Extraction of Peripheral Blood From Acute Myeloid Leukemia Patients and Healthy Individuals

AML patients were diagnosed in accordance with clinical and laboratory criteria, and healthy individuals with normal physical examination indices were used as controls. To extract total RNA, a fivefold volume of erythrocyte lysis buffer was added to fresh whole blood samples, which were placed on a shaker for 15–20 min. The cells were centrifuged for 5 min at 1,000 rpm, and the supernatant was discarded. The cell pellet was washed twice with phosphate-buffered saline (PBS), and the remaining erythrocytes were re-lysed. Total RNA was extracted using TRIzol (Invitrogen, Carlsbad, CA, USA) in accordance with the manufacturer's instructions. Experiments using samples derived from AML patients were approved by the Ethics Committee and Institutional Review Board of University of Science and Technology of China, Anhui, China (approval number: 2019-N(H)-101).

RNA Sequencing

Total RNA was isolated from HL-60 cells treated with LukS-PV or PBS. Paired-end libraries were synthesized using the TruSeq RNA Sample Preparation Kit (Illumina, San Diego, CA, USA) in accordance with the manufacturer's instructions. Briefly, the mRNA molecules were purified using poly-T oligomers attached to magnetic beads. Library construction and sequencing were performed at Shanghai Sinomics Corporation of China.

Separation and Culturing of Primary Bone Marrow Cells

AML patients were diagnosed in accordance with clinical and laboratory criteria. Primary AML cells were harvested from the bone marrow of AML patients immediately after lumbar puncture. Fresh bone marrow mononuclear cells were isolated by Ficoll density-gradient centrifugation, resuspended in RPMI-1640 medium supplemented with 10% FBS, and placed in an incubator. The primary AML cells were then incubated with LukS-PV for 24 h.

Recombinant LukS-PV Production and Purification

The pET28a vector (Roche Diagnostics Corp., Basel, Switzerland) was used to generate six recombinant His-tagged LukS-PV proteins. The LukS-PV sequence was amplified from PVL-positive *S. aureus* isolates. PCR products were digested with *Xho*I and *Bam*HI (Promega Corp., Madison, WI, USA) and ligated into the pET28a vector. Recombinant LukS-PV was purified as previously described (20).

RNA Isolation and Quantitative Real-Time RT-PCR

Total RNA was extracted using TRIzol (Invitrogen, Carlsbad, USA) as described above. Reverse transcription was performed using the RevertAid First Strand cDNA Synthesis Kit (Fermentas, Vilnius, Lithuania). All quantitative real-time PCR (qRT-pCR) assays were carried out using a StepOnePlus RT-PCR system (Applied Biosystems, Carlsbad, CA, USA). Relative expression levels were quantified using the comparative Ct method. Gene-specific primer sequences were as follows: *SET8*: 5′-ACTTACGGATTTCTACCCTGTC-3′ and 5′-CGATGAGG TCAATCTTCATTCC-3′; *PIK3CB*: 5′-ATCGCTCTG GCCTCATTGAAGTTG-3′ and 5′-ATGGCTCGGT CCAGGTCATCC-3′.

Lentiviral Transduction

The lentiviral vectors used for SET8 silencing and overexpression and PIK3CB overexpression (HanBio, Shanghai, China) were transduced into HL-60 and NB4 cells. As controls, lentiviral vectors containing short hairpin RNA sequences targeting a non-mammalian gene were used. After 48 h of transduction, the cells were selected using puromycin and cultured.

Flow Cytometric Analysis

To assess apoptosis, cells were harvested by centrifugation at 1,000 rpm for 5 min, washed twice with cold PBS, resuspended in 500 µl of staining buffer, and co-stained with Annexin V-PE and 7-AAD (eBioscience, San Diego, CA, USA) at room temperature for 15 min in the dark. The cells were analyzed using a FACSCalibur flow cytometer (BD Biosciences, Franklin Lakes, NJ, USA). The data were analyzed using FCS Express software (*De Novo* Software, Pasadena, CA, USA).

Western Blotting

Cells were lysed in radioimmunoprecipitation assay (RIPA) lysis buffer containing 1% phenylmethylsulfonyl fluoride (Beyotime, Shanghai, China) on ice for 30–60 min and centrifuged at 12,000 rpm for 5 min, and the pellet was discarded. The protein samples were boiled in sodium dodecyl sulfate (SDS)-loading dye for 15 min. The proteins were separated by SDS–polyacrylamide gel electrophoresis (SDS-PAGE) and electro-transferred onto a 0.45-µm nitrocellulose membrane (Millipore, Bedford, MA, USA). The membranes were blocked with Protein Free Rapid Blocking Buffer (EpiZyme, Jiangsu, China) and subsequently probed with primary antibodies. The primary antibodies used were as follows: rabbit anti-human SET8 (#2996), anti-PIK3CB (#3011), anti-FOXO1 (#2880), anti-AKT (#4685), anti-p-AKT (#4060), and anti-BAK (#12105), anti-histone H4 (#13919), anti-BCL2 (#15071), and anti-GAPDH (#51332) purchased from Cell Signaling Technology (Beverly, MA, USA) and anti-H4K20me1 (Abcam; #ab177188; Cambridge, UK). Thereafter, the membranes were washed and incubated with the appropriate horseradish peroxidase-conjugated secondary antibody for 1.5 h at room temperature. Immunoreactive bands were visualized using an enhanced chemiluminescence detection system.

Chromatin Immunoprecipitation Sequencing Assay and Chromatin Immunoprecipitation–PCR

Approximately 4×10^6 HL-60 cells were fixed with 1% formaldehyde and subjected to chromatin immunoprecipitation (ChIP) with a ChIP grade anti-H4K20me1 antibody (Abcam; #ab177188) using the SimpleChIP enzymatic ChIP kit (Cell Signaling Technology, #9003) in accordance with the manufacturer's instructions. Input and H4K20me1-immunoprecipitated chromatin samples were sequenced at GeneSky Biotechnologies, Inc. (Suzhou, China). The gene-specific primer sequences used for ChIP-PCR were as follows: *PIK3CB*: 5′-GGAAGAGCGGAATCTCTCGG-3′ and 5′-GCACGGCCTTTCCTAACTCT-3′. The PCR reaction program was as follows: initial denaturation at 95°C for 3 min followed by 40 cycles of denaturing at 95°C for 15 s and annealing/extension at 60°C for 60 s per cycle. The %Input = 2% * 2^($CT_{Input\ sample}$ − $CT_{IP\ sample}$).

Xenograft Mouse Assay

Male BALB/c nude mice (4 weeks old) were obtained from GemPharmatech, Ltd. (Nanjing, Jiangsu, China) and maintained in a specific pathogen-free facility at the Laboratory Animal Center of Anhui Medical University, and care was in accordance with institution guidelines. Mice were injected intraperitoneally (i.p.) with cyclophosphamide (100 mg/kg body weight) on each of three successive days to suppress immunity and then randomized into three groups: normal control (five mice), HL-60 group (10 mice), and NB4 group (10 mice). Mice in the normal control group received only PBS. Each mouse in the HL-60 and NB4 groups was injected with 5×10^6 HL-60 and NB4 cells, respectively, *via* the tail vein and then randomized into PBS (five mice) and LukS-PV (five mice) groups. The LukS-PV mice were injected with LukS-PV (300 µg/kg body weight per mouse) *via* the tail vein for three successive days. After 30 days, mice were sacrificed, and their spleens and peripheral blood samples were collected for the next experiments. CD33, a myeloid lineage-specific antigen, is a sialoadhesin family member that is normally expressed on precursor myeloid cells and can be used as a specific marker to observe leukemic cell proliferation and infiltration in a mouse leukemia model (21). Hence, we used anti-CD33-PE (BD Biosciences, cat #555450) to assess invasion of AML cells *in vivo via* flow cytometry. This study was approved by the Ethics Committee and Institutional Review Board of University of Science and Technology of China, Anhui, China (approval

number: 2019-N(H)-101), and all experiments conformed to the relevant regulatory standards.

Statistical Analysis

All data are expressed as means ± standard deviations (SDs), and all experiments were performed in triplicate. All data met a normal distribution. Statistical analyses were performed using independent-sample t-tests for comparisons between two groups or ANOVA for multiple comparisons followed by Bonferroni's or Dunn's post-test to compare differences between the groups. The log-rank test was used for survival analysis. Sample sizes for all experiments were predetermined from our experience. Animals were randomly assigned, and no samples were excluded from the analyses. The investigators were not blinded to the team allocation at some stages in the draw materials and effect assessments. All statistical analyses were conducted using GraphPad Prism software (Version 5.0; GraphPad Software, Inc., San Diego, CA, USA). A p-value of $p < 0.05$ (*), $p < 0.01$ (**), or $p < 0.001$ (***) was considered statistically significant.

RESULTS

LukS-PV Induced Cell Apoptosis *In Vitro* and Inhibited Cell Invasion *In Vivo*

We randomly isolated bone marrow samples from four AML patients for *in vitro* culture and treated them with different concentrations of LukS-PV to detect apoptosis by flow cytometry. The demographics and clinical features of the four AML patients are described in **Table 1**. The results showed that LukS-PV induced apoptosis in a dose-dependent manner in primary AML blasts (**Figure 1A**). To further study the antileukemia activity of LukS-PV *in vivo*, we injected AML cell lines (HL-60 and NB4) into the tail vein of nude mice and treated the mice with LukS-PV. The results demonstrated that the spleen index for the LukS-PV treatment group was lower than that for the PBS control group (**Figure 1B**). Furthermore, flow cytometric analysis showed that the percentage of AML cells (CD33+ cells) in the peripheral blood and spleens was lower in the LukS-PV treatment group than in the control group (**Figures 1C, D**). These results indicated that Luks-PV induced AML apoptosis *in vitro* and inhibited tumor cell invasion *in vivo*.

TABLE 1 | Clinical features of four AML patients.

	AML 1	AML 2	AML 3	AML 4
Age (years)	47	66	55	47
Gender	Female	Male	Female	Female
FAB	M2	M3	M4	M3
Mutation	AML1/ETO	PML/RARA	MLL/AF9	PML/RARA
Cytogenetic	46, XX, der(7)t(7;8)(p22;q22), t(8;21)(p22;q22)	46, XY, t(15;17)	46, XX, t(9;11)(p21;q23)	46,XX, del(13)t(15;17)
Treatment	IA+ARA-C	IA+ATRA	IA	ATRA+ATO

AML, acute myeloid leukemia.

SET8 Is Downregulated in Acute Myeloid Leukemia Cells After LukS-PV Treatment

Recent studies have revealed that dysregulation of histone modification plays an important role in leukemia pathogenesis. Several histone-modifying enzymes have been investigated as potential therapeutic targets for leukemia. We demonstrated that LukS-PV could inhibit the proliferation and induce apoptosis by downregulating histone acetylation in HCC cells. These studies suggested that LukS-PV may also exert antileukemia activity by targeting histone modification regulators. To determine whether LukS-PV induced apoptosis by regulating histone modification, we identified 31 highly expressed histone epigenetic modifiers in AML patients using The Cancer Genome Atlas (TCGA) database and Genotype-Tissue Expression (GTEx) datasets (22, 23). By RNA sequencing, we determined that LukS-PV downregulated 14 histone epigenetic regulating genes in AML cells. After overlap analysis, we identified a total of eight different histone modification regulators that were potential targets for LukS-PV. Because SET8 was decreased to the greatest extent among these potential targets, we chose SET8 for further evaluation (**Figure 2A**). We verified that both mRNA and protein levels of SET8 were downregulated by LukS-PV in AML cells in a dose- and time-dependent manner (**Figures 2B–E**). Collectively, these data demonstrated that LukS-PV decreased SET8 expression in AML cells.

SET8 Is Highly Expressed in Acute Myeloid Leukemia and Is Associated With Poor Prognosis

To understand the role of SET8 in AML pathogenesis, we evaluated SET8 expression in AML patients and healthy individuals. We sampled peripheral blood from 20 AML patients and 20 healthy control participants and quantified SET8 expression in isolated peripheral blood leukocytes. RT-PCR and Western blotting revealed that SET8 was significantly upregulated in AML patients compared with the healthy controls (**Figures 3A, B**). Then, we analyzed RNA-seq data from the peripheral blood of AML patients using TCGA database and the RNA-seq data from peripheral blood of healthy people using the GTEx database (20) to verify our results. The analysis showed that the expression of *SET8* mRNA in AML patients was significantly higher in AML patients than in healthy people and was associated with a poor prognosis (**Figures 3C, D**).

HL-60 and NB4 cells were transfected with siRNAs or overexpression vectors to silence or overexpress SET8, and SET8 expression was quantified by RT-PCR and Western blotting (**Figures 3E, F**). Furthermore, apoptosis was assessed by flow cytometry after the transfections. The results showed that early apoptosis and late apoptosis were significantly increased after knockdown of SET8 in the AML cell lines. However, SET8 overexpression did not affect apoptosis, which may be explained by the low level of apoptosis in SET8-NC cells (**Figures 3G, H**). These results suggest that SET8 is involved in

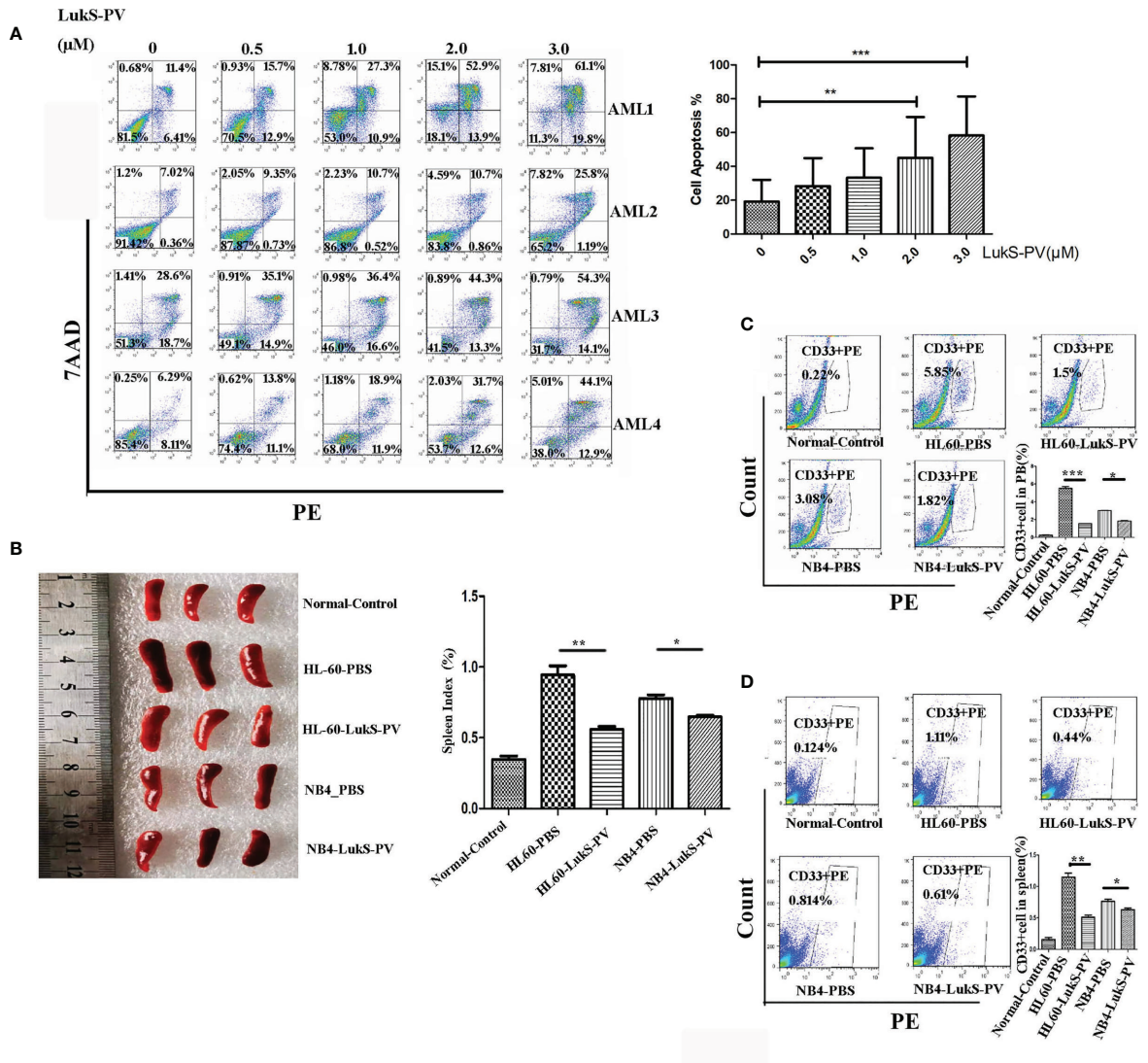

FIGURE 1 | LukS-PV induces apoptosis *in vitro* and inhibits cell invasion *in vivo*. **(A)** Flow cytometric analysis shows that treatment of primary acute myeloid leukemia (AML) blasts with LukS-PV induces apoptosis in a dose-dependent manner. **(B)** The spleen volume (left) and spleen index [(spleen weight/body weight) × 100, right] of mice. **(C)** The percentage of CD33+ cells in PB (peripheral blood). **(D)** The percentage of CD33+ cells in the spleen. Data are expressed as mean ± SD (n = 3). ns, not significant; *p < 0.05; **p < 0.01; ***p < 0.001.

leukemia pathogenesis and may be a potential therapeutic target in AML.

LukS-PV Induced Apoptosis in Acute Myeloid Leukemia Cells by Downregulating SET8 and H4K20me1

SET8 is a member of the SET domain-containing methyltransferase family and the only modifying enzyme known to catalyze the monomethylation of histone H4 Lys-20 (H4K20me1). We used Western blotting to detect H4K20me1 levels in SET8-siRNA and SET8-overexpressing cells. The results demonstrated that the level of H4K20me1 was increased significantly in SET8-overexpressing cells and decreased in SET8-siRNA cells (**Figures 3E, F**). Furthermore, we treated HL-60 and NB4 cells with different concentrations of LukS-PV for different time periods and quantified H4K20me1 expression. The results showed that LukS-PV reduced H4K20me1 levels in a dose- and time-dependent manner, which was consistent with the results from the SET8 expression experiments (**Figures 4A, B**). These results collectively indicated that LukS-PV downregulated H4K20me1 by regulating SET8 in a dose- and time-dependent manner.

To further determine whether LukS-PV exerted antileukemia effects by downregulating SET8 and H4K20me1, we overexpressed or knocked down SET8 in AML cell lines treated in the cells with 3.0 μM of LukS-PV, and apoptosis was assessed

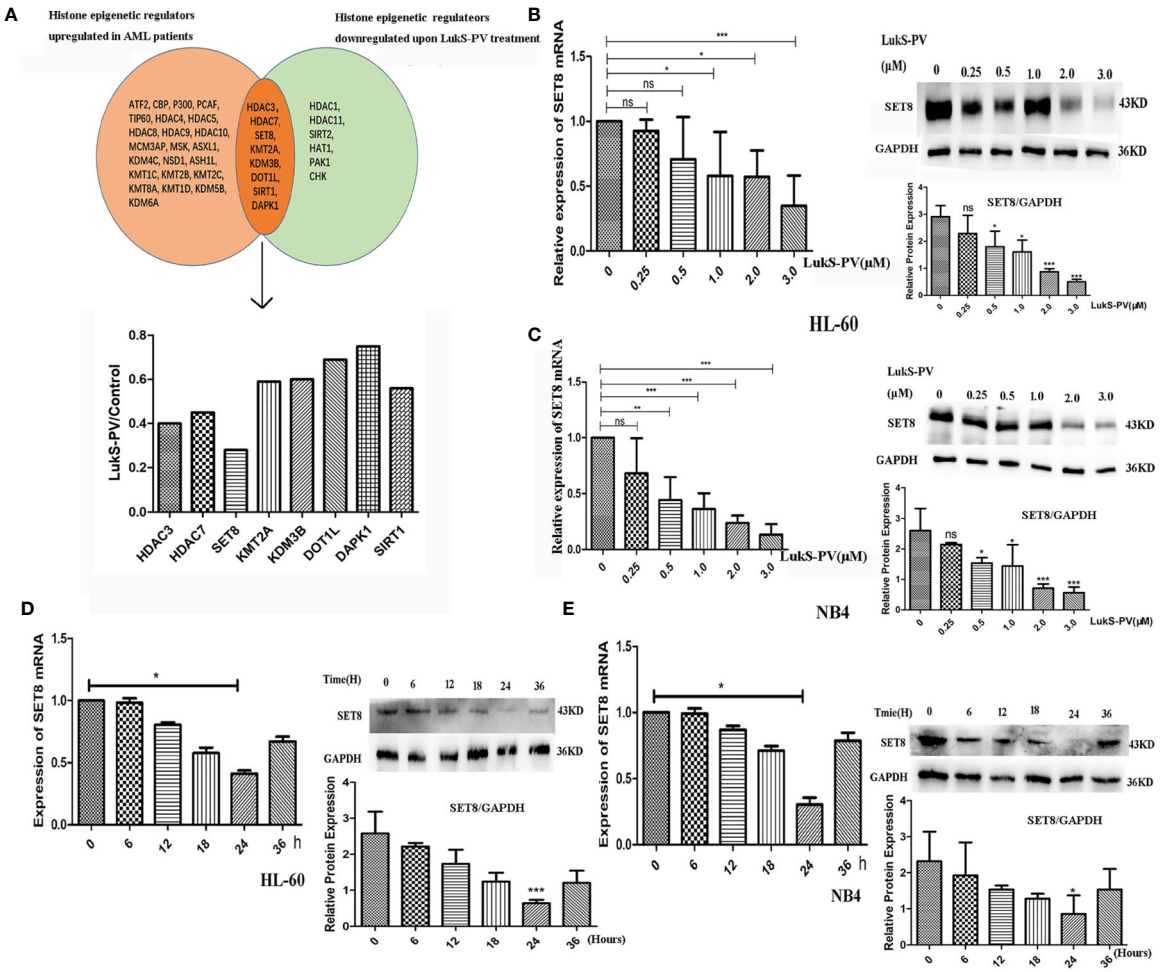

FIGURE 2 | SET8 is downregulated in acute myeloid leukemia (AML) cells after LukS-PV treatment. **(A)** Downregulated histone epigenetic regulators after LukS-PV treatment. **(B)** HL-60 and **(C)** NB4 cells were treated with LukS-PV at different concentrations, and *SET8* mRNA and protein expression levels were determined by quantitative real-time PCR and Western blotting. **(D)** HL-60 and **(E)** NB4 cells were treated with 3.0 μM of LukS-PV at different timepoints, and *SET8* mRNA and protein expression levels were determined by quantitative real-time PCR and Western blotting. ns, not significant; *p < 0.05; **p < 0.01; ***p < 0.001.

by flow cytometry. The LukS-PV-treated cells displayed significantly greater apoptosis than the PBS-treated cells. Apoptosis was further enhanced in SET8-knockdown cells but markedly alleviated in SET8-overexpressing cells, indicating that the effect of LukS-PV on apoptosis was inhibited by SET8 expression (**Figures 4C, D**). Interestingly, we found that the level of apoptosis was the highest in the SET8-siRNA + LukS-PV group, likely because Luks-PV also induced apoptosis through other pathways, and there was an added apoptotic effect after knocking down SET8. These results indicated that SET8 downregulation is one of the mechanisms by which LukS-PV induced apoptosis in AML cells. Additionally, LukS-PV treatment decreased the protein levels of SET8, H4K20me1, and the anti-apoptotic protein BCL2 and increased the pro-apoptotic protein BAK, and this effect was further enhanced by SET8 knockdown and alleviated by SET8 overexpression (**Figure 4E**).

PIK3CB Is a Downstream Target Gene of SET8-H4K20me1

Studies have shown that SET8 is involved in tumor pathogenesis by catalyzing the monomethylation of H4K20 in target gene promoter regions and promoting gene transcription. To further explore the molecular mechanism of LukS-PV-induced apoptosis and downregulation of SET8 in AML cells, we hypothesized that SET8 regulated downstream target genes through H4K20me1. To verify this hypothesis, target genes regulated by SET8/H4K20me1 were determined by ChIP sequencing. ChIP experiments were first performed with HL-60 cells using antibodies against H4K20me1 after LukS-PV treatment. H4K20me1-associated DNA sequences in LukS-PV-treated cells were then amplified under non-biased conditions, labeled, and sequenced. Through HiSeq2000 with a p-value cutoff of 10^{-5}, we identified 2,450 H4K20me1-specific binding

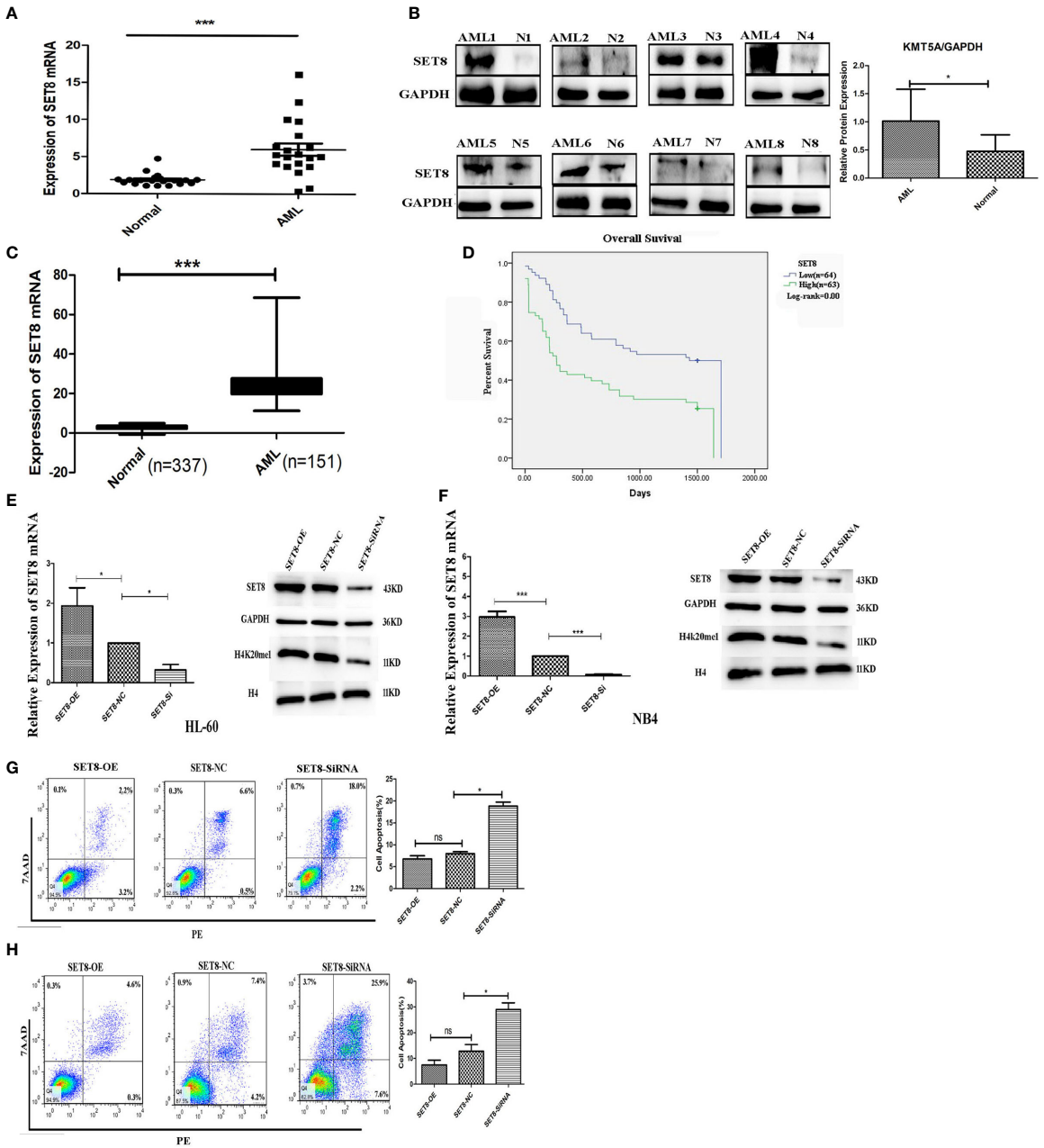

FIGURE 3 | SET8 is highly expressed in acute myeloid leukemia (AML) and is associated with poor prognosis. **(A)** *SET8* mRNA expression in AML patients and healthy control subjects. **(B)** SET8 protein expression in AML patients. **(C, D)** The Cancer Genome Atlas and Genotype-Tissue Expression database analyses of *SET8* expression between AML patients and healthy individuals. **(E, F)** Relative expression of SET8 and H4K20me1 in cells (HL-60 and NB4) transduced with a lentiviral vector determined through quantitative real-time PCR and Western blotting. **(G, H)** Flow cytometric analysis of Annexin V-PE/7-AAD staining shows that the knockdown of *SET8* expression with siRNA induced apoptosis in HL-60 and NB4 cells. ns, not significant; *p < 0.05; ***p < 0.001.

peaks of which 731 were upregulated and 1,719 were downregulated (**Supplementary Table S1**).

Because LukS-PV inhibits downstream gene transcription *via* downregulation of SET8/H4K20me1, we focused on the genes with reduced H4K20 monomethylation enrichment in the promoter region after LukS-PV treatment. Gene Ontology-based analysis showed that these reduced genes were significantly enriched for transcription coactivator activity and magnesium ion binding, were mainly located in dendrites and cytoplasmic regions, and participated in potassium ion transport and viral defense responses (**Figure 5A**). Kyoto Encyclopedia of Genes and Genomes-based functional enrichment analysis demonstrated that the reduced genes were enriched in cAMP signaling, Wnt signaling, and tumor-related pathways

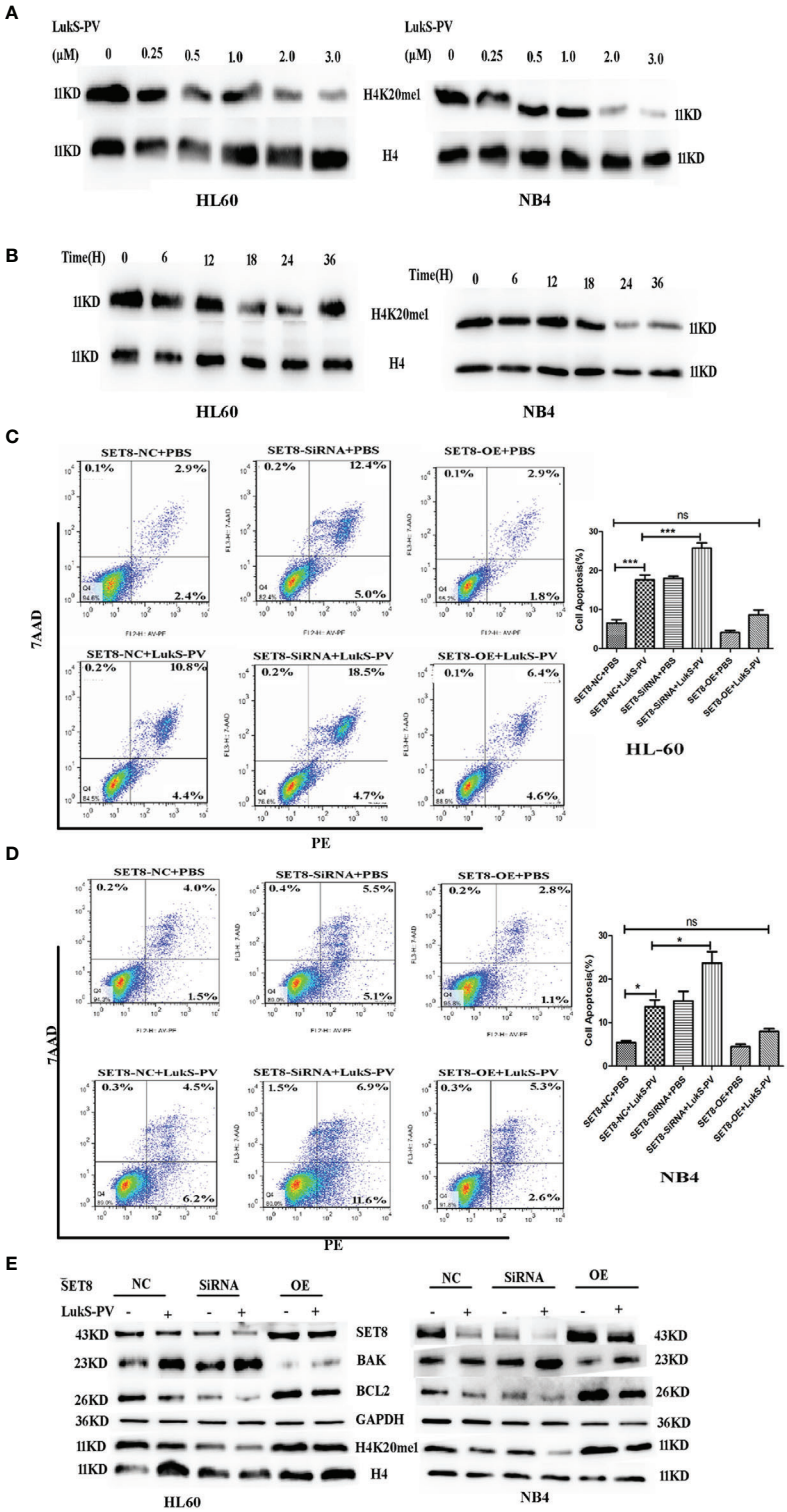

FIGURE 4 | LukS-PV induces apoptosis in acute myeloid leukemia (AML) cells by downregulating SET8/H4K20me1. **(A)** HL-60 and NB4 cells were treated with LukS-PV at different concentrations for 24 h, and H4K20me1 expression was assessed by Western blotting. **(B)** HL-60 and NB4 cells were treated with 3.0 μM of LukS-PV at different timepoints, and H4K20me1 expression was assessed by Western blotting. **(C, D)** SET8 knockdown induced apoptosis and SET8 overexpression inhibited apoptosis in HL-60 **(C)** and NB4 **(D)** cells treated with LukS-PV. **(E)** Expression of SET8 and apoptosis-associated proteins in HL-60 and NB4 cells was assessed by Western blotting. SET8-OE, SET8 overexpression; SET8-NC, SET8 negative control; SET8-siRNA, SET8 small interfering RNA; ns, not significant; *$p < 0.05$; ***$p < 0.001$.

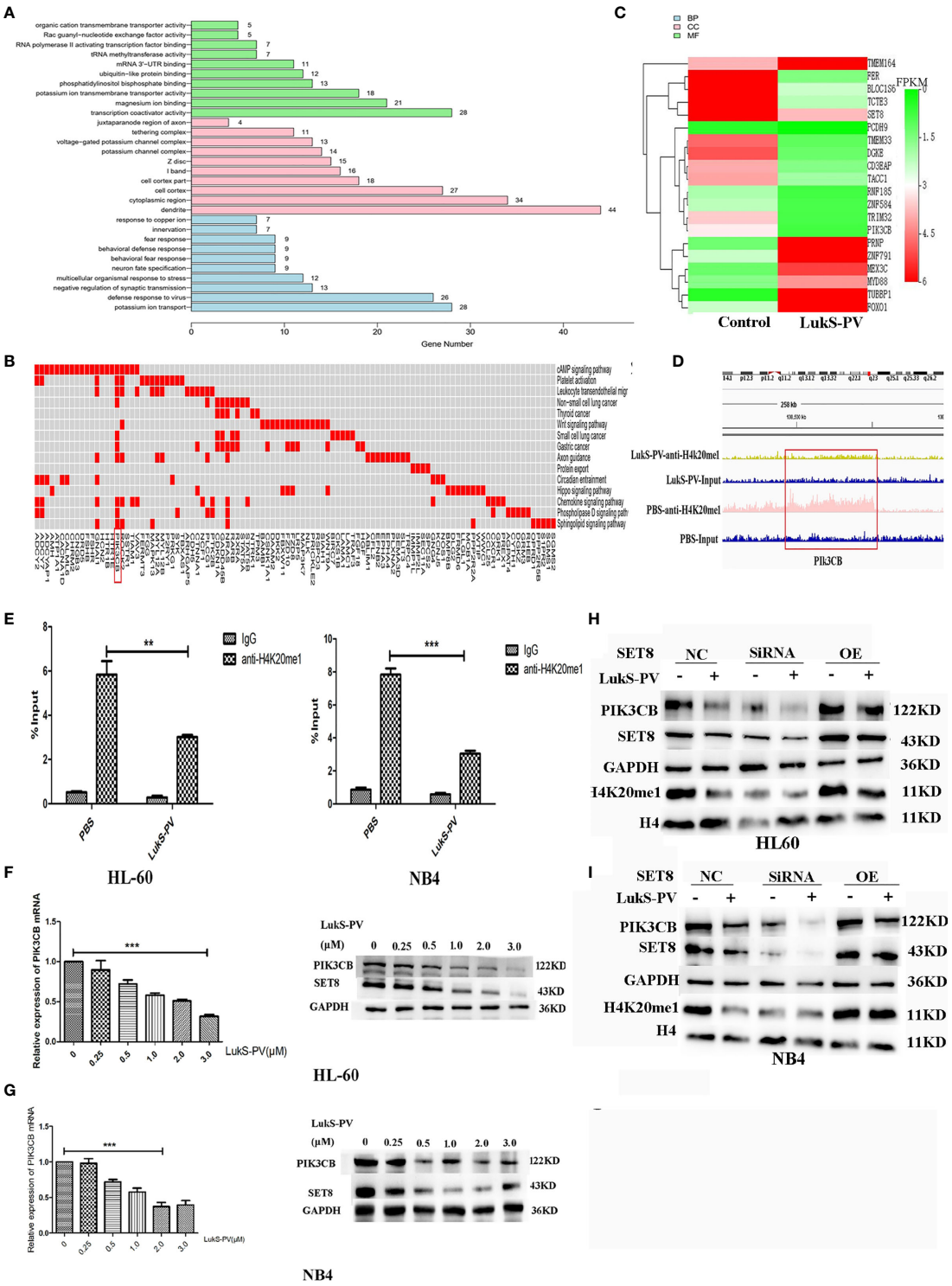

FIGURE 5 | PIK3CB is the target gene for LukS-PV-SET8/H4K20me1. **(A)** Gene Ontology (GO) analysis of downregulated peak related gene binding by LukS-PV-mediated H4K20me1 through ChIP-seq. **(B)** Functional groups in downregulated peak-related genes binding by LukS-PV-mediated H4K20me1. **(C)** Heatmap of different expression genes upon LukS-PV or phosphate-buffered saline (PBS) treatment. **(D)** The binding of LukS-PV and PBS on target gene PIK3CB. **(E)** The binding of H4K20me1 at the PIK3CB promoter was significantly reduced upon LukS-PV treatment *via* quantitative chromatin immunoprecipitation (ChIP)–PCR analysis. Data are presented as fold-change relative to the control with PBS as a negative control. **(F, G)** HL-60 and NB4 cells were treated with LukS-PV at different concentrations for 24 h, and PIK3CB gene and protein expression levels were assessed *via* quantitative real-time PCR and Western blotting. **(H, I)** Western blotting showed that LukS-PV downregulated PIK3CB *via* SET8/H4K20me1 in HL-60 **(H)** and NB4 **(I)** cells. $^{**}p < 0.01$; $^{***}p < 0.001$.

(**Figure 5B**). Data analysis showed that H4K20me1 enrichment in the *PIK3CB*, *ROCK2*, and *GNAI1* promoter regions decreased significantly. Furthermore, PIK3CB is involved in tumor-related signaling pathways, and the decrease in H4K20 methylation in the *PIK3CB* promoter region was the most obvious (**Figure 5D**). Similarly, RNA-seq results showed that *PIK3CB* mRNA was downregulated after LukS-PV treatment (**Figure 5C**). Moreover, Maeda et al. reported that PIK3CB plays a crucial role in apoptosis in renal cell carcinoma (24). Collectively, our data showed that *PIK3CB* was a potential downstream target gene of LukS-PV, and regulation of *PIK3CB* was mediated by SET8/H4K20me1. We verified this finding through ChIP-PCR in HL-60 and NB4 cells. Accordingly, upon LukS-PV treatment, the binding of H4K20me1 to the *PIK3CB* promoter was significantly reduced (**Figure 5E**). We treated HL-60 and NB4 with different concentrations of LukS-PV, and *PIK3CB* mRNA and protein expression levels were reduced in a dose-dependent manner (**Figures 5F, G**). Additionally, knockdown of SET8 reduced the expression of PIK3CB, while overexpression of SET8 promoted the expression of PIK3CB (**Figures 5H, I**). Collectively, LukS-PV inhibited the expression of PIK3CB *via* downregulation of SET8/H4K20me1.

LukS-PV Induced Apoptosis in Acute Myeloid Leukemia Cells by Downregulating PIK3CB *via* SET8/H4K20me1

Because PIK3CB was the downstream target gene of LukS-PV, we investigated whether PIK3CB played a role in apoptosis induced by LukS-PV. PIK3CB was overexpressed in AML cell lines (**Figure 6A**), which were then exposed to 3.0 μM of LukS-PV for 24 h. The flow cytometry results showed that overexpression of PIK3CB inhibited apoptosis induced by LukS-PV (**Figures 6B, D**). Furthermore, we examined the effect of GSK2636771 (a PIK3CB inhibitor) on apoptosis in SET8-overexpressing cells and UNC0379 (a SET8 inhibitor) on apoptosis in PIK3CB-overexpressing cells. The flow cytometry results demonstrated that inhibition of PIK3CB induced apoptosis in SET8-overexpressing cells; however, overexpression of PIK3CB prevented apoptosis induced by SET8 inhibition (**Figures 6B, D**). Finally, the levels of apoptosis-associated proteins were in accordance with the degree of apoptosis (**Figures 6C, E**). Together, our results indicated that LukS-PV induced apoptosis by downregulating the expression of target gene *PIK3CB*, and this downregulation was mediated by SET8/H4K20me1 in AML cells.

LukS-PV Induced Apoptosis *via* the PIK3CB/AKT/FOXO1 Signaling Pathway by Targeting SET8

It was reported that PIK3CB inhibits transcription factor FOXO1 by regulating AKT phosphorylation and inhibits apoptosis by regulating the expression of BAK and BCL2. Furthermore, our RNA sequencing results showed that *FOXO1* mRNA was upregulated after LukS-PV treatment (**Figure 5C**). Therefore, we hypothesized that LukS-PV may induce apoptosis *via* the PIK3CB/AKT/FOXO1 signaling pathway by targeting SET8. We verified this molecular mechanism by Western blotting, and the results were in line with our expectations. We found that LukS-PV-treated HL-60 and NB4 cells had lower levels of PIK3CB, pAKT (Ser 473), and anti-apoptotic BCL2 but higher levels of FOXO1 and pro-apoptotic BAK than PBS-treated control cells. These effects were further enhanced after SET8 knockdown with siRNA and markedly alleviated in SET8-overexpressing cells (**Figure 7A**).

Similarly, we determined the levels of associated proteins in primary AML blasts *via* Western blotting. In accordance, the results showed that treatment with 3.0 μM of LukS-PV significantly decreased the levels of SET8, H4K20me1, PIK3CB, pAKT (Ser 473), and anti-apoptotic BCL2 but increased the levels of FOXO1 and pro-apoptotic BAK as compared with the PBS-treated control group (**Figure 7B**). Together, our results indicated that LukS-PV induced apoptosis *via* the PIK3CB/AKT/FOXO1 signaling pathway by targeting SET8 in primary AML blasts (**Figure 7C**).

DISCUSSION

AML is a complex disease with a diverse genetic landscape, and the current approaches for AML treatment are still far from satisfactory. Target cell specificity and cytotoxicity of bacterial toxins have gained importance in the development of new antitumor drugs (3, 4). In this study with AML cells, we demonstrated that LukS-PV induced apoptosis *in vitro* and inhibited cell invasion *in vivo*. Moreover, we found that SET8 expression was decreased significantly after LukS-PV treatment, and SET8 is highly expressed in AML and is associated with poor prognosis. Furthermore, we confirmed that LukS-PV induced AML apoptosis *via* SET8 and identified *PIK3CB* as a downstream target gene for apoptosis mediated by SET8/H4K20me1. Finally, our results indicated that LukS-PV induced apoptosis *via* the PIK3CB-AKT-FOXO1 signaling pathway by targeting SET8.

Recent studies have revealed that changes in histone modification play an important role in leukemia pathogenesis (25, 26). For example, histone methylation has been reported to regulate stem cell differentiation and leukemia pathogenesis (27). This phenomenon is precisely based on the reversibility of epigenetic modifications that may facilitate targeted leukemia therapy (28). For instance, azacitidine and decitabine are DNA methyltransferase inhibitors approved for clinical treatment of AML (29, 30). Histone methyltransferase (EZH2) and demethylase (LSD1) targeting drugs have entered clinical trials (31, 32). In summary, histone modifications are potentially promising for targeted therapy for leukemia. SET8 is a member of the SET domain-containing methyltransferase family and specifically targets H4K20me1 (33). SET8 is involved in vital cellular processes, including transcriptional regulation (34), S-phase cell cycle progression (35), genomic replication and stability (36), and DNA repair (37). Aberrant SET8 expression has been linked to numerous solid tumors. High SET8 levels are also associated with poor survival in cancer patients (38–40). However, SET8 has so far been poorly studied

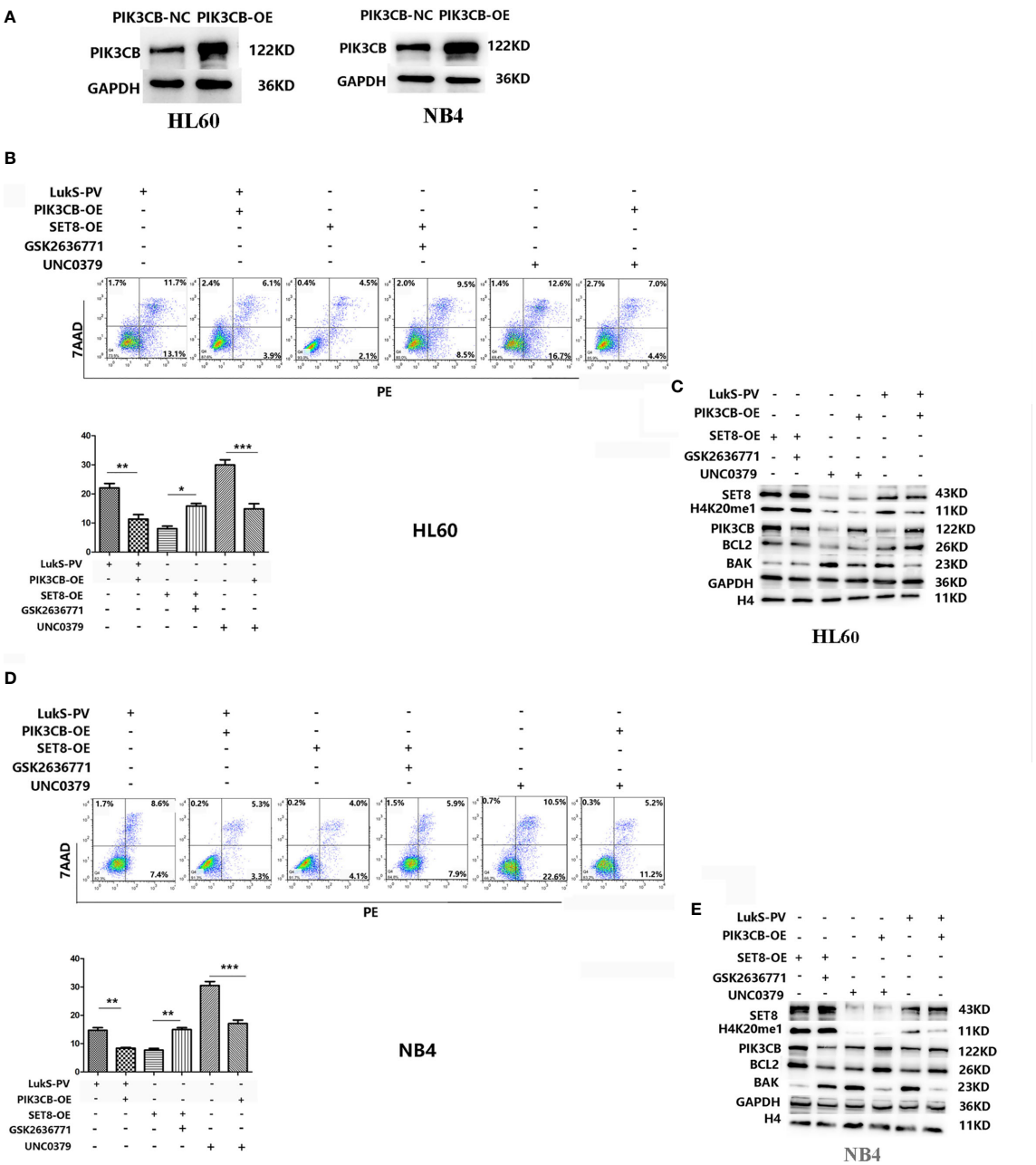

FIGURE 6 | LukS-PV induces apoptosis in acute myeloid leukemia (AML) cells by downregulating PIK3CB *via* SET8/H4K20me1. **(A)** PIK3CB overexpression in HL-60 (left) and NB4 (right) cells. **(B)** Apoptosis was determined in HL-60 cells *via* flow cytometry. **(C)** Apoptosis-related proteins were determined by Western blotting in HL-60 cells. **(D)** Apoptosis was determined in NB4 cells *via* flow cytometry. **(E)** Apoptosis-related proteins were determined by Western blotting in NB4 cells. ns, not significant; *p < 0.05; **p < 0.01; ***p < 0.001.

in leukemia. In this study, we found that SET8 was overexpressed in AML patients and associated with a poor prognosis, and knockdown of SET8 expression induced apoptosis in AML cells. These results suggest that SET8 may be a potential therapeutic target for AML.

Bacterial toxins reportedly have specific cytotoxic effects on target cells, including tumor cells, and they have received increasing attention in the development of antitumor drugs. As a new anti-AML drug, diphtheria toxin has entered the stage of clinical experimentation (41, 42). LukS-PV is the S component of PVL secreted by *S. aureus*. Our previous research has shown that LukS-PV has antileukemia activity *in vivo* and *in vitro* by inhibiting proliferation and inducing apoptosis and differentiation (12–15). Furthermore, we previously demonstrated that LukS-PV inhibited proliferation and induced apoptosis by downregulating histone

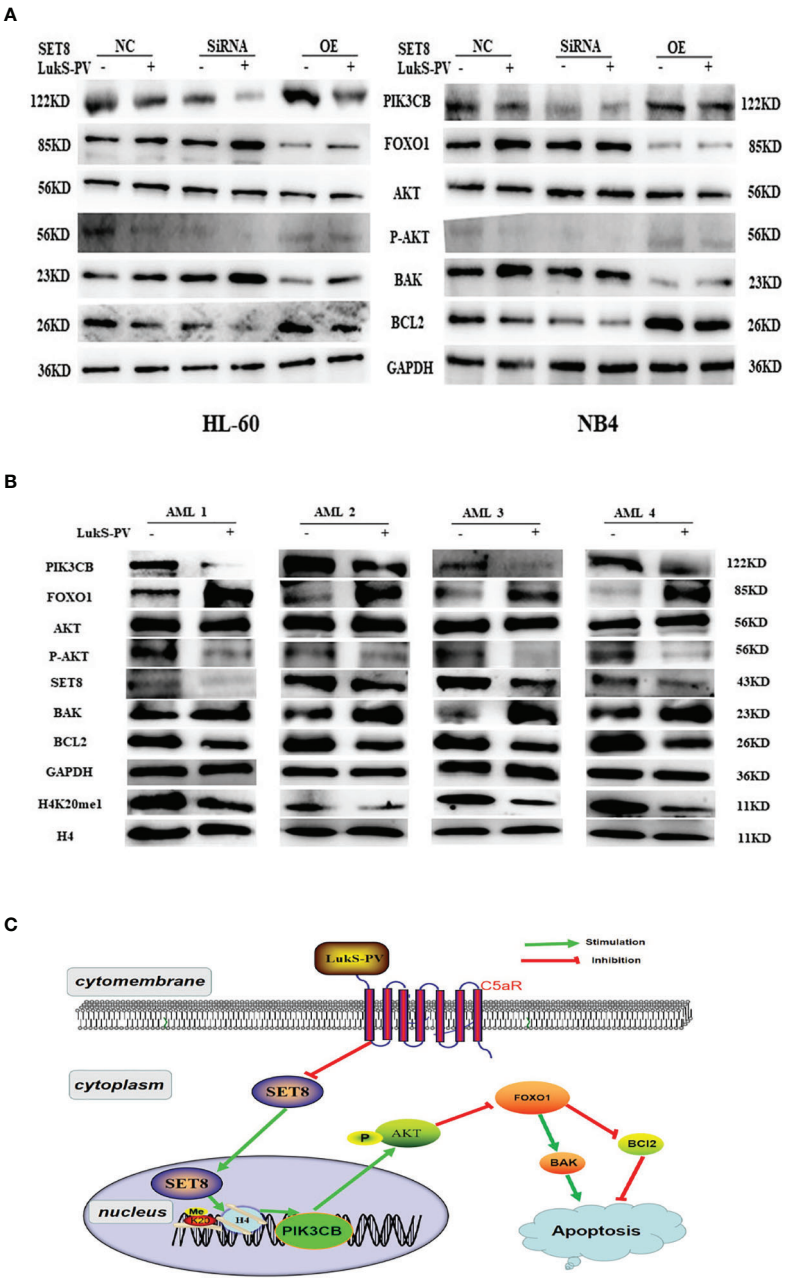

FIGURE 7 | LukS-PV induces apoptosis *via* the PIK3CB signal pathway by targeting SET8. **(A)** Levels of PIK3CB, FOXO1, AKT, apoptosis-associated (BAK/BCL2) proteins, and AKT phosphorylation in HL-60 and NB4 cells were assessed through Western blotting. **(B)** Expression levels of SET8, H4K20me1, PIK3CB, FOXO1, AKT, apoptosis-associated (BAK/BCL2), proteins, and AKT phosphorylation in primary acute myeloid leukemia (AML) blasts were assessed through Western blotting. **(C)** Proposed mechanism of action of LukS-PV in acute myeloid leukemia cells. SET8-OE, SET8 overexpression; SET8-NC, SET8 negative control; SET8-SiRNA, SET8 small interfering RNA.

acetylation in HCC cells (19), suggesting that LukS-PV maybe exert antileukemia activity by targeting histone epigenetic modifiers. In the current study, we found that LukS-PV induced apoptosis by downregulating SET8 and H4K20me1 and identified *PIK3CB* as a potential target gene. Our study indicates that SET8-PIK3CB signaling is one of the mechanisms by which LukS-PV induced apoptosis in AML cells.

The phosphatidylinositol 3-kinase (PI3K) pathway plays a pivotal role in cell growth, proliferation, and survival by integrating extracellular growth signals (43). PIK3CB is a member of the PI3K family, and hyperactivation of the PI3K pathway contributes to cancer progression in humans (44). AKT, a serine/threonine-protein kinase, is one of the most well-characterized targets of the PI3K pathway. Yutaka et al.

reported that TGF-β selectively induces AKT phosphorylation at Ser 473 in a PIK3CB-dependent manner in CD4+ T cells, resulting in the inhibition of FOXO transcription factors (45). Furthermore, studies have shown that FOXO factors promote apoptosis by inducing the expression of multiple pro-apoptotic members of the BCL2 family of mitochondria-targeting proteins (46). The present research revealed that *PIK3CB* is a downstream target gene of LukS-PV signaling. LukS-PV decreased AKT Ser 473 phosphorylation and increased FOXO1 levels, thus inducing apoptosis by decreasing BCL2 and increasing BAK in HL-60 and NB4 cells.

Several limitations to this study need to be acknowledged. First, the number of AML patient samples was small, and further in-depth research will be required using a larger number of clinical samples. Second, we used a xenograft tumor model, and few leukemia cells were present in mouse peripheral blood, which made it difficult to isolate enough leukemia cells for apoptosis experiments. Third, we found that the levels of SET8 and H4K20me1 reduced by LukS-PV were maximally downregulated at the 24 h timepoint and then increased at the 36 h timepoint. Indeed, in previous research, we found that the effects of LukS-PV were time-dependent; apoptosis was induced at an early stage (<24 h), and cell differentiation was induced at a later stage (36–48 h) (15). Whether regulation of SET8 expression by LukS-PV is also time-dependent remains to be further studied.

In conclusion, these results demonstrate that LukS-PV induced apoptosis in AML cells *via* the PIK3CB/AKT/FOXO1 signal transduction pathway by targeting the methyltransferase SET8. Our data suggest that SET8 may be a potential therapeutic target for AML. Furthermore, LukS-PV may be a valuable drug candidate for treatment of AML that targets epigenetic modifications.

DATA AVAILABILITY STATEMENT

The sequence data presented in the study are deposited in the CBI SRA repository, accession number: PRJNA767433, https://www.ncbi.nlm.nih.gov/bioproject/PRJNA767433.

ETHICS STATEMENT

The studies involving human participants were reviewed and approved by Ethics Committee and Institutional Review Board of University of Science and Technology of China, Anhui, China (Approval number: 2019-N(H)-101). The patients/participants provided their written informed consent to participate in this study. The animal study was reviewed and approved by Ethics Committee and Institutional Review Board of University of Science and Technology of China, Anhui, China (Approval number: 2019-N(H)-101).

AUTHOR CONTRIBUTIONS

LX: conceptualization, methodology, formal analysis, writing—original draft, data curation, and investigation. LS: conceptualization, investigation, writing—original draft, and funding acquisition. PD: resources and software. FM: methodology and software. KS: investigation and data curation. PQ: software and formal analysis. WC: visualization and supervision. YD: supervision and project administration. YM: writing—review and editing, and supervision. XM: writing—review and editing, supervision, project administration, and funding acquisition. All authors contributed to the article and approved the submitted version.

FUNDING

This work was supported by the National Natural Science Foundation of China (Grant No. 81972001, No. 81572065), the Anhui Natural Science Foundation (Grant No. 1808085QH259), and Fundamental Research Funds for Central Universities (WK9110000007, WK9110000107).

ACKNOWLEDGMENTS

We thank the Center for Scientific Research of Anhui Medical University for valuable help in our experiment. We thank Susan Zunino, PhD, from Liwen Bianji (Edanz) (www.liwenbianji.cn/), for editing the English text of a draft of this manuscript.

SUPPLEMENTARY MATERIAL

The Supplementary Material for this article can be found online at: https://www.frontiersin.org/articles/10.3389/fonc.2021.718791/full#supplementary-material

REFERENCES

1. Saultz JN, Garzon R. Acute Myeloid Leukemia: A Concise Review. *J Clin Med* (2016) 5(3):33. doi: 10.3390/jcm5030033
2. Webster JA, Pratz KW. Acute Myeloid Leukemia in the Elderly: Therapeutic Options and Choice. *Leuk Lymphoma* (2018) 59:274–87. doi: 10.1080/10428194.2017.1330956
3. Kramer MG, Masner M, Ferreira FA, Hoffman RM. Bacterial Therapy of Cancer: Promises, Limitations, and Insights for Future Directions. *Front Microbiol* (2018) 9:16. doi: 10.3389/fmicb.2018.00016
4. Weerakkody LR, Witharana C. The Role of Bacterial Toxins and Spores in Cancer Therapy. *Life Sci* (2019) 235:116839. doi: 10.1016/j.lfs.2019.116839
5. Vandenesch F, Naimi T, Enright MC, Lina G, Nimmo. Community-Acquired Methicillin-Resistant Staphylococcus Aureus Carrying Panton-Valentine Leukocidin Genes: Worldwide Emergence. *Emerg Infect Dis* (2003) 9(8):978–84. doi: 10.3201/eid0908.030089
6. Tacconelli E, Pop-Vicas AE, D'Agata EMC. Increased Mortality Among Elderly Patients With Meticillin-Resistant Staphylococcus Aureus Bacteraemia. *J Hosp Infect* (2006) 64:251–6. doi: 10.1016/j.jhin.2006.07.001

7. Boyle-Vavra S, Daum RS. Community-Acquired Methicillin-Resistant Staphylococcus Aureus: The Role of Panton-Valentine Leukocidin. *Lab Invest* (2007) 87:3–9. doi: 10.1038/labinvest.3700501
8. Pédelacq J, Maveyraud L, Prévost G, Baba-Moussa L, González A, Courcelle E, et al. The Structure of a Staphylococcus Aureus Leucocidin Component (LukF-PV) Reveals the Fold of the Water-Soluble Species of a Family of Transmembrane Pore-Forming Toxins. *Structure* (1999) 7:277–87. doi: 10.1016/S0969-2126(99)80038-0
9. Rogolsky M. Nonenteric Toxins of Staphylococcus Aureus. *Microbiological Rev* (1979) 43:320–60. doi: 10.1128/mr.43.3.320-360.1979
10. Ma XX, Ito T, Tiensasitorn C, Jamklang M, Chongtrakool P, Boyle-Vavra S, et al. Novel Type of Staphylococcal Cassette Chromosome Mec Identified in Community-Acquired Methicillin-Resistant Staphylococcus Aureus Strains. *Antimicrob Agents Chemother* (2002) 46:1147. doi: 10.1128/AAC.46.4.1147-1152.2002
11. Genestier AL. Staphylococcus Aureus Panton-Valentine Leukocidin Directly Targets Mitochondria and Induces Bax-Independent Apoptosis of Human Neutrophils. *J Clin Invest* (2005) 115:3117–7. doi: 10.1172/JCI22684
12. Shan W, Bu S, Zhang C, Zhang S, Ding B, Chang W, et al. LukS-PV, a Component of Panton-Valentine Leukocidin, Exerts Potent Activity Against Acute Myeloid Leukemia *In Vitro* and *In Vivo*. *Int J Biochem Cell Biol* (2015) 61:20–8. doi: 10.1016/j.biocel.2015.01.007
13. Sun XX, Zhang SS, Dai CY, Peng J, Pan Q, Xu LF, et al. LukS-PV-Regulated MicroRNA-125a-3p Promotes THP-1 Macrophages Differentiation and Apoptosis by Down-Regulating NF1 and Bcl-2. *Cell Physiol Biochem* (2017) 44:1093–105. doi: 10.1159/000485415
14. Zhang P, Yu WW, Peng J, Xu LF, Zhao CC, Chang WJ, et al. LukS-PV Induces Apoptosis in Acute Myeloid Leukemia Cells Mediated by C5a Receptor. *Cancer Med* (2019) 8:2474–83. doi: 10.1002/cam4.2137
15. Dai C, Zhang C, Sun X, Pan Q, Peng J, Shen J, et al. LukS-PV Induces Differentiation by Activating the ERK Signaling Pathway and C-JUN/c-FOS in Human Acute Myeloid Leukemia Cells. *Int J Biochem Cell Biol* (2016) 76:107–14. doi: 10.1016/j.biocel.2016.04.005
16. Boila L, Sengupta A. Evolving Insights on Histone Methylome Regulation in Human Acute Myeloid Leukemia Pathogenesis and Targeted Therapy. *Exp Hematol* (2020) 92:19–31. doi: 10.1016/j.exphem.2020.09.189
17. Zhou J, Bi C, Cheong LL, Mahara S, Liu SC, Tay KG, et al. The Histone Methyltransferase Inhibitor, DZNep, Up-Regulates TXNIP, Increases ROS Production, and Targets Leukemia Cells in AML. *Blood* (2011) 118:2830–9. doi: 10.1182/blood-2010-07-294827
18. Cusan M, Cai SF, Mohammad HP, Krivtsov A, Chramiec A, Loizou E, et al. LSD1 Inhibition Exerts its Anti-Leukemic Effect by Recommissioning PU.1- and C/Ebpα-Dependent Enhancers in AML. *Blood* (2018) 131(15):1730–42. doi: 10.1182/blood-2017-09-807024
19. Wang Z, Yu W, Qiang Y, Xu L, Ma F, Ding P, et al. LukS-PV Inhibits Hepatocellular Carcinoma Progression by Downregulating HDAC2 Expression. *Mol Ther Oncol* (2020) 17:547–61. doi: 10.1016/j.omto.2020.05.006
20. Ma X, Chang W, Zhang C, Zhou X, Yu F. Staphylococcal Panton-Valentine Leukocidin Induces Pro-Inflammatory Cytokine Production and Nuclear Factor-Kappa B Activation in Neutrophils. *PLoS One* (2012) 7(4):e34970. doi: 10.1371/journal.pone.0034970
21. Dinndorf PA, Andrews RG, Benjamin D, Ridgway D, Wolff L, Bernstein ID. Expression of Normal Myeloid-Associated Antigens by Acute Leukemia Cells. *Blood* (1986) 67:1048–53. doi: 10.1182/blood.V67.4.1048.1048
22. Carithers LJ, Moore HM. The Genotype-Tissue Expression (GTEx) Project. *Biopreservation Biobanking* (2015) 13:307–8. doi: 10.1089/bio.2015.29031.hmm
23. Wu M, Shang X, Sun Y, Wu J, Liu G. Integrated Analysis of Lymphocyte Infiltration-Associated lncRNA for Ovarian Cancer *via* TCGA, GTEx and GEO Datasets. *PeerJ* (2020) 8:e8961. doi: 10.7717/peerj.8961
24. Maeda Y, Kawano Y, Wada Y, Yatsuda J, Motoshima T, Murakami Y, et al. C5aR Is Frequently Expressed in Metastatic Renal Cell Carcinoma and Plays a Crucial Role in Cell Invasion *via* the ERK and PI3 Kinase Pathways. *Oncol Rep* (2015) 33:1844–50. doi: 10.3892/or.2015.3800
25. Dhall A, Zee BM, Yan F, Blanco MA. Intersection of Epigenetic and Metabolic Regulation of Histone Modifications in Acute Myeloid Leukemia. *Front Oncol* (2019) 9:432. doi: 10.3389/fonc.2019.00432
26. Goldman SL, Hassan C, Khunte M, Soldatenko A, Jong Y, Afshinnekoo E, et al. Epigenetic Modifications in Acute Myeloid Leukemia: Prognosis, Treatment, and Heterogeneity. *Front Genet* (2019) 10:133. doi: 10.3389/fgene.2019.00133
27. Ernst P, Wang J, Korsmeyer SJ. The Role of MLL in Hematopoiesis and Leukemia. *Curr Opin Hematol* (2002) 9:282–7. doi: 10.1097/00062752-200207000-00004
28. Greenblatt SM, Nimer SD. Chromatin Modifiers and the Promise of Epigenetic Therapy in Acute Leukemia. *Leukemia* (2014) 28:1396–406. doi: 10.1038/leu.2014.94
29. Dombret H, Seymour JF, Butrym A, Wierzbowska A, Selleslag D, Jang JH, et al. International Phase 3 Study of Azacitidine vs Conventional Care Regimens in Older Patients With Newly Diagnosed AML With >30% Blasts. *Blood* (2015) 126:291–9. doi: 10.1182/blood-2015-01-621664
30. He J, Xiu L, De Porre P, Dass R, Thomas X. Decitabine Reduces Transfusion Dependence in Older Patients With Acute Myeloid Leukemia: Results From a *Post Hoc* Analysis of a Randomized Phase III Study. *Leuk Lymphoma* (2015) 56:1033–42. doi: 10.3109/10428194.2014.951845
31. Harris WJ, Huang X, Lynch JT, Spencer GJ, Hitchin JR, Li Y, et al. The Histone Demethylase KDM1A Sustains the Oncogenic Potential of MLL-AF9 Leukemia Stem Cells. *Cancer Cell* (2012) 21:473–87. doi: 10.1016/j.ccr.2012.03.014
32. McCabe MT, Ott HM, Ganji G, Korenchuk S, Thompson C, Van Aller SG, et al. EZH2 Inhibition as a Therapeutic Strategy for Lymphoma With EZH2-Activating Mutations. *Nature* (2012) 492:108–12. doi: 10.1038/nature11606
33. Nishioka K, Rice JC, Sarma K. PR-Set7 Is a Nucleosome-Specific Methyltransferase That Modifies Lysine 20 of Histone H4 and Is Associated With Silent Chromatin. *Mol Cell* (2002) 9:1201–13. doi: 10.1016/S1097-2765(02)00548-8
34. Li Z, Nie F, Wang S, Li L. Histone H4 Lys 20 Monomethylation by Histone Methylase SET8 Mediates Wnt Target Gene Activation. *Proc Natl Acad Sci USA* (2011) 108:3116–23. doi: 10.1073/pnas.1009353108
35. Tardat M, Brustel J, Kirsh O, Lefevbre C, Callanan M, Sardet C, et al. The Histone H4 Lys 20 Methyltransferase PR-Set7 Regulates Replication Origins in Mammalian Cells. *Nat Cell Biol* (2010) 12:1086–93. doi: 10.1038/ncb2113
36. Centore RC, Havens CG, Manning AL, Li JM, Flynn RL, Tse A, et al. CRL4(Cdt2)-Mediated Destruction of the Histone Methyltransferase Set8 Prevents Premature Chromatin Compaction in S Phase. *Mol Cell* (2010) 40:22–33. doi: 10.1016/j.molcel.2010.09.015
37. Yu N, Huangyang P, Yang X, Han X, Yan R, Jia H, et al. microRNA-7 Suppresses the Invasive Potential of Breast Cancer Cells and Sensitizes Cells to DNA Damages by Targeting Histone Methyltransferase SET8. *J Biol Chem* (2013) 288:19633–42. doi: 10.1074/jbc.M113.475657
38. Zhou HR, Fu H-Y, Wu D-S, Zhang Y-Y, Huang S-H, Chen C-J, et al. Relationship Between Epigenetic Changes in Wnt Antagonists and Acute Leukemia. *Oncol Rep* (2017) 37:2663–71. doi: 10.3892/or.2017.5509
39. Hou L, Li Q, Yu Y, Li M, Zhang D. SET8 Induces Epithelial–Mesenchymal Transition and Enhances Prostate Cancer Cell Metastasis by Cooperating With ZEB1. *Mol Med Rep* (2016) 13:1681–8. doi: 10.3892/mmr.2015.4733
40. Zhang X, Peng Y, Yuan Y, Gao Y, Hu F, Wang J, et al. Histone Methyltransferase SET8 Is Regulated by miR-192/215 and Induces Oncogene-Induced Senescence *via* P53-Dependent DNA Damage in Human Gastric Carcinoma Cells. *Cell Death Dis* (2020) 11:937. doi: 10.1038/s41419-020-03130-4
41. Bachanova V, Cooley S, Defor TE, et al. Clearance of Acute Myeloid Leukemia by Haploidentical Natural Killer Cells Is Improved Using IL-2 Diphtheria Toxin Fusion Protein. *Blood* (2014) 123(25):3855–63. doi: 10.1182/blood-2013-10-532531
42. Frankel A, Liu JS, Rizzieri D, Hogge D. Phase I Clinical Study of Diphtheria Toxin-Interleukin 3 Fusion Protein in Patients With Acute Myeloid Leukemia and Myelodysplasia. *Leuk Lymphoma* (2008) 49:543–53. doi: 10.1080/10428190701799035
43. Cantley LC. The Phosphoinositide 3-Kinase Pathway. *Science* (2002) 296:1655–7. doi: 10.1126/science.296.5573.1655
44. Engelman JA, Luo J, Cantley LC. The Evolution of Phosphatidylinositol 3-Kinases as Regulators of Growth and Metabolism. *Nat Rev Genet* (2006) 7:606–19. doi: 10.1038/nrg1879
45. Kurebayashi Y, Baba Y, Minowa A, Nadya NA, Azuma M, Yoshimura A, et al. TGF-Beta-Induced Phosphorylation of Akt and Foxo Transcription Factors

Negatively Regulates Induced Regulatory T Cell Differentiation. *Biochem Biophys Res Commun* (2016) 480:114–9. doi: 10.1016/j.bbrc.2016.09.153

46. Zhang X, Tang N, Hadden T, Rishi A. Akt, FoxO and Regulation of Apoptosis. *Biochim Biophys Acta* (2011) 1813:1978–86. doi: 10.1016/j.bbamcr.2011.03.010

Conflict of Interest: The authors declare that the research was conducted in the absence of any commercial or financial relationships that could be construed as a potential conflict of interest.

Publisher's Note: All claims expressed in this article are solely those of the authors and do not necessarily represent those of their affiliated organizations, or those of the publisher, the editors and the reviewers. Any product that may be evaluated in this article, or claim that may be made by its manufacturer, is not guaranteed or endorsed by the publisher.

frontiers in Oncology

ORIGINAL RESEARCH
published: 21 October 2021
doi: 10.3389/fonc.2021.761205

LncRNA PPM1A-AS Regulate Tumor Development Through Multiple Signal Pathways in T-Cell Acute Lymphoblastic Leukemia

Guoli Li[1], *Xinyue Lei*[1], *Yingchi Zhang*[2], *Zhe Liu*[1,3,4*] *and Kegan Zhu*[1,3*]

[1] Department of Immunology, Biochemistry and Molecular Biology, 2011 Collaborative Innovation Center of Tianjin for Medical Epigenetics, Tianjin Key Laboratory of Medical Epigenetics, Tianjin Medical University, Tianjin, China, [2] State Key Laboratory of Experimental Hematology, National Clinical Research Center for Blood Diseases, Institute of Hematology & Blood Diseases Hospital, Chinese Academy of Medical Sciences & Peking Union Medical College, Tianjin, China, [3] Key Laboratory of Immune Microenvironment and Disease of the Ministry of Education, Tianjin Medical University, Tianjin, China, [4] Tianjin Key Laboratory of Radiation Medicine and Molecular Nuclear Medicine, Institute of Radiation Medicine, Tianjin, China

OPEN ACCESS

Edited by:
Yonghui Li,
Shenzhen University General Hospital, China

Reviewed by:
Chandraditya Chakraborty,
Dana-Farber Cancer Institute and Harvard Medical School, United States
Albrecht Reichle,
University Medical Center Regensburg, Germany

***Correspondence:**
Kegan Zhu
zhukegan@tmu.edu.cn
Zhe Liu
zheliu@tmu.edu.cn

Specialty section:
This article was submitted to Hematologic Malignancies, a section of the journal Frontiers in Oncology

Received: 19 August 2021
Accepted: 29 September 2021
Published: 21 October 2021

Citation:
Li G, Lei X, Zhang Y, Liu Z and Zhu K (2021) LncRNA PPM1A-AS Regulate Tumor Development Through Multiple Signal Pathways in T-Cell Acute Lymphoblastic Leukemia. Front. Oncol. 11:761205. doi: 10.3389/fonc.2021.761205

ALL (Acute lymphoblastic leukemia) is the most common pediatric malignancy and T-ALL (T-cell acute lymphoblastic leukemia) comprises about 15% cases. Compared with B-ALL (B-cell acute lymphoblastic leukemia), the prognosis of T-ALL is poorer, the chemotherapy is easier to fail and the relapse rate is higher. Previous studies mainly focused in Notch1-related long non-coding RNAs (lncRNAs) in T-ALL. Here, we intend to investigate lncRNAs involved in T-ALL covering different subtypes. The lncRNA PPM1A-AS was screened out for its significant up-regulation in 10 T-ALL samples of different subtypes than healthy human thymus extracts. Besides, the PPM1A-AS expression levels in 3 T-ALL cell lines are markedly higher than that in $CD45^+$ T cells of healthy human. We further demonstrate that PPM1A-AS can promote cell proliferation and inhibit cell apoptosis *in vitro* and can influence T-ALL growth *in vivo*. Finally, we verified that PPM1A-AS can regulate core proteins, Notch4, STAT3 and Akt, of 3 important signaling pathways related to T-ALL. These results confirm that lncRNA PPM1A-AS can act as an oncogene in T-ALL and maybe a potential clinical target of patients resistant to current chemotherapy or relapsed cases.

Keywords: PPM1A-AS, T-ALL, Notch4, STAT3, Akt

INTRODUCTION

T-cell acute lymphoblastic leukemia (T-ALL) is a hematologic malignancy induced by the transformation of T-cell progenitors (1). The prominent feature of T-ALL is the uncontrolled proliferation of immature T lymphocyte, frequent large thymic masses, enlarged spleen and pleural effusions (1, 2). T-ALL accounts for 15% of childhood and 25% of adult ALL cases and childhood

acute lymphoblastic leukemia (cALL) causes the most frequent death from cancer in pediatrics (3). So far, genetic alterations, including point mutations, chromosomal rearrangements and the loss or gain of chromosome, have been well studied due to the development of genome-wide sequencing. Dozens of oncogenes or tumor suppressors are found to be dys-regulated in T-ALL. As a result, modern combined chemotherapy remarkably raised the overall survive rate in patients especially pediatric patients with T-ALL. Although T-ALL cases are divided into different subgroups characterized by one particular transcription factor which is ectopic expressed, for example TLX1、TLX3、LMO、HOXA and so on, but almost T-ALL cases owe not only one biologically relevant genomic lesion (4). In some cases, more than 10 mutated genes work together and thus lead to the transformation of T cells into aggressive leukemia cells with enhanced proliferation and survival characteristics, impaired differentiation, altered cell cycle and metabolism properties (5). In fact, there are more than 100 genes were found abnormal in T-ALL (5). The screening out of novel molecules that participate in several regulating pathways may contribute to the clinical treatment of complex T-ALL cases which are resistant to given drugs or relapsed cases.

LncRNAs are a new class of RNAs which is more than 200 nucleotides in size with no defined open reading frames. LncRNAs are usually much lower expressed than mRNAs but can be specially expressed in particular tissue. LncRNAs are found to play roles in many normal life processes, such as neuroregulation, spermatogenesis, muscle regeneration and erythropoiesis (6). Besides, ectopic expression of lncRNA is closely related to different diseases including cancers (6). The latest researches show that lncRNAs participate in tumorigenesis, tumor proliferation, migration, invasion and metabolism (7). Thus, lncRNAs may be used as diagnostic markers, novel therapeutic targets and potential prognostic markers in cancers. In leukemia, lncRNAs also have important functions (7). For example, in BLL (B-cell lymphoblastic leukemia), lncRNA GAS5 was proved to regulate metastasis by repressing miR-222 (8) and lncRNA ZEB-AS1 could influence tumor development by targeting IL11/STAT3 signal pathway (9). Besides, Trimarchi et al. focused in Notch-regulated lncRNAs while Takaomi Sanda et al. focused in TAL1 complex-regulated lncRNAs in T-ALL (10, 11). Furthermore, another lncRNA, NALT, was also involved in T-ALL development by inducing Notch1 activation (12). Despite of these findings, more efforts are needed to make the lncRNA regulatory network in leukemia clearer.

In the current study, we found a new lncRNA, which we named as PPM1A-AS, was overexpressed in patients with T-ALL at the first time. Then, we demonstrated that T-ALL tumor cell proliferation ability was closely connected to the PPM1A-AS expression level. Moreover, PPM1A-AS could influence the tumor cell apoptosis *in vitro*. Next, we established tumor model in NOD-SCID mice and demonstrated that PPM1A-AS could also promote T-ALL development *in vivo*. Finally, we performed whole-transcriptome deep sequencing in wild- or PPM1A-AS-knockdown-Jurkat cells. Compared to the wild group, we detected 288 up expressed genes and 313 down expressed genes in PPM1A-AS-knockdown group. By KEGG pathway analysis, the differentially expressed genes are enriched in Notch signal pathway and PI3K-Akt signaling pathway, which take important roles in T-ALL tumor development. We then verified that phosphorylated Akt, phosphorylated STAT3 and Notch4 protein levels are positive related with PPM1A-AS. To conclude, we find that PPM1A-AS can work as an oncogene and can regulate several pathways in T-ALL, and thus may be provided as a potential clinic target for T-ALL patients with multiple gene mutations.

MATERIALS AND METHODS

Cell Culture

The T-ALL cell lines Jurkat, CEM and MOLT4 were cultured in RPMI1640 (Gibco, NY, USA) with 10% fetal bovine serum (FBS). They were maintained at 37°C in a humidified incubator with 5% CO2.

Human CD45$^+$ T Cell Isolation

The peripheral blood were collected from healthy human and red blood cell lysis was conducted with lysis buffer (Solarbio, Beijing, China). The CD45$^+$ T cells were isolated with magnetic beads (Stemcell, Vancouver, Canada) according to the manufacturer's instructions.

Quantitative Real Time PCR

Total RNA of T-ALL cells was extracted with TRIzol Reagent (Thermo Fisher Scientific, MA, USA) and 1ug total RNA was reverse-transcribed into complementary DNA(cDNA) using the RevertAid First Strand cDNA Synthesis Kit (Thermo). Quantitative real-time PCR was performed to determine the RNA expression using SYBR Green master mix (DBI®Bioscience, Ludwigshafen, German) with specific primers listed below. All of the reactions were run in triplicate and the relative levels of lncRNA were normalized to 18S rRNA. The sequences of the primers were as follows: hGAPDH Forward: 5'- CTTTTGCGTCGCCAGCCGAG -3'; hGAPDH Reverse: 5'- CCAGGCGCCCAATACGACCA -3'; PPM1A-AS Forward: 5'- AGTCCTGGACAGTCTTTAGGC -3'; PPM1A-AS Reverse: 5'- AGGTGTGTGCTGGGAAATGT -3'.

Cell Nucleus/Cytoplasm Fraction Isolation

Cytoplasmic and nuclear RNA were isolated and purified using the PARIS™ Kit (ThermoFisher, #AM1921) according to the manufacturer's instructions.

Knockdown and Overexpression

For knockdown assay, oligos encoding shRNA specific for PPM1A-AS were ligated into pSUPER.retro.puro, and the fragment containing the H1 promoter and hairpin sequences was subcloned into the lentiviral shuttle pCCL.PPT.hPGK.GFP.Wpre. The shRNA target sequences were as follows: shPPM1A-AS-1, GCATCAAGAAGAACAGCTA; shPPM1A-AS-2, GGTTGA

TCTGTGCGGCAAA. For overexpression assay, lncRNA PPM1A-AS sequence was ligated into the lentiviral shuttle pCCL.PPT.hPGK.IRES.GFP/pre. These plasmids were used to produce lentivirus in HEK293T cells with the packaging plasmids pMD2.BSBG, pMDLg/pRRE and pRSV-REV. Cells were infected with lentivirus and sorted by GFP signal to generate a stable cell line.

Cell Counting Kit-8 Assay

To assess cell proliferation ability, Jurkat, CEM and MOTL4 cells infected with control lentivirus, lncRNA PPM1A-AS-knockdown lentivirus or lncRNA PPM1A-AS-overexprssion lentivirus were seeded into 96-well plates at a density of 2000 cells per well. At 0, 24, 48, 72, 96, 120 hours after the cells were seeded, CCK-8 reagent (Dojingdo, Japan) was mixed with the cells for 1h incubation at 37°C. The absorbance value was measured at 450nm with Microplate reader.

EdU Assay

The EdU assay was conducted with Cell-Light EdU Apollo567 In Vitro Kit (RiboBio Co., Guangzhou, China) according to the manufacturer's instructions of suspension cell. Briefly, Jurkat, CEM and MOTL4 cells were infected with control, lncRNA PPM1A-AS-knockdown or lncRNA PPM1A-AS-overexprssion lentivirus and then 5000 cells of each group were planted in 24-well plates. 24 hours later, the cells were remarked with EdU and made smears. After cell fixation and Apollo staining, the slides were observed and took photos under a microscope at 100×magnification.

Cell Apoptosis Assay

Jurkat and CEM cells infected with control lentivirus, lncRNA PPM1A-AS-knockdown lentivirus or lncRNA PPM1A-AS-overexprssion lentivirus were collected and incubated with annexin V and PIfor 15min. The apoptotic cells were detected by BD flow cytometer. The annexin positive but PI negative staining indicated the early apoptotic cells. The annexin V and PI both positive staining indicated cells in necrosis (post-apoptotic necrosis or late apoptosis). The proportion of total apoptotic cells are the sum of these two parts of cells.

Western Blotting

The control or infected cells were rinsed with PBS and lysed in RIPA Lysisbuffer (Beyotime, China) supplemented with Protease and Phosphatase Inhibitor (Cell Signaling Technology Inc., USA) on ice for 30min. The cell lysates were centrifuged for 10min (12000 g, 4°C) and the supernatant was collected. The protein concentration was calculated with Pierce BCA protein assay kit (Thermo) and equivalent quantities of protein were separated on 10% SDS-PAGE gels. Then the proteins were transferred onto a nitrocellulose membrane (Bio-Rad, CA, USA). After blocking with 5% non-fat milk at room temperature for 1h, the membranes were immunostained with primary antibodies at 4°C overnight, washed three times in TBST, and then incubated with secondary antibody at room temperature for 1h. Finally, the protein bands on membranes were detected with an enhanced chemiluminescence reagent (Millipore) and captured using a luminescence instrument (Tanon, Shanghai, China). The gray density of protein bands was determined by Image J software. The primary antibodies were listed below: Akt (#9272, Cell Signaling Technology); T308-pAkt (#13038, Cell Signaling Technology), S473-pAkt (#4060, Cell Signaling Technology); STAT-3(#9132, Cell Signaling Technology), T705-pSTAT3 (#9131, Cell Signaling Technology), S727-pSTAT3 (#9134, Cell Signaling Technology); Notch4 (ab184742, Abcam).

T-ALL Xenograft Model

Female NOD-SCID mice (4-6 weeks old) were purchased from the Model Animal Research Center of Nanjing University (Nanjing, China) and housed under pathogen-free conditions in Tianjin Medical University. Jurkat cells were infected with control lentivirus or lncRNA PPM1A-AS-knockdown lentivirus (2×10^6), suspended in 200ul PBS and then injected into the mice by tail intravenous injection. After 45 days later, the peripheral blood was taken from mice, the mice were sacrificed, the spleens were photographed and weighed and the bone marrow were dissected. The animal study was reviewed and approved by Tianjin Medical University Animal Care and Use Committee.

RNA Sequencing

RNA was isolated from Jurkat cells injected with control lentivirus or lncRNAPPM1A-AS-knockdownlentivirus using Trizol (Invitrogen) following manufacture instructions. Biological samples in duplicate were submitted to Novogene Co., Ltd for RNA sequencing. Barcoded sequence libraries were constructed using TruSeq RNA Sample Prep kit (Illumina), and sequenced on a HiSeq 2000 instrument.

Statistical Analysis

Data analyses were undertaken with GraphPad PRISM 8.0. The results were shown as mean ± standard deviation (SD), from three independent experiments and analyzed *via* the Student's t-test. The value $p < 0.05$ was considered statistically significant.

RESULTS

LncRNA PPM1A-AS Is Up-Regulated in T-ALL

To identify lncRNAs differentially expressed in T-ALL, we collected and analyzed RNA sequencing (RNA-seq) data of 10 T-ALL patients and 2 human whole thymus extracts from public database (GSE110636 (13), GSE57982 (10), the sample numbers were listed in **Supplementary Table 1**). The 10 T-ALL patients were belonging to different genetic subgroups. The heatmap was showed in **Figure 1A**. Among these lncRNAs, we found that CTD-2184C24.2 (ENST00000553775) was obviously increased in T-ALL patients (**Figure 1B**). CTD-2184C24.2 is a transcript antisense to *PPM1A*. So, we named this lncRNA as PPM1A-AS after this gene. Moreover, we tested the expression level of PPM1A-AS in T-ALL cell lines Jurkat, CCRF-CEM and MOLT4. The T cells extracted from healthy human blood with $CD45^+$ magnetic beads were used as control. As a result, PPM1A-AS was significantly overexpressed in all three T-ALL

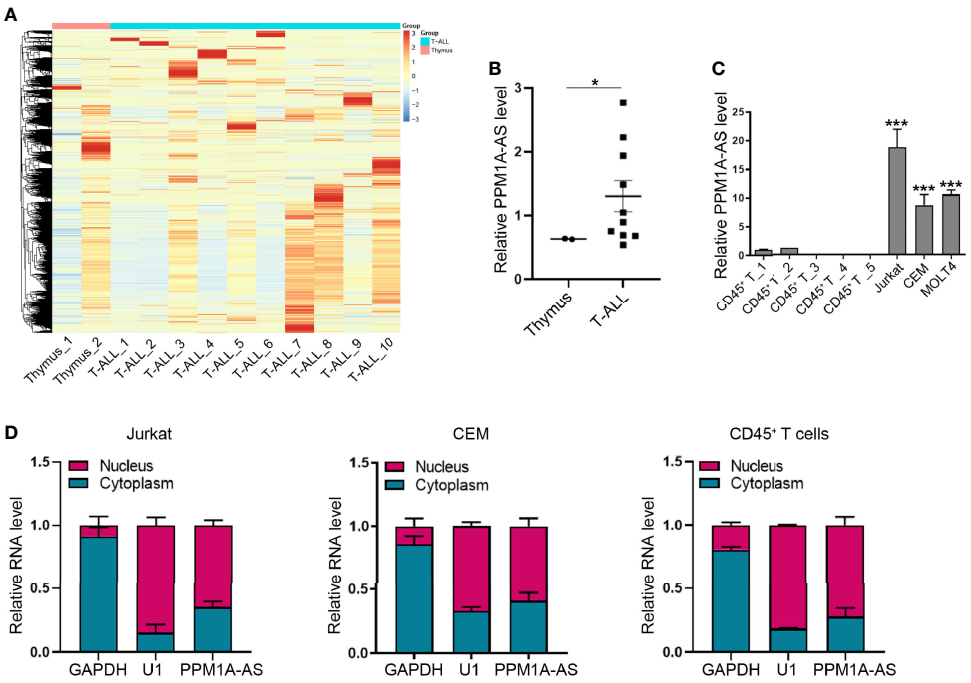

FIGURE 1 | LncRNA PPM1A-AS is up expressed in T-ALL. **(A)** The heatmap of lncRNA expression in 10 T-ALL samples and 2 healthy human whole thymus extracts. **(B)** The relative expression level of lncRNA PPM1A-AS in 10 T-ALL samples and 2 healthy human thymus extracts. **(C)** RT-qPCR analysis of lncRNA PPM1A-AS in T-ALL cell lines and healthy human CD45$^+$ T cells. **(D)** The nuclear and cytoplasmic distribution of lncRNA PPM1A-AS in Jurkat, CEM and T cells extracted from healthy human. Mean ± SD. *P < 0.05. ***P < 0.001.

cell lines than T cells extracted from healthy persons (**Figure 1C**). Finally, we verified the distribution of PPM1A-AS in T cells. No matter in normal or cancerous T cells, PPM1A-AS was existing in both nucleus and cytoplasm, mainly in nucleus (**Figure 1D**). These results also indicated that the PPM1A-AS had no shuttle between nucleus and cytoplasm during T-ALL formation.

LncRNA PPM1A-AS Promotes Cell Proliferation and Inhibits Cell Apoptosis in T-ALL Cell Lines

In order to explore the function of PPM1A-AS, stable clones with knockdown and overexpression of PPM1A-AS were generated with shRNA and plasmid *via* lentivirus technology in T-ALL cell lines, Jurkat, CEM and MOTL4. Firstly, we evaluated the efficiency of PPM1A-AS knockdown (**Figure 2A** and **Supplementary Figure 1A**) and overexpression by RT-qPCR (**Figure 3A** and **Supplementary Figure 1D**). The PPM1A-AS RNA level was about 25% lower by two different shRNAs and hundreds higher by overexpression vector. Then we performed CCK-8 and EdU assays to test the cell proliferation ability. Compared to the control group, cells infected with PPM1A-AS shRNA lentivirus showed significantly slower proliferation rates (**Figures 2B, C** and **Supplementary Figures 1B, C**) while overexpression of PPM1A-AS enhanced cell proliferation (**Figures 3B, C** and **Supplementary Figures 1E, F**). Besides, we examined cell apoptosis by flow cytometry. We found that knockdown of PPM1A-AS could induce T-ALL cell death (**Figure 2D**). Taken together, we conclude that lncRNA PPM1A-AS may have the potential to serve as an oncogene in T-ALL.

LncRNA PPM1A-AS Regulates T-ALL Development *In Vivo*

To further determine the role of lncRNA PPM1A-AS in T-ALL, we established tumor xenograft model in NOD-SCID mice. We cultured Jurkat cells infected with blank lentivirus or lncRNA PPM1A-AS-konckdown lentivirus and transplanted mice by tail intravenous injection. About 45 days later, we sacrificed the mice, photographed and measured the spleens, detected the proportion of tumor cells in peripheral blood and bone marrow. As the pictures showed in **Figure 4A**, the spleens from mice of the control group were much enlarged than the PPM1A-AS knockdown group. The statistical data were in **Figure 4B** and the spleens' average weight of control mice was obviously larger. Moreover, the proportion of tumor cells in peripheral blood (**Figure 4C**) or bone marrow (**Figure 4D**) from control mice were much more than the mice of PPM1A-AS knockdown group, which means PPM1A-AS knockdown can repress T-ALL tumor development *in vivo*.

LncRNA PPM1A-AS Target Genes in Multiple Signal Pathways

To further investigate the mechanism by which PPM1A-AS promotes T-ALL progression, we performed RNA-seq in

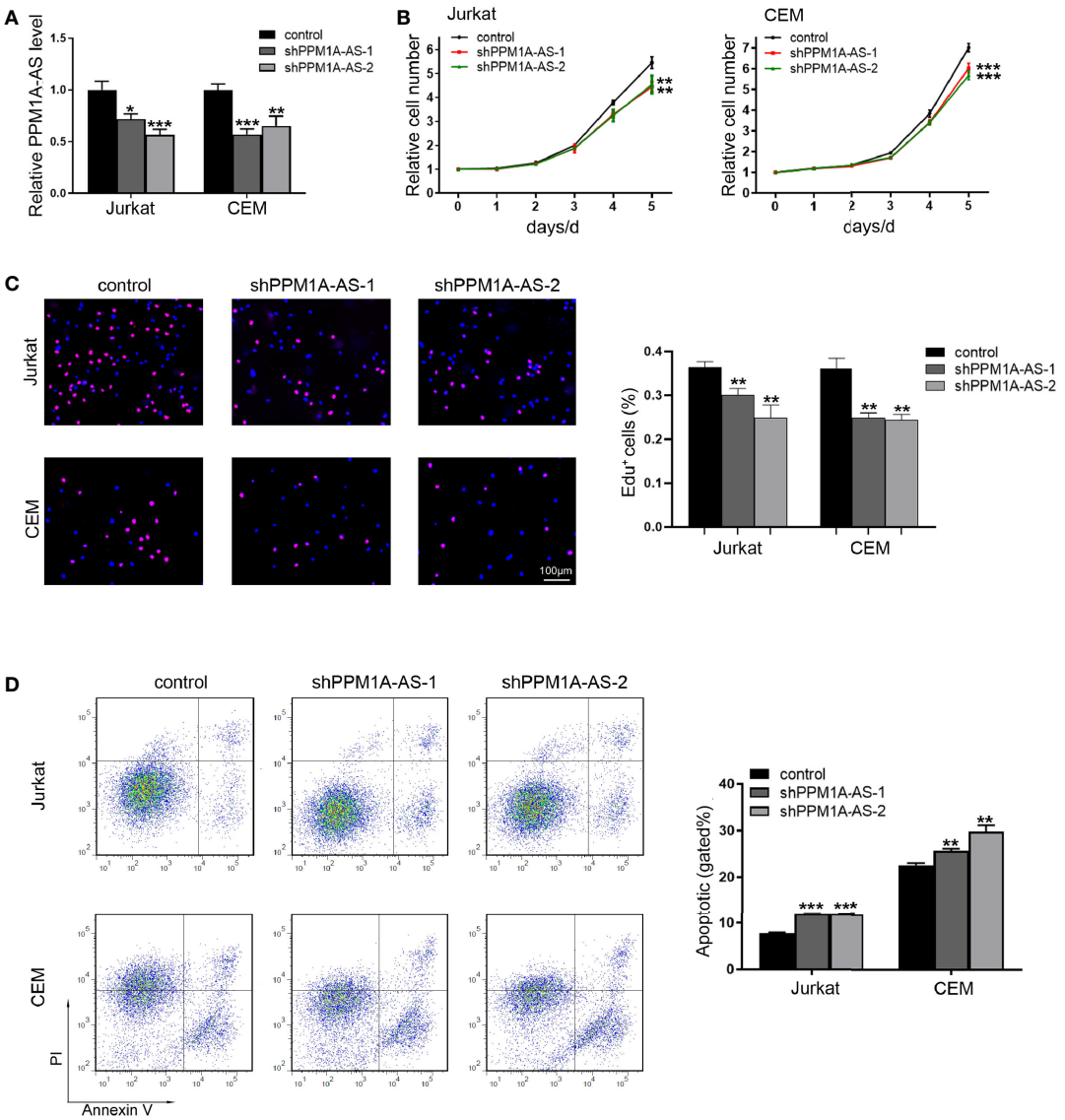

FIGURE 2 | Knockdown of lncRNA PPM1A-AS can inhibit cell proliferation and promote cell apoptosis. **(A)** The efficiency of PPM1A-AS shRNAs in Jurkat and CEM cell lines. **(B)** CCK-8 analyses of the proliferation rates of Jurkat and CEM cells infected with control or PPM1A-AS-knockdown lentivirus. **(C)** EdU analyses of the proliferative ability of Jurkat and CEM cells infected with control or PPM1A-AS-knockdown lentivirus. Left panel: representative images; right panel: average percentage of EdU^+ cells counted in each field. Scale bar, 100μm. **(D)** Flow cytometry analyses of T-ALL cell apoptosis after infected with control or PPM1A-AS-knockdown lentivirus. Left panel: representative images; right panel: percentage of apoptotic cells. Mean ± SD. *P < 0.05. **P < 0.01. ***P < 0.001.

Jurkat cells stably transduced with shRNAs targeting PPM1A-AS or a non-targeting control. Two biological replicates were included in each group and high correlations were observed between the replicates (**Figure 5A**). We then performed differential gene expression analysis, and identified 288 and 313 genes significantly upregulated and downregulated after knockdown of PPM1A-AS (**Figure 5B** and **Supplementary Table 2**). The major signal pathways that the differently expressed genes involved in were analyzed by KEGG database (**Figure 5C**). Among these pathways, Notch signaling pathway and PI3K-Akt signaling pathway are the major pathways participated in T-ALL tumorigenesis and development (14). We then tested if PPM1A-AS has any role in the well-known oncogenic pathways involved in T-ALL. *AKT*, *NOTCH* and *STAT* are core genes of PI3K-Akt signaling pathway, Notch signaling pathway and JAK-STAT3 signaling pathway respectively (15). We chose proteins of these genes and examined their expression after PPM1A-AS knockdown. The whole protein levels of STAT3 and Akt were not changed but the phosphorylated protein (T308, S473 of Akt and T705, S727 of

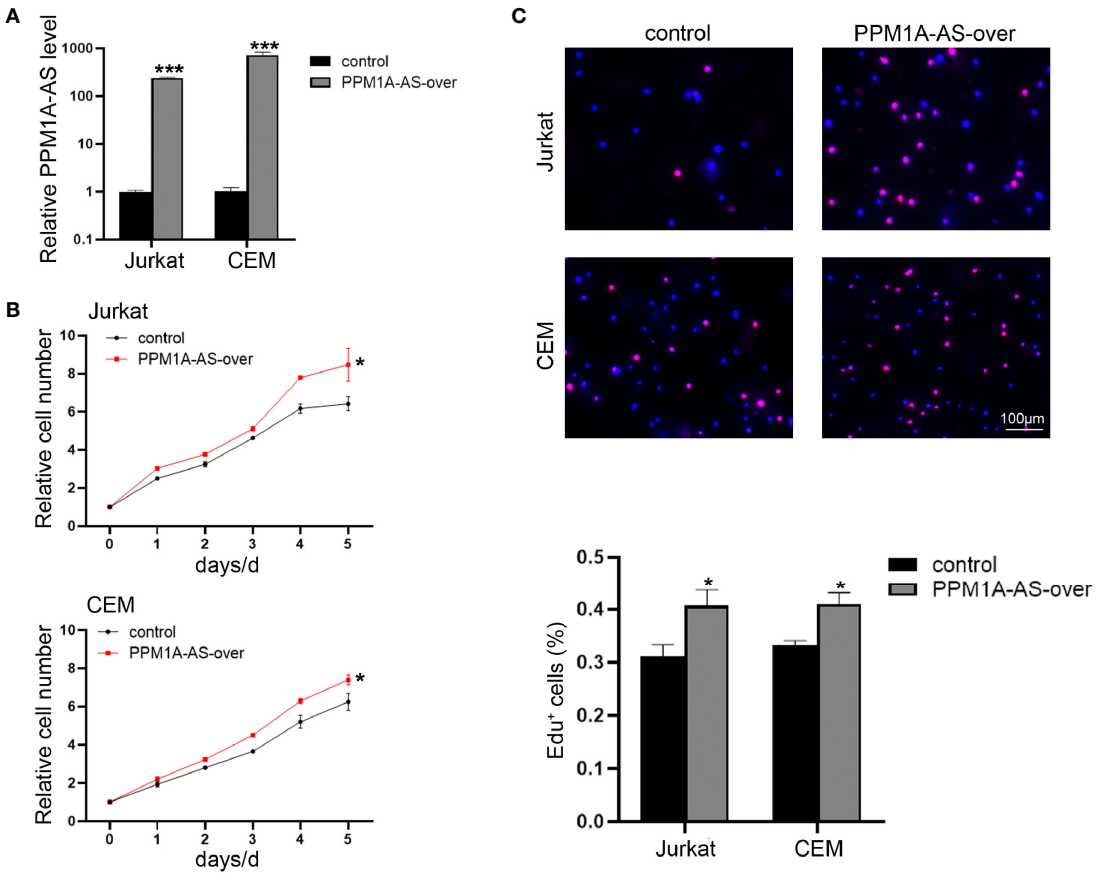

FIGURE 3 | Overexpression of lncRNA PPM1A-AS can promote cell proliferation. **(A)** The efficiency of PPM1A-AS overexpression in Jurkat and CEM cell lines. **(B)** CCK-8 analyses of the proliferation rates of Jurkat and CEM cells infected with control or PPM1A-AS-overexpression lentivirus. **(C)** EdU analyses of the proliferative ability of Jurkat and CEM cells infected with control or PPM1A-overexpression lentivirus. Upper panel: representative images; bottom panel: average percentage of EdU$^+$ cells counted in each field. Scale bar, 100μm. Mean ± SD. *P < 0.05. ***P < 0.001.

STAT3) were significantly downregulated by PPM1A-AS knockdown (**Figure 5D**). Besides, the Notch4 (**Figure 5D**) but not Notch1 (data were not showed) protein level was also consistent with PPM1A-AS RNA level. Therefore, these data showed that PPM1A-AS could regulate multiple proteins and thus have roles in several T-ALL related pathways.

DISCUSSION

ALL is the most common pediatric malignancy and T-ALL comprises about 15% cases (16). Till now, scientists have discovered many oncogenic and tumor suppressor pathways that participate in T-ALL transformation and development. Notch signaling is an oncogenic pathway which is activated in more than 65% of T-ALL patients by activating Notch1 gene mutations (14, 17). Notch4 is also a member of NOTCH family of receptors but its role in T-ALL is not as clear as Notch1 (18). James et al. (2014) discovered that Notch4 did not signal in response to ligand but it could repress the signaling from Notch1 receptor. Notch4 could bind unprocessed, full-length Notch1 and altered the subcellular localization of Notch1 (19). Costa et al. found that genetic deletion of Notch4 did not result in an overt phenotype in mice as well as other publications. But the expression of Notch4 was required for tumor onset and early tumor perfusion in a mouse model of breast cancer, despite the phenomenon that the final tumor size was similar between tumors grown in wild type and Notch4-null hosts (20). Besides, PI3K-AKT signaling is also an important oncogenic signaling pathway in T-ALL (17). Transgenic overexpression of an active form of AKT in T cell progenitors results in increased PI3K signaling and induces T-ALL in mice (21). Moreover, there is another oncogenic signaling pathway, JAK-STAT signaling, playing roles in T-ALL (17). Approximately 10% of T-ALLs show gain-of-function mutations in IL7R and result in constitutive JAK-STAT signaling (22). In the research of 116 clinical cases, authors found that phosphorylated STAT3, but not pSTAT5 or pSTAT6, predicts better prognosis in the smoldering type of T-ALL (23). Due to these findings of oncogenic or tumor suppressed mechanism contributing to T-ALL, abundant

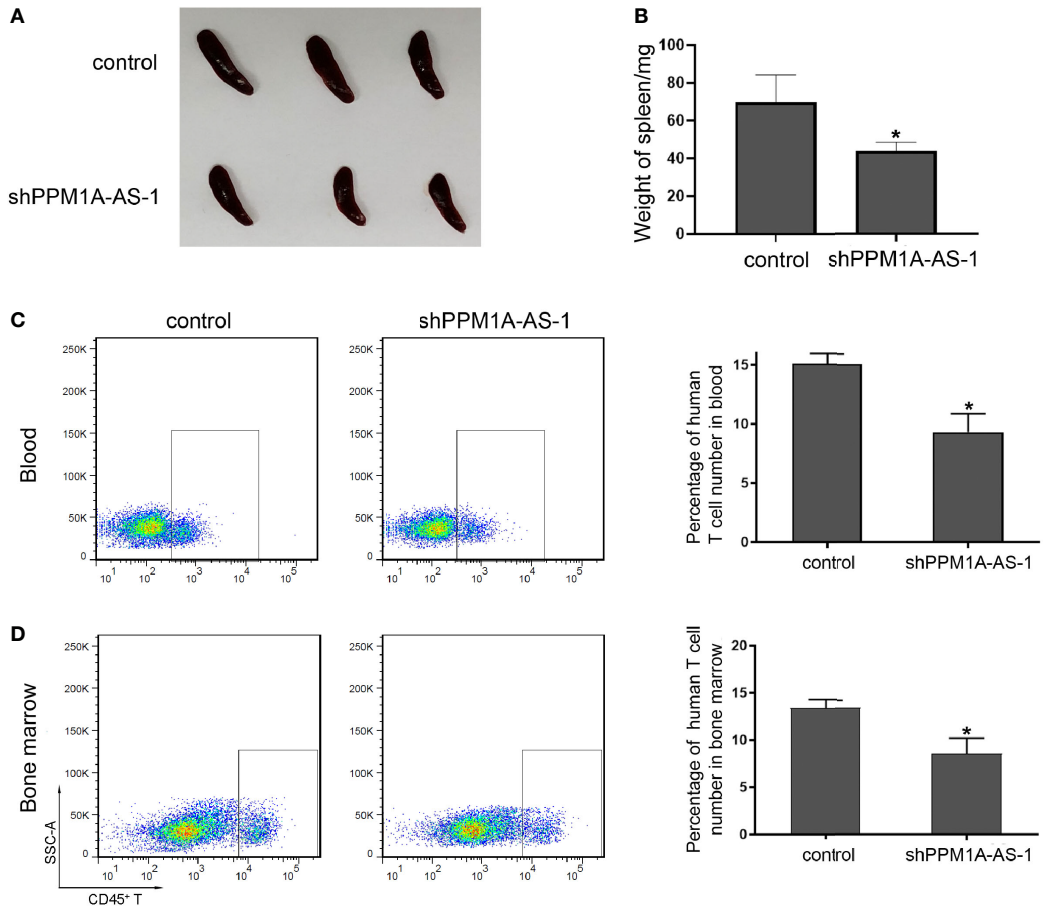

FIGURE 4 | LncRNA PPM1A-AS can enhance tumor development in NOD-SCID mice. Jurkat cells were infected with control or PPM1A-AS-overexpression lentivirus and transplanted mice by tail intravenous injection. About 45 days later, the mice were sacrificed, the photos were taken and relative data were detected. **(A)** Representative images of spleens from mice. **(B)** Quantitative analyses of the weights of the spleens. **(C)** Flow cytometry analyses of human $CD45^+$ T cells in peripheral blood of mice. Left panel: representative images; right panel: average percentage of $CD45^+$ T cells in peripheral blood from each mouse. **(D)** Flow cytometry analyses of human $CD45^+$ T cells in bone marrow of mice. Left panel: representative images; right panel: average percentage of $CD45^+$ T cells in bone marrow from each mouse. Mean ± SD. *$P < 0.05$.

chemotherapy protocols are drawn into clinical treatment and lead to a consequent gradual progress in cure rate. Despite this improvement, patients with primary resistant T-ALL or those with relapsed disease still faced terrible prognosis. So, we need more efforts to reveal other specific therapeutic targets underlying T-ALL development. In fact, many clinical T-ALL cases contain more than one gene mutation and may involve several signaling pathways which function in cancer transformation and grown (24). Combined application of chemotherapy drugs may be benefit to these complicated cases. Here, we discover that lncRNA PPM1A-AS can regulate Notch4, phosphorylated AKT, phosphorylated STAT3 expression in the same time and thus affect Notch signaling, PI3K-AKT signaling as well as JAK-STAT signaling pathways. This finding indicates the existence of lncRNA regulating different oncogenic or tumor suppressor pathways in T-ALL and may provide a new thought to solve complex clinical cases.

Due to the establishment of Sanger sequencing, the Human Genome Project was conducted in the worldwide which discovered that only 1.2% of the human genome represents protein coding exons and most genomic DNA is non-coding (25). The same phenomena were also verified in other eukaryotes and gave rise to heated debates in the scientific community about if they are transcriptional noises. The first long non-coding RNA H19 was found in the late 1980s, even though it was classified as an mRNA at that time (25). The function of lncRNA remained a mystery through a century until another lncRNA, Xist, was characterized to function in X-chromosome inactivation in mammals in the early 1990s (25). The rapid development of high-throughput sequencing technologies led to an explosion in the number of newly identified and uncharacterized lncRNAs. But many challenges in lncRNA biology remain, including accurate annotation, functional characterization and clinical relevance. Here, we focus on lncRNAs in T-ALL and tried to

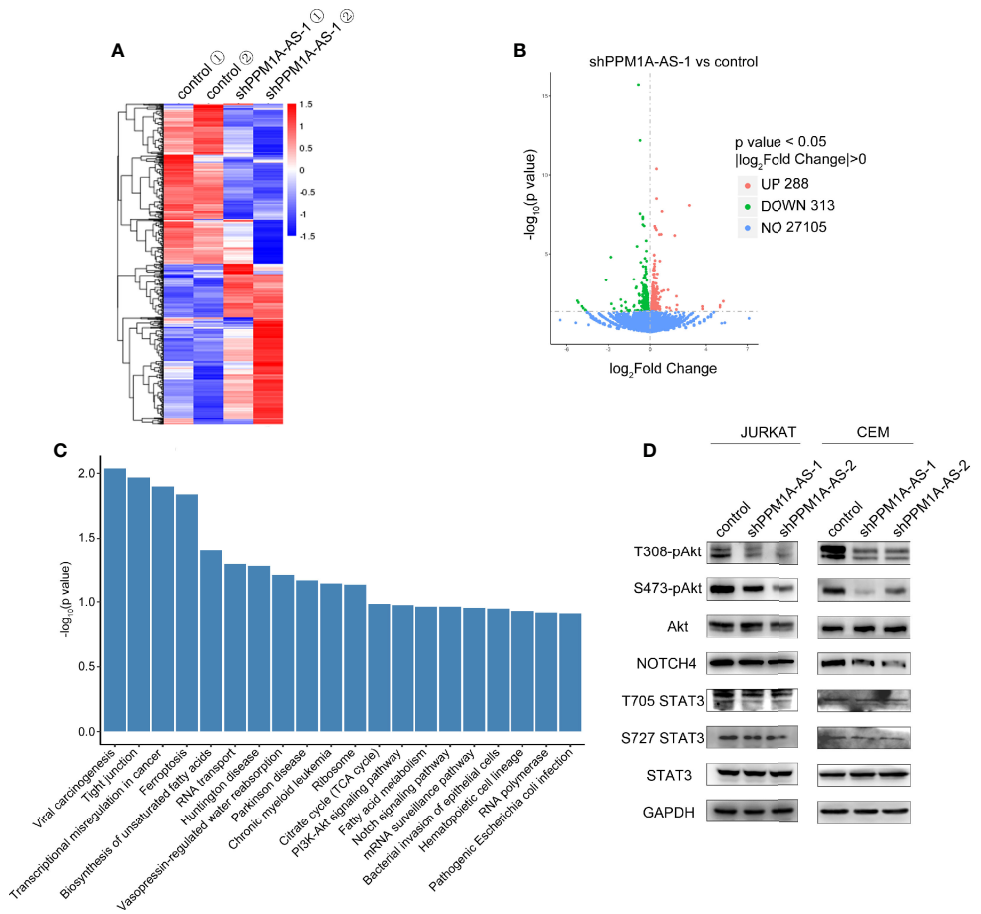

FIGURE 5 | LncRNA PPM1A-AS regulates multiple signaling pathways in T-ALL. **(A)** The heatmap of transcriptome sequencing of Jurkat cells infected with control or PPM1A-AS-knockdown lentivirus. **(B)** The volcano plot representation of differentially expressed mRNAs upon PPM1A-AS knockdown. **(C)** Significantly enriched pathways relative to differentially expressed mRNAs upon PPM1A-AS knockdown. **(D)** Western blot analysis of core proteins belonging to T-ALL relative signaling pathways.

do our bit for the improvement of lncRNA regulatory network. We researched a new lncRNA, which we named as PPM1A-AS because it's an antisense lncRNA of gene *PPM1A*, at the first time. We found PPM1A-AS was up-expressed in T-ALL patients and cell lines. By *in vitro* and *in vivo* assays, PPM1A-AS was proved to be benefit for T-ALL development through regulating cell proliferation and apoptosis. Next, we performed transcriptome sequencing using RNAs extracted from Jurkat cells which were infected with control or PPM1A-AS-knockdown lentivirus. KEGG pathway analysis revealed that PPM1A-AS was probably involved in Notch signaling and PI3K-Akt signaling pathways. We then tested if PPM1A-AS could influence expression of core proteins in these pathways by western blotting. The results showed that knockdown of PPM1A-AS didn't affect the level of Notch1 and total protein of Akt but could decrease the phosphorylated Akt and Notch4 expression. Furthermore, we also detected lncRNA PPM1A-AS's role in another oncogenic pathway, JAK-STAT signaling pathway. PPM1A-AS can impact phosphorylated STAT3 but not total STAT3 protein level. In conclusion, we not only make a break of functions of a new lncRNA but also make a contribution to the new roles of lncRNA in T-ALL. Finally, the particular mechanism which lncRNA PPM1A-AS took to affect Noth4, p-Akt and p-STAT3 is not clear and needs more efforts in the future.

DATA AVAILABILITYSTATEMENT

The datasets presented in this study can be found in online repositories. The names of the repository/repositories and accession number(s) can be found below: GSE182998, GSM5548426-29.

ETHICS STATEMENT

The animal study was reviewed and approved by Tianjin Medical University Animal Care and Use Committee.

AUTHOR CONTRIBUTIONS

KZ and ZL contributed to conception and design of the study. GL and XL performed the laboratory studies. YZ and KZ carried out data analyses. KZ contributed to drafting the manuscript. All authors contributed to the article and approved the submitted version.

FUNDING

This work was supported by grants from the Science & Technology Development Fund of the Tianjin Education Commission for Higher Education (2017KJ227).

ACKNOWLEDGMENTS

The authors sincerely appreciate all members who participated in this work.

SUPPLEMENTARY MATERIAL

The Supplementary Material for this article can be found online at: https://www.frontiersin.org/articles/10.3389/fonc.2021.761205/full#supplementary-material

REFERENCES

1. Sanchez-Martin M, Ferrando A. The NOTCH1-MYC Highway Toward T-Cell Acute Lymphoblastic Leukemia. *Blood* (2017) 129(9):1124–33. doi: 10.1182/blood-2016-09-692582
2. Cook LB, Fuji S, Hermine O, Bazarbachi A, Ramos JC, Ratner L, et al. Revised Adult T-Cell Leukemia-Lymphoma International Consensus Meeting Report. *J Clin Oncol* (2019) 37(8):677–87. doi: 10.1200/jco.18.00501
3. Vadillo E, Dorantes-Acosta E, Pelayo R, Schnoor M. T Cell Acute Lymphoblastic Leukemia (T-ALL): New Insights Into the Cellular Origins and Infiltration Mechanisms Common and Unique Among Hematologic Malignancies. *Blood Rev* (2018) 32(1):36–51. doi: 10.1016/j.blre.2017.08.006
4. Porcher C, Chagraoui H, Kristiansen MS. SCL/TAL1: A Multifaceted Regulator From Blood Development to Disease. *Blood* (2017) 129 (15):2051–60. doi: 10.1182/blood-2016-12-754051
5. Zhang J, Ding L, Holmfeldt L, Wu G, Heatley SL, Payne-Turner D, et al. The Genetic Basis of Early T-Cell Precursor Acute Lymphoblastic Leukaemia. *Nature* (2012) 481(7380):157–63. doi: 10.1038/nature10725
6. Kopp F, Mendell JT. Functional Classification and Experimental Dissection of Long Noncoding RNAs. *Cell* (2018) 172(3):393–407. doi: 10.1016/j.cell.2018.01.011
7. Bhan A, Soleimani M, Mandal SS. Long Noncoding RNA and Cancer: A New Paradigm. *Cancer Res* (2017) 77(15):3965–81. doi: 10.1158/0008-5472.Can-16-2634
8. Jing Z, Gao L, Wang H, Chen J, Nie B, Hong Q. Long Non-Coding RNA GAS5 Regulates Human B Lymphocytic Leukaemia Tumourigenesis and Metastasis by Sponging miR-222. *Cancer Biomark* (2019) 26(3):385–92. doi: 10.3233/cbm-190246
9. Wang Q, Du X, Yang M, Xiao S, Cao J, Song J, et al. LncRNA ZEB1-AS1 Contributes to STAT3 Activation by Associating With IL-11 in B-Lymphoblastic Leukemia. *Biotechnol Lett* (2017) 39(12):1801–10. doi: 10.1007/s10529-017-2421-3
10. Trimarchi T, Bilal E, Ntziachristos P, Fabbri G, Dalla-Favera R, Tsirigos A, et al. Genome-Wide Mapping and Characterization of Notch-Regulated Long Noncoding RNAs in Acute Leukemia. *Cell* (2014) 158(3):593–606. doi: 10.1016/j.cell.2014.05.049
11. Ngoc PCT, Tan SH, Tan TK, Chan MM, Li Z, Yeoh AEJ, et al. Identification of Novel lncRNAs Regulated by the TAL1 Complex in T-Cell Acute Lymphoblastic Leukemia. *Leukemia* (2018) 32(10):2138–51. doi: 10.1038/s41375-018-0110-4
12. Wang Y, Wu P, Lin R, Rong L, Xue Y, Fang Y. LncRNA NALT Interaction With NOTCH1 Promoted Cell Proliferation in Pediatric T Cell Acute Lymphoblastic Leukemia. *Sci Rep* (2015) 5:13749. doi: 10.1038/srep13749
13. Verboom K, Van Loocke W, Volders PJ, Decaesteker B, Cobos FA, Bornschein S, et al. A Comprehensive Inventory of TLX1 Controlled Long Non-Coding RNAs in T-Cell Acute Lymphoblastic Leukemia Through polyA Plus and Total RNA Sequencing. *Haematologica* (2018) 103(12):E585–9. doi: 10.3324/haematol.2018.190587
14. Gutierrez A, Look AT. NOTCH and PI3K-AKT Pathways Intertwined. *Cancer Cell* (2007) 12(5):411–3. doi: 10.1016/j.ccr.2007.10.027
15. Luo K. Signaling Cross Talk Between TGF-β/Smad and Other Signaling Pathways. *Cold Spring Harb Perspect Biol* (2017) 9(1):a022137. doi: 10.1101/cshperspect.a022137
16. Karrman K, Johansson B. Pediatric T-Cell Acute Lymphoblastic Leukemia. *Genes Chromosomes Cancer* (2017) 56(2):89–116. doi: 10.1002/gcc.22416
17. Girardi T, Vicente C, Cools J, De Keersmaecker K. The Genetics and Molecular Biology of T-ALL. *Blood* (2017) 129(9):1113–23. doi: 10.1182/blood-2016-10-706465
18. Lobry C, Oh P, Mansour MR, Look AT, Aifantis I. Notch Signaling: Switching an Oncogene to a Tumor Suppressor. *Blood* (2014) 123(16):2451–9. doi: 10.1182/blood-2013-08-355818
19. James AC, Szot JO, Iyer K, Major JA, Pursglove SE, Chapman G, et al. Notch4 Reveals a Novel Mechanism Regulating Notch Signal Transduction. *Biochim Biophys Acta* (2014) 1843(7):1272–84. doi: 10.1016/j.bbamcr.2014.03.015
20. Costa MJ, Wu X, Cuervo H, Srinivasan R, Bechis SK, Cheang E, et al. Notch4 Is Required for Tumor Onset and Perfusion. *Vasc Cell* (2013) 5(1):7. doi: 10.1186/2045-824x-5-7
21. Somervaille TC, Linch DC, Khwaja A. Growth Factor Withdrawal From Primary Human Erythroid Progenitors Induces Apoptosis Through a Pathway Involving Glycogen Synthase Kinase-3 and Bax. *Blood* (2001) 98 (5):1374–81. doi: 10.1182/blood.v98.5.1374
22. Delgado-Martin C, Meyer LK, Huang BJ, Shimano KA, Zinter MS, Nguyen JV, et al. JAK/STAT Pathway Inhibition Overcomes IL7-Induced Glucocorticoid Resistance in a Subset of Human T-Cell Acute Lymphoblastic Leukemias. *Leukemia* (2017) 31(12):2568–76. doi: 10.1038/leu.2017.136
23. Brender C, Nielsen M, Kaltoft K, Mikkelsen G, Zhang Q, Wasik M, et al. STAT3-Mediated Constitutive Expression of SOCS-3 in Cutaneous T-Cell Lymphoma. *Blood* (2001) 97(4):1056–62. doi: 10.1182/blood.v97.4.1056
24. Belver L, Ferrando A. The Genetics and Mechanisms of T Cell Acute Lymphoblastic Leukaemia. *Nat Rev Cancer* (2016) 16(8):494–507. doi: 10.1038/nrc.2016.63
25. Gibb EA, Brown CJ, Lam WL. The Functional Role of Long Non-Coding RNA in Human Carcinomas. *Mol Cancer* (2011) 10:38. doi: 10.1186/1476-4598-10-38

Conflict of Interest: The authors declare that the research was conducted in the absence of any commercial or financial relationships that could be construed as a potential conflict of interest.

Publisher's Note: All claims expressed in this article are solely those of the authors and do not necessarily represent those of their affiliated organizations, or those of the publisher, the editors and the reviewers. Any product that may be evaluated in this article, or claim that may be made by its manufacturer, is not guaranteed or endorsed by the publisher.

frontiers in Oncology

ORIGINAL RESEARCH
published: 12 November 2021
doi: 10.3389/fonc.2021.763232

Lin28A/CENPE Promoting the Proliferation and Chemoresistance of Acute Myeloid Leukemia

Mingyue Shi[1†], Junwei Niu[1†], Xiaona Niu[1], Honggang Guo[1], Yanliang Bai[1], Jie Shi[1], Weiya Li[1], Kai Sun[1], Yuqing Chen[1] and Fengmin Shao[2*]*

[1] Department of Hematology, Zhengzhou University People's Hospital and Henan Provincial People's Hospital, Zhengzhou, China, [2] Department of Nephrology, Henan Provincial Key Laboratory of Kidney Disease and Immunology, Zhengzhou University People's Hospital and Henan Provincial People's Hospital, Zhengzhou, China

OPEN ACCESS

Edited by:
Yonghui Li,
Shenzhen University General Hospital, China

Reviewed by:
Sk. Kayum Alam,
University of Minnesota Twin Cities, United States
Xiaohua Tan,
Shenzhen Third People's Hospital, China

***Correspondence:**
Yuqing Chen
henanblood@sina.com
Fengmin Shao
shaofengmin1818@163.com

[†]These authors have contributed equally to this work

Specialty section:
This article was submitted to Hematologic Malignancies, a section of the journal Frontiers in Oncology

Received: 23 August 2021
Accepted: 22 October 2021
Published: 12 November 2021

Citation:
Shi M, Niu J, Niu X, Guo H, Bai Y, Shi J, Li W, Sun K, Chen Y and Shao F (2021) Lin28A/CENPE Promoting the Proliferation and Chemoresistance of Acute Myeloid Leukemia. Front. Oncol. 11:763232. doi: 10.3389/fonc.2021.763232

The prognosis of chemoresistant acute myeloid leukemia (AML) is still poor, mainly owing to the sustained proliferation ability of leukemic cells, while the microtubules have a major role in sustaining the continuity of cell cycle. In the present study, we have identified CENPE, a microtubular kinesin-like motor protein that is highly expressed in the peripheral blood of patients with chemoresistant AML. In our *in vitro* studies, knockdown of CENPE expression resulted in the suppression of proliferation of myeloid leukemia cells and reversal of cytarabine (Ara-C) chemoresistance. Furthermore, Lin28A, one of the RNA-binding oncogene proteins that increase cell proliferation and invasion and contribute to unfavorable treatment responses in certain malignancies, was found to be remarkably correlated with CENPE expression in chemoresistance AML. Overexpression of LIN28A promoted the proliferation and Ara-C chemoresistance of leukemic cells. RIP assay, RNA pull-down, and dual luciferase reporter analyses indicated that LIN28A bound specifically to the promoter region GGAGA of CENPE. In addition, the impacts of LIN28A on cell growth, apoptosis, cell cycle progression, and Ara-C chemoresistance were reverted by the knockdown of CENPE. Hence, Lin28A/CENPE has enhanced the proliferation and chemoresistance of AML, and therefore, it could be a prospective candidate for AML treatment.

Keywords: CENPE, LIN28A, AML, chemoresistance, cell cycle

INTRODUCTION

The prognosis of chemoresistant acute myeloid leukemia (AML) remains poor due to the sustained proliferative capacity of leukemic cells (1–3). The dysregulated cell cycle could induce raised proliferation, which predisposes leukemic cells to gain mutations and may privilege chemoresistant leukemic transformation (4–6). Cell cycle-specific agent cytarabine (Ara-C) and cell cycle-nonspecific

agents anthracycline chemotherapeutics are the standard treatment of AML in both induction and consolidation therapies, but still a proportion of patients present intrinsic or acquired chemotherapy resistance (7, 8). Thus, there is an urgent need for new targets and therapeutic approaches to treat chemoresistant AML. Cell cycle checkpoint, including microtubules, is critical in the maintenance of a continuous cell cycle. Targeting cell cycle checkpoints has showed promising results in preclinical models and provides a potential combination therapy for AML patients (3, 5, 9).

Centromere protein E (CENPE), a microtubule kinesin, localizes to unlinked kinesins during mitosis and slides monomeric chromosomes toward the spindle equator using end-directed microtubule movement (10). The upregulated CENPE has been found to be involved in the tumorigenesis of breast cancer, prostate cancer, neuroblastoma, etc., and CENPE deletion could lead to the apoptosis of tumor cells (11–14). A most recent study demonstrated that in medulloblastoma cells, CENPE depletion triggered the endogenous DNA damaging, which activated TP53 or TP73 and cell death signaling pathways (15). In a research of 1,195 non-small cell lung cancer (NSCLC) patients' samples, CENPE was revealed to be highly expressed and patients with strong CENPE expression had a relatively low overall survival rate (16). In prostate cancer, CENPE expression could be activated by LSD through binding to the promoter region (13). To understand the mechanism of CENPE depletion in tumor cell growth, an *in vitro* study has further identified that the overexpressed FOXM1 could facilitate CENPE expression and lung cancer cell proliferation by specifically binding to the CENPE promoter region (17).

In leukemia, attention has already been devoted to antimitotic agents. For example, in HL-60 cells, the antimitotic agent HKL-1 was found to evoke mitotic catastrophes by downregulating the mitotic stage-specific kinase CENPE and downregulating Bcl-2 (18). Moreover, an anti-mitogenic agent GSK923295A, capable of inhibiting CENPE motility activity, exhibited substantial remission-inducing antileukemia activities towards acute lymphoblastic leukemia (ALL) xenografts (19). In 38,410 cells from aspirates of AML patients and healthy volunteers, single-cell RNA-seq and genotyping were performed and CENPE was found to be related to minimal residual diseases (MRD) >2-fold standard deviation of all residuals (20). However, the mechanism of CENPE in AML progression and chemoresistance is rarely studied.

RNA binding proteins (RBPs) are key modulators of cancers and mRNAs (21, 22). Previous studies have explored the effect and molecular mechanisms of the RBPs LIN28A in the development of various tumors and revealed the underlying role of LIN28A on cell cycle-related mRNAs (23–26). Lin28 has been found to enhance the growth of dental pulp cells by upregulating the cyclin-dependent proteins and by interacting with the let-7a/IGF2BP2 pathway (23). In epithelial tumors, LIN28A promoted cell cycle procession by moderating the expression of CDK2, Cyclin D1, and CDC25A (26). Highly expressed LIN28A can serve as a potential oncogenic factor that contributes to the tumorigenesis, development, and migration of ovarian, breast, liver, and colon cancers (27–33). Mechanism-wise, LIN28A can modulate the translation of its targeted mRNA and restrain let-7 expression in the posttranscriptional level, which both depend on the LIN28A protein's RNA-binding motif (34–42). For example, in a study on colorectal cancer, LIN28A was found to promote the development and progression of disease by regulating the expression of the mRNA GEFT (38). Moreover, LIN28A has been confirmed to have the capacity to stabilize and modulate the expression of various mRNAs, including YB-packaged mRNA, RAN, and HSBP1 mRNA in tumors (40–42). More interestingly, it has been shown that LIN28A participated in regulating the differentiation and cell cycle progression of AML cells (43). However, the mechanism of LIN28A in AML progression and chemoresistance is not definitively understood.

In our study, we found that CENPE was overexpressed in patients with chemoresistant AML. Furthermore, Lin28A was found to be remarkably correlated with CENPE expression in chemoresistance AML. Knockdown of CENPE expression led to the suppression of growth of myeloid leukemia cells and reversal of Ara-C chemoresistance. Overexpression of LIN28A promoted the growth and Ara-C of leukemic cells by specifically binding to the promoter region GGAGA of CENPE, while knockdown of CENPE reverted this influence. Our findings indicated that Lin28A may have a pivotal role in AML tumorigenesis and chemoresistance by modulating CENPE, and that targeting Lin28A/CENPE could be a potential effective treatment or combined chemotherapy regimen for chemoresistant AML patients.

MATERIALS AND METHODS

Clinical Samples

Peripheral blood samples of three refractory/relapsed AML patients (R/R-AML, relapsed/refractory AML patients who failed to achieve complete remission/CR after two courses of induction chemotherapy), three refractory secondary AML patients (S-AML-, MDS-, or MPN-derived AML patients did not reach CR after two rounds of induction chemotherapy), four *de novo* AML patients (AML, CR after standard "3+7" induction chemotherapy), and three healthy controls (HC) were collected in Henan Provincial People's Hospital. Permission of this study was obtained from the Ethics Committee of Henan Provincial People's Hospital, and written informative consent was granted to all subjects.

Cell Separation and RNA Extraction

Peripheral blood mononuclear cells (PBMCs) from all individuals were collected and separated by density centrifugation (Ficoll-Hypaque). All specimens were obtained from EDTA peripheral blood in 4 h and then preserved at −80°C. Total PBMC RNA was obtained by TRIzol reagent (ThermoFisher Scientific) following directions of the manufacturer. Add 0.5 ml of Trizol, RT 2–3 min. Add 0.25 ml of chloroform and shake vigorously for 20–30 s, RT 2–3 min.

Then, centrifuge for 10 min at 12,000 rpm at 4°C. Carefully transfer the supernatant to another tube, add 0.5 ml of isopropanol, mix, and put in RT 10 min. Then, centrifuge for 10 min at 4°C at 12,000 rpm. Wash with 70% EtOH and air-dry the pellet. Using 50 μl of DEPC-H_2O, dissolve the pellet. Measure OD260. Store at −80°C.

RNA-seq and Bioinformatic Analysis

Nanodrop was applied to quantify the total RNA samples. Illumina kits were used to prepare the RNA-seq library. Ultimately, after quantifying and qualifying the RNA-seq libraries, the sequencing is detected by Illumina Hiseq 4000. Differentially expressed genes (DEGs) were screened for adjusted $p < 0.05$ and fold change ≥2. DEGs between each of the two groups were presented by scatter plot, volcano plot, and hierarchical clustering. To discover the potential underlying biological procedures and pathways in R/R-AML, S-AML, and *de novo* AML, we conducted GO and KEGG pathway analysis.

Downloaded TCGA and GEO RNA-seq Data

Whole blood RNA-seq dataset of Recurrence-AML (R-AML) was downloaded from TCGA (151 cases) and primary AML dataset was downloaded from GEO (7 cases). The DEGs between R-AML and primary AML samples were identified based on screening criteria: $|\log2FC| \geq 1$ and $p \leq 0.05$. The clinical data of R-AML patients from TCGA were extracted. The expression profiles of CENPE were extracted and compared in R-AML and primary AML groups. X-tile software was used to calculate the cutoff values of CENPE in R-AML patients, and survival analysis was conducted in R-AML patients with CENPE high expression and R-AML patients with CENPE low expression.

Cell Culture and Transfection

K562 and THP-1 cell lines were obtained from the American Type Culture Collection (ATCC). Cells were incubated in RPMI 1640 media (Sigma Aldrich, USA) with 1% penicillin/streptomycin (37°C, 5% CO_2) and 10% fetal bovine serum (Gibco, USA). 293T cells were cultivated in DMEM media (Sigma Aldrich, USA). Search the gene sequences of CENPE on the NCBI GENE bank database, and design RNA interference sequences according to the design principles. Small interference RNA (siRNA)-directed CENPE and the negative control (NC) were made by Wuzhou Kangjian Biological Technology Co., Ltd. (Tianjin, China). The LIN28A expression plasmid and NC plasmid were purchased from Wuhan GeneCreate Biological Engineering Co., Ltd. (Wuhan, China) and transfected into K562 and THP-1 cells. Transfections were carried out in six-well plates applying Lipofectamine 3000 (Thermo Fisher Scientific, Inc.). The sequences of the siRNAs are as follows: CENPE#1: AGG CTACAATGGTACTATATT, CENPE#2: CCAAAGATTCA GCACTACTAA, Lin28A#1: CTTTCGAGAGGAAGAAGA AGA, Lin28A#2: GAGTAAGCTGCACATGGAAGG.

Cell Proliferative Ability Analysis

Use Cell Counting Kit-8 (CCK-8, Solarbio) to observe the *in vitro* cell proliferation after transfection. In the CCK8 assay, 12 h post-transfection, 100 μl of cell suspension (about 5,000 cells/well) was transferred into a 96-well plate and then cultured at 37°C, in 5% CO_2. Add to each well of the plate 10 μl of CCK-8 solution. Incubate the plate for 1–4 h. Thereafter, the absorbance was evaluated at 450 nm (OD450) using an automatic microplate reader. The experiment was performed at 12 h, 24 h, 48 h, and 72 h to create a cell growth curve.

Actinomycin D Assay to Analyze mRNA Stability

Actinomycin D (ActD) was added to si-NC or si-LIN28A transfected K562 and THP-1 cells 48 h after transfection. CENPE mRNA expression was measured by RT-qPCR after 0, 2, 4, and 6 h of ActD treatment.

Drug Treatment and IC50 Calculation

IC50 value is the drug concentration value corresponding to the cell survival rate of 50%. IC50 values were examined by the CCK-8 assay (Solarbio). To calculate K562 and THP-1 IC50 values, cells were treated with Ara-C at concentrations of 0.125 μM, 0.25 μM, 0.5 μM, 1 μM, 2 μM, 4 μM, and 8 μM at 37°C with 5% CO_2. After 48 h, under light-proof conditions, 10 μl of CCK-8 solvent was pipetted to every well and placed at 37°C for 2 h. The absorbance was evaluated at OD450. Calculate the cell survival rates.

Cell Apoptosis Analysis

Cells were treated either with or not with Ara-C for 48 h before collection, the cell culture supernatant was discarded, and then the cells were collected. The cells were washed twice with the phosphate buffered saline (PBS, Servicebio) and 500 μl of 1× binding buffer was added. Continue to add 5 μl each of Annexin V-FITC and PI staining solution (Solarbio) to the tube, incubate for 15 min in the dark (room temperature), and detect apoptosis by flow cytometry within 1 h.

Cell Cycle Analysis

Cells were starved before transfection for 24 h and confirmed that most of the cells were in G0/G1 phase. Afterwards, cells were transfected with si-NC or si-CENPE, and the effect of CENPE interference on cell cycle was examined 48 h later. Wash the cells twice with PBS solution, centrifuge them, and discard the supernatant. Add 70% alcohol (pre-cooled) to 2 ml of the EP tube and centrifuge at 4°C for 30 min. The cells were collected, washed once with PBS, and centrifuged; RNase A was added; and the mixture was incubated 30 min at 37°C and then centrifuged. Continue to add 5 μg/ml of PI staining solution (Solarbio, China), place at room temperature in the dark for 15 min, and detect the cell cycle using flow cytometry.

RT-PCR Measurement

K562 and THP-1 cell lines with or without targeted genes knocked down were collected to extracted total RNA. cDNA was synthesized applying a Bio-Rad iScript cDNA Synthesis Kit. RT-PCR was conducted with SYBR Green reaction system (12 μl). PCR primers were synthesized by Wuhan GeneCreate Biological Engineering Co., Ltd. Transfer the diluted (20 μl

cDNA + 280 μl ddH2O) cDNA to an 8-strip PCR tube. Use an electric multi-channel pipette to transfer to a 384-well plate (three replicates for each test sample). Mix 2×SYBR Green Mix (ThermoFisher Scientific, USA) with primers. Centrifuge the sealing plate and test on the machine. The qPCR process is done on a CFX96 real-time system. The relative levels of mRNAs were measured using the $2^{-\Delta\Delta Cq}$ method. The sequences were as follows: CENPE: Forward GATGACC TAGCAACTACACAGTC, Reverse AAAG CACCCAAACTCGAATCA; LIN28A: Forward GGT GGACGTCTTTGTGCACCAGAG, Reverse CGCTCACT CCCAATACAGAACACAC; β-actin: Forward ACCAAC TGGGACGACATGGAG, Reverse GTGAGGATCTTC ATGAGGTAGTC.

Western Blot Analysis

Collect 1×10^6 each of K562 and THP-1 cells, wash the cells three times, then add RIPA protein lysis solution, and place on ice to lyse for 10 min. Take a small amount of protein solution for BCA protein concentration assay (Sangon Biotech, Shanghai, China). Subsequently, 50 μg of protein samples was added to the loading wells of each lane in an SDS-PAGE gel; after electrophoresis at 70 V for 25 min, switch to 120 V and continue electrophoresis for 1 h. The proteins were then moved to PVDF membranes. Block the membranes with 5% BSA (Solarbio) at room temperature for 2 h. Wash with TBST solution and add primary antibodies (anti-CENPE, anti-LIN28A, and anti-β-actin), and then incubate at 4°C overnight. Wash the PVDF membranes and then place in HRP-labeled secondary antibodies for 1.5 h, at 37°C. After sufficient washing with TBST solution, ECL chemiluminescence was performed and protein levels were analyzed.

RIP-qPCR to Identify the Targeting Relationship Between LIN28A and CENPE

After 48 h transfection of LIN28A and si-CENPE, the K562 cells were collected, lysed, and stored at −80°C. In transfected (after 48 h) or un-transfected K562 cells, RIP Kit (Millipore) with IgG (Abcam, Cambridge, MA, USA) or LIN28A antibody (Abcam) was used to assess the binding potential of LIN28A to CENPE. The level of CENPE mRNA that was enriched by IgG or LIN28A antibodies was measured by RT-qPCR.

RNA Pull-Down

The interaction between CENPE mRNA 3'UTR and LIN28A protein was analyzed using the RNA Pull-Down kit (Thermo Scientific). Lyse the cells with IP Lysis Buffer. Biotin-labeled CENPE mRNA 3'UTR probes for the sense or antisense strands of LIN28A were prepared. RNA pull-down experiments were performed in the whole cell lysates of K562 cells with a magnetic RNA pull-down kit. LIN28A protein levels that were pulled down by biotin-labeled transcripts were detected by Western blot.

Dual Luciferase Report Analysis

The wild-type CENPE (CENPE Wt) 3'UTR sequence containing a LIN28A binding site was constructed onto the pGL3-Basic vector to build the CENPE Wt reporter vector. The CENPE 3'UTR and LIN28A binding site in CENPE Wt was mutated to construct the CENPE mutation (CENPE Mut) reporter vector. The LIN28A overexpression plasmid (LIN28A) and empty plasmid (Vector) were provided by Wuhan GeneCreate Biological Engineering Co., Ltd. In K562 cells, CENPE Wt and CENPE Mut were transfected with the groups of CENPE Wt+ Vector, CENPE Wt+LIN28A, CENPE Mut+Vector, and CENPE Mut+LIN28A, respectively. After 48 h of cell transfection, the change of luciferase activity was detected by luciferase activity assay kit (Promega).

Statistical Analysis

All experiments were independently repeated three times. Differences between two groups were analyzed by *t*-test, and one-way ANOVA was applied to analyze differences between multiple groups. Experimental data were analyzed using GraphPad prism 7.0 software and shown in Mean ± SEM. Pearson correlation analysis was performed to analyze correlations, and $p < 0.05$ was thought as a significant difference (SPSS22.0).

RESULTS

Mitosis Cell Cycle-Related Gene CENPE Was Upregulated in Chemoresistance AML Patients

In the present study, RNA-seq results indicated that 1,017 genes (303 upregulated and 714 downregulated) were observed in patients with *de novo* AML in comparison to HC (**Figure 1A**). A total of 329 DEGs were acquired (202 upregulated and 127 downregulated) in chemoresistance S-AML patients compared with *de novo* AML patients (**Figure 1D**). Among S-AML samples and *de novo* AML samples, Gene Set Enrichment Analysis (GSEA) enrichment plots of DEGs of GO biological processes were predominantly engaged in mitotic spindle organization (GO:0007052) and regulation of mitotic metaphase/anaphase transition (GO:0030071) (**Figures 1B, E**). CENPE gene was in the top five upregulated DEGs (**Figures 1B, E**). In the KEGG Pathway profiling, the majority of the upregulated DEGs were as well enriched in the cell cycle pathway (hsa04110) (**Figures 1C, F**). Moreover, as to identify our hypothesis, the DEGs between R-AML from TCGA and primary AML from GEO were analyzed. When $|\log2FC| \geq 1$ and $p \leq 0.05$, a total of 7,957 DEGs were identified (5,964 upregulated and 1,993 downregulated) (**Figure 1G**). In order to identify the key upregulated genes in chemoresistance AML, we performed a Venn diagram analysis of the upregulated DEGs among R/R-AML, S-AML, R-AML, and primary/*de novo* AML patients, and the result revealed a total of 12 overlapping genes: CENPE, ASPM, CENPF, DLGAP5, KIF15, HMMR, BUB1B, KIF11, CEP55, NCAPG2, CCNB2, and CDCA8 (**Figure 1H**). The 12 upregulated genes were all upregulated in AML patients with relapsed and chemoresistance disease. Among the 12 overlapping genes, the *p*-value and log2 fold change of CENPE

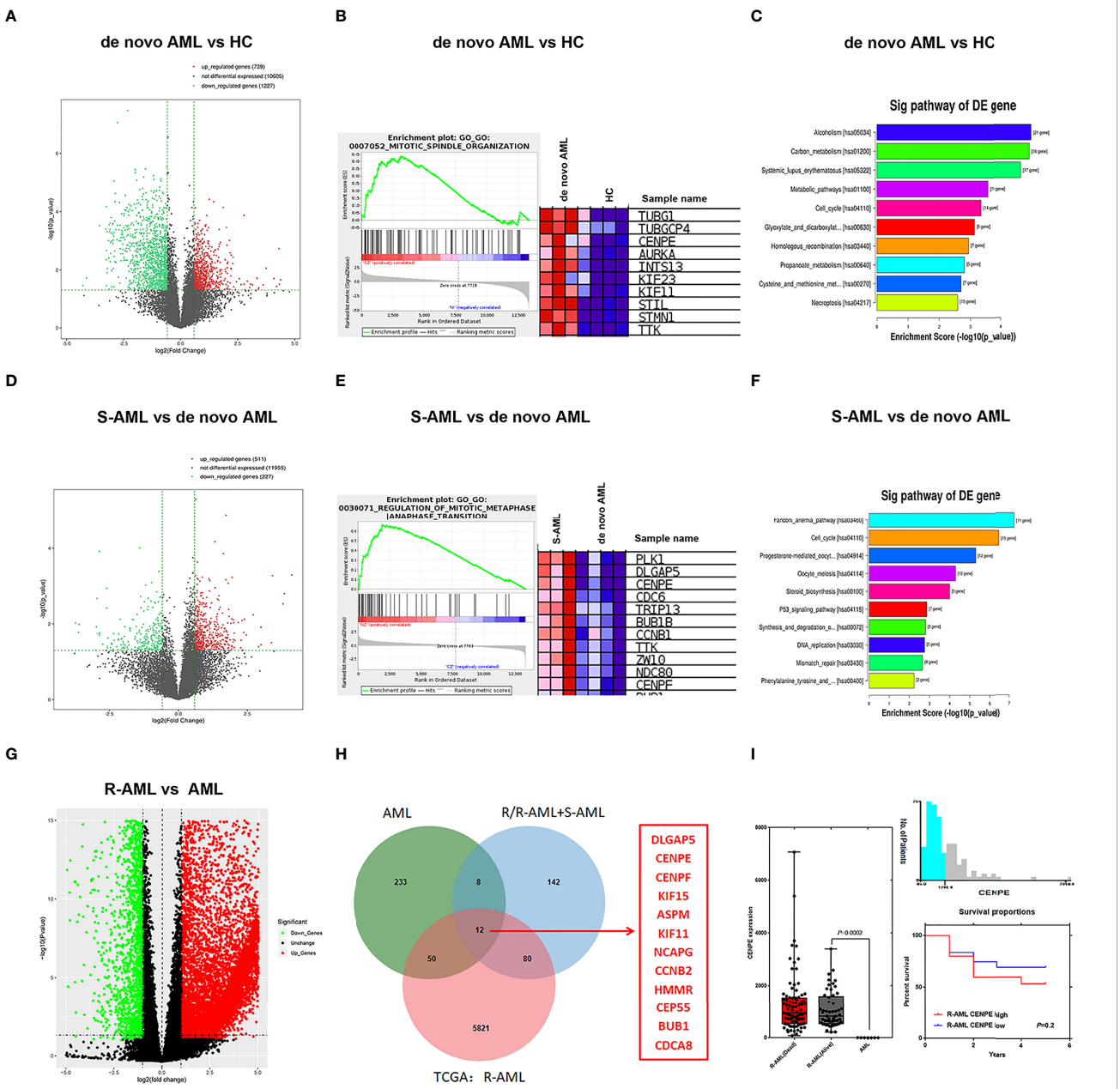

FIGURE 1 | Mitosis-related gene CENPE was highly expressed in chemoresistance AML patients. **(A)** DEGs in *de novo* AML patients compared with HC. **(B)** GSEA enrichment plots of DEGs of GO biological processes were predominantly engaged in mitotic spindle organization (GO:0007052) in *de novo* AML patients compared with HC. **(C)** Upregulated DEGs enriched KEGG pathways in *de novo* AML patients compared with HC. **(D)** DEGs in S-AML versus *de novo* AML patients. **(E)** GSEA enrichment plots of DEGs of GO biological processes were predominantly engaged in regulation of mitotic metaphase/anaphase transition (GO:0030071) in S-AML versus *de novo* AML patients. **(F)** Upregulated DEGs enriched KEGG pathways in S-AML versus *de novo* AML patients. **(G)** The DEGs in R-AML from TCGA versus primary AML from GEO. **(H)** Twelve targeted upregulated DEGs among R/R-AML, S-AML, R-AML, and primary/*de novo* AML patients. **(I)** CENPE in R-AML was significantly higher than that of primary AML patients. X-tile software calculated the cutoff values of CENPE in R-AML patients, and survival analysis was conducted in R-AML patients with CENPE high expression and R-AML patients with CENPE low expression.

were the most significant (**Table 1**). Combined with the GSEA analysis results of DEGs in AML patients, we selected CENPE, which was enriched in the mitotic spindle organization (GO:0007052) and regulation of mitotic metaphase/anaphase transition (GO:0030071) (**Figures 1B, E**) for further study (**Figure 1E**). Moreover, we found that CENPE expression was considerably increased in R-AML compared to primary AML (**Figure 1I**). It is worth noting that the expression of CENPE in the R-AML patients ended with dead was slightly higher than that in the alive patients (**Figure 1I**). We applied X-tile software

TABLE 1 | The expression profiles of 12 upregulated overlapping genes in AML samples.

	baseMean	log2FoldChange	lfcSE	stat	pvalue	padj
CENPE	1049.802	5.191935	0.425723	12.19556	3.28E-34	1.88E-32
ASPM	1919.416	4.978494	0.427757	11.6386	2.62E-31	1.26E-29
CENPF	3083.29	4.450087	0.375638	11.84674	2.24E-32	1.16E-30
DLGAP5	570.4089	2.538413	0.434018	5.848632	4.96E-09	2.46E-08
KIF15	746.446	2.504048	0.361179	6.932982	4.12E-12	3.11E-11
HMMR	660.9024	2.39525	0.401993	5.958438	2.55E-09	1.32E-08
BUB1B	1155.31	2.240073	0.306405	7.310828	2.66E-13	2.33E-12
KIF11	1913.824	1.412275	0.27741	5.090932	3.56E-07	1.35E-06
CEP55	482.5731	1.334555	0.403412	3.308172	0.000939	0.001988
NCAPG2	1700.24	1.326956	0.272845	4.863398	1.15E-06	4.02E-06
CCNB2	795.6173	1.318156	0.33368	3.950366	7.80E-05	0.0002
CDCA8	692.7212	1.238473	0.308255	4.017694	5.88E-05	0.000154

to calculate the cutoff values of CENPE in R-AML patients and divided R-AML patients into a CENPE high-expression group and a CENPE low-expression group according to the cutoff values. Although a relatively shorter survival time could be seen in the CENPE high-expression group, however, the difference between the two groups was not statistically significant (**Figure 1I**).

Effect of CENPE Interference on Cell Cycle, Cell Apoptosis, and Ara-C Drug Sensitivity

To further explore the functional role of CENPE in AML progression and chemoresistance, we have designed and synthesized siRNAs against CENPE (si-CENPE) and NC siRNAs (si-NC). The knockdown efficiency was analyzed and showed that si-CENPE transfection resulted in markedly reduced CENPE expression in K562 and THP-1 cells when compared with the si-NC (**Figures 2A, B**). Cell proliferation activities of K562 and THP-1 cells were analyzed by CCK-8 assay. The results showed that transfection with si-CENPE significantly inhibited K562 and THP-1 cell activities ($p < 0.05$, **Figures 2C, D**). The apoptosis of K562 and THP-1 cells after CENPE interference was analyzed by flow cytometry. The results demonstrated that CENPE interference increased the incidence of apoptosis in K562 and THP-1 cells (**Figures 3A, B**). Also, cell cycles were analyzed by PI single-staining method. The results revealed that si-CENPE transfection induced G1 phase block and reduced the number of cells of G2/M phase in K562 and THP-1 cells compared to the si-NC group (**Figures 3C, D**). Western blot was used to analyze the expression of cycle-associated proteins Cyclin B1 and p21. Compared with the si-NC group, CENPE knockdown suppressed Cyclin B1 expression and promoted p21 expression in K562 and THP-1 cells (**Figures 3E, F**), indicating that CENPE interference caused arrest and hindered the progression of the cell cycle. Moreover, Ara-C drug sensitivity after CENPE interference was detected. Following the treatment of Ara-C with different concentrations, the IC50 values were measured and analyzed by the CCK-8 method. The results showed that si-CENPE transfection reduced the IC50 values of K562 and THP-1 cells and led to enhanced sensitivity of Ara-C compared to the si-NC group (**Figures 4A, B**). In conclusion, the proliferation of myeloid leukemia cells was inhibited and chemoresistance was reversed after knocking down the expression of CENPE.

CENPE Expression Was Highly Correlated With RBP LIN28A

Starbase database was used to predict the RBPs, which might bind to CENPE. Combined with the DEGs screened by TCGA R-AML patients, 25 RBPs that were differentially expressed in R-AML and might interact with CENPE were screened (**Figure 5A** and **Table 2**). The correlation between the expression of each of the above RBPs in AML and CENPE expression was analyzed using the GEPIA database (**Table 2**). LIN28A was among the top five RBPs that most correlated with CENPE in AML. CENPE expression was shown to be highly correlated with RBP LIN28A ($r = 0.24$; $p < 0.05$) (**Figure 5B**). Taking into consideration the crucial modulatory effects of LIN28A in oncogenes and mRNAs and the potential roles of LIN28A on cell cycle-related genes. LIN28A was selected for further study. LIN28A gene expression levels were analyzed in the 151 R-AML whole blood samples from the TCGA database and 7 primary AML samples from the GEO database. Our preliminary analysis revealed that the expression of LIN28A was dramatically increased in R-AML patients when compared with primary AML patients ($p < 0.05$, **Figure 5C**), which means patients with high expression of LIN28A are more likely to relapse. Therefore, we further explored the modulatory role of LIN28A on CENPE.

LIN28A Effected CENPE Expression and mRNA Stability

Analysis of transfection efficiency revealed that the si-LIN28A group led to a significant downregulation of LIN28A levels in K562 and THP-1 cells compared to the si-NC group (**Figures 6A, B**). RT-qPCR and Western blot assays further showed that knockdown of LIN28A suppressed the CENPE mRNA and protein production in K562 and THP-1 cells (**Figures 6C, D**). The influence of the LIN28A deletion on the stability of CENPE mRNA was investigated by ActD assays. At the same time after ActD treatment, the half-lives of CENPE mRNA were dramatically shortened in K562 and THP-1 cells that were transfected with si-LIN28A in

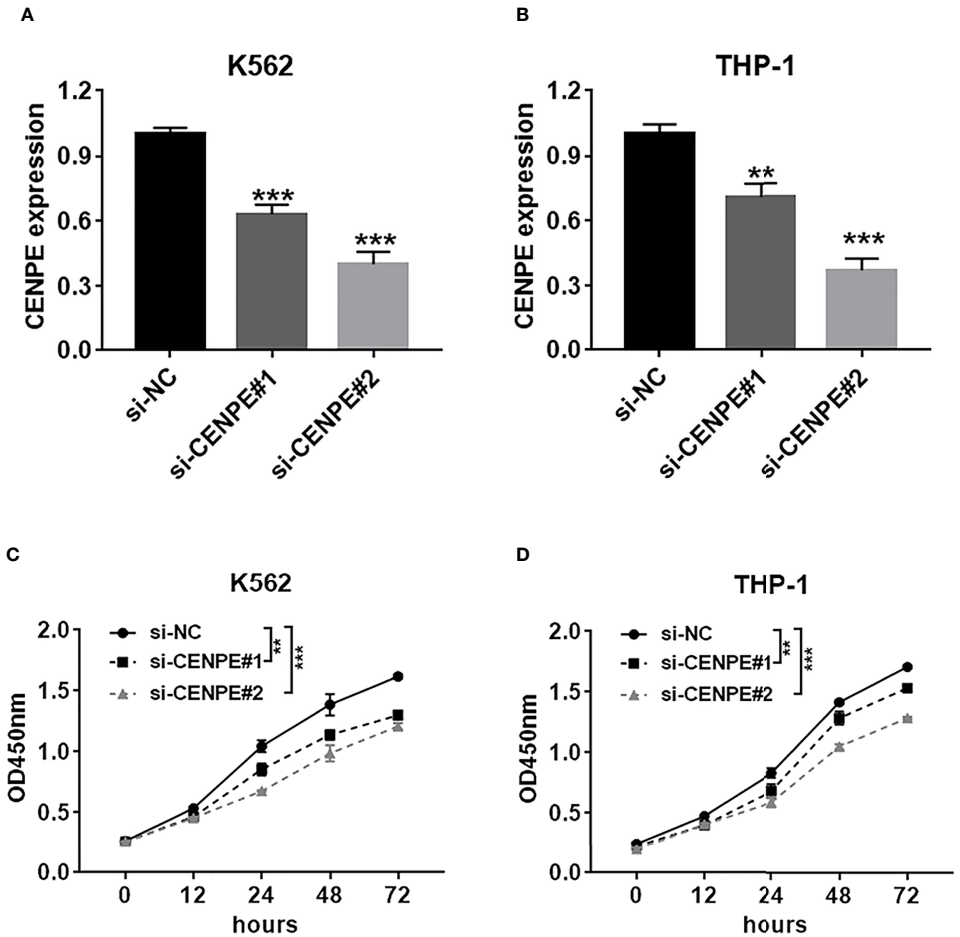

FIGURE 2 | CENPE interference inhibited K562 and THP-1 cell proliferation. **(A, B)** K562 and THP-1 cells were transfected with si-NC, si-CENPE#1, or si-CENPE#2. Knockdown efficiency of CENPE in K562 and THP-1 cells was measured by RT-qPCR. **(C, D)** Cell proliferation was evaluated by CCK-8 assay, and si-CENPE significantly inhibited K562 and THP-1 cell activities compared with the si-NC group. $^{**}p < 0.01$. $^{***}p < 0.001$.

comparison with the si-NC group (**Figures 6E, F**). It indicated that LIN28A interference reduced CENPE mRNA stability. In conclusion, LIN28A inhibited the CENPE mRNA and protein production, and reduced CENPE mRNA stability in myeloid leukemia cells.

LIN28A Interacted With CENPE by Binding to the 3'UTR Region

The binding capacity was investigated between LIN28A and CENPE mRNA by RIP assay. The results indicated that LIN28A antibody was able to enrich a significant amount of CENPE in K562 cells compared to the IgG group ($p < 0.05$, **Figure 7A**). Predictive analysis showed the existence of a GGAGA motif that bound to LIN28A in the CENPE 3'UTR; therefore, we hypothesized that LIN28A might impact the stability of CENPE by interacting with the CENPE 3'UTR GGAGA motif. The CENPE 3'UTR was obtained by *in vitro* transcription and labeled with a biotin synthetic probe, and we also analyzed the interaction of LIN28A with the CENPE 3'UTR by RNA pull-down assay and luciferase assay. RNA pull-down and Western blot analyses indicated that in K562 cells, LIN28A could be markedly enriched with biotinylated sense CENPE 3'UTR, whereas it could not be enriched with biotinylated antisense CENPE 3'UTR (**Figure 7B**). The LIN28A mRNA and protein levels were obviously increased in LIN28A-transfected K562 cells when compared to the Vector group ($p < 0.05$, **Figure 7C**). It indicated that the overexpression plasmid of LIN28A had a good overexpression efficiency. Wild-type (Wt) and mutant (Mut) luciferase plasmids of 100 bp upstream and downstream of the CENPE 3'UTR binding site were constructed, and CENPE Wt and CENPE Mut were transfected into K562 cells, including CENPE Wt+Vector, CENPE Wt+LIN28A, CENPE Mut +Vector, and CENPE Mut+LIN28A. Forty-eight hours after transfection, the change of luciferase activity was measured by the luciferase activity assay kit. The results revealed that the luciferase activity was remarkably stronger in the Wt group after LIN28A overexpression when compared to the Wt+Vector group ($p < 0.05$, **Figure 7C**). However, the promotion effect of

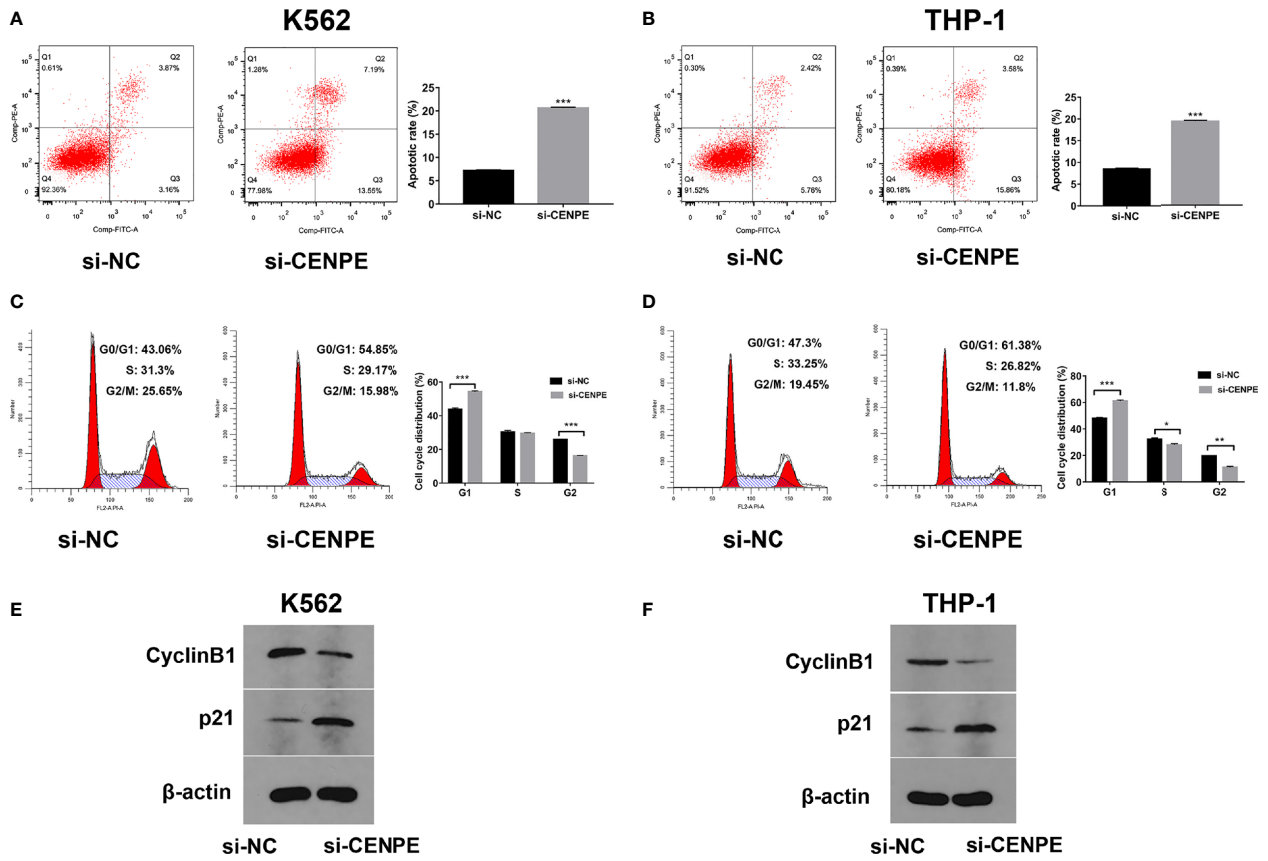

FIGURE 3 | CENPE interference effected K562 and THP-1 cell apoptosis and cell cycle and drug resistance. **(A, B)** After 48 h of transfection, cell apoptosis was measured by flow cytometry. The cell apoptotic rates between si-NC and si-CENPE groups were analyzed in K562 and THP-1 cells. **(C, D)** After 48 h of transfection, cell cycle was measured by PI single-staining method. **(E, F)** After 48 h, Western blot analyzed the expression of cycle-related proteins Cyclin B1 and p21 in K562 and THP-1 cells. $^{*}p < 0.05$. $^{**}p < 0.01$. $^{***}p < 0.001$.

LIN28A on luciferase activity in the Wt group disappeared after CENPE 3'UTR mutation (**Figure 7D**). This suggested that LIN28A can target binding to the GGAGA site of the CENPE 3'UTR.

Interaction of LIN28A and CENPE Effected AML Cell Proliferation, Apoptosis, Cell Cycle, and Ara-C Resistance

After LIN28A was overexpressed, the CCK-8 results revealed a significantly increased proliferation rate in K562 and THP-1 cells ($p < 0.05$, **Figures 8A, C**). The effect of CENPE interference on cell proliferation regulated by LIN28A overexpression was further analyzed. The results showed that compared with LIN28A overexpression plus si-NC group (LIN28A+si-NC), CENPE interference reversed the proliferation of K562 and THP-1 cells promoted by LIN28A overexpression ($p < 0.05$, **Figures 8A, C**). This indicated that LIN28A promoted AML cell proliferation, and CENPE interference diminished the pro-proliferative effect of LIN28A. LIN28A overexpression reduced the apoptosis rate of K562 and THP-1 cells compared with Vector (**Figures 8B, D**). Furthermore, LIN28A overexpression inhibited AML cell apoptosis, and compared with the LIN28A overexpression plus si-NC group, CENPE interference reversed the apoptosis-inhibiting ability of LIN28A overexpression (**Figures 8B, D**). In K562 and THP-1, LIN28A overexpression triggered cell cycle progression to the G2/M phase compared to the Vector group (**Figures 9A, B**). Compared with the LIN28A overexpression plus si-NC group, CENPE interference reversed the promotive effect of LIN28A overexpression on K562 and THP-1 cell cycles (**Figures 9A, B**). LIN28A overexpression induced Cyclin B1 expression and inhibited p21 expression in K562 and THP-1 cells in comparison with the Vector group (**Figures 9C, D**). Compared with the LIN28A overexpression plus si-NC group, CENPE interference reversed the regulation of Cyclin B1 and p21 expression by LIN28A overexpression (**Figures 9C, D**). Moreover, Ara-C drug sensitivity after LIN28A overexpression and CENPE interference was detected. Following the treatment of Ara-C with concentrations of 0.125 μM, 0.25 μM, 0.5 μM, 1 μM, 2 μM, 4 μM, and 8 μM in K562 and THP-1 cells, the IC50 values were measured and analyzed by the CCK-8 method. The results showed that LIN28A overexpression increased IC50 values compared to the Vector group in K562

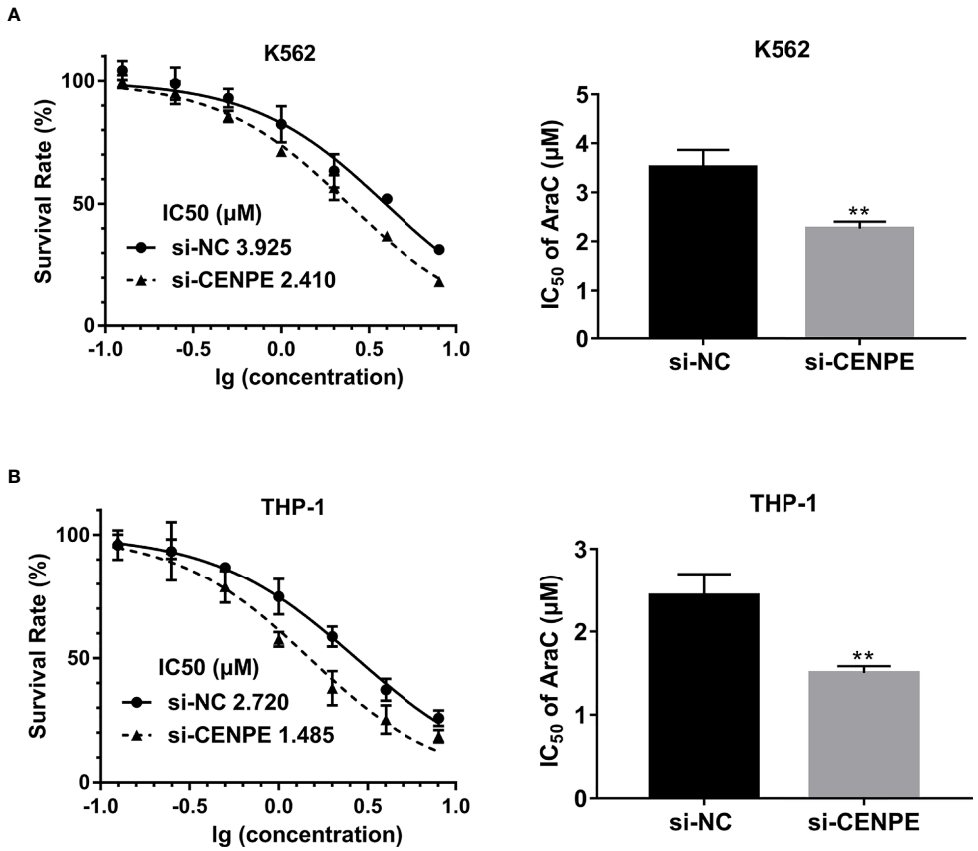

FIGURE 4 | CENPE interference effected Ara-C resistance in K562 and THP-1 cells. **(A, B)** K562 and THP-1 cells were treated with ascending concentrations of Ara-C (0.125 μM, 0.25 μM, 0.5 μM, 1 μM, 2 μM, 4 μM, and 8 μM). After 48 h, IC50 values were measured and analyzed by the CCK-8 method. The experiment was independently repeated three times and statistical differences between the si-NC and si-CENPE groups were analyzed. $^{**}p < 0.01$.

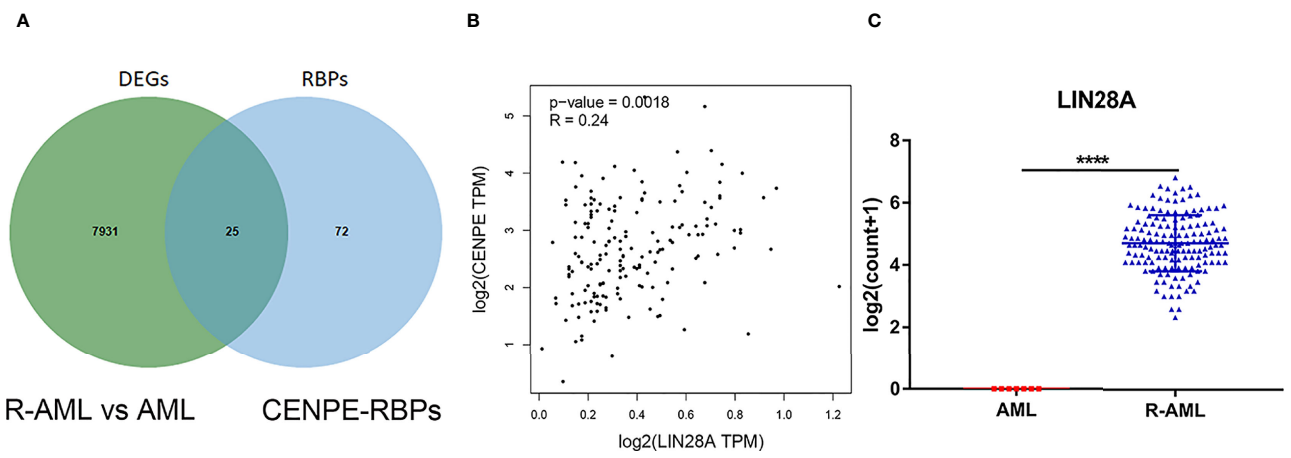

FIGURE 5 | CENPE expression was highly correlated with RBP LIN28A. **(A)** Starbase database was used to screen out 25 RBPs, which might bind to CENPE and were differentially expressed in R-AML. **(B)** CENPE expression was strongly related to RBP LIN28A ($r = 0.24$; $p < 0.05$). **(C)** LIN28A gene expression were higher in the 151 R-AML whole blood samples from the TCGA database versus 7 primary AML samples from the GEO database. $^{****}p < 0.0001$.

TABLE 2 | The correlation between CENPE and RBPs.

Gene	Correlation coefficient	*p*-value
VIM	–0.24	0.0016
LIN28A	0.24	0.0018
MSI1	0.22	0.0041
SLTM	0.17	0.026
FMR1	0.17	0.029
FBL	–0.16	0.038
ACIN1	–0.16	0.04
TARDBP	0.15	0.047
SRSF3	0.15	0.05
HNRNPK	0.15	0.054
HNRNPC	0.15	0.056
U2AF1	0.14	0.063
TNRC6A	0.12	0.11
NPM1	0.12	0.12
RBM5	–0.098	0.2
SRSF9	–0.098	0.2
HNRNPA1	0.091	0.23
CNBP	–0.065	0.4
LARP4B	0.065	0.4
EIF4A3	0.056	0.46
YWHAG	0.042	0.58
IGF2BP3	–0.019	0.8
SBDS	–0.0096	0.9
KHDRBS2	0.0032	0.97
KHDRBS3	–0.023	0.77

and THP-1 cells (**Figures 10A, B**). Compared with the LIN28A overexpression plus si-NC group, CENPE interference attenuated the IC50 values of cells increased by LIN28A overexpression (**Figures 10A, B**). In conclusion, LIN28A promoted AML cell cycle progression and inhibited AML cell apoptosis, and CENPE interference repressed the cell cycle progression-promoting effect of LIN28A and facilitated apoptosis in leukemic cells. Moreover, it indicated that LIN28A enhanced drug resistance of AML cells to Ara-C, but CENPE interference reversed LIN28A-regulated Ara-C resistance in leukemic cells.

DISCUSSION

The prognosis for AML patients remains poor, with a 5-year survival rate of <30%, even with novel therapeutic agents (8). AML is partially triggered by dysregulated cell proliferation, which involves cell cycle modulation and DNA reparation. One mechanism of chemoresistance is related to the recognition of DNA damage by cell cycle regulators (39). Hence, inhibition of cell cycle pathways can have a synergistic impact on chemotherapy (9, 44). Previous studies have shown that mitotic regulator inhibitors, such as balaceltib and polo-like kinase-1 (PLK1), are found to be effective in combination with

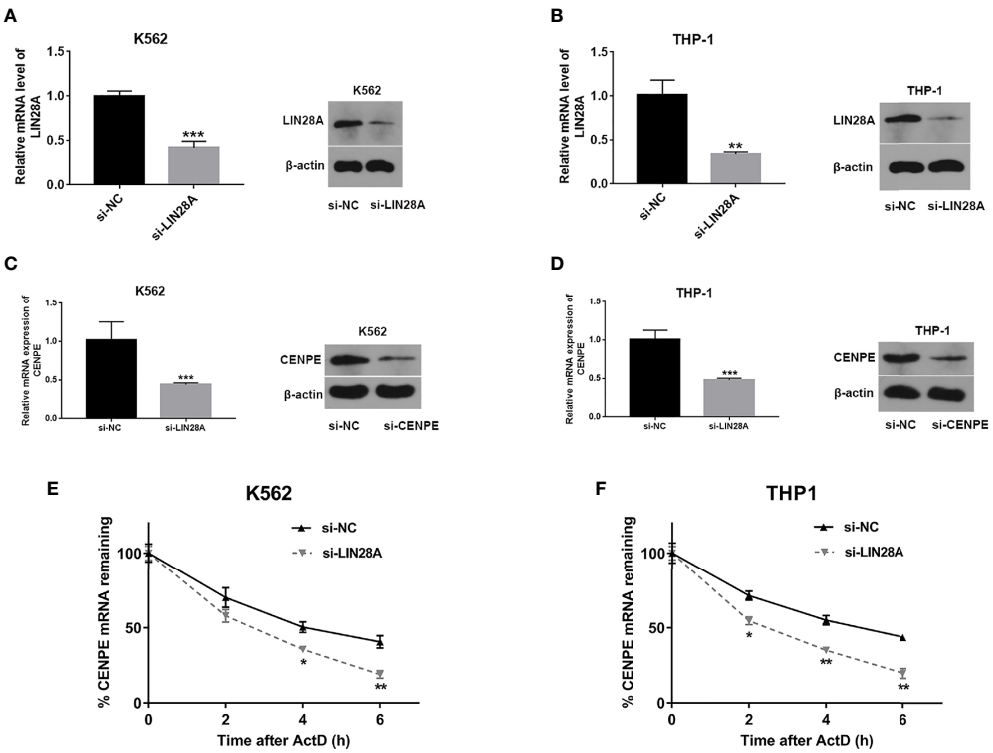

FIGURE 6 | LIN28A effected CENPE expression and mRNA stability. **(A, B)** Transfected K562 and THP-1 cells with si-NC or si-LIN28A, and LIN28A mRNA and protein were detected by RT-qPCR and Western blot 48 h after transfection. **(C, D)** Forty-eight hours after transfection of LIN28A in K562 and THP-1 cells, CENPE mRNA and protein were examined by RT-qPCR and Western blot. **(E, F)** The impact of the knockdown of LIN28A on the stability of CENPE mRNA was evaluated by the actinomycin D assay. *$p < 0.05$. **$p < 0.01$. ***$p < 0.001$.

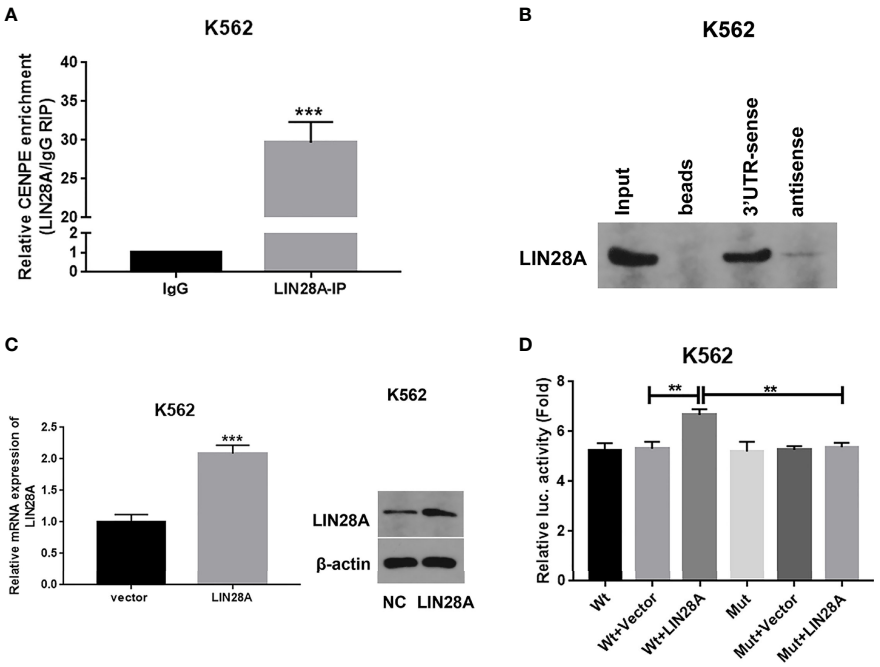

FIGURE 7 | LIN28A interacted with CENPE by binding to the 3'UTR region. **(A)** CENPE mRNA enriched by IgG or LIN28A antibodies in K562 cells were detected by RIP-conjugated RT-qPCR. **(B)** RNA pull-down and Western blot assays were conducted to detect the LIN28A protein levels being pulled down by biotin sense or antisense CENPE 3'UTR. **(C)** K562 cells were transfected with empty vector or LIN28A overexpression plasmid, and LIN28 expression was detected by RT-qPCR and Western blot. **(D)** The CENPE Wt and CENPE Mut were transfected in K562 cells, including CENPE Wt+Vector, CENPE Wt+LIN28A, CENPE Mut+Vector, and CENPE Mut+LIN28A, and 48 h after cell transfection, changes in luciferase activity were measured with a luciferase activity assay kit. $^{**}p < 0.01$. $^{***}p < 0.001$.

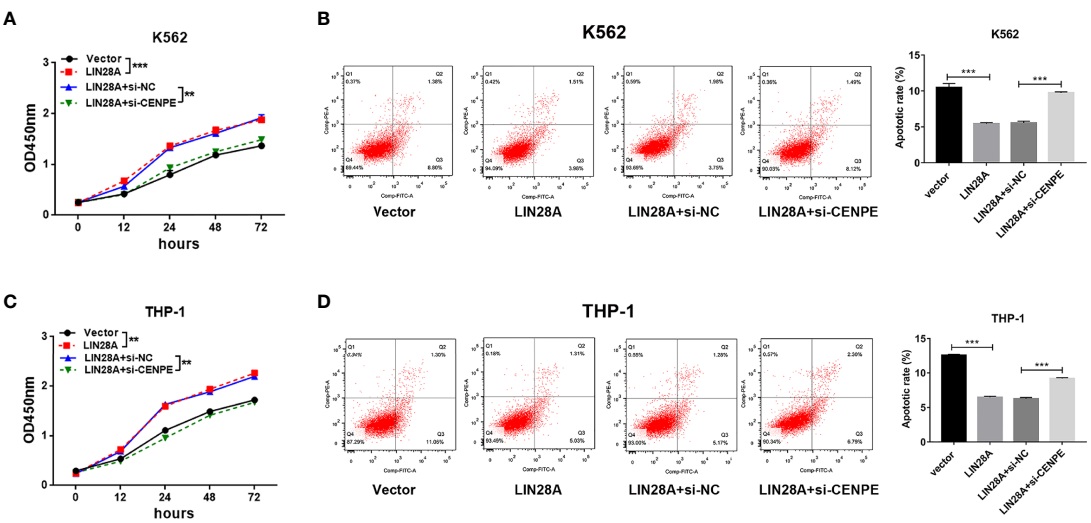

FIGURE 8 | Interaction of LIN28A and CENPE effected cell proliferation and apoptosis in K562 and THP-1 cells. **(A)** CCK8 assay was used to explore the effect of LIN28A overexpression and CENPE interference on cell proliferation regulated by LIN28A overexpression of K562 cells. **(B)** After 48 h of transfection, cell apoptosis was measured by Annexin V-FITC/PI double-staining method flow cytometry in LIN28A overexpressed and CENPE interfered LIN28A overexpressed K562 cells. The cell apoptotic rates were analyzed in K562 cells. **(C)** CCK8 assay was used to explore the effect of LIN28A overexpression and CENPE interference on cell proliferation regulated by LIN28A overexpression of THP-1 cells. **(D)** After 48 h of transfection, cell apoptosis was detected by Annexin V-FITC/PI double-staining method flow cytometry in LIN28A overexpressed and CENPE interfered LIN28A overexpressed THP-1 cells. The cell apoptotic rates were analyzed in THP-1 cells. $^{**}p < 0.01$. $^{***}p < 0.001$.

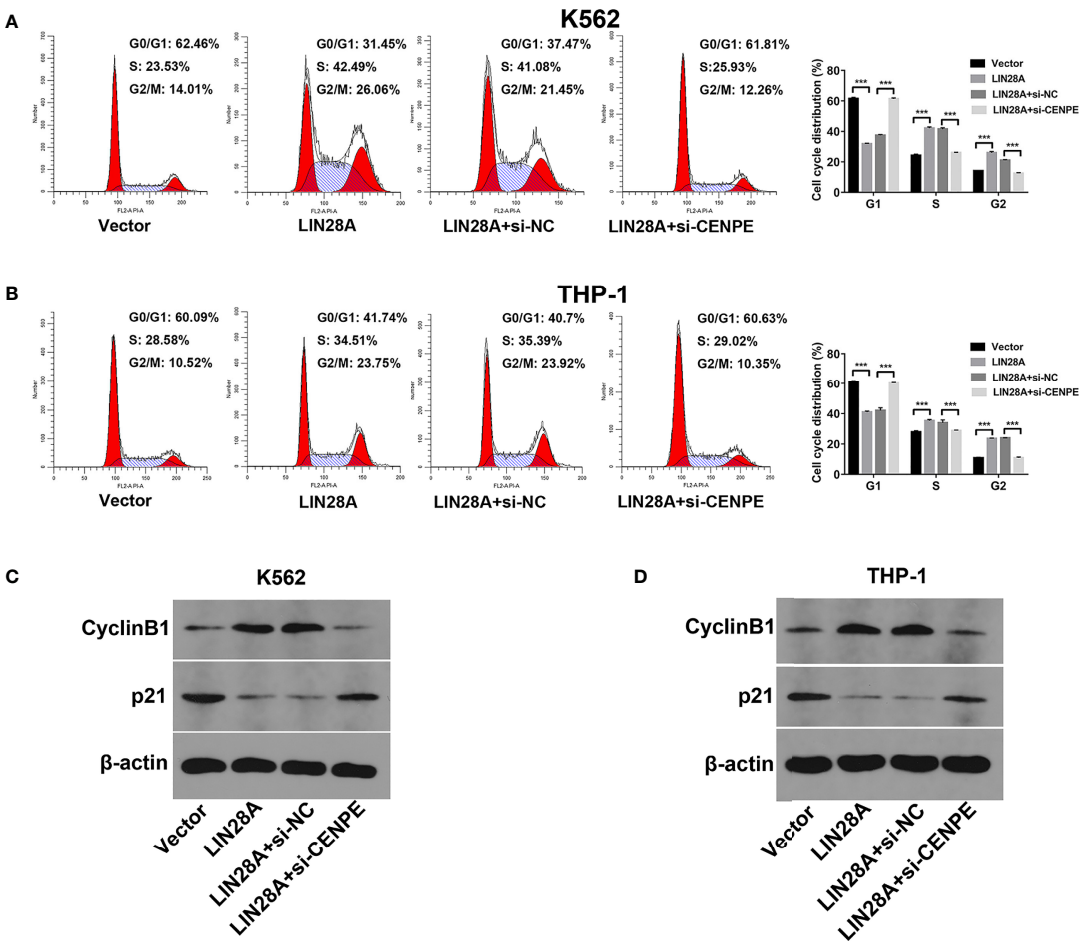

FIGURE 9 | LIN28A/CENPE inhibited the cell cycle progression in K562 and THP-1 cells. **(A, B)** After 48 h of transfection, cell cycle was measured by PI single-staining method in LIN28A overexpressed and CENPE interfered LIN28A overexpressed K562 and THP-1 cells. **(C, D)** After 48 h, Western blot analyzed the expression of cycle-related proteins Cyclin B1 and p21 in LIN28A overexpressed and CENPE interfered LIN28A overexpressed K562 and THP-1 cells. ***$p < 0.001$.

other chemotherapeutic agents, such as low-dose Ara-C, for the treatment of patients with leukemia, AML, myelodysplastic syndrome (MDS), and MDS-progressive AML (45–48). Therefore, targeting cell cycle regulators could be a potential therapeutic target for chemoresistant AML.

In this study, we have shown that the expression of mitosis cell cycle-related gene CENPE was notably elevated in chemoresistant AML patients compared to chemosensitive AML patients, which was in line with public data of R-AML *versus* primary AML. CENPE is a microtubule motility protein that is implicated in oncogenesis of various kinds of cancer (10, 11, 15). Knockdown of CENPE in breast cancer, prostate cancer, and neuroblastoma leads to repression of the tumor proliferation (12–14). In a study of NSCLC, CENPE was found to be highly expressed and predicted poor prognosis (16). *In vitro* studies further determined that the pro-proliferative effect of CENPE expression on lung cancer cells is modulated directly by FOXM1 *via* binding to the promoter region of CENPE (17). In leukemia, GSK923295A, which inhibited CENPE motility activity, exhibited significant remission induced anti-leukemia effect in the ALL xenografts (19). In AML, single-cell RNA-seq result showed that CENPE was correlated with higher residuals (20). In the present study, we demonstrated that CENPE was increased in chemoresistance AML patients and R-AML patients from the TCGA database. Moreover, CENPE interference significantly inhibited AML cell activity and promoted cell cycle arrest and apoptosis, which is consistent with previous findings, but whether CENPE can be involved in regulating the drug sensitivity of AML to Ara-C has not been reported. In our study, our functional analysis confirmed that CENPE interference enhanced the drug sensitivity of AML cells to Ara-C.

Given the important role of CENPE in AML progression and chemoresistance, we further explored the mechanisms of upstream regulation of CENPE. It was revealed that LIN28A was significantly correlated with CENPE expression. Highly expressed RBPs LIN28A can act as a potential oncogenic factor to promote tumorigenesis, progression, and metastasis in various human cancers (27). As in previous studies, by analyzing publicly

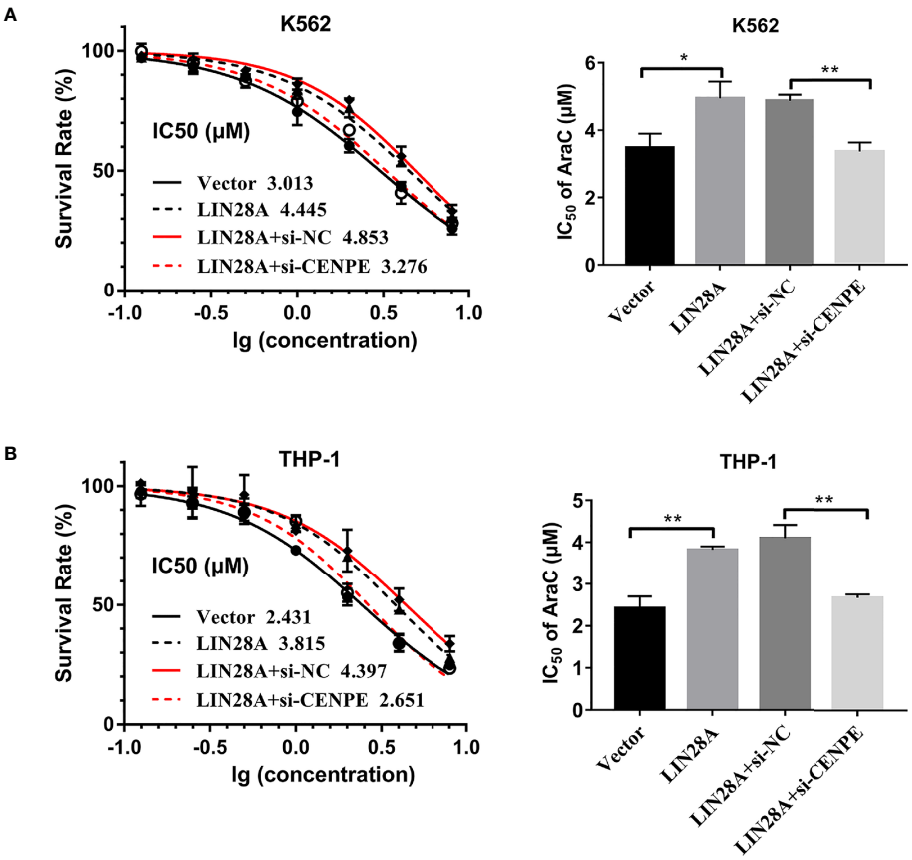

FIGURE 10 | LIN28A/CENPE interaction effected Ara-C resistance in K562 and THP-1 cells. **(A, B)** LIN28A overexpressed and CENPE interfered LIN28A overexpressed K562 and THP-1 cells were treated with ascending concentrations of Ara-C (0.125 μM, 0.25 μM, 0.5 μM, 1 μM, 2 μM, 4 μM, and 8 μM). After 48 h, IC50 values were measured and analyzed by the CCK-8 method. The experiment was independently repeated three times and statistical differences were analyzed. $^{*}p < 0.05$. $^{**}p < 0.01$.

available data, our preliminary results show that LIN28A expression is substantially increased in R-AML patients compared to primary AML patients, which indicated poor prognosis in AML. Mechanistically, LIN28A can regulate its target mRNA translation (24, 28). In papillary thyroid carcinoma cells, LIN28A interference inhibited c-myc expression, which in turn reduced cell proliferation, migration, and invasion (49). Additionally, by binding to LINC00355 or GEFT 3'UTR, LIN28A moderated LINC00355-mediated GEFT expression, increased GEFT mRNA stability, and facilitated colorectal cancer formation, development, and aggression (38). In ovarian cancer, Lin28A enriched the mRNA of RAN and HSBP1, which was negatively correlated with survival and prognosis (41). In glioma cells, the Lin28A/SNHG14/IRF6 axis is pivotal for the reprogramming of glucose metabolism and the spurring of oncogenesis, and depletion of Lin28A reduced *in vivo* xenograft tumor outgrowth and prolonged nude mice survival (42). Several studies (23–26) have also revealed the underlying role of LIN28A on cell cycle-related mRNAs. For instance, tissue microarrays identified that LIN28A expression was increased in epithelial tumors and promoted cell cycle progression by regulating CDK2, CCND1, and CDC25A in cancer cells. Moreover, it has been shown that LIN28A is involved in regulating AML cell differentiation and cycle progression (43). However, the mechanism of LIN28A in regulating cell cycle progression in chemoresistance AML is rarely studied.

In our study, LIN28A highly correlated with CENPE in R-AML. We also confirmed that LIN28A, which is upregulated in R-AML, has a predicted binding site to CENPE. RIP experiments showed that LIN28A antibody significantly enriched CENPE in K562 cells. Sequence analysis revealed that the CENPE mRNA 3'UTR contains the GGAGA motif. RNA pull-down experiments confirmed that the biotin-labeled CENPE 3'UTR positive strand could enrich a large quantity of LIN28A protein, indicating that LIN28A directly interacted with CENPE mRNA 3'UTR. Subsequently, dual luciferase reporter assay showed that the binding activity of LIN28A and CENPE mRNA 3'UTR was mediated by the GGAGA motif. In summary, LIN28A promoted CENPE mRNA expression and stability through direct binding to the GGAGA motif in the CENPE 3'UTR. More importantly, by performing functional remediation studies, we further investigated the role of LIN28A in AML development and drug resistance by

affecting the stability of CENPE mRNA. The results showed that CENPE interference reduced the proliferation and cycle-promoting effects of LIN28A overexpression. In drug sensitivity assays, CENPE interference reversed the promoting effect of LIN28A on Ara-C resistance in leukemic cells.

Our findings demonstrated the underlying value of CENPE and LIN28A for the early detection of chemoresistant AML. In addition, a better understanding of the functional and molecular modulation mechanisms of LIN28A/CENPE may help provide potential therapeutic targets and synergistic agents for chemotherapy-resistant AML.

DATA AVAILABILITY STATEMENT

The datasets presented in this study can be found in online repositories. The names of the repository/repositories and accession number(s) can be found below: GEO, GSE183817.

ETHICS STATEMENT

The studies involving human participants were reviewed and approved by the Ethics Committee of Henan Provincial People's Hospital. Written informed consent to participate in this study was provided by the participants' legal guardian/next of kin. Written informed consent was obtained from the individual(s), and minor(s)' legal guardian/next of kin, for the publication of any potentially identifiable images or data included in this article.

AUTHOR CONTRIBUTIONS

MS, JN, XN, HG, YB, JS, and WL performed the experiments, analyzed the data, and wrote the manuscript. KS, YC, and FS contributed to the conception and design of the experiments and supervision of the study. All authors contributed to the article and approved the submitted version.

FUNDING

This study was partially supported by the National Natural Science Foundation of China (No. 81971508, No. 81471589, and No. 81273259), the Health Bureau of Henan Province, P.R. China (No. 201201005), the Foundation and Frontier Research Grant of Henan Provincial Science and Technology Bureau, P.R. China (No. 142300410078), and Sansheng Chunya Funds for Young Scientists.

REFERENCES

1. Akinduro O, Weber TS, Ang H, Haltalli MLR, Ruivo N, Duarte D, et al. Proliferation Dynamics of Acute Myeloid Leukaemia and Haematopoietic Progenitors Competing for Bone Marrow Space. *Nat Commun* (2018) 9 (1):519. doi: 10.1038/s41467-017-02376-5
2. Feitelson MA, Arzumanyan A, Kulathinal RJ, Blain SW, Holcombe RF, Mahajna J, et al. Sustained Proliferation in Cancer: Mechanisms and Novel Therapeutic Targets. *Semin Cancer Biol* (2015) 35 Suppl(Suppl):S25–54. doi: 10.1016/j.semcancer.2015.02.006
3. Dong Y, Zhao X, Feng X, Zhou Y, Yan X, Zhang Y, et al. SETD2 Mutations Confer Chemoresistance in Acute Myeloid Leukemia Partly Through Altered Cell Cycle Checkpoints. *Leukemia* (2019) 33(11):2585–98. doi: 10.1038/s41375-019-0456-2
4. Schnerch D, Yalcintepe J, Schmidts A, Becker H, Follo M, Engelhardt M, et al. Cell Cycle Control in Acute Myeloid Leukemia. *Am J Cancer Res* (2012) 2 (5):508–28.
5. Ghelli Luserna di Rora A, Iacobucci I, Martinelli G. The Cell Cycle Checkpoint Inhibitors in the Treatment of Leukemias. *J Hematol Oncol* (2017) 10(1):77. doi: 10.1186/s13045-017-0443-x
6. Richter A, Schoenwaelder N, Sender S. Cyclin-Dependent Kinase Inhibitors in Hematological Malignancies-Current Understanding, (Pre-)Clinical Application and Promising Approaches. *Cancers (Basel)* (2021) 13 (10):2497. doi: 10.3390/cancers13102497
7. Tang K, Schuh AC, Yee KW. 3 + 7 Combined Chemotherapy for Acute Myeloid Leukemia: Is It Time to Say Goodbye? *Curr Oncol Rep* (2021) 23 (10):120. doi: 10.1007/s11912-021-01108-9
8. Levin M, Stark M, Ofran Y, Assaraf YG. Deciphering Molecular Mechanisms Underlying Chemoresistance in Relapsed AML Patients: Towards Precision Medicine Overcoming Drug Resistance. *Cancer Cell Int* (2021) 21(1):53. doi: 10.1186/s12935-021-01746-w
9. Jammal N, Rausch CR, Kadia TM, Pemmaraju N. Cell Cycle Inhibitors for the Treatment of Acute Myeloid Leukemia: A Review of Phase 2 & 3 Clinical Trials. *Expert Opin Emerg Drugs* (2020) 25(4):491–9. doi: 10.1080/14728214.2020.1847272
10. Craske B, Welburn JPI. Leaving No-One Behind: How CENP-E Facilitates Chromosome Alignment. *Essays Biochem* (2020) 64(2):313–24. doi: 10.1042/ebc20190073
11. El-Arabey AA, Salama SA, Abd-Allah AR. CENP-E as a Target for Cancer Therapy: Where Are We Now? *Life Sci* (2018) 208:192–200. doi: 10.1016/j.lfs.2018.07.037
12. Kung PP, Martinez R, Zhu Z, Zager M, Blasina A, Rymer I, et al. Chemogenetic Evaluation of the Mitotic Kinesin CENP-E Reveals a Critical Role in Triple-Negative Breast Cancer. *Mol Cancer Ther* (2014) 13(8):2104–15. doi: 10.1158/1535-7163.mct-14-0083-t
13. Liang Y, Ahmed M, Guo H, Soares F, Hua JT, Gao S, et al. LSD1-Mediated Epigenetic Reprogramming Drives CENPE Expression and Prostate Cancer Progression. *Cancer Res* (2017) 77(20):5479–90. doi: 10.1158/0008-5472.can-17-0496
14. Balamuth NJ, Wood A, Wang Q, Jagannathan J, Mayes P, Zhang Z, et al. Serial Transcriptome Analysis and Cross-Species Integration Identifies Centromere-Associated Protein E as a Novel Neuroblastoma Target. *Cancer Res* (2010) 70 (7):2749–58. doi: 10.1158/0008-5472.can-09-3844
15. Iegiani G, Gai M, Di Cunto F. CENPE Inhibition Leads to Mitotic Catastrophe and DNA Damage in Medulloblastoma Cells. *Cancers (Basel)* (2021) 13 (5):1028. doi: 10.3390/cancers13051028
16. Hao X, Qu T. Expression of CENPE and Its Prognostic Role in Non-Small Cell Lung Cancer. *Open Med (Warsaw Poland)* (2019) 14:497–502. doi: 10.1515/med-2019-0053
17. Shan L, Zhao M, Lu Y, Ning H, Yang S, Song Y, et al. CENPE Promotes Lung Adenocarcinoma Proliferation and Is Directly Regulated by FOXM1. *Int J Oncol* (2019) 55(1):257–66. doi: 10.3892/ijo.2019.4805
18. Hsu MH, Liu CY, Lin CM, Chen YJ, Chen CJ, Lin YF, et al. 2-(3-Methoxyphenyl)-5-Methyl-1,8-Naphthyridin-4(1H)-One (HKL-1) Induces G2/M Arrest and Mitotic Catastrophe in Human Leukemia HL-60 Cells. *Toxicol Appl Pharmacol* (2012) 259(2):219–26. doi: 10.1016/j.taap.2011.12.026
19. Lock RB, Carol H, Morton CL, Keir ST, Reynolds CP, Kang MH, et al. Initial Testing of the CENP-E Inhibitor GSK923295A by the Pediatric Preclinical Testing Program. *Pediatr Blood Cancer* (2012) 58(6):916–23. doi: 10.1002/pbc.23176

20. van Galen P, Hovestadt V, Wadsworth Ii MH, Hughes TK, Griffin GK, Battaglia S, et al. Single-Cell RNA-Seq Reveals AML Hierarchies Relevant to Disease Progression and Immunity. *Cell* (2019) 176(6):1265–81.e1224. doi: 10.1016/j.cell.2019.01.031
21. Pereira B, Billaud M, Almeida R. RNA-Binding Proteins in Cancer: Old Players and New Actors. *Trends Cancer* (2017) 3(7):506–28. doi: 10.1016/j.trecan.2017.05.003
22. Moore S, Järvelin AI, Davis I, Bond GL, Castello A. Expanding Horizons: New Roles for Non-Canonical RNA-Binding Proteins in Cancer. *Curr Opin Genet Dev* (2018) 48:112–20. doi: 10.1016/j.gde.2017.11.006
23. Liu Y, Dong N, Miao J, Li C, Wang X, Ruan J. Lin28 Promotes Dental Pulp Cell Proliferation *via* Upregulation of Cyclin-Dependent Proteins and Interaction With Let-7a/IGF2BP2 Pathways. *Biomed Pharmacother Biomed Pharmacother* (2019) 113:108742. doi: 10.1016/j.biopha.2019.108742
24. Mayr F, Heinemann U. Mechanisms of Lin28-Mediated miRNA and mRNA Regulation–A Structural and Functional Perspective. *Int J Mol Sci* (2013) 14 (8):16532–53. doi: 10.3390/ijms140816532
25. Xu B, Zhang K, Huang Y. Lin28 Modulates Cell Growth and Associates With a Subset of Cell Cycle Regulator mRNAs in Mouse Embryonic Stem Cells. *RNA (N Y NY)* (2009) 15(3):357–61. doi: 10.1261/rna.1368009
26. Li N, Zhong X, Lin X, Guo J, Zou L, Tanyi JL, et al. Lin-28 Homologue A (LIN28A) Promotes Cell Cycle Progression *via* Regulation of Cyclin-Dependent Kinase 2 (CDK2), Cyclin D1 (CCND1), and Cell Division Cycle 25 Homolog A (CDC25A) Expression in Cancer. *J Biol Chem* (2012) 287 (21):17386–97. doi: 10.1074/jbc.M111.321158
27. Zhang J, Xu A, Miao C, Yang J, Gu M, Song N. Prognostic Value of Lin28A and Lin28B in Various Human Malignancies: A Systematic Review and Meta-Analysis. *Cancer Cell Int* (2019) 19:79. doi: 10.1186/s12935-019-0788-z
28. Wang T, Wang G, Hao D, Liu X, Wang D, Ning N, et al. Aberrant Regulation of the LIN28A/LIN28B and Let-7 Loop in Human Malignant Tumors and Its Effects on the Hallmarks of Cancer. *Mol Cancer* (2015) 14:125. doi: 10.1186/s12943-015-0402-5
29. Balzeau J, Menezes MR, Cao S, Hagan JP. The LIN28/let-7 Pathway in Cancer. *Front Genet* (2017) 8:31. doi: 10.3389/fgene.2017.00031
30. He Y, Wang H, Yan M, Yang X, Shen R, Ni X, et al. High LIN28A and PLK4 Co–Expression Is Associated With Poor Prognosis in Epithelial Ovarian Cancer. *Mol Med Rep* (2018) 18(6):5327–36. doi: 10.3892/mmr.2018.9562
31. Shen H, Zhao L, Feng X, Xu C, Li C, Niu Y. Lin28A Activates Androgen Receptor *via* Regulation of C-Myc and Promotes Malignancy of ER-/Her2+ Breast Cancer. *Oncotarget* (2016) 7(37):60407–18. doi: 10.18632/oncotarget.11004
32. Gaza A, Fritz V, Malek L, Wormser L, Treiber N, Danner J, et al. Identification of Novel Targets of miR-622 in Hepatocellular Carcinoma Reveals Common Regulation of Cooperating Genes and Outlines the Oncogenic Role of Zinc Finger CCHC-Type Containing 11. *Neoplasia (NY NY)* (2021) 23(5):502–14. doi: 10.1016/j.neo.2021.04.001
33. Weng M, Feng Y, He Y, Yang W, Li J, Zhu Y, et al. Hypoxia-Induced LIN28A mRNA Promotes the Metastasis of Colon Cancer in a Protein-Coding-Independent Manner. *Front Cell Dev Biol* (2021) 9:642930. doi: 10.3389/fcell.2021.642930
34. Jain M, Tran S, Thakur S, Nagashima Y, Anderson R, Narendran A. Lin28A/let-7 Oncogenic Circuit Is a Potential Therapeutic Target in Neurocutaneous Melanosis-Associated CNS Tumors in Children. *Neuro-Oncol Adv* (2020) 3 (1):vdaa174. doi: 10.1093/noajnl/vdaa174
35. Parisi S, Castaldo D, Piscitelli S, D'Ambrosio C, Divisato G, Passaro F, et al. Identification of RNA-Binding Proteins That Partner With Lin28a to Regulate Dnmt3a Expression. *Sci Rep* (2021) 11(1):2345. doi: 10.1038/s41598-021-81429-8
36. Gibadulinova A, Bullova P, Strnad H, Pohlodek K. CAIX-Mediated Control of LIN28/let-7 Axis Contributes to Metabolic Adaptation of Breast Cancer Cells to Hypoxia. *Int J Mol Sci* (2020) 21(12):4299. doi: 10.3390/ijms21124299
37. Dou J, Zhang H, Chen R, Shu Z, Yuan H, Zhao X, et al. SUMOylation Modulates the LIN28A-Let-7 Signaling Pathway in Response to Cellular Stresses in Cancer Cells. *Mol Oncol* (2020) 14(9):2288–312. doi: 10.1002/1878-0261.12694
38. Wang Y, Zhang B, Gao G, Zhang Y, Xia Q. Long Non-Coding RNA LINC00355 Promotes the Development and Progression of Colorectal Cancer by Elevating Guanine Nucleotide Exchange Factor T Expression *via* RNA Binding Protein Lin-28 Homolog A. *Front Oncol* (2020) 10:582669. doi: 10.3389/fonc.2020.582669
39. Shrivastava G, Aljabali AA. Targeting LIN28: A New Hope in Prostate Cancer Theranostics. *Future Oncol* (2021) 7(29):3873–80. doi: 10.2217/fon-2021-0247
40. Samsonova A, El Hage K. Lin28, A Major Translation Reprogramming Factor, Gains Access to YB-1-Packaged mRNA Through Its Cold-Shock Domain. *Commun Biol* (2021) 4(1):359. doi: 10.1038/s42003-021-01862-3
41. Zhong Y, Cao L, Ma H, Wang Q, Wei P, Yang J, et al. Regulates Stem-Like Properties of Ovarian Cancer Cells by Enriching RAN and HSBP1 mRNA and Up-Regulating Its Protein Expression. *Int J Biol Sci* (2020) 16(11):1941–53. doi: 10.7150/ijbs.43504
42. Lu J, Liu X, Zheng J, Song J, Liu Y, Ruan X, et al. Lin28A Promotes IRF6-Regulated Aerobic Glycolysis in Glioma Cells by Stabilizing SNHG14. *Cell Death Dis* (2020) 11(6):447. doi: 10.1038/s41419-020-2650-6
43. De Luca L, Trino S, Laurenzana I, Tagliaferri D, Falco G, Grieco V, et al. Knockdown of miR-128a Induces Lin28a Expression and Reverts Myeloid Differentiation Blockage in Acute Myeloid Leukemia. *Cell Death Dis* (2017) 8 (6):e2849. doi: 10.1038/cddis.2017.253
44. Winer ES, Stone RM. Novel Therapy in Acute Myeloid Leukemia (AML): Moving Toward Targeted Approaches. *Ther Adv Hematol* (2019) 10:2040620719860645. doi: 10.1177/2040620719860645
45. Yang J, Ikezoe T, Nishioka C, Tasaka T, Taniguchi A, Kuwayama Y, et al. AZD1152, A Novel and Selective Aurora B Kinase Inhibitor, Induces Growth Arrest, Apoptosis, and Sensitization for Tubulin Depolymerizing Agent or Topoisomerase II Inhibitor in Human Acute Leukemia Cells *In Vitro* and In Vivo. *Blood* (2007) 110(6):2034–40. doi: 10.1182/blood-2007-02-073700
46. Döhner H, Lübbert M, Fiedler W, Fouillard L, Haaland A, Brandwein JM, et al. Randomized, Phase 2 Trial of Low-Dose Cytarabine With or Without Volasertib in AML Patients Not Suitable for Induction Therapy. *Blood* (2014) 124(9):1426–33. doi: 10.1182/blood-2014-03-560557
47. Garcia-Manero G, Fenaux P, Al-Kali A, Baer MR, Sekeres MA, Roboz GJ, et al. Rigosertib Versus Best Supportive Care for Patients With High-Risk Myelodysplastic Syndromes After Failure of Hypomethylating Drugs (ONTIME): A Randomised, Controlled, Phase 3 Trial. *Lancet Oncol* (2016) 17(4):496–508. doi: 10.1016/s1470-2045(16)00009-7
48. Navada SC, Fruchtman SM, Odchimar-Reissig R, Demakos EP, Petrone ME, Zbyszewski PS, et al. A Phase 1/2 Study of Rigosertib in Patients With Myelodysplastic Syndromes (MDS) and MDS Progressed to Acute Myeloid Leukemia. *Leukemia Res* (2018) 64:10–6. doi: 10.1016/j.leukres.2017.11.006
49. Huang J, Lin H, Zhong M, Huang J, Sun S, Lin L, et al. Role of Lin28A/let-7a/C-Myc Pathway in Growth and Malignant Behavior of Papillary Thyroid Carcinoma. *Med Sci Monitor: Int Med J Exp Clin Res* (2018) 24:8899–909. doi: 10.12659/msm.908628

Conflict of Interest: The authors declare that the research was conducted in the absence of any commercial or financial relationships that could be construed as a potential conflict of interest.

Publisher's Note: All claims expressed in this article are solely those of the authors and do not necessarily represent those of their affiliated organizations, or those of the publisher, the editors and the reviewers. Any product that may be evaluated in this article, or claim that may be made by its manufacturer, is not guaranteed or endorsed by the publisher.

frontiers in Oncology

REVIEW
published: 01 February 2022
doi: 10.3389/fonc.2022.806137

Acute Myeloid Leukemia With *CEBPA* Mutations: Current Progress and Future Directions

Long Su[1], *Yuan-Yuan Shi*[2], *Zeng-Yan Liu*[3] *and Su-Jun Gao*[1*]

[1] Department of Hematology, The First Hospital of Jilin University, Changchun, China, [2] State Key Laboratory of Experimental Hematology, National Clinical Research Center for Blood Diseases, Institute of Hematology & Blood Diseases Hospital, Chinese Academy of Medical Sciences & Peking Union Medical College, Tianjin, China, [3] Department of Hematology, Binzhou Medical University Hospital, Binzhou, China

Mutations in *CCAAT enhancer binding protein A gene* (*CEBPA*) are one of the common genetic alterations in acute myeloid leukemia (AML). Recently, the emergence of new evidence makes it necessary to reconsider the subsets and treatment of AML patients with *CEBPA* mutations. This review will summarize the history of research progress of *CEBPA* mutations in AML, the heterogeneities of AML with *CEBPA* double mutations (*CEBPA*^{dm}), and two special subtypes of *CEBPA* mutated AML. We will discuss the treatment of AML with *CEBPA* mutations as well, and finally propose a new algorithm for the treatment of these patients, including both familial and sporadic *CEBPA* mutated AML patients. This review may be beneficial for further investigation and optimizing clinical management of AML patients with *CEBPA* mutations.

Keywords: acute myeloid leukemia, *CEBPA* mutations, subsets, prognosis, treatment

OPEN ACCESS

Edited by:
Yonghui Li,
Shenzhen University General Hospital, China

Reviewed by:
Cosimo Cumbo,
University of Bari Aldo Moro, Italy
Xiaoxia Hu,
Ruijin Hospital, China

***Correspondence:**
Su-Jun Gao
sjgao@jlu.edu.cn

Specialty section:
This article was submitted to Hematologic Malignancies, a section of the journal Frontiers in Oncology

Received: *31 October 2021*
Accepted: *03 January 2022*
Published: *01 February 2022*

Citation:
Su L, Shi Y-Y, Liu Z-Y and Gao S-J (2022) Acute Myeloid Leukemia With CEBPA Mutations: Current Progress and Future Directions. Front. Oncol. 12:806137. doi: 10.3389/fonc.2022.806137

INTRODUCTION

CCAAT enhancer binding protein alpha (CEBPα) is a crucial transcription factor for the differentiation of granulocytes, which also plays a critical role in regulating glucose metabolism (1). CEBPα is encoded by the *CEBPA* gene located in chromosome 19 of human, which contains two transactivation domains (TAD) in the N-terminal and one basic leucine zipper region (bZIP) in the C-terminal. *CEBPA* mutations are one of the most frequent genetic lesions in patients with acute myeloid leukemia (AML). Although mutations of *CEBPA* gene can occur across the whole gene, they cluster in two main hotspots: N-terminal frame-shift insertions/deletions and/or C-terminal in-frame insertions/deletions. Mutations in the N-terminal result in the production of a truncated protein p30, which has a dominant negative effect over the full-length p42 protein, while mutations in the C-terminal will disrupt the binding of CEBPα to DNA or dimerization (2). *CEBPA* mutations include those locate in one terminal (*CEBPA* single mutation; *CEBPA*^{sm}) and those that occur in both N- and C-terminals (*CEBPA* double mutations; *CEBPA*^{dm}). Although *CEBPA* mutations are widely investigated in numerous studies and several reviews have already been published to discuss their molecular mechanisms and clinical relevance (3–7), newly emerging evidence makes it necessary to reconsider the pathogenesis, subsets, and treatment choice of AML with *CEBPA* mutations. The aim of this perspective review is to summarize the latest findings in this field and propose a new treatment algorithm based on the available evidence.

KEY RESEARCH PROGRESS OF *CEBPA* MUTATIONS IN AML

The frequency of *CEBPA* mutations in AML is 6.86%–20.33%, and a higher incidence rate is observed in AML patients from Asia compared to that in Western countries. Moreover, the frequencies of $CEBPA^{sm}$ and $CEBPA^{dm}$ are similar in AML patients from Caucasian populations, but more patients present with $CEBPA^{dm}$ in Asian populations (2, 6, 8–13) (**Figure 1**).

The first study was published in 2001, reporting that *CEBPA* mutations were identified in 10 of 137 patients with AML, which was also the first report showing *CEBPA* mutations in human neoplasia (14). In the following year, the prognostic significance of *CEBPA* mutations was retrospectively analyzed in 135 AML (non-M3) patients. Fifteen patients were found harboring *CEBPA* mutations, which was demonstrated to be an independent favorable prognostic factor for long-term outcomes (15). In 2009, the prognostic significance of $CEBPA^{sm}$ and $CEBPA^{dm}$ was put forward by investigators from the Netherlands (13). Only patients with $CEBPA^{dm}$ show a unique gene expression profile and favorable event-free survival (EFS) and overall survival (OS). However, both gene expression signature and outcomes were similar between patients with $CEBPA^{sm}$ and wild-type *CEBPA* (13). Subsequently, a series of studies confirmed the favorable prognosis of AML with $CEBPA^{dm}$, both in the whole patient cohort and those with normal karyotype (9, 10, 16, 17). Thus, AML with $CEBPA^{dm}$ is recognized as a definite entity in "The 2016 revision to the World Health Organization classification of myeloid neoplasm and acute leukemia", given its distinct biological and clinical characteristics (18). However, recent studies suggest that the classification of single and double mutations may not be sufficient to reflect the biological essence and clinic significance of such kind of AML. Recently, in a retrospective study including 4,708 adult patients with AML, the results showed that patients with $CEBPA^{dm}$ and $CEBPA^{sm}$ affecting bZIP ($CEBPA^{smbZIP}$) shared similar gene expression profiles and clinical features, including younger age, higher leukocytes at diagnosis, and improved survival compared to those with $CEBPA^{sm}$ affecting TAD ($CEBPA^{smTAD}$). Further analysis revealed that the clinical and molecular characteristics and favorable outcomes were confined to patients carrying in-frame mutations in bZIP, regardless of single or double mutations, in terms of superior complete remission (CR) rates and long-term survival (19). The favorable prognosis of $CEBPA^{smbZIP}$ was also observed in another independent patient cohort of 1,028 AML patients, and presence of $CEBPA^{smbZIP}$ was a strong indicator of a higher chance to achieve CR, better survival, and lower risk of relapse (20). These studies may challenge the current concept of *CEBPA* mutations in diagnosis and treatment of patients with AML. New subsets of AML with bZIP or non-bZIP mutations of *CEBPA* may be recognized rather than single and double mutations. Moreover, the prognostic and therapeutic implications of AML with $CEBPA^{smbZIP}$ may be similar to those with $CEBPA^{dm}$. The major research progress of *CEBPA* mutated AML in the last two decades was summarized in **Figure 2**.

HETEROGENEITIES OF AML WITH $CEBPA^{DM}$

Although AML patients with $CEBPA^{dm}$ show favorable outcomes, relapse after treatment is inevitable in many patients. Therefore, the heterogeneities of AML with $CEBPA^{dm}$ have been noticed and discussed by our team and other investigators (2–6). Here, we divide these heterogeneities into two major categories, namely, genetic and treatment response heterogeneities.

Genetic Heterogeneity

Mutations in transcription factor GATA2 were one of the most common molecular alterations in AML patients with $CEBPA^{dm}$. In the preliminary study, whole exome sequencing was performed with five patients with $CEBPA^{dm}$ and *GATA2* zinc finger 1 (ZF1) mutations were identified in two patients (21). The authors also found that the frequency of *GATA2* ZF1 mutations was 39.4% in AML patients with $CEBPA^{dm}$, which tended to be a favorable indicator (21). Thereafter, several studies evaluated the prognostic significance of *GATA2* mutations in patients with $CEBPA^{dm}$ (22–26) (summarized in **Table 1**). However, controversial results were found in those reports. Notably, high

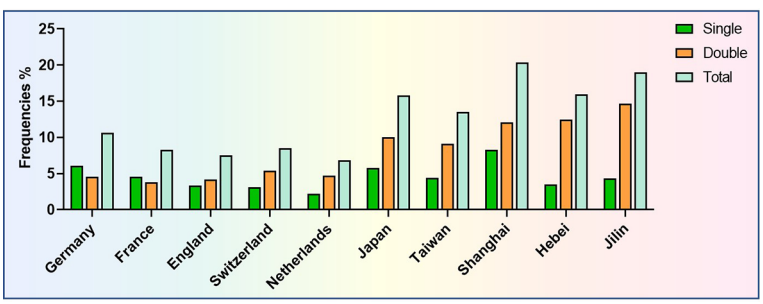

FIGURE 1 | Frequencies of *CEBPA* mutations in AML patients from different countries or different regions of China.

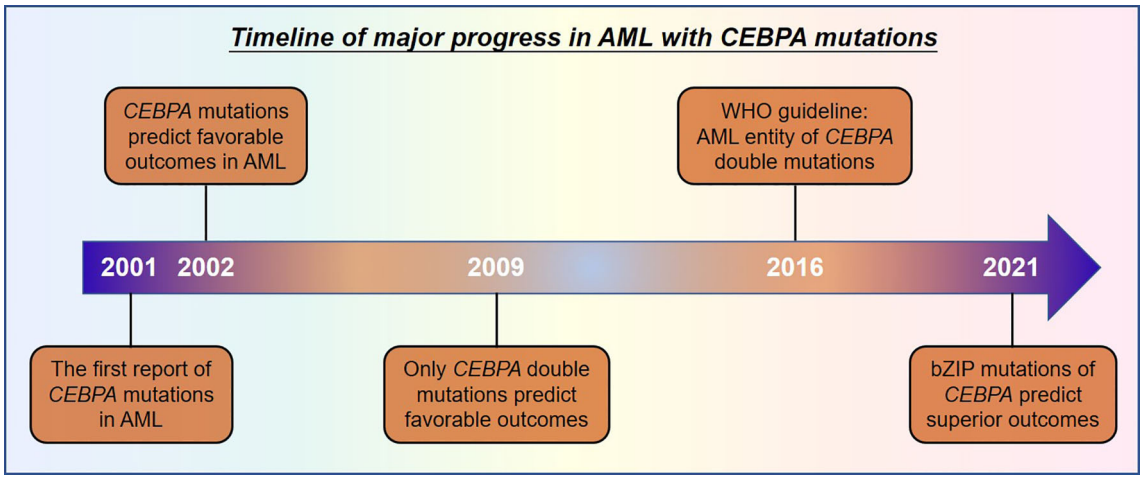

FIGURE 2 | Major research progress of AML patients with *CEBPA* mutations.

TABLE 1 | Frequencies and clinical significance of *GATA2* mutations in AML with *CEBPA*^{dm}.

Studies	Frequencies	ED	CR	EFS	OS
Fasan et al. (22)	18.3% (9/98)	NA	NA	Fav tendency	Fav
Grossmann et al. (24)	21.0% (20/95)	NA	NA	Fav tendency	Fav
Green et al. (23)	27.3% (15/55)	NS	NS	NA	NS
Marceau-Renaut et al. (25)	28.7% (25/87)	NA	NA	NA	NS
Theis et al. (26)	31.9% (36/113)	NS	NS	NS	NS

ED, early death; CR, complete remission; EFS, event-free survival; OS, overall survival; Fav, favorable; NA, not available; NS, not significant.

co-occurrence of other genetic mutations, such as *FLT3*-ITD in patients with wide-type *GATA2*, may produce unfavorable impact on the survival compared to those with mutated *GATA2*.

CSF3R is the receptor of granulocyte-colony stimulating factor (G-CSF), which functions through activation of the JAK/STAT signaling pathway. High occurrence of *CSF3R* mutations in AML patients with *CEBPA*^{dm} was first identified by RNA-sequencing in four of 14 patients, and all were T681I mutations (27). Meanwhile, high-frequency recurrent mutations in *CSF3R* were found with TARGET dataset of pediatric AML patients with *CEBPA* mutations (28). For the first time, we demonstrated that *CSF3R* mutations were associated with inferior survival in patients with AML with *CEBPA*^{dm} (5). Interestingly, *CSF3R* mutations were included in two recent studies as a parameter for prognostic nomograph models (29, 30). Thus, a high degree of overlap between *CSF3R* and *CEBPA* mutations may facilitate an in-depth understanding of the role of *CSF3R* in the pathogenesis and prognosis of AML patients with *CEBPA*^{dm}, and development of new targeted therapy, which will be discussed in a subsequent section.

Other mutated genes, such as *TET*2 and *WT1*, were reported to be negative indicators for the prognoses of AML patients with *CEBPA*^{dm} (2, 3, 6, 24). Further studies are still needed to confirm these conclusions due to limited studies and relatively small numbers of patients with mutations. One effective way to solve the issue of small patient size is to combine patients with mutations according to gene family or pathways. Mutations of tyrosine kinase genes, including *FLT3*, *CSF3R*, *KIT*, and *JAK*3, confer adverse prognosis (31). Two genetic subgroups were defined by the presence (positive; pos) or absence (negative; neg) of mutations in chromatin/DNA modifiers (C), cohesin complex (C), and splicing (S) genes: CCSpos and CCSneg, respectively. Only patients with *CEBPA*^{dm} with CCSneg had distinct genetic and clinical features and favorable outcomes compared to those with *CEBPA*^{sm} (3). Interestingly, most patients (20/25, 80%) in the CCSpos group were defined by *TET2* mutations in this study, which may reflect the unfavorable impact of *TET2* mutations on the survival of AML with *CEBPA*^{dm}.

Treatment Response Heterogeneity

Although CR rate after induction chemotherapy is very high in patients with *CEBPA*^{dm}, a substantial proportion of the patients (30%–50%) will relapse consolidated with chemotherapeutic agents only (2, 32, 33), which suggests the heterogeneity of treatment responses of these patients. Measurable residual disease (MRD) status is a very important indicator for treatment responses and prognosis in patients with AML, which is also a potential biomarker for prognostic restratification of AML with *CEBPA*^{dm}. In the preliminary single-center study, patients with *CEBPA*^{dm} were divided into MRD high-risk (positive after two consolidation cycles and/or negative status loss at any time) and low-risk (persistent negative) groups based on MRD status during

consolidation therapy (33). As expected, MRD risk groups were the only independent risk factor for relapse and long-term survival in multivariate analysis (33). Subsequently, we conducted a multicenter retrospective study that also confirmed the previous findings that only MRD low risk associated with low recurrence rate and superior outcomes in multivariate analysis (unpublished). Therefore, MDR status may be a potential indicator to be considered for treatment choice in patients with *CEBPA*^{dm}. However, it should be noted that these two categories of heterogeneities may not be separated absolutely, because we notice that patients with high-risk genetic mutations, such as mutated *CSF3R*, had a significantly higher rate of positive MRD than those with wide-type *CSF3R* after consolidation therapy (82.0% vs. 56.25%, respectively).

SPECIFIC SUBTYPES OF AML WITH *CEBPA* MUTATIONS

Pediatric Patients With *CEBPA* Mutations

AML in adults and children may show different biological behaviors, treatment responses, or prognoses. In 2005, the first study reported that the frequency of *CEBPA* mutations was 6.19% (7/113) in pediatric patients with AML, including two with single and five with double mutations. Four of the seven patients had cooperating mutations with *FLT3*-ITD or *NRAS* mutations (34). The prevalence and prognostic significance of *CEBPA* mutations were evaluated in 847 children with AML from 3 consecutive clinical trials. *CEBPA* mutations were detected in 38 patients (4.49%), with 31 cases harboring double mutations. Patients with *CEBPA* mutations had significantly improved EFS and OS, and lower cumulative incidence rate of relapse compared to those with wide-type *CEBPA* (35). Single (n = 7) or double (n = 31) mutations had no significant impact on the prognosis of these patients (35), which may be due to the small size of patients in each arm. In another study from Japan, a high frequency of *CEBPA* mutations (14.92%, 47/315) was observed, and *CEBPA*^{dm} is an independent favorable prognostic risk factor in pediatric AML patients in multivariate analysis in the total patient cohort (36). Hence, the favorable prognostic significance of *CEBPA* mutations could also be confirmed in pediatric patients with AML.

Familial AML With *CEBPA* Mutations

As early as 1978, a large familial aggregation leukemia was reported, and 13 individuals over four generations of a family comprising 293 members were diagnosed (37). After screening of genetic markers, karyotypes, and virus infections, the authors postulated that such aggregation of leukemia cases likely resulted from undefined genetic, probably polygenic, predisposition, in association with the activity of leukemogenic factors (37). However, the riddle was solved 30 years later. In 2010, a report based on one member of this family (III-45) was diagnosed as AML carrying a single heterozygous base pair deletion of the N-terminal (c.68delC) in somatic sample and a probable acquired three-base pair duplication (c.937_939dupAAG) in the C-terminal of *CEBPA* in a proportion of peripheral blood cells, indicating familial AML with *CEBPA* mutations (38). Small cases of familial AML with *CEBPA* mutations were also reported by other studies (23, 39). In 2015, the first study exploring the disease evolution and outcomes of familial AML with germline *CEBPA* mutations was reported, and 24 members from 10 *CEBPA*-mutated families were enrolled (40). Germline *CEBPA* mutations clustered within the N-terminal and acquired mutations preferentially targeting the C-terminal in diagnostic leukemia samples. AML patients with germline *CEBPA* mutations showed absence of diagnostic *CEBPA* mutations in relapse (40) and younger age than those with sporadic *CEBPA* mutations (41). Furthermore, patients with familial *CEBPA* mutations showed a favorable long-term outcome with 10-year OS of 67% (40). Although familial AML with *CEBPA* mutations is a rare disease, these studies discovered the unique biological behaviors and favorable prognosis of these patients.

TREATMENT STRATEGIES FOR PATIENTS WITH *CEBPA* MUTATIONS

High CR rates of *de novo* (~90%) and relapsed (~80%) AML patients with *CEBPA*^{dm} induced by chemotherapy indicate that this subtype of AML is highly sensitive to chemotherapeutic agents (42). Furthermore, with the insight into the pathogenesis and clinical features of *CEBPA* mutated AML in recent years, therefore, it is necessary to reconsider the treatment choice for these patients. A comparison between hematopoietic stem cell transplantation (HSCT) and chemotherapy was performed with 124 patients with *CEBPA*^{dm} in CR1. Thirty-two patients were treated with allogeneic HSCT (allo-HSCT), 20 with autologous HSCT (auto-HSCT), and the remaining 72 received chemotherapy. Although patients consolidated with chemotherapy showed significantly higher relapse rates compared to those in both auto-HSCT and allo-HSCT groups, such advantage did not translate into survival benefit for HSCT. Furthermore, there is no significant difference between patients in auto-HSCT and allo-HSCT groups in terms of relapse-free survival and OS (32). Relapsed patients still have a favorable outcome after reinduction followed by allo-HSCT with a 3-year OS of 46% (32). Allo-HSCT and chemotherapy were also compared in AML patients with *CEBPA*^{dm} in other studies. Allo-HSCT (n = 25) resulted in significantly lower incidence rate of relapse than chemotherapy (n = 24), but OS was similar between those two groups (43). Another study favored chemotherapy, not allo-HSCT, for patients with *CEBPA*^{dm} (44). In a recent study, *CEBPA*^{dm} AML patients were divided into low- and high-risk groups according to a nomograph model that was constructed with high white blood cell counts, DNA methylation related gene, *CSF3R*, and *KMT2A* mutations. Allo-HSCT was superior to chemotherapy and was only observed in high-risk, but not low-risk subgroups (29). Collectively, these results suggest that the majority of studies showed that allo-HSCT was not superior to chemotherapy or auto-HSCT in AML with *CEBPA*^{dm}. Nevertheless, certain AML patients with *CEBPA*^{dm} may benefit from allo-HSCT, but further study is needed to explore and validate.

With the emerging research advances, other potential targets that are reported in AML with *CEBPA*^{dm} may be used for treatment. AML with *CEBPA*^{dm} showed a low genetic expression signature, and reactivation of these low expressed genes promoted granulocytic differentiation of primary samples by histone deacetylase inhibitors that may be a candidate for treatment (45). High frequency of *CSF3R* mutations was discovered in AML with *CEBPA*^{dm}, which was sensitive to JAK inhibition; furthermore, AML patients with *CEBPA*^{dm} with special gene expression prolife without *CSF3R* mutations were uniformly sensitive to JAK inhibitors as well, which suggests the possibility of using JAK inhibitors in those patients (27). In addition, a combination of inhibitors of JAK signaling pathway and lysine-specific demethylase 1 is effectively capable of controlling the growth of *CSF3R*/*CEBPA* mutant leukemia *in vivo* (46). The interaction between MLL histone-methyltransferase complex with CEBPα p30 plays a critical role in leukemogenesis of *CEBPA* mutated AML, while MLL inhibition impairs proliferation and restores myeloid differentiation in AML cells with *CEBPA* mutations (47). As both histone deacetylase inhibitor Chidamide and JAK inhibitor Ruxolitinib have been used in clinic, integration of these inhibitors with chemotherapy or HSCT may possibly improve the prognosis of AML with *CEBPA* mutations.

CONCLUSION AND FUTURE DIRECTIONS

From what was discussed above, we could see that AML patients with *CEBPA*^{dm} are sensitive to chemotherapy, which suggests a critical role of chemotherapy and auto-HSCT in the treatment of those patients. Although some genetic mutations are associated with high risk of relapse (*CSF3R*, *WT1*, and *TET2*; high-risk factors) in AML with *CEBPA*^{dm}, the total frequency of those mutations is higher than the recurrence rate of *CEBPA*^{dm} patients consolidated with auto-HSCT, which indicates that patients with those high-risk factors may also benefit from auto-HSCT. Furthermore, as the majority of patients with *CEBPA*^{dm} carry mutations in bZIP, it will result in limited significance to divide *CEBPA*^{dm} into those with or without bZIP mutations. However, recent research indicates that *CEBPA*^{sm} located in bZIP showed similar clinical features and prognosis to those with *CEBPA*^{dm}. Therefore, we propose that AML patients with sporadic *CEBPA* mutations should be divided into *CEBPA*$^{smnon\text{-}bZIP}$, *CEBPA*^{smbZIP}, and *CEBPA*^{dm} for further treatment. For those with *CEBPA*^{smbZIP} and *CEBPA*^{dm}, they should be treated according to MRD status and genetic high-risk factors for choosing chemotherapy, auto-HSCT, or allo-HSCT as we presented in **Figure 3**. Optimization of prognostic evaluation and treatment choice for AML patients with *CEBPA*

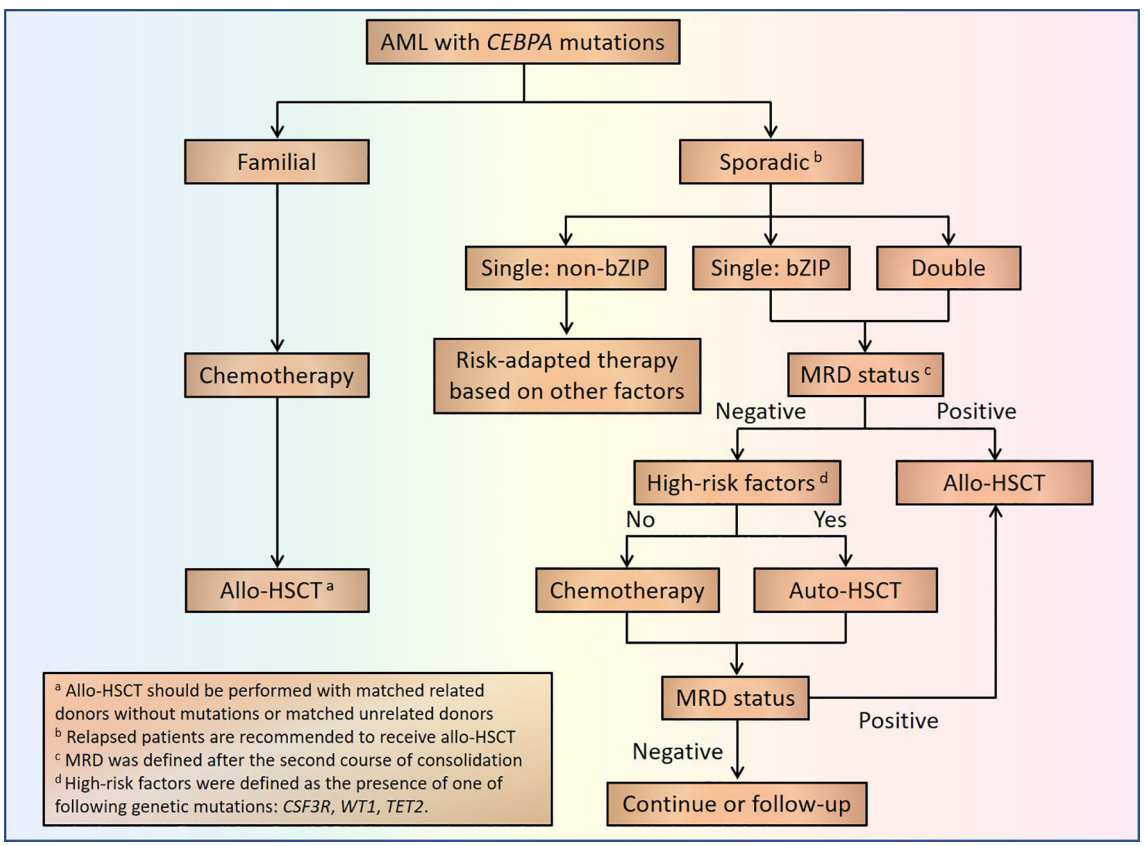

FIGURE 3 | Treatment flowchart of AML patients with *CEBPA* mutations.

mutations by MRD status during treatment here may suggest that an integrated prognostic system should be established with both pre-treatment (cytogenetic and genetic alterations) and post-treatment (MRD status) parameters, in order to direct choosing treatment strategies post remission. As to those with familial AML with *CEBPA* mutations, favorable outcomes could be achieved by chemotherapy, and those with refractory or relapse disease should receive allo-HSCT to eliminate the germline mutations with related donors without mutations or unrelated donors (**Figure 3**).

More beneficial evidence that *CEBPA* bZIP mutations may define a subset of AML is still anticipated, especially in the settings of different populations or treatment plans. Some investigators suggested the classification of *CEBPA* mutated AML as *CEBPA* with in-frame bZIP mutations and those without. However, two points must be mentioned. First, the frequency of frame-shift bZIP mutations in $CEBPA^{dm}$ is very low in AML in some patient cohorts; it is only 4.38% (6/137) in patients from our center. Second, a comparison between in-frame and frame-shift bZIP mutations of *CEBPA* is still needed. Furthermore, whether such phenomenon could be observed in pediatric AML patients needs further exploration. Although AML with $CEBPA^{dm}$ is sensitive to chemotherapy, evidence of auto-HSCT is limited, which may be helpful to prevent disease relapse in some patients because auto-HSCT is more intensive than chemotherapy alone. Finally, with the discovery of new potential targets or development and application of new drugs in the treatment of those patients, the prognoses of *CEBPA* mutated AML may be further improved, which may challenge the diagnosis and treatment dogma of the current concept.

AUTHOR CONTRIBUTIONS

LS wrote the manuscript. LS, Y-YS, Z-YL, and S-JG collected, analyzed, and summarized the data. LS, Y-YS, Z-YL, and S-JG conceptualized this review. LS and S-JG revised the review. All authors contributed to the article and approved the submitted version.

FUNDING

This work was supported by grants from NSFC (81900174) and the Clinical Research Foundation of First Hospital of Jilin University (No. LCFYJJ2017005).

REFERENCES

1. Nerlov C. C/EBPalpha Mutations in Acute Myeloid Leukaemias. *Nat Rev Cancer* (2004) 4:394–400. doi: 10.1038/nrc1363
2. Su L, Tan Y, Lin H, Liu X, Yu L, Yang Y, et al. Mutational Spectrum of Acute Myeloid Leukemia Patients With Double CEBPA Mutations Based on Next-Generation Sequencing and its Prognostic Significance. *Oncotarget* (2018) 9:24970–9. doi: 10.18632/oncotarget.23873
3. Konstandin NP, Pastore F, Herold T, Dufour A, Rothenberg-Thurley M, Hinrichsen T, et al. Genetic Heterogeneity of Cytogenetically Normal AML With Mutations of CEBPA. *Blood Adv* (2018) 2:2724–31. doi: 10.1182/bloodadvances.2018016840
4. Nie Y, Su L, Li W, Gao S. Novel Insights of Acute Myeloid Leukemia With CEBPA Deregulation: Heterogeneity Dissection and Re-Stratification. *Crit Rev Oncol Hematol* (2021) 163:103379. doi: 10.1016/j.critrevonc.2021.103379
5. Su L, Gao S, Tan Y, Lin H, Liu X, Liu S, et al. CSF3R Mutations Were Associated With an Unfavorable Prognosis in Patients With Acute Myeloid Leukemia With CEBPA Double Mutations. *Ann Hematol* (2019) 98:1641–6. doi: 10.1007/s00277-019-03699-7
6. Tien FM, Hou HA, Tang JL, Kuo YY, Chen CY, Tsai CH, et al. Concomitant WT1 Mutations Predict Poor Prognosis in Acute Myeloid Leukemia Patients With Double Mutant CEBPA. *Haematologica* (2018) 103:e510–3. doi: 10.3324/haematol.2018.189043
7. Wilhelmson AS, Porse BT. CCAAT Enhancer Binding Protein Alpha (CEBPA) Biallelic Acute Myeloid Leukaemia: Cooperating Lesions, Molecular Mechanisms and Clinical Relevance. *Br J Haematol* (2020) 190:495–507. doi: 10.1111/bjh.16534
8. Fasan A, Haferlach C, Alpermann T, Jeromin S, Grossmann V, Eder C, et al. The Role of Different Genetic Subtypes of CEBPA Mutated AML. *Leukemia* (2014) 28:794–803. doi: 10.1038/leu.2013.273
9. Green CL, Koo KK, Hills RK, Burnett AK, Linch DC, Gale RE. Prognostic Significance of CEBPA Mutations in a Large Cohort of Younger Adult Patients With Acute Myeloid Leukemia: Impact of Double CEBPA Mutations and the Interaction With FLT3 and NPM1 Mutations. *J Clin Oncol* (2010) 28:2739–47. doi: 10.1200/JCO.2009.26.2501
10. Pabst T, Eyholzer M, Fos J, Mueller BU. Heterogeneity Within AML With CEBPA Mutations; Only CEBPA Double Mutations, But Not Single CEBPA Mutations Are Associated With Favourable Prognosis. *Br J Cancer* (2009) 100:1343–6. doi: 10.1038/sj.bjc.6604977
11. Renneville A, Boissel N, Gachard N, Naguib D, Bastard C, de Botton S, et al. The Favorable Impact of CEBPA Mutations in Patients With Acute Myeloid Leukemia is Only Observed in the Absence of Associated Cytogenetic Abnormalities and FLT3 Internal Duplication. *Blood* (2009) 113:5090–3. doi: 10.1182/blood-2008-12-194704
12. Shen Y, Zhu YM, Fan X, Shi JY, Wang QR, Yan XJ, et al. Gene Mutation Patterns and Their Prognostic Impact in a Cohort of 1185 Patients With Acute Myeloid Leukemia. *Blood* (2011) 118:5593–603. doi: 10.1182/blood-2011-03-343988
13. Wouters BJ, Löwenberg B, Erpelinck-Verschueren CA, van Putten WL, Valk PJ, Delwel R. Double CEBPA Mutations, But Not Single CEBPA Mutations, Define a Subgroup of Acute Myeloid Leukemia With a Distinctive Gene Expression Profile That Is Uniquely Associated With a Favorable Outcome. *Blood* (2009) 113:3088–91. doi: 10.1182/blood-2008-09-179895
14. Pabst T, Mueller BU, Zhang P, Radomska HS, Narravula S, Schnittger S, et al. Dominant-Negative Mutations of CEBPA, Encoding CCAAT/enhancer Binding Protein-Alpha (C/EBPalpha), in Acute Myeloid Leukemia. *Nat Genet* (2001) 27:263–70. doi: 10.1038/85820
15. Preudhomme C, Sagot C, Boissel N, Cayuela JM, Tigaud I, de Botton S, et al. Favorable Prognostic Significance of CEBPA Mutations in Patients With De Novo Acute Myeloid Leukemia: A Study From the Acute Leukemia French Association (ALFA). *Blood* (2002) 100:2717–23. doi: 10.1182/blood-2002-03-0990
16. Dufour A, Schneider F, Metzeler KH, Hoster E, Schneider S, Zellmeier E, et al. Acute Myeloid Leukemia With Biallelic CEBPA Gene Mutations and Normal Karyotype Represents a Distinct Genetic Entity Associated With a Favorable Clinical Outcome. *J Clin Oncol* (2010) 28:570–7. doi: 10.1200/JCO.2008.21.6010
17. Taskesen E, Bullinger L, Corbacioglu A, Sanders MA, Erpelinck CA, Wouters BJ, et al. Prognostic Impact, Concurrent Genetic Mutations, and Gene Expression Features of AML With CEBPA Mutations in a Cohort of 1182 Cytogenetically Normal AML Patients: Further Evidence for CEBPA Double Mutant AML as a Distinctive Disease Entity. *Blood* (2011) 117:2469–75. doi: 10.1182/blood-2010-09-307280
18. Arber DA, Orazi A, Hasserjian R, Thiele J, Borowitz MJ, Le Beau MM, et al. The 2016 Revision to the World Health Organization Classification of

Myeloid Neoplasms and Acute Leukemia. *Blood* (2016) 127:2391–405. doi: 10.1182/blood-2016-03-643544
19. Taube F, Georgi JA, Kramer M, Stasik S, Middeke JM, Röllig C, et al. CEBPA Mutations in 4708 Patients With Acute Myeloid Leukemia - Differential Impact of bZIP and TAD Mutations on Outcome. *Blood* (2022) 139:87–103. doi: 10.1182/blood.2020009680
20. Wakita S, Sakaguchi M, Oh I, Kako S, Toya T, Najima Y, et al. Prognostic Impact of CEBPA bZIP Domain Mutation in Acute Myeloid Leukemia. *Blood Adv* (2021) 6:238–47. doi: 10.1182/bloodadvances.2021004292
21. Greif PA, Dufour A, Konstandin NP, Ksienzyk B, Zellmeier E, Tizazu B, et al. GATA2 Zinc Finger 1 Mutations Associated With Biallelic CEBPA Mutations Define a Unique Genetic Entity of Acute Myeloid Leukemia. *Blood* (2012) 120:395–403. doi: 10.1182/blood-2012-01-403220
22. Fasan A, Eder C, Haferlach C, Grossmann V, Kohlmann A, Dicker F, et al. GATA2 Mutations Are Frequent in Intermediate-Risk Karyotype AML With Biallelic CEBPA Mutations and Are Associated With Favorable Prognosis. *Leukemia* (2013) 27:482–5. doi: 10.1038/leu.2012.174
23. Green CL, Tawana K, Hills RK, Bödör C, Fitzgibbon J, Inglott S, et al. GATA2 Mutations in Sporadic and Familial Acute Myeloid Leukaemia Patients With CEBPA Mutations. *Br J Haematol* (2013) 161:701–5. doi: 10.1111/bjh.12317
24. Grossmann V, Haferlach C, Nadarajah N, Fasan A, Weissmann S, Roller A, et al. CEBPA Double-Mutated Acute Myeloid Leukaemia Harbours Concomitant Molecular Mutations in 76·8% of Cases With TET2 and GATA2 Alterations Impacting Prognosis. *Br J Haematol* (2013) 161:649–58. doi: 10.1111/bjh.12565
25. Marceau-Renaut A, Guihard S, Castaigne S, Dombret H, Preudhomme C, Cheok M. Classification of CEBPA Mutated Acute Myeloid Leukemia by GATA2 Mutations. *Am J Hematol* (2015) 90:E93–94. doi: 10.1002/ajh.23949
26. Theis F, Corbacioglu A, Gaidzik VI, Paschka P, Weber D, Bullinger L, et al. Clinical Impact of GATA2 Mutations in Acute Myeloid Leukemia Patients Harboring CEBPA Mutations: A Study of the AML Study Group. *Leukemia* (2016) 30:2248–50. doi: 10.1038/leu.2016.185
27. Lavallée VP, Krosl J, Lemieux S, Boucher G, Gendron P, Pabst C, et al. Chemo-Genomic Interrogation of CEBPA Mutated AML Reveals Recurrent CSF3R Mutations and Subgroup Sensitivity to JAK Inhibitors. *Blood* (2016) 127:3054–61. doi: 10.1182/blood-2016-03-705053
28. Maxson JE, Ries RE, Wang YC, Gerbing RB, Kolb EA, Thompson SL, et al. CSF3R Mutations Have a High Degree of Overlap With CEBPA Mutations in Pediatric AML. *Blood* (2016) 127:3094–8. doi: 10.1182/blood-2016-04-709899
29. Wu LX, Jiang H, Chang YJ, Zhou YL, Wang J, Wang ZL, et al. Risk Stratification of Cytogenetically Normal Acute Myeloid Leukemia With Biallelic CEBPA Mutations Based on a Multi-Gene Panel and Nomogram Model. *Front Oncol* (2021) 11:706935. doi: 10.3389/fonc.2021.706935
30. Xu X, Cai W, Cai P, Zhang L, Yao H, Zhang T, et al. Prognostic Nomogram for Acute Myeloid Leukemia Patients With Biallelic CEBPA Mutations. *Front Oncol* (2021) 11:628248. doi: 10.3389/fonc.2021.628248
31. Zhang Y, Wang F, Chen X, Zhang Y, Wang M, Liu H, et al. Companion Gene Mutations and Their Clinical Significance in AML With Double Mutant CEBPA. *Cancer Gene Ther* (2020) 27:599–606. doi: 10.1038/s41417-019-0133-7
32. Schlenk RF, Taskesen E, van Norden Y, Krauter J, Ganser A, Bullinger L, et al. The Value of Allogeneic and Autologous Hematopoietic Stem Cell Transplantation in Prognostically Favorable Acute Myeloid Leukemia With Double Mutant CEBPA. *Blood* (2013) 122:1576–82. doi: 10.1182/blood-2013-05-503847
33. Wang J, Lu R, Wu Y, Jia J, Gong L, Liu X, et al. Detection of Measurable Residual Disease may Better Predict Outcomes Than Mutations Based on Next-Generation Sequencing in Acute Myeloid Leukaemia With Biallelic Mutations of CEBPA. *Br J Haematol* (2020) 190:533–44. doi: 10.1111/bjh.16535
34. Liang DC, Shih LY, Huang CF, Hung IJ, Yang CP, Liu HC, et al. CEBPalpha Mutations in Childhood Acute Myeloid Leukemia. *Leukemia* (2005) 19:410–4. doi: 10.1038/sj.leu.2403608
35. Ho PA, Alonzo TA, Gerbing RB, Pollard J, Stirewalt DL, Hurwitz C, et al. Prevalence and Prognostic Implications of CEBPA Mutations in Pediatric Acute Myeloid Leukemia (AML): A Report From the Children's Oncology Group. *Blood* (2009) 113:6558–66. doi: 10.1182/blood-2008-10-184747
36. Matsuo H, Kajihara M, Tomizawa D, Watanabe T, Saito AM, Fujimoto J, et al. Prognostic Implications of CEBPA Mutations in Pediatric Acute Myeloid Leukemia: A Report From the Japanese Pediatric Leukemia/Lymphoma Study Group. *Blood Cancer J* (2014) 4:e226. doi: 10.1038/bcj.2014.47
37. Gunz FW, Gunz JP, Vincent PC, Bergin M, Johnson FL, Bashir H, et al. Thirteen Cases of Leukemia in a Family. *J Natl Cancer Inst* (1978) 60:1243–50. doi: 10.1093/jnci/60.6.1243
38. Carmichael CL, Wilkins EJ, Bengtsson H, Horwitz MS, Speed TP, Vincent PC, et al. Poor Prognosis in Familial Acute Myeloid Leukaemia With Combined Biallelic CEBPA Mutations and Downstream Events Affecting the ATM, FLT3 and CDX2 Genes. *Br J Haematol* (2010) 150:382–5. doi: 10.1111/j.1365-2141.2010.08204.x
39. Smith ML, Cavenagh JD, Lister TA, Fitzgibbon J. Mutation of CEBPA in Familial Acute Myeloid Leukemia. *N Engl J Med* (2004) 351:2403–7. doi: 10.1056/NEJMoa041331
40. Tawana K, Wang J, Renneville A, Bödör C, Hills R, Loveday C, et al. Disease Evolution and Outcomes in Familial AML With Germline CEBPA Mutations. *Blood* (2015) 126:1214–23. doi: 10.1182/blood-2015-05-647172
41. Shih LY, Liang DC, Huang CF, Wu JH, Lin TL, Wang PN, et al. AML Patients With CEBPalpha Mutations Mostly Retain Identical Mutant Patterns But Frequently Change in Allelic Distribution at Relapse: A Comparative Analysis on Paired Diagnosis and Relapse Samples. *Leukemia* (2006) 20:604–9. doi: 10.1038/sj.leu.2404124
42. Kurosawa S, Yamaguchi H, Yamaguchi T, Fukunaga K, Yui S, Kanamori H, et al. The Prognostic Impact of FLT3-ITD, NPM1 and CEBPa in Cytogenetically Intermediate-Risk AML After First Relapse. *Int J Hematol* (2020) 112:200–9. doi: 10.1007/s12185-020-02894-x
43. Ahn JS, Kim JY, Kim HJ, Kim YK, Lee SS, Jung SH, et al. Normal Karyotype Acute Myeloid Leukemia Patients With CEBPA Double Mutation Have a Favorable Prognosis But No Survival Benefit From Allogeneic Stem Cell Transplant. *Ann Hematol* (2016) 95:301–10. doi: 10.1007/s00277-015-2540-7
44. Kurosawa S, Yamaguchi H, Yamaguchi T, Fukunaga K, Yui S, Wakita S, et al. Decision Analysis of Postremission Therapy in Cytogenetically Intermediate-Risk Acute Myeloid Leukemia: The Impact of FLT3 Internal Tandem Duplication, Nucleophosmin, and CCAAT/Enhancer Binding Protein Alpha. *Biol Blood Marrow Transplant* (2016) 22:1125–32. doi: 10.1016/j.bbmt.2016.03.015
45. Liss A, Ooi CH, Zjablovskaja P, Benoukraf T, Radomska HS, Ju C, et al. The Gene Signature in CCAAT-Enhancer-Binding Protein α Dysfunctional Acute Myeloid Leukemia Predicts Responsiveness to Histone Deacetylase Inhibitors. *Haematologica* (2014) 99:697–705. doi: 10.3324/haematol.2013.093278
46. Braun TP, Coblentz C, Smith BM, Coleman DJ, Schonrock Z, Carratt SA, et al. Combined Inhibition of JAK/STAT Pathway and Lysine-Specific Demethylase 1 as a Therapeutic Strategy in CSF3R/CEBPA Mutant Acute Myeloid Leukemia. *Proc Natl Acad Sci USA* (2020) 117:13670–9. doi: 10.1073/pnas.1918307117
47. Schmidt L, Heyes E, Scheiblecker L, Eder T, Volpe G, Frampton J, et al. CEBPA-Mutated Leukemia Is Sensitive to Genetic and Pharmacological Targeting of the MLL1 Complex. *Leukemia* (2019) 33:1608–19. doi: 10.1038/s41375-019-0382-3

Conflict of Interest: The authors declare that the research was conducted in the absence of any commercial or financial relationships that could be construed as a potential conflict of interest.

frontiers in Oncology

REVIEW
published: 09 March 2022
doi: 10.3389/fonc.2022.787108

Antigen-Specific TCR-T Cells for Acute Myeloid Leukemia: State of the Art and Challenges

Synat Kang[1], Yisheng Li[2], Jingqiao Qiao[2], Xiangyu Meng[2], Ziqian He[2], Xuefeng Gao[1,2] and Li Yu[1]**

[1] Department of Hematology and Oncology, International Cancer Center, Shenzhen Key Laboratory of Precision Medicine for Hematological Malignancies, Shenzhen University General Hospital, Shenzhen University Clinical Medical Academy, Shenzhen University Health Science Center, Shenzhen, China, [2] Central Laboratory, Shenzhen University General Hospital, Shenzhen, China

OPEN ACCESS

Edited by:
Shujun Liu,
University of Minnesota Twin Cities, United States

Reviewed by:
Yong-Chen Lu,
University of Arkansas for Medical Sciences, United States
Xiaowen Tang,
The First Affiliated Hospital of Soochow University, China

***Correspondence:**
Xuefeng Gao
xfgao@szu.edu.cn
Li Yu
yuli@szu.edu.cn

Specialty section:
This article was submitted to Hematologic Malignancies, a section of the journal Frontiers in Oncology

Received: 30 September 2021
Accepted: 10 February 2022
Published: 09 March 2022

Citation:
Kang S, Li Y, Qiao J, Meng X, He Z, Gao X and Yu L (2022) Antigen-Specific TCR-T Cells for Acute Myeloid Leukemia: State of the Art and Challenges. Front. Oncol. 12:787108. doi: 10.3389/fonc.2022.787108

The cytogenetic abnormalities and molecular mutations involved in acute myeloid leukemia (AML) lead to unique treatment challenges. Although adoptive T-cell therapies (ACT) such as chimeric antigen receptor (CAR) T-cell therapy have shown promising results in the treatment of leukemias, especially B-cell malignancies, the optimal target surface antigen has yet to be discovered for AML. Alternatively, T-cell receptor (TCR)-redirected T cells can target intracellular antigens presented by HLA molecules, allowing the exploration of a broader territory of new therapeutic targets. Immunotherapy using adoptive transfer of WT1 antigen-specific TCR-T cells, for example, has had positive clinical successes in patients with AML. Nevertheless, AML can escape from immune system elimination by producing immunosuppressive factors or releasing several cytokines. This review presents recent advances of antigen-specific TCR-T cells in treating AML and discusses their challenges and future directions in clinical applications.

Keywords: acute myeloid leukemia, TCR-T cells, immunotherapy, allo-HSCT, immune escape

INTRODUCTION

Acute myeloid leukemia (AML), which is a relatively common leukemia in adult patients, results from aberrant growth in the hematopoietic system, and it has multiple clinical appearances (1, 2). Complete remission for AML remains difficult to achieve despite recent advances in chemotherapy and molecularly targeted therapies (3), and chemotherapy is the first-line treatment option for AML

Abbreviations: allo-HSCT, allogeneic hematopoietic stem cell transplant; ATL, adult T-cell leukemia/lymphoma; CAR-T, chimeric antigen receptor modified-T cells; CLL, acute lymphoid leukemia; CR, complete response; CTA, cancer-testis antigen; GM-SCF, granulocyte-macrophage colony-stimulating factor; HA-1, minor histocompatibility antigen; IDO, indoleamine 2,3-dioxygenase; IFN-γ, interferon gamma; IL-10, interleukin-10; IL-15, interleukin-15; IL-1, interleukin-1; LCLs, lymphoblastoid cell lines cells; MDS, myelodysplastic syndrome; MDSC, myeloid-derived suppressor cells; mHag, minor histocompatibility antigen; RFS, relapse-free survival; PBLs, peripheral blood lymphocytes; PD-L1, programmed cell death-ligand 1; ROS, reactive oxygen species; TCB, TCR-like T-cell bispecific antibody; TCR-T, T-cell receptor modified-T cells; TERT, telomerase reverse transcriptase; TKI, tyrosine kinase inhibitor; Treg, regulatory T cells.

patients. The 5-year survival rates of patients below the age of 60 years are 30% to 35% and less than 15% for those aged 60 years and above (4, 5).

Allogeneic hematopoietic stem cell transplantation (allo-HSCT) remains the only established curative strategy for some types of relapsed or refractory AML (6–8). Analyses of adult AML patients have revealed that allo-HSCT treatment prior to the first complete remission resulted in a reduction of the risk of disease relapse by more than 60% compared with chemotherapy alone (9). Similarly, several studies using haploidentical donors have shown therapeutic effects on the first complete remission of 34% to 47% (10, 11). Moreover, patients receiving allo-HSCT demonstrated significantly higher OS than patients receiving chemotherapeutic postremission therapy (12). However, the results from these modest adoptive cell therapy (ACT) strategies for AML remain unsatisfactory due to high rates of graft-vs.-host disease (GVHD) and relapse (6), which could be explained by immune escape reasons (13–16).

ACT with antigen-specific T cells, including chimeric antigen receptor T cells (CAR-T cells) and T-cell receptor-engineered T cells (TCR-T cells), involves the generation and modification of targeted T cells. These therapies have shown high potency against diverse tumors, including AML **(Figure 1)** (14, 17–30). The FDA approved the first CD19 CAR-T-cell product, KYMRIAH (tisagenlecleucel), to treat acute lymphoblastic leukemia in children and adults (19). CD19 CAR-T cells are widely used for treating hematological cancers, especially leukemia (20–22). Two clinical trials exploring the use of CD19 CAR-T in the treatment of AML are currently recruiting (NCT04257175, NCT03896854). Clinical trial NCT04257175 is a phase II/III, while clinical trial NCT03896854 is a phase I/II trial in which the primary goal is to measure adverse events. Importantly, the use of second-generation autologous CD123 CAR-T cells has demonstrated a potent efficacy (NCT02159495). Here, six patients were enrolled in the study and were administered various doses of CD123 CAR-T cells: two patients received 5.0×10^7 CD123 CAR-T and four patients received 2.0×10^8 CD123 CAR-T cells. One of the patients who was treated with the lower dose of cells experienced a reduction of leukemia blast counts (from 77.9% to 0.9%), while one of the patients who was treated the higher dose achieved complete remission. The other three patients experienced reductions of blast counts but not complete remission (23).

In addition to the use of CAR-T cells, the success of adoptive transfer of antigen-specific TCR-T cells in murine studies was originally reported by Dembic et al. in the late 1986. Here, α and β TCR genes were transduced into T cells in order to enhance recognition of antigen-specific peptides presented by major histocompatibility complex (MHC) I (31). Subsequently, αβ-TCR-T cell specific for melanoma antigen recognized by T cell (MART)-1 were generated by Clay et al., who found that the redirecting of human peripheral blood lymphocytes (PBL) with αβ TCR efficiently allowed for recognition of a peptide antigen specific to melanoma cells (32). In addition, adoptive transfer of autologous TCR-T cells specific for New York esophageal squamous cell carcinoma (NY-ESO)-1 has resulted in remarkable clinical responses and a safe profile in the treatment of several cancers, including melanoma, synovial cell sarcoma, and nonsmall cell lung cancer (24–27). Treatment with autologous T cells transduced with NY-ESO-1 TCR with an increased affinity has achieved clinical responses in 80% of patients with myeloma (33).

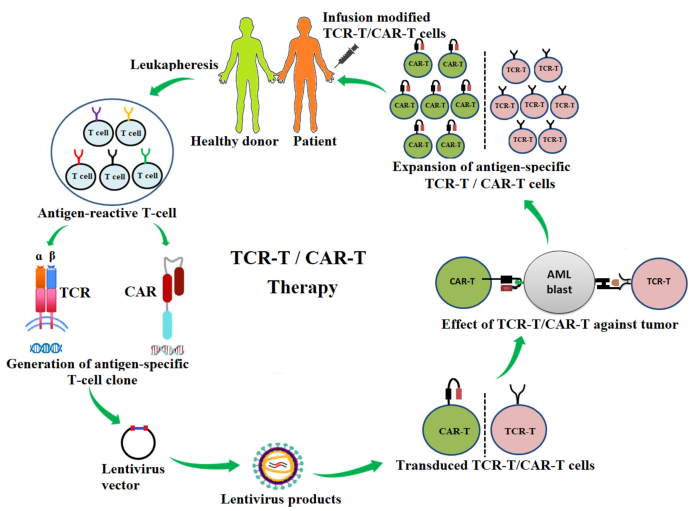

FIGURE 1 | Schematic diagram of the adoptive transfer of antigen-specific T-cell receptor redirecting T cells (TCR-T) and chimeric-antigen receptor redirecting T cells (CAR-T) for AML immunotherapy. Antigen-specific T-cell clones are generated from antigen-reactive T cells of healthy donors or patients and are inserted into a lentivirus vector. The lentivirus vector is transfected into the packing cells for the production of lentiviral particles. The lentiviral particle products containing desired αβ-TCR or CAR genes are then used to infect T cells (TCR-T, CAR-T). These genetically modified TCR-T or CAR-T cells are tested for effectiveness against cancers. TCR-T or CAR-T products are then expanded *in vitro* and infused into patients.

Several relevant breakthroughs in leukemia immunotherapy have been reported over the past few years (28–30). Treatment of high-risk AML patients with adoptive transfer of Wilms' tumor antigen 1 (WT1)-specific allogeneic TCR-T cells has shown promising results and helped prevent relapse (28). Another clinical trial (NCT02550535) of autologous WT1-specific TCR-T cells was performed to assess treatment of high-risk myeloid malignancies, and it demonstrated strong efficacy with a good safety profile (30). These findings highlight the potential for TCR-T cell therapies to improve outcomes in AML. Unfortunately, cancer cells produce several immunosuppressive factors that facilitate escape from detection by the immune system.

In this review, we present the state of the art and challenges of antigen-specific TCR-T cell immunotherapy for managing myeloid malignancies and discuss future directions of TCR-T for treating AML.

THE CURRENT STATE OF TCR-T CELL IMMUNOTHERAPY FOR AML

TCR-T Cell Immunotherapy for AML in Preclinical Studies

Selecting the appropriate target is crucial for the success of TCR-T therapy. Optimally, the antigen target must be highly overexpressed in cancerous cells but have limited expression in the healthy hematopoietic system. However, if the target antigen is expressed in normal blood cells, it must be at a low level, it must be dispensable in normal cells, and it must not be displayed as a human leukocyte antigen (HLA). If the target antigen is expressed in normal blood cells, short-lived TCR-T must be used for targeting (34). Thus far, several types of tumor-associated antigens (TAAs) and other potential targets have been reported in preclinical studies of TCR-T therapy in AML (**Table 1**). WT1, minor histocompatibility A (HA)-1, telomerase (TERT), and survivin,

TABLE 1 | Adoptive transfer of antigen-specific TCR-T cells against AML in the preclinical study.

Tumor-associated antigens	Antigen-specific TCRs	Types of T cells	Manipulation	HLA restriction	Effect of TCR-T against AML	References
Overexpressed antigens	TERT TCR-T	T cells	High-affinity TCR	HLA-A*0201	Efficiently lysed primary and AML cell lines *in vitro* and inhibited tumor growth prolong survival rate of AML xenograft model.	(35)
	Survivin-TCR-T	$CD8^+$ T cells	Codon optimization of TCRs	HLA-A*0201	Specifically lysed AML *in vitro*.	(36)
Lineage-restricted antigens	WT1 TCR-T (NTLA5001)	$CD4^+$ T cells, $CD8^+$ T cells	CRISPR/Cas9 genome editing	HLA-A*02:01	High effectiveness in controlling tumor growth and increased survival in the animal model. No GVHD was observed.	(37)
	WT1 TCR-T	T cells	High-affinity TCRs	HLA-A*02:01	Highly lysed fresh BM or PBL of AML blasts and eliminated AML in xenograft	(38)
	WT1 TCB-T	T cells	TCR-like TCBs combining with lenalidomide	HLA-A*02:01	Mediated killing primary AML *in vitro* and animal model.	(39)
Minor histocompatibility antigens	HA1 TCR-T	$CD4^+$ T cells, $CD8^+$ T cells	iCasp9 genome editing	HLA-A*02:01	Potential killing cell lines and primary relapsed/ refractory AML or LCL.	(40)
	HA1 TCR-T	T cells	Codon optimization of TCRs	HLA-A*02:01	Increased cytolytic function against AML/LCL.	(41)
	mHagHA-2-TCR, TCR-mHag DBY, CMV pp65-TCR	γδ T cells	αβ TCR transduced γδ T cells	HLA-A*0201 HLA-B*07:02 HLA-DQ5	Highly lysed primary AML blasts.	(42)
Cancer-testis antigen	PRAME TCR-T	T cells	High-avidity TCRs	HLA-A*02:01	High efficacy lysis several tumor cells, including primary AML blasts.	(43)
Neoantigens	NPM1 TCR-T	$CD4^+$ T cells, $CD8^+$ T cells	Codon optimization of TCRs	HLA A*02:01	Specifically killed AML cell lines and primary AML blasts and controlled tumor outgrowth and prolonged survival in a xenograft model.	(44)
	CBFB-MYH11 TCR-T	$CD8^+$ T cells	High-avidity TCR	HLA-B*40:01	Potent antileukemic activity against primary AML cells and in xenograft model.	(45)
	HMMR-TCR	T cells	High-affinity TCR	HLA-A*0201	High-effective controlling solid tumor growth and hematopoietic malignant such as AML.	(46)
	MDM2-TCR	$CD8^+$ T cells	High-affinity TCR	HLA-A*0201	Highly lysed the specific target cells.	(47)
	FMNL-TCR	$CD4^+$ T cells	DC-pulsed FMNL1	HLA-DRB1*0101, HLADRB1*1101	Increased several cytokines release again AML *in vitro*.	(48)
	HLA-DPB1 TCR	$CD4^+$ T cells	Codon optimization of TCR	HLA-DPA1*01:03, HLA-DPB1*04:01	Highly lysed AML *in vitro* and xenograft model.	(49)

neoantigens, and cancer-testis antigens (CTAs) have been reported as TAAs and have been explored in preclinical trials (34, 50). TAAs have been classified into several categories: overexpressed antigens (e.g. survivin and TERT), lineage-restricted antigens (e.g., WT1), cancer-testis antigens (e.g., NY-ESO-1, MAGE, and PRAME), neoantigens (e.g., NPM1 and CBFB-MYH11), and HA-1 (34, 50, 51).

Overexpressed Antigens

Telomerase TCR-T

Telomerase (TERT) is a ribonucleoprotein enzyme that acts as an organizer at the ends of eukaryotic chromosomes. It is expressed and activated under the control of multiple regulatory mechanisms, which include trafficking and posttranscriptional and posttranslational modifications, to maintain homeostasis of telomere lengths. Alterations to these regulatory mechanisms result in the dysfunction of telomeres and the development of multiple human diseases (52).

TERT is absent in most human somatic tissues but is expressed highly in most AML patients (~85%) and is most highly expressed in patients with relapsed AML (35). An earlier study demonstrated cytolytic activity of TERT-specific cytotoxic T lymphocytes (CTLs) against several cancers, including leukemia (53–55). TERT-specific CTLs, which were generated by stimulating CTLs with artificial antigen-presenting cells (APCs), have also been demonstrated to have cytotoxic activities against solid tumors and hematopoietic malignancies (55). Increasing antitumor activities were associated with expression of TERT and HLA serotype A*02:01 by the target cells (55). Moreover, adoptive transfers of high-avidity TERT-specific TCR-T cells in the context of HLA-A*02:01-restricted targets have been shown potential for controlling tumor growth and prolonging the survival of tumor-bearing mice in AML (35). However, the targeting of AML by TERT-specific TCR-T cells has not yet been evaluated clinically. Intriguingly, several clinical trials of a TERT-peptide vaccine have been shown to have activity against several cancers, including nonsmall cell lung cancer, prostate cancer, and multiple myeloma (56–59).

Survivin TCR-T

Survivin, which is encoded by the *BIRC5* gene, plays an essential role in inhibiting apoptosis, regulating the cell cycle, and regulating the anti-tumor activities of T cells (60). Survivin is not expressed, or is expressed at very low levels, in normally differentiated cells (60), but it has been found to be highly expressed in various cancers, including AML (61–65). Survivin-specific CTLs in the context of HLA-A2 restriction have been demonstrated to efficiently lyse diverse types of tumor cell lines and primary leukemia cells, including those from AML, acute lymphoblastic leukemia (ALL), and chronic lymphocytic leukemia (CLL) (66). Stimulating T cells with dendritic cells expressing survivin-specific mRNA have been shown to be effective against an AML patient-derived blast and xenograft model (67). Moreover, survivin-specific CTLs have been demonstrated to sufficiently recognize and kill survivin- and HLA-A2-positive leukemia cells in patients with AML, without cross-reactivity against healthy progenitor cells (68). Subsequently, Arbor et al. (36) generated survivin-specific TCR-T cells in the context of HLA-A*02:01. These cells were shown to avoid fratricidal effects or toxicity during normal hematopoietic stem-cell transplantation (HSCT). Survivin-specific TCR-T cells also have been shown to have high specificity and efficacy against AML targets without on-target, off-tumor toxicity. Notably, in *in vivo* studies, survivin-specific TCR-T showed potent antitumor activity and prolonged survival in a xenograft mouse model (36).

Lineage-Restricted Antigens

WT1 TCR-T

The gene encoding WT1 is located on chromosome 11p13. The protein includes an N-terminal domain and a C-terminus containing four zinc-fingers that are organized as multiple isoforms (69, 70). Different isoforms tend to be differentially expressed in patients with relapsed AML (69). WT1 is an intracellular antigen highly expressed in the bone marrow of patients with leukemia, particularly those with AML, myelodysplasia (MDS), and CLL (39, 69, 71). WT1 is an ideal target for cancer immunotherapy due to its limited expression on healthy tissues. The success of WT1-specific CTLs and WT1-specific TCR-T cells for eliminating leukemia cells was demonstrated *in vitro* and in xenograft models several years ago (38, 72). WT1-specific CTLs showed specific cytotoxicity against leukemia cells and achieved sustained remission in patients with refractory AML (73). Moreover, studies of high-avidity WT1-specific TCR-transduced CTLs in the context of HLA-A*02:01 were conducted, and they demonstrated a high degree of lysis of $CD34^+$ cells in fresh bone marrow or blood samples from AML patients and the potential elimination of leukemia blast cells in xenograft models (38). In addition, a WT1-specific TCR-like T-cell bispecific antibody (TCB) redirecting T cells showed enhanced efficiency in killing AML cell lines and primary AML cells (39).

A concern regarding therapies that involve the adoptive transfer of TCR-T cells is that mispairing of introduced and endogenous TCR chains may decrease the avidity of T cells against primary cancers and subsequently lead to the presentation of low levels of relevant peptides on cell surfaces (74, 75). Therapeutic strategies must, then, avoid such mispairings and competition with endogenous TCR α and TCR β chains, which could result in off-tumor toxicity and GVHD or negatively impact T-cell specificity and TCR expression levels. To that end, Ruggiero et al. (37) created high avidity of WT1 TCR-T cells modified through a strategy involving CRISPR/Cas9 to eliminate the endogenous TCR α and TCR β chains. Resulting WT1-specific TCR-T cells exhibited high efficacy in killing primary AML from bone marrow and ALL tumor-bearing NOD SCID gamma mice (37). The treatment of these mice with genetically modified WT1-specific TCR-T cells significantly reduced tumor growth and enhanced survival without inducing GVHD (37). Rather than using CRISPR/Cas9, Fujiwara et al. (76) alternatively generated appropriately

modified T cells with both WT1-specific TCRs and siRNAs (siTCRs) to avoid the primary concern of autoimmune reactivity caused by mispairing between introduced and endogenous TCR chains with unknown specificity (76). $WT1_{235-243}$-specific siTCR-T cells in the context of restricted HLA-A*24:02 were shown to have significantly enhanced antileukemia efficacies, and they extended animal survival. These positive results were associated with the presence of memory T cells in the mice modified with WT1-siTCR/$CD8^+$ T cells (76). Thus, preclinical studies of WT1-specific TCR-T cells demonstrated advanced benefits; clinical studies of WT1-specific TCR-T cells will be discussed further, below.

Minor Histocompatibility Antigens

HA-1 TCR-T

HA-1 is a peptide of nine amino acids encoded by a diallelic gene on human chromosome 19 (77). Significant differences in the immunogenicity of the HA-1 T-cell epitope can be traced to the identity of the amino acid at position 3 (i.e., VL**H**DDLLEA genotype RS_1801284 A/G or A/A vs. VL**R**DDLLEA, genotype RS_1801284 G/G) (77). Between these two peptides, the $HA\text{-}1^H$ (VL**H**DDLLEA) peptide can only be presented on the cell surface with highly HLA-A*0201-restricted CTLs (78), while the $HA\text{-}1^R$ (VL**R**DDLLEA) peptide cannot be delivered to the cell surface, even though both nanopeptides can bind to HLA-A*0201.

The $HA\text{-}1^H$ (hereafter referred to as HA-1) antigen is abundantly expressed in leukemia and normal hematopoietic cells, but its expression is restricted in nonhematopoietic cells (34). In HA-1-mismatched HCT, the $HA\text{-}1^-$ donor immune system is not tolerant to HA-1 because it is considered self-antigens (40). A study of HA-1-specific $CD8^+$ CTL showed that APCs coated with HLA-A*02:01/HA-1 stimulated $CD8^+$ CTL (donor-derived HLA-A*02:01/$HA\text{-}1^-$) to kill HA-1-positive cells in primary leukemia blasts (79).

Based on this success, additional approaches to generate HA-1-specific TCR redirecting T cells have been developed (41, 80). The transduction of PBL or cord blood (CB) with HA-1-specific αβ TCR demonstrated cytolytic activity against HLA-$A2^+$/$HA\text{-}1^+$ of AML and lymphoblastoid cell lines (LCLs). However, the detection of HA-1 TCR-positive cells showed a low level of HA-1-specific tetramer affinity due to the mismatched TCR structure between exogenous TCR and endogenous TCR (80). The affinity of HA-1-specific TCR has been improved by TCR codon optimization to increase TCR expression on the cell surface (41). HA-1-specific TCR-T showed efficient expression in transduced TCR and enhanced HA-1-specific functional activity against primary AML cells and LCL lines (41). Moreover, high-affinity HA-1-specific TCR-T cells containing an inducible caspase 9 safety switch, generated from the repertoire of a healthy HLA-A*02:01-positive HA-1-negative cell, have demonstrated high efficiency in killing $HA\text{-}1^+$ primary AML and LCL (40). Notably, the coexpression of CD8 receptor and high-affinity HA-1-TCR by $CD4^+$ cells led to specific killing of HA-1-containing target cells without cross-reactivity (40).

Cancer-Testis Antigens

CTA-Specific TCR-T

CTAs are a group of TAAs that exhibit normal expression in the adult testis but aberrant expression in several types of cancers (51). So far, more than 200 CTA genes from 44 gene families have been found to be encoded in the human genome *via* analysis of the CTdatabase (51). These CTAs can be classified into two groups depending on whether they are localized to the X-chromosome (Xq21-q28) or to non-X-chromosomes (51). Chromosome X-encoded CTAs include melanoma antigen (MAGE), NY-ESO-1, G antigen (GAGE), CT45, and synovial sarcoma, X chromosome (SSX), whereas non-X CTAs, located on autosomes, include B melanoma antigen (BAGE), helicase antigen (HAGE), and sperm protein 17 (SP17) (81, 82).

The CTA expression level mainly depends on the tumor type, the degree of differentiation, and the stage of progression. CTAs are potential targets for adoptive T-cell therapy because they are not expressed in normal somatic tissues accompanied by their relatively high expression in malignant cancers and their re-expression in several tumors (83). Immunotherapies targeting CTAs, including NY-ESO-1, MAGE-A3, and preferentially expressed antigen in melanoma (PRAME), have demonstrated high antitumor efficacies (84, 85). PRAME-specific CTLs in the context of HLA-A*02:01-restricted epitope have been generated from AML patients after allo-HSCT (86). Moreover, high-avidity PRAME-specific TCR-T cells generated from severe GVHD after HLA-mismatched HSCT have demonstrated high efficacy against a wide variety of tumor cell lines and AML primary cells (43). Multileukemia antigen-specific T cells, which included TCRs against PRAME and MAGE-A3, have shown antitumor reactivity against AML blasts (87). Accordingly, clinical testing of the utilization of *ex vivo*-stimulated HSCT donors against PRAME, MAGE-A3, and other tumor-associated antigens (WT1, NY-ESO-1, and survivin) is ongoing (NCT02494167 and NCT02203903).

Neoantigens

Neoantigen TCR-T

Neoantigens, which are highly immunogenic, are found in several solid tumors and hematopoietic malignancies, including AML (88, 89). Neoantigens can be divided into shared neoantigens and personalized (uniquely mutated) neoantigens (90). Shared neoantigens are mutated antigens that are common across different cancer patients but are not expressed in the normal genome (90). Personalized neoantigens have unique mutations and are significantly different from patient to patient (91). Nucleophosmin1 (NPM1) mutations are present in approximately 30% to 35% of AML cases and regarded as an optimal immunotherapy target (89). NPM1-specific $CD8^+$ T cells in the context of the HLA-A*02:01-restricted NPM1 epitope CLAVEEVSL were generated from healthy donors by Van der Lee et al. (44). This clone effectively lysed the primary AML blasts. Subsequently, a codon-optimized TCR was generated from these clones, and adoptive transfer of NPM1/HLA-A*02:01-specific TCR-transduced T cells specifically killed both AML cell lines and primary AML blasts and controlled tumor outgrowth and

prolonged survival in a xenograft model (44). These studies may suggest a role for shared neoantigens in TCR-based immunotherapy of AML and other hematologic malignancies.

Another neoantigen that is critical in leukemogenesis is a type-A variant of the fusion of core-binding factor β and myosin heavy chain 11 (CBFB-MYH11). The gene fusion event that leads to the formation of CBFB-MYH11 involves the inv(16) or t (16;16) cytogenetic abnormalities, and fusion occurs in approximately 90% of AML patients and 10% of individuals (92). Biernacki et al. generated CBFB-MYH11-specific $CD8^+$ T cells in the context of CBFB-MYH11 and HLA-B*40:01-restricted T cells from healthy donors (45). A high-avidity $CD8^+$ T cell clone showed the potential to kill relevant AML cell lines and primary human AML cells *in vitro* and *in vivo*. The construction of high-avidity TCR-specific CBFB-MYH11/HLA-B*40:01 T cells from this clone also demonstrated highly effective antileukemia activities *in vitro* and *in vivo*. The study concluded that the CBFB-MYH11 fusion neoantigen is immunologically targeting AML-initiating fusions. This study may represent the first critical step toward developing TCR-T cell immunotherapy targeting fusion gene-driven AML.

Other Antigen-Specific TCR-T Cells

Murine double minute 2 (MDM2) is an oncoprotein that is a potential inhibitor of wild-type p53 (wtp53) and can induce cell proliferation and promote cell survival (93). The MDM2 oncoprotein is overexpressed in several tumors, including hematopoietic malignancies (47, 94), and it has found to be an ideal target for AML immunotherapy. Thomas et al. generated MDM2-specific high-affinity TCR redirecting CTL in the context of HLA-A*02:01 for targeting leukemia. MDM2-specific TCR-CTL efficiently killed several human tumor and leukemia targets (47). Hyaluronan-mediated motility receptor (HMMR/Rhamm), a novel hyaluronan receptor complex component, was first purified from the supernatants of murine cells in 1992 (95). HMMR is broadly expressed in the neural crest and during embryogenesis, but its expression is limited to adult bone marrow (BM), thymus, and tonsils and in the placenta (46). It became an attractive target for cancer immunotherapy due to its overexpression in several tumors, including AML (46, 96). HMMR-specific TCR-T cells demonstrated high efficacy in killing AML *in vitro* and *in vivo*, and treating mice with HMMR-specific TCR-T combined with interleukin (IL)-15 exhibited potent efficiency in eliminating tumors and prolonged survival of AML-bearing mice (46). Human leukocyte antigen-DP β1 (HLA-DPB1) is a class of major histocompatibility complex (MHC)-II. The use of HLA-DPB1 in unrelated donor hematopoietic stem cell transplantation has been shown to improve outcomes in patients with leukemia relapse (97). Due to a common linkage imbalance between HLA-DR, HLA-DQ, and HLA-DP, approximately 80% of 10/10 matched unrelated donor-patient pairs are mismatched for one or both HLA-DPB1 alleles. Therefore, HLA-DPB1 mismatches predict a significantly lower risk of leukemia relapse (98). Herr et al. (98) generated AML-reactive CD4 CTL by stimulation of CD45RA-selected naive-enriched CD4 T cells of unrelated stem-cell donors with AML blasts of 10/10 HLA-matched patients. HLA-DPB1-mismatch-specific CD4 CTL effectively lysed HLA-DPB1 mismatch-expressing AML blasts and effectively eliminated human AML blasts in a xenograft model (98). Consistent with this study, Klobuch et al. have generated the HLA-DPB1-specific T-cell receptors from HLA-DPB1 mismatch-reactive allogeneic donor CD4 T-cell clones. They subsequently genetically optimized the receptor to enhance TCR expression and increase its activity against AML (49). HLA-DPB1-specific TCR-transduced $CD4^+$ T and $CD8^+$ T cells were strongly effective against primary AML blasts *in vitro*; however, *in vivo*, only DPB1 TCR-$CD4^+$ T cells showed high-efficacy in the eradication of AML blasts in xenograft NOD SCID gamma mice (49).

TCR-T Cell-Based Immunotherapy for AML in Clinical Studies

Adoptive transfer of antigen-specific TCR-T cells has demonstrated remarkable clinical outcomes in treating patients with relapsed or refractory AML; particular success has been seen with WT1-specific TCR-T cells (28, 29). The first human confirmation of the utility of WT1-specific TCR-transduced autologous T cells in the context of HLA-A*24:02 for treatment of refractory AML or high-risk MDS came in clinical trial UMIN000011519 (29). Among the eight patients enrolled in this study, two showed decreased blast counts in bone marrow, which predicted a regression from leukemia. Moreover, the WT1-specific TCR-T cells showed persistence in five patients, and four out of these five patients survived for more than 12 months. None of the patients experienced the adverse events related to toxicity in normal tissues (29).

HLA-A*0201-restricted WT1-specific donor-derived $CD8^+$ cytotoxic T-cells (CTLs) for treating high-risk or relapses of 11 patients with leukemia, including those with AML, was reported early by Chapuis et al. in clinical trial NCT00052520 (99). Transduction of the cells led to demonstrated clinical responses in two patients: one patient experienced reduction of advanced progressive disease and another experienced prolonged remission. In addition, three patients at high risk for relapse post-HSCT survived without leukemia relapse or GVHD (99). Subsequently, Chapuis et al. continued to generate high-affinity WT1-specific TCR from HLA-A*02:01 healthy donor repertoires and cloned the TCR into Epstein–Barr virus (EBV)-specific donor $CD8^+$ T cells to reduce GVHD and to enhance the transferring of T-cell survival (28). In clinical trial NCT01640301, 12 patients with relapsed or high-risk AML received allogeneic high-avidity WT1-specific TCR-T cells prophylactically. Interestingly, no toxicity was observed after the patients received adoptive transfer of WT1-specific TCR cells. The adoptive transfer of WT1-specific TCR-T cells led to 100% relapse-free survival at a median of 44 months, as compared with the control group with similar risk AML, which experienced approximately 54% RFS (28).

Moreover, a second study of WT1-specific TCR-transduced autologous T cells in the treatment of patients with high-risk AML and other myeloid malignancies has been reported by Morris et al. (30). In clinical trial NCT02550535, a total of 10 patients, including 6 AML, 3 MDS, and 1 tyrosine kinase inhibitor (TKI)-resistant CML, received the gene-modified T cells.

No severe adverse events were associated with on-target, off-tumor toxicity in the ten patients treated with autologous WT1-specific TCR-T cells. Notably, seven out of ten patients who received the autologous WT1-specific TCR-T cells proliferated *in vivo* and persisted through the 12 month study period (30). Currently, a phase I/II clinical trial (NCT04284228), studying WT1, PRAME, and cyclin A1-specific stem cell donor $CD8^+$ T cells in the context of HLA-A*02:01 (NEXI-001 T-cell product), is still enrolling. In addition, several studies of the WT1 antigen target and other antigen-specific autologous/allogeneic TCR-T cells also have been registered on ClinicalTrials.gov, including HA-1 (allogeneic, NCT03326921; autologous, NCT04464889) and PRAME (autologous, NCT03503968) (**Table 2**).

THE CHALLENGES OF ADOPTIVE TCR-T CELL IMMUNOTHERAPY FOR AML

Several TCR-T cell immunotherapies for AML are in use in the clinic, but some obstacles relevant to this approach need to be overcome to enhance the clinical benefits. The benefits of TCR-T cell therapy for AML may remain limited unless a thorough evaluation is made of its on-target/off-tumor toxicity, its dose-related toxicity, the persistence of TCR-T cells *in vivo*, and the chance of immune escape by AML after TCR-T administration.

On-Target, Off-Tumor Toxicity

One concern of therapies involving the adoptive transfer of antigen-specific TCR-T cells is on-target/off-tumor toxicity that may occur if nontarget tissues, such as those of the hematopoietic system, are recognized as targets. This possibility is exacerbated when antigen targets are expressed in normal tissues. Two clinical trials have reported the occurrence of off-target toxicity-related adverse effects upon adoptive transfer of autologous TCR-T cells, including neurotoxicity and cardiac toxicity (100, 101). Two patients treated with high-affinity TCR-T cells, for example, showed symptoms of cardiogenic shock and died within a few days of T-cell infusion. Here, the TCR-T cells recognized a similar peptide epitope derived from the entirely unrelated protein titin expressed in cardiac tissue (100). Similarly, two out of nine melanoma patients treated with TCR-T cells that recognized epitope MAGE-A3/9/12 lapsed into comas. They died after T-cell infusion due to the expression of MAGE-A12 in the human brain, which may have been attacked by the MAGE-specific TCR-T cells (101).

Adverse events of on-target toxicity have also been reported in metastatic melanoma treated with high-avidity TCR-transduced autologous T cells specific for MART-1 and gp100 in the context of HLA-A*0201. After infusion, these patients showed a therapeutic response but experienced adverse events, including skin rash, hearing loss, and uveitis (102). Severe inflammatory colitis has been demonstrated in colon cancer patients who received adoptive transfer of carcinoembryonic antigen-specific autologous TCR-T cells in the context of HLA-A*0201 (103).

Several clinical trials reported high efficacy and safe use of NY-ESO-1 antigen-specific TCR-T in clinics (25–27, 104). AML blasts have a low level of NY-ESO-1 expression due to the silencing of CTA expression *via* promoter methylation (105, 106). Several groups have reported that treatment of AML with the hypomethylating agent decitabine *in vitro* and *in vivo* resulted in upregulation of the expression of CTAs such as NY-ESO-1 (104, 106, 107). NY-ESO-1 vaccination combined with decitabine in the targeting of AML has shown impressive results in clinical studies (104). These clinical results evoked the idea that demethylating agents could promote NY-ESO-1-specific TCR-T cells to target and kill AML. Accordingly, our group recently demonstrated that the use of NY-ESO-$1_{157–165}$ HLA-A*02:01-specific TCR-T cells against decitabine-induced AML efficiently lysed AML cell lines and primary AML blasts and targeted AML in a xenograft model (data not shown). Therefore, NY-ESO-1-specific TCR-T combined with decitabine could be a potent approach for future clinical investigations in patients with relapsed or high-risk AML.

T cells referred to as γδ T cells, which represent from 1% to 10% of peripheral blood T cells, express a γδTCR that is not able to form a complex with αβ TCRs (108). Therefore, strategies designed to redirect γδ T cells with αβ TCR or to redirect αβ T cells with γδTCR may overcome the limitation of TCR mispairing, which can risk mediating self-reactivity (42, 109). Accordingly, αβ TCR-specific mHag HA-2-transduced γδ T cells have shown high-potency and antigen-specific killing or primary leukemia blasts with a good safety profile (42). The γδ T cells transduced with αβ TCR and CD8 receptor in the context of HLA-A*02:01-restricted HA-2 showed high levels of antigen-specific cytolytic activity against HA-2-expressing AML and CML blasts (42). In addition, transduction of γδ T cells with αβ TCR and CD4 receptor in the context of HLA class II-restricted human Y chromosome antigen DBY-TCR also showed high cytotoxicity against target cells (42). Some clinical trials of αβ TCR-modified allogeneic γδ T cells have been described in a literature review (110).

Alternatively, it is possible to redirect the αβ T cells (T cells) with γδ TCR cells (109). Redirecting $CD4^+$ and $CD8^+$ αβ T cells with γ9δ2TCR also has been shown to lead to efficient killing of primary AML *in vitro* and in a xenograft model (109). Vyborova et al. have successfully generated γ9δ2TCR clones from healthy donors, and the clones mediated antitumor responses against malignant cancers. In addition, the γ9δ2TCR-transduced αβ T cells, a product known as TEG001, were shown to recognize the butyrophilin subfamily 2 member A1 peptide antigen, and demonstrated functional enhancement activity against leukemia *in vitro* and *in vivo* (111, 112). Analysis of TEG001 is underway in a first-in-human clinical trial (NTR6541).

Dose-Related Toxicity

Dose-related toxicity has been reported in some patients receiving a high concentration of MAGE-A3-specific TCR-transduced autologous T cells (101). Patients developed neurologic toxicity after receiving a total dose higher than 6.73×10^{10} cells (101). In a phase I clinical trial (NCT02858310), one patient with metastatic

TABLE 2 | Clinical studies of adoptive transfer of antigen-specific TCR-T cells against AML.

Identifier	TCR-T therapy	Leukemia	Phase	Outcome measures	Status	Locations
NCT02550535	Autologous WT1 TCR-T cells	■ Myelodysplastic syndromes; ■ Acute myeloid leukaemia	Phase 1 Phase 2	■ Safety following gene-modified WT1 TCR T-cell therapy as measured by suspected unexpected serious adverse reactions (SUSARS); ■ Proportion of subjects achieving 1 or more IWG response criteria following gene-modified WT1 TCR T-cell therapy; ■ Safety and tolerability of gene-modified WT1 TCR therapy as measured by clinical laboratory parameters and adverse events. ■ Among 10 patients (6 AML, 3 MDS, and 1 TKI-resistant CML) enrolled in the study, All 6 AML patients survived, at last, follow-up (median 12 months) and median 3 months in the 3 patients with MDS. 3 deaths: 2 from disease progression and 1 from other causes.	Completed	■ AZ St. Jan Brugge-Oostende AV Brugge, Belgium ■ UZ Leuven Leuven, Belgium ■ Uniklinikum Dresden, Germany
UMIN00001159	Autologous WT1 siTCR-T cells	■ Acute myeloid leukemia; ■ Myelodysplastic syndromes	Unknown	■ No adverse events of normal tissue were seen. ■ 2 patients showed transient decreases in blast counts in bone marrow, which was associated with recovery of hematopoiesis.	Completed	■ Mie University Hospital, Japan ■ Ehime University Hospital, Japan ■ Fujita Health University Hospital, Japan ■ Nagoya University Hospital, Japan
NCT01621724	Autologous WT1 TCR-T cells	■ Acute myeloid leukemia; ■ Chronic myeloid leukemia	Phase 1 Phase 2	■ Identify organ toxicities and other side effects ■ Transduction efficiency and TCR expression on TCR-transduced cells ■ WT1-specific immune responses of TCR-transduced T cells	Completed	■ University Hospitals Bristol NHS Foundation Trust Bristol, UK ■ University College London Hospitals NHS Trust London, UK, NW1 2PG
NCT01640301	Allogeneic WT1 TCR-T cells	■ Recurrent adult acute myeloid leukemia; ■ Recurrent childhood acute myeloid leukemia; ■ Secondary acute myeloid leukemia	Phase 1 Phase 2	■ Antileukemic potential efficacy, in terms of duration of response (Arm II). ■ Efficacy, in terms of relapse rate (Arm I). ■ Incidence of chronic graft versus host disease (GVHD) (Arm I).	Active, not recruiting	■ Fred Hutch University of Wash ington Cancer Consortium Seattle, Washington, USA
NCT04284228	Allogeneic WT1/PRAME/Cyclin A1-antigen-specific $CD8^+$ T cells (NEXI-001 T-cell product)	■ Acute myeloid leukemia; ■ Myelodysplastic syndrome	Phase 1 Phase 2	■ Adverse events of special interest (AESIs) events of dose-limiting toxicities (DLTs) ■ AESI events of infusion-related reactions and cytokine release syndrome (CRS) ■ Survival, including median progressive-free survival (PFS), overall response rate (ORR), overall survival (OS).	Recruiting	■ City of Hope Comprehensive Cancer Center Duarte, California, USA ■ Advent Health Medical Group Blood & Marrow Transplant Orlando, Florida, USA ■ Karmanos Cancer Institute Detroit, Michigan, United States
NCT03503968	Autologous PRAME TCR-T cells (MDG1011 cell product)	■ High-risk myeloid; ■ Lymphoid neoplasms (including relapse AML after allo-HSCT)	Phase 1 Phase 2	■ Adverse events and dose limiting toxicities (safety and tolerability). ■ Maximum tolerated dose (MTD) and/or recommended phase II dose (RP2D) of MDG101.	Recruiting	■ University Hospital Dresden, Dresden, Germany ■ University Hospital Erlangen, Erlangen, Germany

(Continued)

TABLE 2 | Continued

Identifier	TCR-T therapy	Leukemia	Phase	Outcome measures	Status	Locations
				■ For feasibility: percent of all subjects who receive the planned target dose of MDG1011.		■ University Hospital Frankfurt, Frankfurt, Germany
NCT03326921	Allogeneic HA-1 TCR-T cells	■ Juvenile myelomonocytic leukemia ■ Recurrent acute biphenotypic leukemia ■ Recurrent acute undifferentiated leukemia	Phase 1	■ Feasibility of manufacturing minor H antigen (HA-1) T-cell receptor (TCR) CD8+ and CD4+ T cells. ■ Feasibility of administering minor H antigen (HA-1) T-cell receptor (TCR) CD8+ and CD4+ T cells. ■ Incidence of dose-limiting toxicities of HA-1 T-cell receptor (TCR) T cells.	Recruiting	■ Fred Hutch University of Washington Cancer Consortium Seattle, Washington, United States
NCT04464889	Autologous HA-1 H TCR-T cells	■ Acute myeloid leukemia ■ Myelodysplastic syndromes	Phase 1	■ Safety and tolerability of HA-1H TCR-transduced T cells: incidence and severity of adverse events. ■ Maximum tolerated dose (MTD) of HA-1H TCR-transduced T cells. ■ Recommended phase 2 doses (RP2D) of HA-1H TCR-transduced T cells.	Active, not recruiting	■ Leiden University Medical Centre Leiden, Zuid Holland, Netherlands

human papillomavirus (HPV)-associated epithelial cancer experienced dose-limiting toxicities (DLTs) at dose level 3 after receiving 1×10^{11} HPV E7-specific autologous TCR-T cells (E7 TCR-T) (113). Adverse events and DLTs were also identified in patients treated with a higher dose of autologous genetically modified MAGE-A10^{c796}TCR-T cells (114).

Several clinical studies have also revealed issues with dose-related toxicity of CD19 CAR-T cells (115–117). The dose-related toxicity may be associated with cytokine release syndrome triggered by the administration of higher doses of CAR-T cells or the achieving of higher cell numbers due to *in vivo* proliferation of CAR-T cells (118). Toxicity induced by the administration a large number of cells may occur immediately after transfusion and may be caused by the triggering of cytokine release by the recognition of low levels of antigen on the surfaces of cells. In one related report, toxicity manifest as severe encephalopathy of was observed in 3 out of 28 patients who received doses between 1.0 and 5.0×10^8 cells in an anti-CD19 CAR-transduced autologous T-cell (CTL019) treatment. One out of the three patients who experienced this encephalopathy died due to follicular lymphoma progressive neurologic deterioration (119). In a phase I clinical trial (NCT01593696), a dose-escalation experiment was conducted to study treatment of children and young adult patients with ALL and non-Hodgkin's lymphoma (NHL) with autologous transfusion of doses of 1.0×10^6/kg (dose 1) or 3.0×10^6/kg (dose 2) CD19 CAR-T cells (117). Two of twenty-one patients who received dose 2 demonstrated dose-limiting toxicity, specifically manifested as grade 3 and grade 4 cytokine release syndrome. Other high-grade toxicities resulting from various doses of CD19 CAR-T cells have been summarized elsewhere (116).

Therefore, dose optimization of TCR-T cells is necessary to overcome the limitation of adverse events related to dose toxicity in clinical applications. Accordingly, in clinical trial NCT02858310, Nagarsheth et al. (113) have demonstrated dose optimization of E7 TCR-transduced autologous T cells to treat HPV-related cancers. The patients were treated with various doses (1×10^9, 1×10^{10}, and 1×10^{11}) of TCR-T cells. This study suggested that administering the maximum amount of 1×10^{11} TCR-T cells was not limited by toxicity in most patients. Other clinical studies, including NCT03503968 and NCT04464889, are ongoing to evaluate the dose titration of autologous TCR-T cells to target myeloid leukemia and other hematopoietic malignancies for avoiding adverse events or dose-related toxicity.

Persistence of TCR-T Cells *In Vivo*

The localization and persistence of adoptively transferred therapeutic T cells are critical factors in cancer elimination and relapse prevention (29, 120). However, a challenge associated with ACT is the short lifespan of T cells, which limits the long-term persistence and expansion of these cells *in vivo*, therefore reducing the therapeutic efficacy. The enhanced persistence of T cells *in vivo* can be achieved through several strategies, including genetic modification of T-cell signaling and stimulation of T cells with cytokines or drugs. For example, the proliferation and persistence of TCR-T cells can be boosted by inserting the intracellular domain (ICD) of moieties that activate T-cell

signaling (CD28 or 4-1BB) into CD3ζ instead of modifying TCR affinity. These modified TCR-T cells have been demonstrated to have increased efficacy with enhanced proliferation and long-term lifespans *in vivo* (121, 122).

Administration of cytokines together with antigen-specific T cells has been shown to enhance T-cell persistence and to lead to the production of T memory stem (TSCM) cells (99, 123–126). Exposure of WT1 antigen-specific donor-derived $CD8^+$ T cells to IL-21 resulted in prolonged remission of patients with leukemia. In all these patients with leukemia, the T cells remained present and were maintained, and their long-term *in vivo* phenotypic and functional characteristics evolved with long-lived memory T cells (99). Recently, an animal model has been used to show that treatment of CAR-T cells with low-dose decitabine led to high efficacy and persistent antitumor activity (127). Thus, TCR-T cells treated with low-dose decitabine may also increase phenotypic markers of T memory stem cells.

Mechanisms of Immune Evasion in AML

Several mechanisms are involved in immune evasion in AML, including (1) alteration of antigen expression by downregulation or loss of MHC molecules, (2) overexpression of immune checkpoint inhibitors, (3) production of immunosuppressive factors, (4) excessive secretion of anti-inflammatory cytokines, and (5) and reducing proinflammatory cytokines **(Figure 2).**

Alteration of Antigen Expression

The elimination of AML blasts by allo-HSCT depends on the recognition of peptides presented by MHC molecules on the cell surface. AML relapse due to the loss of the mismatched HLA haplotype has been observed in the HSCT of donor T cells or bone marrow transplantation (128, 129). A case study reported a patient with leukemia who had two occurrences of leukemia relapse due to loss of mismatched HLA after receiving allo-HSCT (130). In the context of TCR-T therapy, adoptive transfer of NY-ESO-1 antigen-specific TCR restricted to HLA-A*02:01 against multiple myeloma has shown recurrence after the treatment. In this case, the analysis of myeloma cells demonstrated that tumor relapse was associated with definite loss of HLA-A*02:01 expression from the cell surface (131). Moreover, several studies have shown that AML relapse was associated with downregulation of MHC class II after allo-HSCT or posttransplantation (132–134). Because members of the interferon family (IFN), such as IFN-α, IFN-β, and IFN-γ, play an important role in the promotion of MHC-I expression (135), a strategy based on insertion of IFN-γ into the C-domain of a TCR may overcome the limitation of MHC molecule down-regulation. Tumor targeting of antibody-IFN-γ fusion proteins has shown highly potent anticancer activities associated with a receptor-trapping mechanism (136).

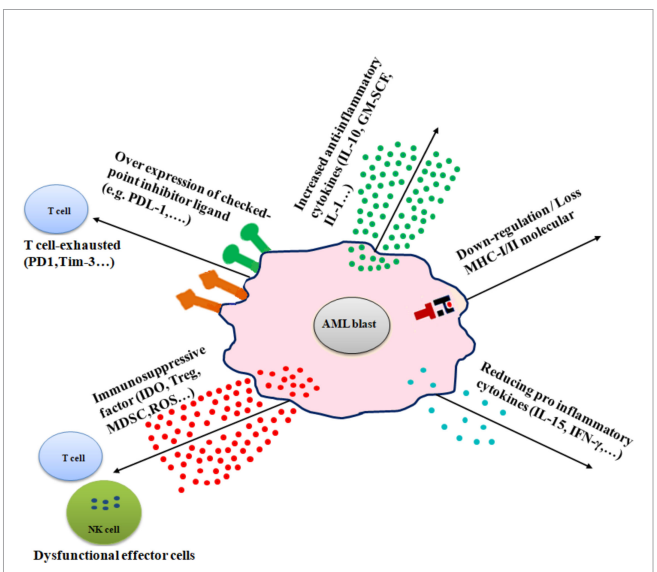

FIGURE 2 | Diverse immune escape mechanisms of AML from immune effector cells. AML cells use several mechanisms to prevent immune effector cell patrolling, including downregulation or loss of MHC molecules (MHC-I/MHC-II), increased inflammatory cytokines (e.g., IL-10, IL-1, and GM-SCF), overexpression of checkpoint inhibitor ligand (e.g., PD-L1 and B7-H3), release of immune-suppressive factors (e.g., IDO, Treg, and MDSC), and reduction of proinflammatory cytokines (e.g., IL-15 and IFN-γ).

Overexpression of Immune Checkpoint-Related Proteins

By upregulating ligands that activate immune checkpoints, AML cells can induce exhaustion in T cells and can thus escape from immune surveillance mechanisms (137). It has been shown that an increased level of expression of programmed cell death protein 1 (PD-1) in $CD8^+$ and $CD4^+$ T cells after allo-HSCT results in T-cell exhaustion, leading to AML relapse (138, 139). In the setting of relapse post-allo-HSCT setting, a study of patient samples showed the upregulation of several ligands on AML blasts, including PD-1 ligand (PD-L1), B7-H3, and poliovirus receptor-related 2 (PVRL2) (133, 140). Overexpression of PD-1 has been reported in patients with metastatic melanoma who received adoptive transfer of MART-1 antigen-specific T cells (141). Exhaustion of tumor-specific $CD8^+$ T cells has been investigated in metastases with melanoma patients caused by upregulation of several inhibitory receptors, including PD-1, CTLA-4, and Tim-3 (142). Therefore, strategies based on blocking inhibitory receptors could represent practical therapeutic approaches by stimulating the synergy of the antileukemia immune response. Treatment of AML relapse with antibodies blocking inhibitory receptors has exhibited remarkable results with high effectiveness in the clinic, as described and reviewed elsewhere (137, 143).

Immunosuppressive Factors

Multiple immunosuppressive factors, such as reactive oxygen species (ROS), indoleamine 2,3-dioxygenase (IDO), regulatory T cells (Treg), and myeloid-derived suppressor cells (MDSC), have been found to be involved in immune escape in AML. It has been found that immature myeloid cells derived from tumor-bearing mice increased ROS levels, inhibiting the cytotoxicity activity of $CD8^+$ T cells as compared with tumor-free animals (144). Moreover, a study of human peripheral blood and bone marrow from AML patients demonstrated that monocytic AML cells secreted ROS to kill T cells and natural killer cells by activating poly-[ADP-ribose] polymerase-1-dependent apoptosis (145).

In addition, the expression of enzymes involved in the production of immunosuppressive products such as IDO is increased in AML patients and can hamper T-cell responses through the induction of high expression of Treg (146).

Low-risk MDS is related to the proliferation of autoimmunity-associated T helper 17 (Th17) cells, whereas a decreased number of Th17 cells and the expansion of Treg are regarded as indicators of high-risk MDS (147). In one study, a positive correlation of the number of Tregs and MDSCs was observed in patients with high-risk MDS but not in those with low-risk MDS, suggesting a role of MDSCs in the *in vivo* expansion of Tregs in MDS and subsequent disease progress (148). The development of the disease can be explained by increased levels of intracellular cytokines IL-10 and TGF-β in MDSCs (148). A higher level of MDSCs in bone marrow may be regarded as a prognostic factor for AML (149, 150). Alternatively, recent studies indicated that MDSC-like blasts from bone marrow mononuclear cells of AML patients could increase the levels of arginase-1 (ARG1) and inducible nitric oxide synthase (iNOS) that restrain $CD8^+$ T-cell proliferation and induce T-cell apoptosis (151). Decreased MDSCs have enormously enhanced the TK/Flt3L gene-induced tumor-specific CD8 T-cell response to patients with gliomas (152). Nagaraj et al. have demonstrated that coculture of antigen-specific $CD8^+$ T cells with peptide-loaded MDSCs disrupted signaling downstream of TCR (153).

Excessive Secretion of Anti-Inflammatory Cytokines

Increased levels of anti-inflammatory cytokines have been identified in the plasma of AML patients (154–156). It is acknowledged that leukemic cells can freely escape from immune surveillance by producing anti-inflammatory cytokines such as TGF-β (157, 158). These studies have reported a dual biological effect of IL-10, including tumor-promoting and antitumor functions, with respect to cancer (159, 160). As a tumor progresses, high levels of IL-10 exhibit powerful immunosuppressive effects through inhibiting the proliferation of T cells and the production of cytokines such as IFN-γ and IL-2 (159). IL-10 suppression was found to enhance the antitumor activity against CLL (161). In addition, combining T-cell therapy with treatments targeting immune cell PD-1 showed high efficacy against leukemia *via* the production of more IFN-γ, the increasing of cytolytic functions, and the increasing of memory $CD8^+$ T cells (161).

Reducing Proinflammatory Cytokines

Proinflammatory cytokines, such as IL-15 and IFN-γ, that are produced by myeloid or lymphoid progenitor cells play an essential role in eliminating leukemia cells (13, 162). Low serum levels of IL-15 in patients with leukemia early post-allo-HSCT were associated with relapse of the disease (163). Moreover, combining NK cells and exogenous IL-15 was demonstrated to enhance the immune effector cells to eradicate leukemia in post-allo-HSCT in a mouse model (164). In a phase I clinical trial (NCT01885897), administration of an IL-15 superagonist complex (ALT-803) significantly improved $CD8^+$ T cell and NK cell functions in relapsed patients with leukemia post-allo-HSCT (165). Thus, high levels of IL-15 in the microenvironment may contribute to suppressing leukemia, since it can boost the effector cells. The strategy to modify TCR-T cells with proinflammatory cytokines such as IL-18 or IL-12 has been found to increase persistence and high antitumor efficacy with a good safety profile in animal models (166, 167).

Low levels of IFN-γ cytokine secretion also have been observed in patients with leukemia. Analyses of clinical samples from B-lineage ALL patients showed that high-risk groups were associated with low IFN-γ expression, which causes leukemia to evade immune cells (168). In addition, leukemia cells may bypass the immune system by suppressing inflammatory growth factors, including IL-1b and G-CSF (13).

COMPARISON BETWEEN TCR-T AND CAR-T CELL THERAPIES FOR AML

Although CAR-T and TCR-T cells have been successfully used as a paradigm-shifting in cancer immunotherapy for treating several cancers, each approach has advantages and disadvantages (**Table 3**). The significant benefit for TCR-T over CAR-T is the ability to target peptide proteins intracellularly or cell surface proteins (169). CAR-T can only recognize target peptides on the cell surface antigens. Most proteins have been reported to express intracellular cells instead of the small number of proteins (~28%) expressed on the cell surface, making them unable to be selected as antigen for CARs (170). TCRs also have structural advantages than CARs, including more subunit receptors (ten subunits vs. one subunit), more costimulate receptors, and less dependent on antigen requirement for T-cell activation (one vs. 100) (171).

AML has been reported to have lower mutational burden compared with solid cancers. Therefore, AML seems to possess relatively fewer neoantigens that can be targeted by CAR-T therapy compared with other malignancies (172). Unlike CAR-T, TCR-T has been shown expressing several mutational neoantigens in AML, as described in the following section. CARs have a higher affinity than TCRs but have less sensitivity than TCR in comparing the affinity of a single-chain TCR (Vβ-linker-Vα) with scFv that serves as a CAR-like receptor (use the same recognition domain) (173). Thus, TCRs offer an expanded capacity to address a larger variety of carcinomas.

One major obstacle is that TCR-T cell therapy is restricted to MHC proteins of certain HLA alleles. Thereby, each TCR-T cell treatment is only suitable to patients who have a matched HLA genotype. This characteristic decreased the number of eligible patients enrolled in the TCR-T clinical trials. In contrast, CAR-T cells are MHC independent and can be applied in patients of all HLA types (169).

Both CAR-T cells and TCR-T cells have on-target, off-tumor (i.e., antigen on normal tissue) toxicities resulting from the target antigens expressed on nonmalignant cells. B-cell aplasia (43), cytokine release syndrome (87, 88), and central nervous system toxicity (88, 89) have been observed in patients receiving CAR-T cells. Although TCR-T cells are designed to redirect antigen reactivity and maintain specificity, preclinical and clinical data have demonstrated the potential for TCR-T cells to exhibit on-target, off-tumor recognition or off-target

TABLE 3 | Comparison between CAR-T and TCR-T cell therapies.

	Advantages	Disadvantages
TCR-T	■ Recognizing antigens expressed on the cell surface or intracellular antigens ■ High sensitivity and more specificity ■ Structural advantages: more subunit receptor, more costimulate receptor, and less dependence on antigens ■ Several AML specific antigens have been reported (e.g., WT1 and neoantigens)	■ Recognizing antigen targets in MHC-restricted manner ■ TCR-T is still underway the phase of clinical trials ■ Possible toxicity due to misparing between exogenous with endogenous TCR or on-target/off-tumor toxicity dose-related toxicity
CAR-T	■ Enables antigen targets without MHC restriction. ■ FDA have been approved CAR-T therapy for several forms of cancers	■ Targeting antigens expressed on the cell surface ■ Toxicity due to cytokine release syndrome ■ Lack of AML-specific antigens. Common specific antigen found (e.g., CD19, CD33, and CD34) ■ Less sensitivity and low specificity

cross-reactivity (i.e., related or unrelated antigen on target or nontarget tissue). In an early clinical trial, two treated patients developed cardiogenic shock and died within a few days of anti-MAGE-A3 affinity-enhanced TCR-T cells, due to off-target reaction directed against an unrelated protein (titin) in striated muscles (100). Thus, more advanced methods to predict or experimentally probe the risk of off-target toxicities are needed for ACT therapies prior to clinical trial.

CONCLUSIONS AND FUTURE PROSPECTS

Adoptive transfer of antigen-specific TCR-T cells is a promising tool for AML immunotherapy due to the ability of these cells to distinguish between normal and malignant tissues. Several clinical studies have demonstrated significant clinical responses with safe profiles and have improved survival, particularly WT1-specific TCR-T cell therapy. Moreover, the analyses of multiple antigen-specific TCR-T cells also are underway in a clinical trial for AML immunotherapy (**Table 2**). However, there are several limitations to the adoptive transfer of antigen-specific TCR-T cells in AML therapy. Although clinical trials of TCR-engineered T cells demonstrated impressive results and efficacy, this treatment strategy is disrupted by treatment-related on-target/off-tumor toxicity or dose-related toxicity. Many potential antigen targets of CTAs, including NY-ESO-1, PRAME, and MAGE, are rarely expressed in AML. Moreover, the persistence of ***in vivo*** TCR-T cells remains a hurdle in AML immunotherapy due to inhibition of T-cell expansion by AML blasts. As a heterogeneous and complex disease, AML evaded the immune cells by several immunosuppressive mechanisms.

Some challenges need to be overcome to ensure the safe and effective use of TCR-T cells in AML therapy. To overcome the limitations of on-target/off-tumor toxicity, choosing an appropriate antigen target is an effective strategy for eliminating malignant cancers. In this respect, tumor-restricted CTAs may be considered potentially safe target antigens. As mentioned above, combining treatment with DNA hypomethylation agents also can induce the expression of several tumor antigens to engage cognate TCRs, thereby potentially activating the adoptively transferred T cells. Dose optimization of TCR-T cells also can prevent patients from experiencing dose-related toxicities. In addition, other improvements have also expanded the persistence of TCR-T cells *in vivo*, including combining the treatment with exogenous cytokines (e.g., IL-21, IL-7, and IL-15) during cell expansion and with demethylating agents such as decitabine. Alternatively, the addition of genetically engineered constitutively signaling cytokine receptors in TCR-T cells also can lead to secretion of immunostimulatory cytokines such as IL-15 and IL-12. The use of adoptive transfer of TCR-T cells in combination with immune checkpoint blockade also can provide a novel strategy to improve immunotherapies. Thus, adoptive transfer of TCR-T therapy is a promising treatment technique for AML immunotherapy, but further investigations are warranted.

AUTHOR CONTRIBUTIONS

SK and XG contributed to the conception and design of the article. SK was accountable for the drafting and writing of the manuscript. XG, YL, JQ, ZH, and XM made critical revisions of the manuscript for important intellectual content. XG and LY were the supervisors. All authors listed have made a substantial, direct, and intellectual contribution to the work and approved it for publication.

FUNDING

This work was supported by grants from the Chinese National Major Project for New Drug Innovation (2019ZX 09201002003), National Natural Science Foundation of China (82030076, 82070161, 81970151, 81670162, 81870134 and 81900474), Shenzhen Science and Technology Foundation (JCYJ20190808163601776, JCYJ20200109113810154), Shenzhen Key Laboratory Foundation (ZDSYS20200811143757022), Sanming Project of Medicine in Shenzhen (SZSM202111004), and Natural Science Foundation of Shenzhen University General Hospital (SUGH2019QD012).

REFERENCES

1. Döhner H, Weisdorf DJ, Bloomfield CD. Acute Myeloid Leukemia. *N Engl J Med* (2015) 373:1136–52. doi: 10.1056/NEJMra1406184
2. Estey EH. Acute Myeloid Leukemia: 2019 Update on Risk-Stratification and Management. *Am J Hematol* (2018) 93:1267–91. doi: 10.1002/ajh.25214
3. Walter RB, Estey EH. Selection of Initial Therapy for Newly-Diagnosed Adult Acute Myeloid Leukemia: Limitations of Predictive Models. *Blood Rev* (2020) 44:100679. doi: 10.1016/j.blre.2020.100679
4. Lowenberg B, Ossenkoppele GJ, van Putten W, Schouten HC, Graux C, Ferrant A, et al. High-Dose Daunorubicin in Older Patients With Acute Myeloid Leukemia. *N Engl J Med* (2009) 361:1235–48. doi: 10.1056/NEJMoa0901409
5. Naina HV, Patnaik MM, Harris S. Anthracycline Dose Intensification in Acute Myeloid Leukemia. *N Engl J Med* (2009) 361:2578; author reply 2578. doi: 10.1056/NEJMc0910366
6. Wakamatsu M, Terakura S, Ohashi K, Fukuda T, Ozawa Y, Kanamori H, et al. Impacts of Thymoglobulin in Patients With Acute Leukemia in Remission Undergoing Allogeneic HSCT From Different Donors. *Blood Adv* (2019) 3:105–15. doi: 10.1182/bloodadvances.2018025643
7. Sharma P, Purev E, Haverkos B, Pollyea DA, Cherry E, Kamdar M, et al. Adult Cord Blood Transplant Results in Comparable Overall Survival and Improved GRFS vs Matched Related Transplant. *Blood Adv* (2020) 4:2227–35. doi: 10.1182/bloodadvances.2020001554
8. Bittencourt MCB, Ciurea SO. Recent Advances in Allogeneic Hematopoietic Stem Cell Transplantation for Acute Myeloid Leukemia. *Biol Blood Marrow Transplant J Am Soc Blood Marrow Transplant* (2020) 26:e215–21. doi: 10.1016/j.bbmt.2020.06.007
9. Cornelissen JJ, Breems D, van Putten WL, Gratwohl AA, Passweg JR, Pabst T, et al. Comparative Analysis of the Value of Allogeneic Hematopoietic Stem-Cell Transplantation in Acute Myeloid Leukemia With Monosomal Karyotype Versus Other Cytogenetic Risk Categories. *J Clin Oncol Off J Am Soc Clin Oncol* (2012) 30:2140–6. doi: 10.1200/JCO.2011.39.6499
10. Ruggeri A, Labopin M, Sanz G, Piemontese S, Arcese W, Bacigalupo A, et al. Comparison of Outcomes After Unrelated Cord Blood and Unmanipulated Haploidentical Stem Cell Transplantation in Adults With Acute Leukemia. *Leukemia* (2015) 29:1891–900. doi: 10.1038/leu.2015.98
11. Ciurea SO, Zhang M-J, Bacigalupo AA, Bashey A, Appelbaum FR, Aljitawi OS, et al. Haploidentical Transplant With Posttransplant Cyclophosphamide vs Matched Unrelated Donor Transplant for Acute Myeloid Leukemia. *Blood* (2015) 126:1033–40. doi: 10.1182/blood-2015-04-639831
12. Cornelissen JJ, Blaise D. Hematopoietic Stem Cell Transplantation for Patients With AML in First Complete Remission. *Blood* (2016) 127:62–70. doi: 10.1182/blood-2015-07-604546
13. Zeiser R, Vago L. Mechanisms of Immune Escape After Allogeneic Hematopoietic Cell Transplantation. *Blood* (2019) 133:1290–7. doi: 10.1182/blood-2018-10-846824
14. Acheampong DO, Adokoh CK, Asante DB, Asiamah EA, Barnie PA, Bonsu DOM, et al. Immunotherapy for Acute Myeloid Leukemia (AML): A Potent Alternative Therapy. *Biomed Pharmacother = Biomed Pharmacother* (2018) 97:225–32. doi: 10.1016/j.biopha.2017.10.100
15. Bernasconi P, Borsani O. Immune Escape After Hematopoietic Stem Cell Transplantation (HSCT): From Mechanisms to Novel Therapies. *Cancers* (2019) 12:69. doi: 10.3390/cancers12010069
16. Vago L, Gojo I. Immune Escape and Immunotherapy of Acute Myeloid Leukemia. *J Clin Invest* (2020) 130:1552–64. doi: 10.1172/JCI129204
17. Mikkilineni L, Kochenderfer JN. Chimeric Antigen Receptor T-Cell Therapies for Multiple Myeloma. *Blood* (2017) 130:2594–602. doi: 10.1182/blood-2017-06-793869
18. Gu B, Chu J, Wu D. Chimeric Antigen Receptor T Cell Therapies for Acute Myeloid Leukemia. *Front Med* (2020) 14:701–10. doi: 10.1007/s11684-020-0763-z
19. June CH, Sadelain M. Chimeric Antigen Receptor Therapy. *N Engl J Med* (2018) 379:64–73. doi: 10.1056/NEJMra1706169
20. Zhang X, Yang J, Li W, Zhang G, Su Y, Shi Y, et al. Feasibility, and Efficacy of Donor-Derived Cd19-Targeted Car T-Cell Therapy in Refractory/Relapsed (r/r)b-Cell Acute Lymphoblastic Leukemia (B-All) Patients. *Blood* (2020) 136:4–6. doi: 10.1182/blood-2020-139390
21. Maude SL, Teachey DT, Porter DL, Grupp SA. CD19-Targeted Chimeric Antigen Receptor T-Cell Therapy for Acute Lymphoblastic Leukemia. *Blood* (2015) 125:4017–23. doi: 10.1182/blood-2014-12-580068
22. Zhang C, He J, Liu L, Wang J, Wang S, Liu L, et al. CD19-Directed Fast CART Therapy for Relapsed/Refractory Acute Lymphoblastic Leukemia: From Bench to Bedside. *Blood* (2019) 134:1340–0. doi: 10.1182/blood-2019-128006
23. Budde L, Song JY, Kim Y, Blanchard S, Wagner J, Stein AS, et al. Remissions of Acute Myeloid Leukemia and Blastic Plasmacytoid Dendritic Cell Neoplasm Following Treatment With CD123-Specific CAR T Cells: A First-In-Human Clinical Trial. *Blood* (2017) 130:811–1. doi: 10.1182/blood.V130.Suppl_1.811.811
24. Hunder NN, Wallen H, Cao J, Hendricks DW, Reilly JZ, Rodmyre R, et al. Treatment of Metastatic Melanoma With Autologous CD4+ T Cells Against NY-ESO-1. *N Engl J Med* (2008) 358:2698–703. doi: 10.1056/NEJMoa0800251
25. Robbins PF, Morgan RA, Feldman SA, Yang JC, Sherry RM, Dudley ME, et al. Tumor Regression in Patients With Metastatic Synovial Cell Sarcoma and Melanoma Using Genetically Engineered Lymphocytes Reactive With NY-ESO-1. *J Clin Oncol Off J Am Soc Clin Oncol* (2011) 29:917–24. doi: 10.1200/JCO.2010.32.2537
26. Xia Y, Tian X, Wang J, Qiao D, Liu X, Xiao L, et al. Treatment of Metastatic Non-Small Cell Lung Cancer With NY-ESO-1 Specific TCR Engineered-T Cells in a Phase I Clinical Trial: A Case Report. *Oncol Lett* (2018) 16:6998–7007. doi: 10.3892/ol.2018.9534
27. Robbins PF, Kassim SH, Tran TL, Crystal JS, Morgan RA, Feldman SA, et al. A Pilot Trial Using Lymphocytes Genetically Engineered With an NY-ESO-1-Reactive T-Cell Receptor: Long-Term Follow-Up and Correlates With Response. *Clin Cancer Res* (2015) 21:1019–27. doi: 10.1158/1078-0432.CCR-14-2708
28. Chapuis AG, Egan DN, Bar M, Schmitt TM, McAfee MS, Paulson KG, et al. T Cell Receptor Gene Therapy Targeting WT1 Prevents Acute Myeloid Leukemia Relapse Post-Transplant. *Nat Med* (2019) 25:1064–72. doi: 10.1038/s41591-019-0472-9
29. Tawara I, Kageyama S, Miyahara Y, Fujiwara H, Nishida T, Akatsuka Y, et al. Safety and Persistence of WT1-Specific T-Cell Receptor Gene-Transduced Lymphocytes in Patients With AML and MDS. *Blood* (2017) 130:1985–94. doi: 10.1182/blood-2017-06-791202
30. Morris EC, Tendeiro-Rego R, Richardson R, Fox TA, Sillito F, Holler A, et al. A Phase I Study Evaluating the Safety and Persistence of Allorestricted WT1-TCR Gene Modified Autologous T Cells in Patients With High-Risk Myeloid Malignancies Unsuitable for Allogeneic Stem Cell Transplantation. *Blood* (2019) 134:1367–7. doi: 10.1182/blood-2019-128044
31. Dembić Z, Haas W, Weiss S, McCubrey J, Kiefer H, von Boehmer H, et al. Transfer of Specificity by Murine Alpha and Beta T-Cell Receptor Genes. *Nature* (1986) 320:232–8. doi: 10.1038/320232a0
32. Clay TM, Custer MC, Sachs J, Hwu P, Rosenberg SA, Nishimura MI. Efficient Transfer of a Tumor Antigen-Reactive TCR to Human Peripheral Blood Lymphocytes Confers Anti-Tumor Reactivity. *J Immunol (Baltimore Md 1950)* (1999) 163:507–13.
33. Rapoport AP, Stadtmauer EA, Binder-Scholl GK, Goloubeva O, Vogl DT, Lacey SF, et al. NY-ESO-1-Specific TCR-Engineered T Cells Mediate Sustained Antigen-Specific Antitumor Effects in Myeloma. *Nat Med* (2015) 21:914–21. doi: 10.1038/nm.3910
34. Biernacki MA, Brault M, Bleakley M. T-Cell Receptor-Based Immunotherapy for Hematologic Malignancies. *Cancer J (Sudbury Mass.)* (2019) 25:179–90. doi: 10.1097/PPO.0000000000000378
35. Sandri S, De Sanctis F, Lamolinara A, Boschi F, Poffe O, Trovato R, et al. Effective Control of Acute Myeloid Leukaemia and Acute Lymphoblastic Leukaemia Progression by Telomerase Specific Adoptive T-Cell Therapy. *Oncotarget* (2017) 8:86987–7001. doi: 10.18632/oncotarget.18115
36. Arber C, Feng X, Abhyankar H, Romero E, Wu MF, Heslop HE, et al. Survivin-Specific T Cell Receptor Targets Tumor But Not T Cells. *J Clin Invest* (2015) 125:157–68. doi: 10.1172/JCI75876
37. Ruggiero E, Liu D, Prodeus A, Becker AM, Foisey M, Balwani I, et al. NTLA5001, a T Cell Product Candidate With CRISPR-Based Targeted

Insertion of a High-Avidity, Natural, WT1-Specific TCR, Shows Efficacy in *In Vivo* Models of AML and ALL. *Blood* (2020) 136:32–3. doi: 10.1182/blood-2020-143119
38. Xue SA, Gao L, Hart D, Gillmore R, Qasim W, Thrasher A, et al. Elimination of Human Leukemia Cells in NOD/SCID Mice by WT1-TCR Gene-Transduced Human T Cells. *Blood* (2005) 106:3062–7. doi: 10.1182/blood-2005-01-0146
39. Klein C, Augsberger C, Xu W, Heitmüller C, Hanisch L, Sam J, et al. Targeting Intracellular WT1 in AML Utilizing a T Cell Bispecific Antibody Construct: Augmenting Efficacy Through Combination With Lenalidomide. *Blood* (2019) 134:4450–0. doi: 10.1182/blood-2019-130121
40. Dossa RG, Cunningham T, Sommermeyer D, Medina-Rodriguez I, Biernacki MA, Foster K, et al. Development of T-Cell Immunotherapy for Hematopoietic Stem Cell Transplantation Recipients at Risk of Leukemia Relapse. *Blood* (2018) 131:108–20. doi: 10.1182/blood-2017-07-791608
41. van Loenen MM, de Boer R, Hagedoorn RS, van Egmond EHM, Falkenburg JHF, Heemskerk MHM. Optimization of the HA-1-Specific T-Cell Receptor for Gene Therapy of Hematologic Malignancies. *Haematologica* (2011) 96:477–81. doi: 10.3324/haematol.2010.025916
42. van der Veken LT, Hagedoorn RS, van Loenen MM, Willemze R, Falkenburg JH, Heemskerk MH. Alphabeta T-Cell Receptor Engineered Gammadelta T Cells Mediate Effective Antileukemic Reactivity. *Cancer Res* (2006) 66:3331–7. doi: 10.1158/0008-5472.CAN-05-4190
43. Amir AL, van der Steen DM, van Loenen MM, Hagedoorn RS, de Boer R, Kester MD, et al. PRAME-Specific Allo-HLA-Restricted T Cells With Potent Antitumor Reactivity Useful for Therapeutic T-Cell Receptor Gene Transfer. *Clin Cancer Res* (2011) 17:5615–25. doi: 10.1158/1078-0432.CCR-11-1066
44. van der Lee DI, Reijmers RM, Honders MW, Hagedoorn RS, de Jong RC, Kester MG, et al. Mutated Nucleophosmin 1 as Immunotherapy Target in Acute Myeloid Leukemia. *J Clin Invest* (2019) 129:774–85. doi: 10.1172/JCI97482
45. Biernacki MA, Foster KA, Woodward KB, Coon ME, Cummings C, Cunningham TM, et al. CBFB-MYH11 Fusion Neoantigen Enables T Cell Recognition and Killing of Acute Myeloid Leukemia. *J Clin Invest* (2020) 130:5127–41. doi: 10.1172/JCI137723
46. Spranger S, Jeremias I, Wilde S, Leisegang M, Stärck L, Mosetter B, et al. TCR-Transgenic Lymphocytes Specific for HMMR/Rhamm Limit Tumor Outgrowth *In Vivo*. *Blood* (2012) 119:3440–9. doi: 10.1182/blood-2011-06-357939
47. Stanislawski T, Voss RH, Lotz C, Sadovnikova E, Willemsen RA, Kuball J, et al. Circumventing Tolerance to a Human MDM2-Derived Tumor Antigen by TCR Gene Transfer. *Nat Immunol* (2001) 2:962–70. doi: 10.1038/ni1001-962
48. Weigand LU, Liang X, Schmied S, Mall S, Klar R, Stötzer OJ, et al. Isolation of Human MHC Class II-Restricted T Cell Receptors From the Autologous T-Cell Repertoire With Potent Anti-Leukaemic Reactivity. *Immunology* (2012) 137:226–38. doi: 10.1111/imm.12000
49. Klobuch S, Hammon K, Vatter-Leising S, Neidlinger E, Zwerger M, Wandel A, et al. HLA-DPB1 Reactive T Cell Receptors for Adoptive Immunotherapy in Allogeneic Stem Cell Transplantation. *Cells* (2020) 9:1264. doi: 10.3390/cells9051264
50. Leung W, Heslop HE. Adoptive Immunotherapy With Antigen-Specific T Cells Expressing a Native TCR. *Cancer Immunol Res* (2019) 7:528–33. doi: 10.1158/2326-6066.CIR-18-0888
51. Fan C, Qu H, Wang X, Sobhani N, Wang L, Liu S, et al. Cancer/testis Antigens: From Serology to mRNA Cancer Vaccine. *Semin Cancer Biol* (2021) 76:218–31. doi: 10.1016/j.semcancer.2021.04.016
52. Wright WE, Piatyszek MA, Rainey WE, Byrd W, Shay JW. Telomerase Activity in Human Germline and Embryonic Tissues and Cells. *Dev Genet* (1996) 18:173–9. doi: 10.1002/(SICI)1520-6408(1996)18:2<173::AID-DVG10>3.0.CO;2-3
53. Sandri S, Bobisse S, Moxley K, Lamolinara A, De Sanctis F, Boschi F, et al. Feasibility of Telomerase-Specific Adoptive T-Cell Therapy for B-Cell Chronic Lymphocytic Leukemia and Solid Malignancies. *Cancer Res* (2016) 76:2540–51. doi: 10.1158/0008-5472.CAN-15-2318
54. Nair SK, Heiser A, Boczkowski D, Majumdar A, Naoe M, Lebkowski JS, et al. Induction of Cytotoxic T Cell Responses and Tumor Immunity Against Unrelated Tumors Using Telomerase Reverse Transcriptase RNA Transfected Dendritic Cells. *Nat Med* (2000) 6:1011–7. doi: 10.1038/79519
55. Dupont J, Latouche JB, Ma C, Sadelain M. Artificial Antigen-Presenting Cells Transduced With Telomerase Efficiently Expand Epitope-Specific, Human Leukocyte Antigen-Restricted Cytotoxic T Cells. *Cancer Res* (2005) 65:5417–27. doi: 10.1158/0008-5472.CAN-04-2991
56. Gridelli C, Ciuleanu T, Domine M, Szczesna A, Bover I, Cobo M, et al. Clinical Activity of a Htert (Vx-001) Cancer Vaccine as Post-Chemotherapy Maintenance Immunotherapy in Patients With Stage IV Non-Small Cell Lung Cancer: Final Results of a Randomised Phase 2 Clinical Trial. *Br J Cancer* (2020) 122:1461–6. doi: 10.1038/s41416-020-0785-y
57. Lilleby W, Gaudernack G, Brunsvig PF, Vlatkovic L, Schulz M, Mills K, et al. Phase I/IIa Clinical Trial of a Novel hTERT Peptide Vaccine in Men With Metastatic Hormone-Naive Prostate Cancer. *Cancer Immunol Immunother CII* (2017) 66:891–901. doi: 10.1007/s00262-017-1994-y
58. Rapoport AP, Aqui NA, Stadtmauer EA, Vogl DT, Fang HB, Cai L, et al. Combination Immunotherapy Using Adoptive T-Cell Transfer and Tumor Antigen Vaccination on the Basis of hTERT and Survivin After ASCT for Myeloma. *Blood* (2011) 117:788–97. doi: 10.1182/blood-2010-08-299396
59. Georgoulias V, Douillard JY, Khayat D, Manegold C, Rosell R, Rossi A, et al. A Multicenter Randomized Phase IIb Efficacy Study of Vx-001, a Peptide-Based Cancer Vaccine as Maintenance Treatment in Advanced Non-Small-Cell Lung Cancer: Treatment Rationale and Protocol Dynamics. *Clin Lung Cancer* (2013) 14:461–5. doi: 10.1016/j.cllc.2013.02.001
60. Garg H, Suri P, Gupta JC, Talwar GP, Dubey S. Survivin: A Unique Target for Tumor Therapy. *Cancer Cell Int* (2016) 16:49. doi: 10.1186/s12935-016-0326-1
61. Zaffaroni N, Daidone MG. Survivin Expression and Resistance to Anticancer Treatments: Perspectives for New Therapeutic Interventions. *Drug Resist Updates Rev Commentaries Antimicrob Anticancer Chemother* (2002) 5:65–72. doi: 10.1016/S1368-7646(02)00049-3
62. Kelly RJ, Lopez-Chavez A, Citrin D, Janik JE, Morris JC. Impacting Tumor Cell-Fate by Targeting the Inhibitor of Apoptosis Protein Survivin. *Mol Cancer* (2011) 10:35. doi: 10.1186/1476-4598-10-35
63. Zareifar S, Ghorbani S, Monabbati A, Bordbar MR, Zekavat OR, Abdolkarimi B, et al. Expression of Antiapoptotic Proteins Livin and Survivin in Pediatric AML Patients, as Prognostic Markers. *Pediatr Hematol Oncol* (2018) 35:250–6. doi: 10.1080/08880018.2018.1530702
64. Huang J, Lyu H, Wang J, Liu B. Influence of Survivin-Targeted Therapy on Chemosensitivity in the Treatment of Acute Myeloid Leukemia. *Cancer Lett* (2015) 366:160–72. doi: 10.1016/j.canlet.2015.05.033
65. Carter BZ, Qiu Y, Huang X, Diao L, Zhang N, Coombes KR, et al. Survivin Is Highly Expressed in CD34+38– Leukemic Stem/Progenitor Cells and Predicts Poor Clinical Outcomes in AML. *Blood* (2012) 120:173–80. doi: 10.1182/blood-2012-02-409888
66. Schmidt SM, Schag K, Müller MR, Weck MM, Appel S, Kanz L, et al. Survivin Is a Shared Tumor-Associated Antigen Expressed in a Broad Variety of Malignancies and Recognized by Specific Cytotoxic T Cells. *Blood* (2003) 102:571–6. doi: 10.1182/blood-2002-08-2554
67. Sohn HJ, Lee JY, Lee HJ, Sohn DH, Cho HI, Kim HJ, et al. Simultaneous *In Vitro* Generation of CD8 and CD4 T Cells Specific to Three Universal Tumor Associated Antigens of WT1, Survivin and TERT and Adoptive T Cell Transfer for the Treatment of Acute Myeloid Leukemia. *Oncotarget* (2017) 8:44059–72. doi: 10.18632/oncotarget.17212
68. Siegel S, Steinmann J, Schmitz N, Stuhlmann R, Dreger P, Zeis M. Identification of a Survivin-Derived Peptide That Induces HLA-A*0201-Restricted Antileukemia Cytotoxic T Lymphocytes. *Leukemia* (2004) 18:2046–7. doi: 10.1038/sj.leu.2403510
69. Rampal R, Figueroa ME. Wilms Tumor 1 Mutations in the Pathogenesis of Acute Myeloid Leukemia. *Haematologica* (2016) 101:672–9. doi: 10.3324/haematol.2015.141796
70. Wang Y, Weng WJ, Zhou DH, Fang JP, Mishra S, Chai L, et al. Wilms Tumor 1 Mutations Are Independent Poor Prognostic Factors in Pediatric Acute Myeloid Leukemia. *Front Oncol* (2021) 11:632094. doi: 10.3389/fonc.2021.632094
71. Sugiyama H. WT1 (Wilms' Tumor Gene 1): Biology and Cancer Immunotherapy. *Jpn J Clin Oncol* (2010) 40:377–87. doi: 10.1093/jjco/hyp194

72. Stauss HJ, Thomas S, Cesco-Gaspere M, Hart DP, Xue SA, Holler A, et al. WT1-Specific T Cell Receptor Gene Therapy: Improving TCR Function in Transduced T Cells. *Blood Cells Mol Dis* (2008) 40:113–6. doi: 10.1016/j.bcmd.2007.06.018
73. Kim YJ, Cho SG, Lee S, Kim MS, Kim EK, Cho BS, et al. Potential Role of Adoptively Transferred Allogeneic WT1-Specific CD4+ and CD8+ T Lymphocytes for the Sustained Remission of Refractory AML. *Bone Marrow Transplant* (2010) 45:597–9. doi: 10.1038/bmt.2009.191
74. Cohen CJ, Li YF, El-Gamil M, Robbins PF, Rosenberg SA, Morgan RA. Enhanced Antitumor Activity of T Cells Engineered to Express T-Cell Receptors With a Second Disulfide Bond. *Cancer Res* (2007) 67:3898–903. doi: 10.1158/0008-5472.CAN-06-3986
75. Bendle GM, Linnemann C, Hooijkaas AI, Bies L, de Witte MA, Jorritsma A, et al. Lethal Graft-Versus-Host Disease in Mouse Models of T Cell Receptor Gene Therapy. *Nat Med* (2010) 16:565–70, 1p following 570. doi: 10.1038/nm.2128
76. Fujiwara H, Ochi T, Ochi F, Miyazaki Y, Asai H, Narita M, et al. Antileukemia Multifunctionality of CD4(+) T Cells Genetically Engineered by HLA Class I-Restricted and WT1-Specific T-Cell Receptor Gene Transfer. *Leukemia* (2015) 29:2393–401. doi: 10.1038/leu.2015.155
77. den Haan JM, Meadows LM, Wang W, Pool J, Blokland E, Bishop TL, et al. The Minor Histocompatibility Antigen HA-1: A Diallelic Gene With a Single Amino Acid Polymorphism. *Sci (New York NY)* (1998) 279:1054–7. doi: 10.1126/science.279.5353.1054
78. Mutis T, Verdijk R, Schrama E, Esendam B, Brand A, Goulmy E. Feasibility of Immunotherapy of Relapsed Leukemia With *Ex Vivo*-Generated Cytotoxic T Lymphocytes Specific for Hematopoietic System-Restricted Minor Histocompatibility Antigens. *Blood* (1999) 93:2336–41. doi: 10.1182/blood.V93.7.2336
79. Schilbach K, Kerst G, Walter S, Eyrich M, Wernet D, Handgretinger R, et al. Cytotoxic Minor Histocompatibility Antigen HA-1–Specific CD8+ Effector Memory T Cells: Artificial APCs Pave the Way for Clinical Application by Potent Primary *In Vitro* Induction. *Blood* (2005) 106:144–9. doi: 10.1182/blood-2004-07-2940
80. Mommaas B, van Halteren AG, Pool J, van der Veken L, Wieles B, Heemskerk MH, et al. Adult and Cord Blood T Cells Can Acquire HA-1 Specificity Through HA-1 T-Cell Receptor Gene Transfer. *Haematologica* (2005) 90:1415–21. doi: 10.3324/%25x
81. Gjerstorff MF, Andersen MH, Ditzel HJ. Oncogenic Cancer/Testis Antigens: Prime Candidates for Immunotherapy. *Oncotarget* (2015) 6:15772–87. doi: 10.18632/oncotarget.4694
82. Caballero OL, Chen YT. Cancer/testis (CT) Antigens: Potential Targets for Immunotherapy. *Cancer Sci* (2009) 100:2014–21. doi: 10.1111/j.1349-7006.2009.01303.x
83. Fratta E, Coral S, Covre A, Parisi G, Colizzi F, Danielli R, et al. The Biology of Cancer Testis Antigens: Putative Function, Regulation and Therapeutic Potential. *Mol Oncol* (2011) 5:164–82. doi: 10.1016/j.molonc.2011.02.001
84. Thomas R, Al-Khadairi G, Roelands J, Hendrickx W, Dermime S, Bedognetti D, et al. NY-ESO-1 Based Immunotherapy of Cancer: Current Perspectives. *Front Immunol* (2018) 9:947. doi: 10.3389/fimmu.2018.00947
85. Yao J, Caballero OL, Yung WK, Weinstein JN, Riggins GJ, Strausberg RL, et al. Tumor Subtype-Specific Cancer-Testis Antigens as Potential Biomarkers and Immunotherapeutic Targets for Cancers. *Cancer Immunol Res* (2014) 2:371–9. doi: 10.1158/2326-6066.CIR-13-0088
86. Steger B, Milosevic S, Doessinger G, Reuther S, Liepert A, Braeu M, et al. CD4+ and CD8+T-Cell Reactions Against Leukemia-Associated- or Minor-Histocompatibility-Antigens in AML-Patients After Allogeneic SCT. *Immunobiology* (2014) 219:247–60. doi: 10.1016/j.imbio.2013.10.008
87. Weber G, Gerdemann U, Caruana I, Savoldo B, Hensel NF, Rabin KR, et al. Generation of Multi-Leukemia Antigen-Specific T Cells to Enhance the Graft-Versus-Leukemia Effect After Allogeneic Stem Cell Transplant. *Leukemia* (2013) 27:1538–47. doi: 10.1038/leu.2013.66
88. Yamamoto TN, Kishton RJ, Restifo NP. Developing Neoantigen-Targeted T Cell-Based Treatments for Solid Tumors. *Nat Med* (2019) 25:1488–99. doi: 10.1038/s41591-019-0596-y
89. Biernacki MA, Bleakley M. Neoantigens in Hematologic Malignancies. *Front Immunol* (2020) 11:121. doi: 10.3389/fimmu.2020.00121
90. Zhang Z, Lu M, Qin Y, Gao W, Tao L, Su W, et al. Neoantigen: A New Breakthrough in Tumor Immunotherapy. *Front Immunol* (2021) 12:672356. doi: 10.3389/fimmu.2021.672356
91. Türeci Ö, Löwer M, Schrörs B, Lang M, Tadmor A, Sahin U. Challenges Towards the Realization of Individualized Cancer Vaccines. *Nat Biomed Eng* (2018) 2:566–9. doi: 10.1038/s41551-018-0266-2
92. Schnittger S, Bacher U, Haferlach C, Kern W, Haferlach T. Rare CBFB-MYH11 Fusion Transcripts in AML With Inv(16)/T(16;16) Are Associated With Therapy-Related AML M4eo, Atypical Cytomorphology, Atypical Immunophenotype, Atypical Additional Chromosomal Rearrangements and Low White Blood Cell Count: A Study on 162 Patients. *Leukemia* (2007) 21:725–31. doi: 10.1038/sj.leu.2404531
93. Urashima M, Teoh G, Chauhan D, Ogata A, Shirahama S, Kaihara C, et al. MDM2 Protein Overexpression Inhibits Apoptosis of TF-1 Granulocyte-Macrophage Colony-Stimulating Factor–Dependent Acute Myeloblastic Leukemia Cells. *Blood* (1998) 92:959–67. doi: 10.1182/blood.V92.3.959
94. Mayr C, Bund D, Schlee M, Bamberger M, Kofler DM, Hallek M, et al. MDM2 Is Recognized as a Tumor-Associated Antigen in Chronic Lymphocytic Leukemia by CD8+ Autologous T Lymphocytes. *Exp Hematol* (2006) 34:44–53. doi: 10.1016/j.exphem.2005.09.016
95. Hardwick C, Hoare K, Owens R, Hohn HP, Hook M, Moore D, et al. Molecular Cloning of a Novel Hyaluronan Receptor That Mediates Tumor Cell Motility. *J Cell Biol* (1992) 117:1343–50. doi: 10.1083/jcb.117.6.1343
96. Greiner J, Li L, Ringhoffer M, Barth TF, Giannopoulos K, Guillaume P, et al. Identification and Characterization of Epitopes of the Receptor for Hyaluronic Acid-Mediated Motility (RHAMM/CD168) Recognized by CD8+ T Cells of HLA-A2-Positive Patients With Acute Myeloid Leukemia. *Blood* (2005) 106:938–45. doi: 10.1182/blood-2004-12-4787
97. Rutten CE, van Luxemburg-Heijs SA, Griffioen M, Marijt EW, Jedema I, Heemskerk MH, et al. HLA-DP as Specific Target for Cellular Immunotherapy in HLA Class II-Expressing B-Cell Leukemia. *Leukemia* (2008) 22:1387–94. doi: 10.1038/leu.2008.90
98. Herr W, Eichinger Y, Beshay J, Bloetz A, Vatter S, Mirbeth C, et al. HLA-DPB1 Mismatch Alleles Represent Powerful Leukemia Rejection Antigens in CD4 T-Cell Immunotherapy After Allogeneic Stem-Cell Transplantation. *Leukemia* (2017) 31:434–45. doi: 10.1038/leu.2016.210
99. Chapuis AG, Ragnarsson GB, Nguyen HN, Chaney CN, Pufnock JS, Schmitt TM, et al. Transferred WT1-Reactive CD8+ T Cells Can Mediate Antileukemic Activity and Persist in Post-Transplant Patients. *Sci Trans Med* (2013) 5:174ra27. doi: 10.1126/scitranslmed.3004916
100. Linette GP, Stadtmauer EA, Maus MV, Rapoport AP, Levine BL, Emery L, et al. Cardiovascular Toxicity and Titin Cross-Reactivity of Affinity-Enhanced T Cells in Myeloma and Melanoma. *Blood* (2013) 122:863–71. doi: 10.1182/blood-2013-03-490565
101. Morgan RA, Chinnasamy N, Abate-Daga D, Gros A, Robbins PF, Zheng Z, et al. Cancer Regression and Neurological Toxicity Following Anti-MAGE-A3 TCR Gene Therapy. *J Immunother (Hagerstown Md 1997)* (2013) 36:133–51. doi: 10.1097/CJI.0b013e3182829903
102. Johnson LA, Morgan RA, Dudley ME, Cassard L, Yang JC, Hughes MS, et al. Gene Therapy With Human and Mouse T-Cell Receptors Mediates Cancer Regression and Targets Normal Tissues Expressing Cognate Antigen. *Blood* (2009) 114:535–46. doi: 10.1182/blood-2009-03-211714
103. Parkhurst MR, Yang JC, Langan RC, Dudley ME, Nathan DA, Feldman SA, et al. T Cells Targeting Carcinoembryonic Antigen Can Mediate Regression of Metastatic Colorectal Cancer But Induce Severe Transient Colitis. *Mol Ther J Am Soc Gene Ther* (2011) 19:620–6. doi: 10.1038/mt.2010.272
104. Griffiths EA, Srivastava P, Matsuzaki J, Brumberger Z, Wang ES, Kocent J, et al. NY-ESO-1 Vaccination in Combination With Decitabine Induces Antigen-Specific T-Lymphocyte Responses in Patients With Myelodysplastic Syndrome. *Clin Cancer Res* (2018) 24:1019–29. doi: 10.1158/1078-0432.CCR-17-1792
105. Lim SH, Austin S, Owen-Jones E, Robinson L. Expression of Testicular Genes in Haematological Malignancies. *Br J Cancer* (1999) 81:1162–4. doi: 10.1038/sj.bjc.6690824
106. Almstedt M, Blagitko-Dorfs N, Duque-Afonso J, Karbach J, Pfeifer D, Jager E, et al. The DNA Demethylating Agent 5-Aza-2'-Deoxycytidine Induces Expression of NY-ESO-1 and Other Cancer/Testis Antigens in Myeloid Leukemia Cells. *Leuk Res* (2010) 34:899–905. doi: 10.1016/j.leukres.2010.02.004

107. Atanackovic D, Luetkens T, Kloth B, Fuchs G, Cao Y, Hildebrandt Y, et al. Cancer-Testis Antigen Expression and Its Epigenetic Modulation in Acute Myeloid Leukemia. *Am J Hematol* (2011) 86:918–22. doi: 10.1002/ajh.22141
108. Saito T, Hochstenbach F, Marusic-Galesic S, Kruisbeek AM, Brenner M, Germain RN. Surface Expression of Only Gamma Delta and/or Alpha Beta T Cell Receptor Heterodimers by Cells With Four (Alpha, Beta, Gamma, Delta) Functional Receptor Chains. *J Exp Med* (1988) 168:1003–20. doi: 10.1084/jem.168.3.1003
109. Marcu-Malina V, Heijhuurs S, van Buuren M, Hartkamp L, Strand S, Sebestyen Z, et al. Redirecting αβ T Cells Against Cancer Cells by Transfer of a Broadly Tumor-Reactive γδt-Cell Receptor. *Blood* (2011) 118:50–9. doi: 10.1182/blood-2010-12-325993
110. Kabelitz D, Serrano R, Kouakanou L, Peters C, Kalyan S. Cancer Immunotherapy With γδ T Cells: Many Paths Ahead of Us. *Cell Mol Immunol* (2020) 17:925–39. doi: 10.1038/s41423-020-0504-x
111. Vyborova A, Beringer DX, Fasci D, Karaiskaki F, van Diest E, Kramer L, et al. γ9δ2t Cell Diversity and the Receptor Interface With Tumor Cells. *J Clin Invest* (2020) 130:4637–51. doi: 10.1172/JCI132489
112. Johanna I, Straetemans T, Heijhuurs S, Aarts-Riemens T, Norell H, Bongiovanni L, et al. Evaluating *In Vivo* Efficacy - Toxicity Profile of TEG001 in Humanized Mice Xenografts Against Primary Human AML Disease and Healthy Hematopoietic Cells. *J Immunother Cancer* (2019) 7:69. doi: 10.1186/s40425-019-0558-4
113. Nagarsheth NB, Norberg SM, Sinkoe AL, Adhikary S, Meyer TJ, Lack JB, et al. TCR-Engineered T Cells Targeting E7 for Patients With Metastatic HPV-Associated Epithelial Cancers. *Nat Med* (2021) 27:419–25. doi: 10.1038/s41591-020-01225-1
114. Lam VK, Hong DS, Heymach J, Blumenschein GR, Creelan BC, Bradbury PA, et al. Initial Safety Assessment of MAGE-A10c796TCR T-Cells in Two Clinical Trials. *J Clin Oncol* (2018) 36:3056–6. doi: 10.1200/JCO.2018.36.15_suppl.3056
115. Gust J, Hay KA, Hanafi LA, Li D, Myerson D, Gonzalez-Cuyar LF, et al. Endothelial Activation and Blood-Brain Barrier Disruption in Neurotoxicity After Adoptive Immunotherapy With CD19 CAR-T Cells. *Cancer Discov* (2017) 7:1404–19. doi: 10.1158/2159-8290.CD-17-0698
116. Brudno JN, Kochenderfer JN. Recent Advances in CAR T-Cell Toxicity: Mechanisms, Manifestations and Management. *Blood Rev* (2019) 34:45–55. doi: 10.1016/j.blre.2018.11.002
117. Lee DW, Kochenderfer JN, Stetler-Stevenson M, Cui YK, Delbrook C, Feldman SA, et al. T Cells Expressing CD19 Chimeric Antigen Receptors for Acute Lymphoblastic Leukaemia in Children and Young Adults: A Phase 1 Dose-Escalation Trial. *Lancet (London England)* (2015) 385:517–28. doi: 10.1016/S0140-6736(14)61403-3
118. Gust J, Taraseviciute A, Turtle CJ. Neurotoxicity Associated With CD19-Targeted CAR-T Cell Therapies. *CNS Drugs* (2018) 32:1091–101. doi: 10.1007/s40263-018-0582-9
119. Schuster SJ, Svoboda J, Chong EA, Nasta SD, Mato AR, Anak Ö, et al. Chimeric Antigen Receptor T Cells in Refractory B-Cell Lymphomas. *N Engl J Med* (2017) 377:2545–54. doi: 10.1056/NEJMoa1708566
120. Berger C, Jensen MC, Lansdorp PM, Gough M, Elliott C, Riddell SR. Adoptive Transfer of Effector CD8+ T Cells Derived From Central Memory Cells Establishes Persistent T Cell Memory in Primates. *J Clin Invest* (2008) 118:294–305. doi: 10.1172/JCI32103
121. Miyao K, Terakura S, Okuno S, Julamanee J, Watanabe K, Hamana H, et al. Introduction of Genetically Modified Cd3ζ Improves Proliferation and Persistence of Antigen-Specific CTLs. *Cancer Immunol Res* (2018) 6:733–44. doi: 10.1158/2326-6066.CIR-17-0538
122. Sakai T, Terakura S, Miyao K, Okuno S, Adachi Y, Umemura K, et al. Artificial T Cell Adaptor Molecule-Transduced TCR-T Cells Demonstrated Improved Proliferation Only When Transduced in a Higher Intensity. *Mol Ther Oncol* (2020) 18:613–22. doi: 10.1016/j.omto.2020.08.014
123. Deshpande P, Cavanagh MM, Le Saux S, Singh K, Weyand CM, Goronzy JJ. IL-7- and IL-15-Mediated TCR Sensitization Enables T Cell Responses to Self-Antigens. *J Immunol (Baltimore Md 1950)* (2013) 190:1416–23. doi: 10.4049/jimmunol.1201620
124. McLellan AD, Ali Hosseini Rad SM. Chimeric Antigen Receptor T Cell Persistence and Memory Cell Formation. *Immunol Cell Biol* (2019) 97:664–74. doi: 10.1111/imcb.12254
125. Kalos M, Levine BL, Porter DL, Katz S, Grupp SA, Bagg A, et al. T Cells With Chimeric Antigen Receptors Have Potent Antitumor Effects and Can Establish Memory in Patients With Advanced Leukemia. *Sci Trans Med* (2011) 3:95ra73. doi: 10.1126/scitranslmed.3002842
126. Xu Y, Zhang M, Ramos CA, Durett A, Liu E, Dakhova O, et al. Closely Related T-Memory Stem Cells Correlate With *In Vivo* Expansion of CAR.CD19-T Cells and Are Preserved by IL-7 and IL-15. *Blood* (2014) 123:3750–9. doi: 10.1182/blood-2014-01-552174
127. Wang Y, Tong C, Dai H, Wu Z, Han X, Guo Y, et al. Low-Dose Decitabine Priming Endows CAR T Cells With Enhanced and Persistent Antitumour Potential *via* Epigenetic Reprogramming. *Nat Commun* (2021) 12:409. doi: 10.1038/s41467-020-20696-x
128. Vago L, Perna SK, Zanussi M, Mazzi B, Barlassina C, Stanghellini MT, et al. Loss of Mismatched HLA in Leukemia After Stem-Cell Transplantation. *N Engl J Med* (2009) 361:478–88. doi: 10.1056/NEJMoa0811036
129. McCurdy SR, Iglehart BS, Batista DA, Gocke CD, Ning Y, Knaus HA, et al. Loss of the Mismatched Human Leukocyte Antigen Haplotype in Two Acute Myelogenous Leukemia Relapses After Haploidentical Bone Marrow Transplantation With Post-Transplantation Cyclophosphamide. *Leukemia* (2016) 30:2102–6. doi: 10.1038/leu.2016.144
130. Sano H, Mochizuki K, Kobayashi S, Ono S, Ikeda K, Ohto H, et al. Two Occurrences of Leukemia Relapse Due to Mismatched HLA Loss After Haploidentical Stem Cell Transplantation From Different Family Donors With KIR Ligand Mismatch. *J Pediatr Hematol Oncol* (2020) 42:e104–6. doi: 10.1097/MPH.0000000000001443
131. Klippel ZK, Chou J, Towlerton AM, Voong LN, Robbins P, Bensinger WI, et al. Immune Escape From NY-ESO-1-Specific T-Cell Therapy *via* Loss of Heterozygosity in the MHC. *Gene Ther* (2014) 21:337–42. doi: 10.1038/gt.2013.87
132. Christopher MJ, Petti AA, Rettig MP, Miller CA, Chendamarai E, Duncavage EJ, et al. Immune Escape of Relapsed AML Cells After Allogeneic Transplantation. *N Engl J Med* (2018) 379:2330–41. doi: 10.1056/NEJMoa1808777
133. Toffalori C, Zito L, Gambacorta V, Riba M, Oliveira G, Bucci G, et al. Immune Signature Drives Leukemia Escape and Relapse After Hematopoietic Cell Transplantation. *Nat Med* (2019) 25:603–11. doi: 10.1038/s41591-019-0400-z
134. Christopher M, Petti AA, Miller CA, Rettig MP, Duncavage EJ, Klco JM, et al. Downregulation of MHC Class II in Relapsed AML Cells After Allogeneic Transplantation. *Blood* (2017) 130:2678–8. doi: 10.1182/blood.V130.Suppl_1.2678.2678
135. Cornel AM, Mimpen IL, Nierkens S. MHC Class I Downregulation in Cancer: Underlying Mechanisms and Potential Targets for Cancer Immunotherapy. *Cancers* (2020) 12:1760. doi: 10.3390/cancers12071760
136. Hemmerle T, Neri D. The Dose-Dependent Tumor Targeting of Antibody-Ifnγ Fusion Proteins Reveals an Unexpected Receptor-Trapping Mechanism *In Vivo*. *Cancer Immunol Res* (2014) 2:559–67. doi: 10.1158/2326-6066.CIR-13-0182
137. Taghiloo S, Asgarian-Omran H. Immune Evasion Mechanisms in Acute Myeloid Leukemia: A Focus on Immune Checkpoint Pathways. *Crit Rev Oncol Hematol* (2021) 157:103164. doi: 10.1016/j.critrevonc.2020.103164
138. Schnorfeil FM, Lichtenegger FS, Emmerig K, Schlueter M, Neitz JS, Draenert R, et al. T Cells Are Functionally Not Impaired in AML: Increased PD-1 Expression Is Only Seen at Time of Relapse and Correlates With a Shift Towards the Memory T Cell Compartment. *J Hematol Oncol* (2015) 8:93. doi: 10.1186/s13045-015-0189-2
139. Williams P, Basu S, Garcia-Manero G, Hourigan CS, Oetjen KA, Cortes JE, et al. The Distribution of T-Cell Subsets and the Expression of Immune Checkpoint Receptors and Ligands in Patients With Newly Diagnosed and Relapsed Acute Myeloid Leukemia. *Cancer* (2019) 125:1470–81. doi: 10.1002/cncr.31896
140. Kong Y, Zhang J, Claxton DF, Ehmann WC, Rybka WB, Zhu L, et al. PD-1 (Hi)TIM-3(+) T Cells Associate With and Predict Leukemia Relapse in AML Patients Post Allogeneic Stem Cell Transplantation. *Blood Cancer J* (2015) 5:e330. doi: 10.1038/bcj.2015.58
141. Ahmadzadeh M, Johnson LA, Heemskerk B, Wunderlich JR, Dudley ME, White DE, et al. Tumor Antigen-Specific CD8 T Cells Infiltrating the Tumor Express High Levels of PD-1 and Are Functionally Impaired. *Blood* (2009) 114:1537–44. doi: 10.1182/blood-2008-12-195792

142. Baitsch L, Baumgaertner P, Devêvre E, Raghav SK, Legat A, Barba L, et al. Exhaustion of Tumor-Specific CD8+ T Cells in Metastases From Melanoma Patients. *J Clin Invest* (2011) 121:2350–60. doi: 10.1172/JCI46102
143. Albring JC, Inselmann S, Sauer T, Schliemann C, Altvater B, Kailayangiri S, et al. PD-1 Checkpoint Blockade in Patients With Relapsed AML After Allogeneic Stem Cell Transplantation. *Bone Marrow Transplant* (2017) 52:317–20. doi: 10.1038/bmt.2016.274
144. Kusmartsev S, Nefedova Y, Yoder D, Gabrilovich DI. Antigen-Specific Inhibition of CD8+ T Cell Response by Immature Myeloid Cells in Cancer Is Mediated by Reactive Oxygen Species. *J Immunol (Baltimore Md 1950)* (2004) 172:989–99. doi: 10.4049/jimmunol.172.2.989
145. Aurelius J, Thorén FB, Akhiani AA, Brune M, Palmqvist L, Hansson M, et al. Monocytic AML Cells Inactivate Antileukemic Lymphocytes: Role of NADPH Oxidase/Gp91(Phox) Expression and the PARP-1/PAR Pathway of Apoptosis. *Blood* (2012) 119:5832–7. doi: 10.1182/blood-2011-11-391722
146. Curti A, Pandolfi S, Valzasina B, Aluigi M, Isidori A, Ferri E, et al. Modulation of Tryptophan Catabolism by Human Leukemic Cells Results in the Conversion of CD25- Into CD25+ T Regulatory Cells. *Blood* (2007) 109:2871–7. doi: 10.1182/blood-2006-07-036863
147. Kordasti SY, Afzali B, Lim Z, Ingram W, Hayden J, Barber L, et al. IL-17-Producing CD4(+) T Cells, Pro-Inflammatory Cytokines and Apoptosis Are Increased in Low Risk Myelodysplastic Syndrome. *Br J Haematol* (2009) 145:64–72. doi: 10.1111/j.1365-2141.2009.07593.x
148. Kittang AO, Kordasti S, Sand KE, Costantini B, Kramer AM, Perezabellan P, et al. Expansion of Myeloid Derived Suppressor Cells Correlates With Number of T Regulatory Cells and Disease Progression in Myelodysplastic Syndrome. *Oncoimmunology* (2016) 5:e1062208. doi: 10.1080/2162402X.2015.1062208
149. Sun H, Li Y, Zhang ZF, Ju Y, Li L, Zhang BC, et al. Increase in Myeloid-Derived Suppressor Cells (MDSCs) Associated With Minimal Residual Disease (MRD) Detection in Adult Acute Myeloid Leukemia. *Int J Hematol* (2015) 102:579–86. doi: 10.1007/s12185-015-1865-2
150. Wang L, Jia B, Claxton DF, Ehmann WC, Rybka WB, Mineishi S, et al. VISTA Is Highly Expressed on MDSCs and Mediates an Inhibition of T Cell Response in Patients With AML. *Oncoimmunology* (2018) 7:e1469594. doi: 10.1080/2162402X.2018.1469594
151. Hyun SY, Na EJ, Jang JE, Chung H, Kim SJ, Kim JS, et al. Immunosuppressive Role of CD11b(+) CD33(+) HLA-DR(-) Myeloid-Derived Suppressor Cells-Like Blast Subpopulation in Acute Myeloid Leukemia. *Cancer Med* (2020) 9:7007–17. doi: 10.1002/cam4.3360
152. Kamran N, Kadiyala P, Saxena M, Candolfi M, Li Y, Moreno-Ayala MA, et al. Immunosuppressive Myeloid Cells' Blockade in the Glioma Microenvironment Enhances the Efficacy of Immune-Stimulatory Gene Therapy. *Mol Ther J Am Soc Gene Ther* (2017) 25:232–48. doi: 10.1016/j.ymthe.2016.10.003
153. Nagaraj S, Schrum AG, Cho HI, Celis E, Gabrilovich DI. Mechanism of T Cell Tolerance Induced by Myeloid-Derived Suppressor Cells. *J Immunol (Baltimore Md 1950)* (2010) 184:3106–16. doi: 10.4049/jimmunol.0902661
154. Sanchez-Correa B, Bergua JM, Campos C, Gayoso I, Arcos MJ, Bañas H, et al. Cytokine Profiles in Acute Myeloid Leukemia Patients at Diagnosis: Survival Is Inversely Correlated With IL-6 and Directly Correlated With IL-10 Levels. *Cytokine* (2013) 61:885–91. doi: 10.1016/j.cyto.2012.12.023
155. Min CK, Lee WY, Min DJ, Lee DG, Kim YJ, Park YH, et al. The Kinetics of Circulating Cytokines Including IL-6, TNF-Alpha, IL-8 and IL-10 Following Allogeneic Hematopoietic Stem Cell Transplantation. *Bone Marrow Transplant* (2001) 28:935–40. doi: 10.1038/sj.bmt.1703258
156. Binder S, Luciano M, Horejs-Hoeck J. The Cytokine Network in Acute Myeloid Leukemia (AML): A Focus on Pro- and Anti-Inflammatory Mediators. *Cytokine Growth Factor Rev* (2018) 43:8–15. doi: 10.1016/j.cytogfr.2018.08.004
157. Naka K, Hoshii T, Muraguchi T, Tadokoro Y, Ooshio T, Kondo Y, et al. TGF-Beta-FOXO Signalling Maintains Leukaemia-Initiating Cells in Chronic Myeloid Leukaemia. *Nature* (2010) 463:676–80. doi: 10.1038/nature08734
158. Selnø ATH, Schlichtner S, Yasinska IM, Sakhnevych SS, Fiedler W, Wellbrock J, et al. Transforming Growth Factor Beta Type 1 (TGF-β) and Hypoxia-Inducible Factor 1 (HIF-1) Transcription Complex as Master Regulators of the Immunosuppressive Protein Galectin-9 Expression in Human Cancer and Embryonic Cells. *Aging* (2020) 12:23478–96. doi: 10.18632/aging.202343
159. Mocellin S, Marincola FM, Young HA. Interleukin-10 and the Immune Response Against Cancer: A Counterpoint. *J Leuk Biol* (2005) 78:1043–51. doi: 10.1189/jlb.0705358
160. Zamarron BF, Chen W. Dual Roles of Immune Cells and Their Factors in Cancer Development and Progression. *Int J Biol Sci* (2011) 7:651–8. doi: 10.7150/ijbs.7.651
161. Rivas JR, Liu Y, Alhakeem SS, Eckenrode JM, Marti F, Collard JP, et al. Interleukin-10 Suppression Enhances T-Cell Antitumor Immunity and Responses to Checkpoint Blockade in Chronic Lymphocytic Leukemia. *Leukemia* (2021) 35:3188–200. doi: 10.1101/2020.07.15.204560
162. Colpitts SL, Stonier SW, Stoklasek TA, Root SH, Aguila HL, Schluns KS, et al. Transcriptional Regulation of IL-15 Expression During Hematopoiesis. *J Immunol (Baltimore Md 1950)* (2013) 191:3017–24. doi: 10.4049/jimmunol.1301389
163. Thiant S, Yakoub-Agha I, Magro L, Trauet J, Coiteux V, Jouet JP, et al. Plasma Levels of IL-7 and IL-15 in the First Month After Myeloablative BMT Are Predictive Biomarkers of Both Acute GVHD and Relapse. *Bone Marrow Transplant* (2010) 45:1546–52. doi: 10.1038/bmt.2010.13
164. Chen G, Wu D, Wang Y, Cen J, Feng Y, Sun A, et al. Expanded Donor Natural Killer Cell and IL-2, IL-15 Treatment Efficacy in Allogeneic Hematopoietic Stem Cell Transplantation. *Eur J Haematol* (2008) 81:226–35. doi: 10.1111/j.1600-0609.2008.01108.x
165. Romee R, Cooley S, Berrien-Elliott MM, Westervelt P, Verneris MR, Wagner JE, et al. First-In-Human Phase 1 Clinical Study of the IL-15 Superagonist Complex ALT-803 to Treat Relapse After Transplantation. *Blood* (2018) 131:2515–27. doi: 10.1182/blood-2017-12-823757
166. Drakes DJ, Rafiq S, Purdon TJ, Lopez AV, Chandran SS, Klebanoff CA, et al. Optimization of T-Cell Receptor-Modified T Cells for Cancer Therapy. *Cancer Immunol Res* (2020) 8:743–55. doi: 10.1158/2326-6066.CIR-19-0910
167. Tucker CG, Mitchell JS, Martinov T, Burbach BJ, Beura LK, Wilson JC, et al. Adoptive T Cell Therapy With IL-12-Preconditioned Low-Avidity T Cells Prevents Exhaustion and Results in Enhanced T Cell Activation, Enhanced Tumor Clearance, and Decreased Risk for Autoimmunity. *J Immunol (Baltimore Md 1950)* (2020) 205:1449–60. doi: 10.4049/jimmunol.2000007
168. Cloppenborg T, Stanulla M, Zimmermann M, Schrappe M, Welte K, Klein C. Immunosurveillance of Childhood ALL: Polymorphic Interferon-Gamma Alleles Are Associated With Age at Diagnosis and Clinical Risk Groups. *Leukemia* (2005) 19:44–8. doi: 10.1038/sj.leu.2403553
169. Zhao Q, Jiang Y, Xiang S, Kaboli PJ, Shen J, Zhao Y, et al. Engineered TCR-T Cell Immunotherapy in Anticancer Precision Medicine: Pros and Cons. *Front Immunol* (2021) 12:658753. doi: 10.3389/fimmu.2021.658753
170. Uhlén M, Fagerberg L, Hallström BM, Lindskog C, Oksvold P, Mardinoglu A, et al. Proteomics. Tissue-Based Map of the Human Proteome. *Sci (New York NY)* (2015) 347:1260419. doi: 10.1126/science.1260419
171. Harris DT, Kranz DM. Adoptive T Cell Therapies: A Comparison of T Cell Receptors and Chimeric Antigen Receptors. *Trends Pharmacol Sci* (2016) 37:220–30. doi: 10.1016/j.tips.2015.11.004
172. Chalmers ZR, Connelly CF, Fabrizio D, Gay L, Ali SM, Ennis R, et al. Analysis of 100,000 Human Cancer Genomes Reveals the Landscape of Tumor Mutational Burden. *Genome Med* (2017) 9:34. doi: 10.1186/s13073-017-0424-2
173. Stone JD, Harris DT, Soto CM, Chervin AS, Aggen DH, Roy EJ, et al. A Novel T Cell Receptor Single-Chain Signaling Complex Mediates Antigen-Specific T Cell Activity and Tumor Control. *Cancer Immunol Immunother CII* (2014) 63:1163–76. doi: 10.1007/s00262-014-1586-z

Conflict of Interest: The authors declare that the research was conducted in the absence of any commercial or financial relationships that could be construed as a potential conflict of interest.

this article, or claim that may be made by its manufacturer, is not guaranteed or endorsed by the publisher.

Advantages of publishing in Frontiers

OPEN ACCESS
Articles are free to read for greatest visibility and readership

FAST PUBLICATION
Around 90 days from submission to decision

HIGH QUALITY PEER-REVIEW
Rigorous, collaborative, and constructive peer-review

TRANSPARENT PEER-REVIEW
Editors and reviewers acknowledged by name on published articles

Frontiers
Avenue du Tribunal-Fédéral 34
1005 Lausanne | Switzerland

Visit us: www.frontiersin.org
Contact us: frontiersin.org/about/contact

REPRODUCIBILITY OF RESEARCH
Support open data and methods to enhance research reproducibility

DIGITAL PUBLISHING
Articles designed for optimal readership across devices

FOLLOW US
@frontiersin

IMPACT METRICS
Advanced article metrics track visibility across digital media

EXTENSIVE PROMOTION
Marketing and promotion of impactful research

LOOP RESEARCH NETWORK
Our network increases your article's readership